science & innovation
Department:
Science and Innovation
REPUBLIC OF SOUTH AFRICA

National Research Foundation

forestry, fisheries & the environment
Department:
Forestry, Fisheries and the Environment
REPUBLIC OF SOUTH AFRICA

SCALE-WIN22 Cruise Report

SCALE
Southern oCean seAsonaL Experiment

Winter Cruise: 11th – 31st July 2022

Southern oCean seAsonal Experiment
Winter 2022

Compiled by Marcello Vichi

DOI: 10.5281/zenodo.7901530

Table of Contents

1 Introduction 1

1.1 Objectives 3

1.2 Participants, planned Itinerary and Narrative 10

1.3 Stations and Activities 16

1.4 Citing this report 18

1.5 Acknowledgements 19

2 Meteorological observations and ocean observing system deployments 20

2.1 Summary of met-ocean conditions 20

2.2 Work packages 25

2.2.1 WP1. Operational marine forecasting and analysis 25

2.2.2 WP2. Met-ocean observation 29

2.2.2.1 Surface synoptic weather observations 29

2.2.2.2 Sea ice remote sensing 30

2.2.2.3 Deployment of oceanographic instrumentation 32

2.2.3 WP3. Research 33

2.3 Challenges and recommendations 34

2.3.1 Freezing of wind sensors 34

2.3.2 XBTs 34

2.3.3 SDS Meteorological Sensors 35

3 Logistics: ocean and ice observations, and autonomous device operations 36

3.1 Ocean operations 36

3.1.1 CTD 36

3.1.2 Kevlar cable 38

3.1.3 Processing and calibration of CTD data 38

3.1.4 Stations 38

3.1.5 Scientific Data system (SDS) 39

3.2 Technical information from the sea-going technician 39

3.3 Sea ice observations (ASPeCt) 51
3.4 Auxiliary satellite observations: SAR from Cosmo-SkyMed 54
3.5 Auxiliary satellite observations: ECICE sea-ice type 54
4 Top predator distribution and abundance in the Southern Ocean 57
4.1 Objectives 57
4.2 Synopsis 57
4.3 Significance 58
4.4 Sampling 58
4.5 Seabirds 59
4.6 Cetaceans 59
5 CO2 and Heat storage and fluxes 67
5.1 Introduction 67
5.2 Continuous pCO_2 measurements 68
5.3 Dissolved inorganic carbon (DIC) and total alkalinity (AT) measurements 69
5.4 Constraining the pCO2 bias on SA Agulhas II 69
5.5 Marine pH measurements 69
5.6 Continuous heat flux measurements: 69
6 Microbiome research 71
6.1 Unravelling the role of Iron and Manganese co-limitation on microbial communities from the Southern Ocean 71
6.1.1 Introduction and Rationale 71
6.1.2 Aims and Objectives 71
6.1.3 Research approach and methodology 71
6.2 2. Elucidating the effects of oceanographic variables on the distribution of viruses in the Southern Ocean 72
6.2.1 Introduction and Rationale 72
6.2.2 Aims and Objectives 72
6.2.3 Research approach and methodology 72
6.3 Exploring the chemical ecology of marine fungi and discovery of important biosynthetic pathways involved in the biological carbon pump 73

6.3.1 Introduction and Rationale 73
6.3.2 Aims and objectives 73
6.3.3 Research approach and Methodology 73
6.4 Investigation of Microbial Genomics to Understand biogeochemical fates of Dimethylsulfoniopropionate in the Southern Ocean 73
6.4.1 Introduction and Rationale 74
6.4.2 Research aims and objectives 74
6.4.3 Research approach and methodology 74
6.5 Closing Remarks 74
7 Seasonal Iron (Fe) speciation in the Southern Ocean 75
7.1 Introduction 75
7.2 Aims and objectives 75
7.3 Methodology 76
7.3.1 Sampling Facilities 76
7.3.2 Sampling and preservations 76
7.3.2.1 Dissolved Fe (dFe) 76
7.3.2.2 Soluble Fe (SFe) 76
7.3.2.3 Humics 76
7.3.3 Fe and Mn addition incubation experiments 76
7.4 Preliminary Results 77
7.5 Future recommendations 77
8 Biological Carbon Pump 78
8.1 Introduction 78
8.2 Routine Measurements (all stations) 79
8.2.1 Chlorophyll a concentration 79
8.2.2 Particulate & Dissolved Organic Carbon 79
8.2.3 Particulate Absorbance 79
8.2.4 Particle Size Distribution 79
8.2.5 HPLC 80
8.3 Student Projects 80

8.3.1 Optical effects of photophysiological changes in Southern Ocean phytoplankton (S. Mpapane, for MSc) 80
8.3.1.1 Background & Rationale 80
8.3.1.2 Measurements 81
8.3.2 Analysis of the sources of variability in photophysiological parameters derived from phytoplankton fluorescence in the Southern Ocean (L. Ruiters, for MSc) 82
8.3.2.1 Background & Rationale 82
8.3.2.2 Methodology 83
8.3.3 Investigating the Dominant Controls of Carbon Export in the Southern Ocean (A. Naicker, for PhD) 83
8.3.3.1 Background & Rationale 83
8.3.3.2 Methodology: MSC Deployment 85
8.3.4 The impacts of ocean acidification and increasing temperatures on phytoplankton primary productivity, physiology, and nutrient uptake (Attang Biyela, for PhD) 86
8.3.4.1 Background & Rationale 86
8.3.4.2 Methodology 87
9 Nitrogen Cycle: Nitrogen cycling in the upper surface Southern Ocean 90
9.1 Introduction 90
9.2 Nitrogen species sampling 92
9.2.1 Field collections 92
9.2.2 Recommendations 95
9.3 Chlorophyll Sampling 95
9.3.1 Methodology 95
9.3.1.1 Filtering for Chlorophyll-a 95
9.3.1.2 Ice Core and frazil ice filtering 96
9.3.1.3 Fluorescence reading 96
9.3.1.4 Lugol's 96
9.3.1.5 Additional work 96
10 IMICROBE project 100
10.1 Methods 100

10.2 mini CTD 101
10.3 Under-ice light measurements 102
10.4 Sea Ice work 103
10.5 Metagenomic samples 104
10.6 Fe manipulation incubations 105
10.7 Phytoplankton characterization 105
10.8 Bacterial abundances 106
10.9 Nanoflagellates grazing 107
10.10 Heterotrophic respiration 108
10.11 FCM demonstration 109
10.12 Seminar on sea ice biome 109
10.13 Acknowledgements 109
11 The Digital SA Agulhas II 110
11.1 Project Details 110
11.2 Prior to Vessel Departure 110
11.3 Ship Structural Response and Propulsion System Measurements 111
11.3.1 Primary Full-Scale Measurement System 111
11.3.1.1 Description of Full-Scale Measurement Infrastructure 111
11.3.1.2 Ship Structural Response Measured Through Acceleration 112
11.3.1.3 Ship Structural Response Measured Through Strain 114
11.3.1.4 Propulsion System Measurements 114
11.3.2 Shaft Line Acoustic Emission Measurement System 115
11.3.3 Hull Stress Monitoring System 117
11.4 Sea Ice and Sea State Observations 119
11.4.1 Visual Sea State Observations 119
11.4.2 Visual Sea Ice Observations 119
11.4.3 Sea Ice Observations with Machine Vision 120
11.4.4 Ice Thickness Measurements 121
11.5 Operational Test Sequences 121

11.5.1 Varying Incident Wave Angles in Open Water 121
11.5.2 Breaking Ice at Constant Speed 123
11.5.3 Turning in Ice Without a Channel 125
11.5.4 Fixed Shaft RPM and Propeller Pitch Test Sequences 127
11.6 Human Responses to Slamming and Motion Sickness 129
11.6.1 Participant Recruitment and Incentive Scheme 129
11.6.2 Daily Diary Distribution and Mariner 4.0 Application Deployment 131
11.6.3 Slamming Observations During Operational Test Sequence 133
11.7 Requested Operational Test Sequences Not Performed 133
11.8 Acknowledgements 134
12 Waves from vessel motion 136
12.1 Introduction 136
12.2 Experiment details 136
12.3 Sensor operation 137
12.4 Acknowledgements 139
13 Sea ice sampling 140
13.1 Sample collection 141
13.1.1 Onboard - Pancake Stations 141
13.1.2 Overboard - Consolidated stations 143
13.1.3 Sea ice sampling methods 145
13.2 Sea ice core processing 146
13.2.1 Uniaxial compressive strength- constant stress 147
13.2.2 Uniaxial compressive strength- constant strain 147
13.2.3 Cross polarisation 148
13.2.4 Temperature and salinity processing 148
13.2.5 Biogeochemical processing 149
13.2.6 Algae Incubation 149
13.2.7 CT scanning 150
13.2.8 Storage biogeochemical processing 150

13.3 Frazil Ice sampling 151

14 A network of autonomous sea ice observation platforms in support of Southern Hemisphere climate predictions 152

14.1 Overview and scientific objectives 152

14.1.1 stations 153

14.2 Ship-based imaging 154

14.2.1 Scientific background 154

14.2.2 Activity report 155

14.2.3 Thermal imaging 155

14.2.3.1 Method and equipment 155

14.2.3.2 Preliminary results 156

14.2.3.3 Recommendation 157

14.2.4 Stereo camera system 157

14.2.4.1 Method and equipment 157

14.2.4.2 Preliminary results 159

14.2.4.3 Recommendation 159

14.2.5 LiDAR imaging for ocean and sea ice elevation monitoring 160

14.2.5.1 Method and equipment 160

14.2.5.2 Preliminary results 160

14.2.5.3 Recommendation 161

14.2.6 Imaging of individual ice pancake floes on deck 161

14.2.6.1 Method and equipment 161

14.2.6.2 Preliminary results 164

14.2.6.3 Recommendations 165

14.2.7 Stereo GoPro recording of buoy deployment and retrievals 165

14.2.7.1 Method and equipment 165

14.2.7.2 Preliminary results 168

14.2.7.3 Recommendations 170

14.3 Buoy deployments and retrievals 170

14.3.1 Scientific background 170

14.3.2 Activity report 171
14.3.3 FMI wave buoy deployment and retrievals 171
14.3.3.1 Method and equipment 171
14.3.3.2 Preliminary results 173
14.3.4 UCT SHARC buoy deployment and retrievals 175
14.3.4.1 Method and equipment 176
14.3.4.2 Preliminary results 177
15 Mercury and bioactive trace metals in the Southern Ocean 181
15.1 Background 181
15.2 Key Research Questions 181
15.3 Sampling strategies 182
15.4 Water 182
15.4.1 Water samples: Stations 182
15.4.2 Water samples: Sampling and sub-sampling 183
15.4.3 Water samples: Sample handling and processing on board 184
15.4.4 Water samples: Limitations 186
15.4.5 Water samples: Stewardship 186
15.5 Ice 186
15.5.1 Ice samples: Stations 186
15.5.2 Ice samples: Ice coring and subsampling 187
15.5.3 Ice samples: Snow 188
15.5.3.1 Ice samples: Frazil ice 188
15.6 Atmosphere 188
15.6.1 Atmospheric gaseous elemental mercury: Sampling and analysis 188
15.6.2 Atmospheric gaseous elemental mercury: Data 189
15.6.3 Atmospheric gaseous elemental mercury: Initial results 189
15.6.4 Atmospheric gaseous elemental mercury: Recommendations 190
16 SAPRI Trainees 191
16.1 Seminar Series 191

16.2Science Participation 192

16.3Images 193

Figure 1 Participants of the SCALE-WIN22 expedition upon arrival in Cape Town on 31st July 2022

1 INTRODUCTION

The SCALE winter 2022 (SCALE-WIN22) cruise was funded by the DSI and NRF in support of the South African scientific community involved in Southern Ocean projects. This included active projects from the South African National Antarctic Program (SANAP) and other projects funded by the NRF. It also involved collaborations with international projects.

HIGHLIGHTS

- Planning and departure under COVID-19 constraints
- 75 science participants from 20 institutions
- 10 NRF funded projects; 3 international projects; 3 projects sponsored by own institutions
- 8 SAPRI trainees: UNISA, WSU, UKZN, RU, UFS, UCT (humanities) and one artist
- Planned stations: 23 (including 5 Process Stations)
- Executed stations: 20 (all 5 PS)
- Departed and returned on time with 85% of the science plan completed (causes of missing parts: shipment issues and weather)

The South African Polar Research Infrastructure (SAPRI) and the Department of Forestry, Fisheries & Environment (DFFE) facilitated the coordination of logistics. The following people were responsible for the organization of voyage:

- Captain: Knowledge Bengu
- Chief scientist (on board): Marcello Vichi (marcello.vichi@uct.ac.za)
- Chief scientist (land): Sarah Fawcett (sarah.fawcett@uct.ac.za)
- SAPRI Logistics: Tahlia Henry (tahliahenry@gmail.com)
- SAPRI Administration: Juliet Hermes (SAPRI manager; jc.hermes@saeon.nrf.ac.za)

The list of participating projects and principal investigators (PI) is given in Table 1.

Table 1 List of scientific teams

NAME	**PI and institution**	**Funding**	**Topic**
NCYCLE	Fawcett and Walker (UCT, CPUT)	NRF SANAP	Nitrogen cycle in Southern Ocean
IMICROBE	Kaartokallio (SYKE)	Finnish Academy of Science	Iron and microbiome in the Southern ocean and Antarctic sea ice
SEAICE	Rampai and Vichi (UCT, CPUT)	NRF SANAP	Mechanical and biogeochemical properties of sea ice
CO2-HEAT	Nicholson (CSIR)	NRF SANAP	Submesoscale dynamics - CO2 and Heat
MICROBIOME	Makhalanyane (UP)	NRF SANAP EU	Microbiome dynamics and co-limitation experiments. AtlantECO Atlantic Ecosystem Assessment, Forecasting and Sustainability https://www.atlanteco.eu/
Fe-PROD	Mtshali and Ryan-Keogh (CSIR, DFFE)	NRF SANAP	Seasonal iron speciation in the Southern Ocean
VESSEL4	Bekker (SUN)	NRF SANAP	Towards a digital twin of the SA Agulhas II
ANTGRAD	Tuhkuri (Aalto University)	Academy of Finland	Sea ice loads on the hull of SA Agulhas II
TOP	Newi Makhado (DFFE)	DFFE	Top predators- distribution and abundance
BUOYS	Verrinder and Vichi (UCT, NMU and Wits)	NRF ESSRP	SHARC – array of autonomous devices for Antarctic sea ice

BGCPUMP	Thomalla and Lain (CSIR)	NRF Marine & Coastal RG	Climate sensitivity of the Southern ocean biological carbon pump
METEO + SAMOC	Tamaryn Morris and Marc de Vos (SAWS) Ansorge and Lamont (UCT, DFFE)	DFFE NRF SANAP	Underway meteorological observations, YOPP, ice edge detection Monitoring of the South Atlantic Meridional Overturning Circulation through XBTs
MERCURY + SEAICE-TM	Susanne Fietz (SUN), Lynwill Martin (SAWS), Lars-Eric Heimbuerger (CNRS-MIO) Roychoudhury (SUN)	NRF PROTEA, UID138132 SUN	Knowledge and technology transfer to investigate marine mercury Trace metals in sea ice
SAPRI	Hermes, Vichi, Morris	SAPRI	Training in polar sciences
VESSEL-WAVES	Butteur Ntamba Ntamba (CPUT)	own	Waves reconstruction from ship movement
GLIDERS	Brearley (BAS), Swart (Gothenburg)	EU	SO-CHIC Southern Ocean – Carbon and Heat Impact on Climate. http://www.sochic-h2020.eu/

1.1 OBJECTIVES

This cruise was included as a final component of the SCALE programme (Southern oCean seAsonaL Experiment, https://scale.org.za), a bottom-up endeavour of the SA scientific community to address the limited multidisciplinary knowledge on the seasonal cycle of the Southern Ocean. The seasonal cycle is an important mode of variability that couples the physical mechanisms of climate forcing to ecosystem response in phytoplankton diversity, primary production, and carbon export. Model simulations of the Southern Hemisphere tend to misestimate the magnitude and miss the timing of the Southern Ocean seasonal cycle both in terms of the seasonality of surface ocean warming and cooling, sea ice advancement/retreat, carbon dioxide exchanges and simulated primary production. Our capability to predict the ongoing shifts and future responses is therefore limited. This drives the need for more physical and biogeochemical data sets that address the problem of knowledge and model biases; firstly, to identify them, and secondly to characterise the associated mechanisms that will allow improved projections.

SCALE is a novel interdisciplinary experiment that spans seasonal to longer-term time scales in the southeast Atlantic sector of the Southern Ocean. SCALE contributes both long-term and experimental observations towards a greater understanding of the role of fine scale dynamics in shaping the phasing and magnitude of the Southern Ocean seasonal cycle through novel integrated ship and robotics experiments.

The main SCALE hypothesis is that detecting and recognizing changes in seasonal variability is more sensitive indicator of long-term trends than changes in the magnitude of annual means based on

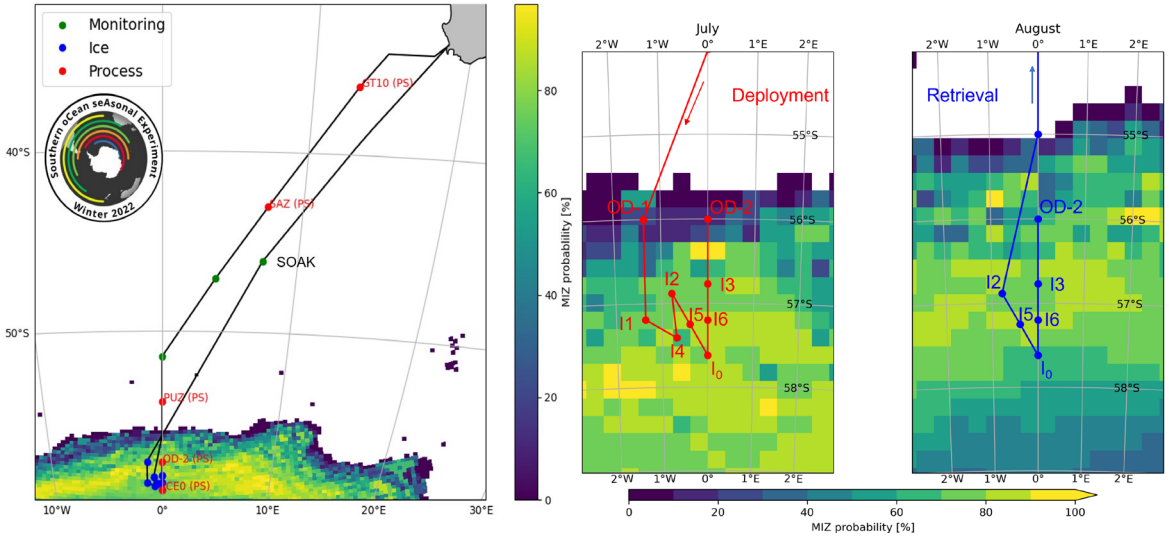

Figure 2 Planned cruise track as reported in the sailing orders, with details of the sampling network for the ice-tethered wave buoys. The shading indicates the probability of exceeding high variability in sea ice concentration, indicative of the typical, variable MIZ conditions (Vichi, 2022).

summer-biased datasets. To verify this hypothesis, a reliable set of observations spanning the various seasons was needed, as well as reliable autonomous devices that would allow to retrieve data throughout the year in combination with the available satellite observations.

The 2019 SCALE expeditions focused on observing the range of seasonal variability through winter, spring, and summer, with a large set of multidisciplinary and interdisciplinary observations that spanned from ocean autonomous devices to marine mammals. The 2022 winter voyage was dedicated to a series of process study stations (PS in Figure 2) located at various key regions in the Southern Ocean and in the marginal ice zone. The PS were designed to be long enough to allow multi-disciplinary sampling, incubation with large amount of water and deployment of multiple instruments.

In combination with the previous round of cruises, SCALE-WIN22 will not only provide an additional set of observations to expand the monitoring effort undertaken by South Africa through the SAPRI, but it will increase our knowledge about some of the underlying mechanisms of physical-biogeochemical interactions in the winter Southern Ocean.

Table 2 List of participants and roles

	Team	Name	Affiliation	Country	Gender	Demography	Role
1	LOGISTICS	Marcello Vichi	UCT	South Africa	M	White	Chief Scientist
2		Riesna R. Audh	UCT	South Africa	F	Indian	Ice operations

3		Jonathan Rogerson	UCT	South Africa	M	White	Ocean operations
4		Ashleigh Womack	UCT	South Africa	F	White	Sea ice observations
5		Heino Els	STS	South Africa	M	White	Glider operations
6	NCYCLE	Mhlangabezi Mdutyana	UCT	South Africa	M	Black	Team Leader
7		Amelia Deary	UCT	South Africa	F	White	MSc
8		Sizwekazi Yapi	UCT	South Africa	F	Black	MSc
9		Christina Monteiro	UCT	South Africa	F	White	Hons
10		Sadiyah Rawat	UCT	South Africa	F	Indian	Hons
11		Lumi Haraguchi	SYKE	Finland	F	White	Postdoc
12		Aldean Esau	CPUT	South Africa	F	Coloured	Hons
13		Venecia van Balla	CPUT	South Africa	F	Coloured	Hons
14		Nkateko Maholobela	CPUT	South Africa	M	Black	Hons
15		Brishan Kalyan	NMU	South Africa	M	Indian	MSc
16		Letizia Tedesco	SYKE	Finland	F	White	Researcher
17	SEAICE	Siobhan Johnson	UCT	South Africa	F	White	Team Leader
18		Felix Paul	UCT/ UDE	German	M	White	Tech/PhD
19		Safiyyah Moos	UCT	South Africa	F	Coloured	PhD

20		Tamuka Keche	UCT	South Africa	M	Black	MSc
21		Hayley Swait	UCT	South Africa	F	White	MSc
22		Magata Mangatane	UCT	South Africa	M	Black	PhD
23		Lisa Kumadiro	UCT	South Africa	F	Black	MSc
24		Dayna Collins	UCT	South Africa	F	White	Hons
25	CO2-HEAT	Siyabulela Hamnca	CSIR	South Africa	M	Black	Team leader
26		Baxolele Mdokwana	DFFE	South Africa	M	Black	Technician
27		Bubele Rasmeni	DFFE	South Africa	M	Black	Technician
28	MICROBIOME	Oliver Mogase	UP	South Africa	M	Black	Team Leader
29		Mayibongwe Buthelezi	UP	South Africa	M	Black	PhD
30		Girish Rameshan	UP	South Africa	M	Indian	Postdoc
31		Nyasha Mafumo	UP	South Africa	F	Black	MSc
32		Benjamin Abraham	UP	South Africa	M	Indian	PhD
33	FE	Thato Mtshali	DFFE	South Africa	M	Black	Team Leader
34		Natasha van Horsten	CSIR/UCT	South Africa	F	Coloured	Postdoc
35		Gareth Kiviets	DFFE	South Africa	M	Coloured	Technician

36		Gemma Portlock	University of Liverpool	U.K.	F	White	PhD
37	BGCPUMP	Lisl Lain	CSIR	South Africa	F	White	Team Leader
38		Annicia Naicker	CSIR	South Africa	F	Indian	PhD
39		Attang Biyela	CSIR	South Africa	F	Black	PhD
40		Lillina Ruiters	CSIR	South Africa	F	Coloured	MSc
41		Sifiso Mpapane	CSIR	South Africa	M	Black	MSc
42	VESSEL4	Nicole Taylor	SUN	South Africa	F	White	Team Leader/PhD
43		Marek Muchow	UAalto	Finland	M	White	PhD
44		Markus Gilges	RWTH Aachen	Germany	M	White	PhD
45		Christof van Zijl	SUN	South Africa	M	White	PhD
46	VESSEL-waves	Paul Senda	CPUT	South Africa	M	Black	Team Leader
47	TOP Predators	Makhudu Masotla	DFFE	South Africa	M	Black	Team Leader
48		Mpumalanga Mnyekemfu	DFFE	South Africa	F	Black	Seabirds At sea Observer
49		Matthew Germishuizen	UP	South Africa	M	White	Mammals At sea observer
50		Estefan Pieterse	UP	South Africa	M	White	Mammals At sea observer
51	BUOYS	Robyn Verrinder	UCT	South Africa	F	White	PI/Team Leader

52		Michael Noyce	UCT	South Africa	M	White	MSc
53		Agoritsa Spirakis	UCT	South Africa	F	White	MSc
54		Lawrence Stanton	UCT	South Africa	M	White	MSc
55		Justin Pead	UCT	South Africa	M	White	Senior Tech Officer
56		Alberto Alberello	UEA	U.K.	M	White	Senior Research Associate
57		Ippolita Tersigni	UniMelb	Australia	F	White	PhD
58		Giulio Passerotti	UniMelb	Australia	M	White	PhD
59		Jacques Welgemoed	NMU	South Africa	M	White	PhD
60		Francesca de Santi	UCT	Italy	F	White	Research fellow
61		Jan-Victor Björkqvist	FMI	Finland	M	White	Researcher
62	METEO	Marc de Vos	SAWS	South Africa	M	White	Team Leader
63		Carla-Louise Ramjukadh	SAWS	South Africa	F	Other	Meteo analyst/tech
64		Mark Fourie	SAWS	South Africa	M	White	Forecaster
65		Berhnard Schmitz	Uni Bremen	Germany	M	White	Ice analyst/tech/PhD
66		Shaakirah Sulaiman	CPUT	South Africa	F	Other	XBT, Argo float and drifter deployments
67		Taygan Roberts	CPUT	South Africa	F	Other	XBT, Argo float and drifter deployments

68	MERCURY	Susanne Fietz	SU	South Africa	F	White	PI
69		Liam Quinlan	SU	South Africa	M	White	MSc
70		Jared Walsh	SU	South Africa	M	White	MSc
71		David Amptmeijer	Mediterranean Institute of Oceanography (MIO), , Helmholtz-Zentrum	FRA	M	White	PhD
72		Sonja Gindorf	Mediterranean Institute of Oceanography (MIO), University of Stockholm	FRA	F	White	PhD
73		Casper Labuschagne	SAWS	South Africa	M	White	MSc
74		Kayla Buchanan	SU	South Africa	F	White	Hons
75		Lide Janse van Vuuren	SU	South Africa	F	White	MSc
76	SAPRI trainees	Udoka Ogugua	UNISA	South Africa	M	Black	Trainee SAPRI
77		Yonela Mahamba	WSU	South Africa	F	Black	Trainee SAPRI
78		Sandra Maluleke	UNISA	South Africa	F	Black	Trainee SAPRI
79		Thamsanqa Wanda	UKZN	South Africa	M	Black	Trainee SAPRI
80		Annah Mthombeni	RU	South Africa	F	Black	Trainee SAPRI

81		Lefa Morake	UFS	South Africa	M	Black	Trainee SAPRI
82		Jennifer Whittingham	UCT	South Africa	F	White	Trainee SAPRI
83		Kurt Martin	Self employed	South Africa	M	White	Artist

1.2 PARTICIPANTS, PLANNED ITINERARY AND NARRATIVE

The planned cruise track as indicated in the sailing orders signed by the DDG of the Department of Fisheries, Forestry & Environment on 1st July 2022 is shown in Figure 2. A few components of the sailing orders related to Team GLIDERS could not be fulfilled due to shipping issues for a density glider, and to the unfortunate loss of one of the gliders deployed during the previous SO-CHIC campaign. Station SOAK, which was originally at the latitude of the expected glider recovery, was then moved further south, at a latitude that ensured 24 hrs of soaking before the first process station.

The 86 participants (Table 2) represented a broad range of expertise, with a majority of early-stage researchers and students. The median age of participants on the ship was 28. The SCALE-WIN22 expedition was planned and departed during a period of mixed COVID-19 protocols. South Africa relaxed the containment measures at the beginning of July 2022, although the maritime industry was still operating on precautional grounds. During a meeting between DFFE, AMSOL, SAPRI, and the cruise chief scientists of SEAmester and SCALE-WIN22, it was decided to relax the hard week-long quarantine and to apply the procedure implemented by AMSOL: everyone boarding the ship must take a PCR test and then quarantine for one day prior to departure. Only those who tested negative have been allowed on board, with minimized contacts with any other external people.

The cruise was scheduled after the return of SEAmester (27th June – 8th July), which had participants from various regions of the country, who were PCR tested right before the departure of the ship. The ship was then assumed to be a green zone, and only people that tested negative were allowed on board. The COVID testing and transport to the ship was organized by Meiheizen International and funded by SAPRI through the UCT contract. Participants were quarantined on Sunday 10th July at the Lagoon Beach Hotel and transported by bus in the morning after for the check-in procedures on the ship. were tested and quarantined; all participants but two tested negatives. The viral charge was however very low, and the participants received a certificate of compliance from the doctors to embark under conditions of isolation on the ship. They were allocated individual cabins and monitored for the next 3 days by the ship doctor, Dr Truiter. It must be reported that the protocols were not strictly maintained by the hotel, since people were supposed to go straight to their room after the PCR test, but they had been kept in a common room for up to 4 hours waiting for their rooms to be ready. This may have risked to invalidate the quarantine procedure, and it was a matter of luck that there was no outbreak during the cruise.

Ship time was maintained at SA standard time (GMT+2). All reported data and table are UTC time. The CS, the Captain and the METEO team met every morning at 8:30 in the bridge to analyse the weather conditions and to plan the daily scientific activities. The CS updated the science plan daily using a custom python software developed during the SCALE 2019 cruises.

The realised ship track is presented in Figure 3. The total distance travelled was about 3900 nm.

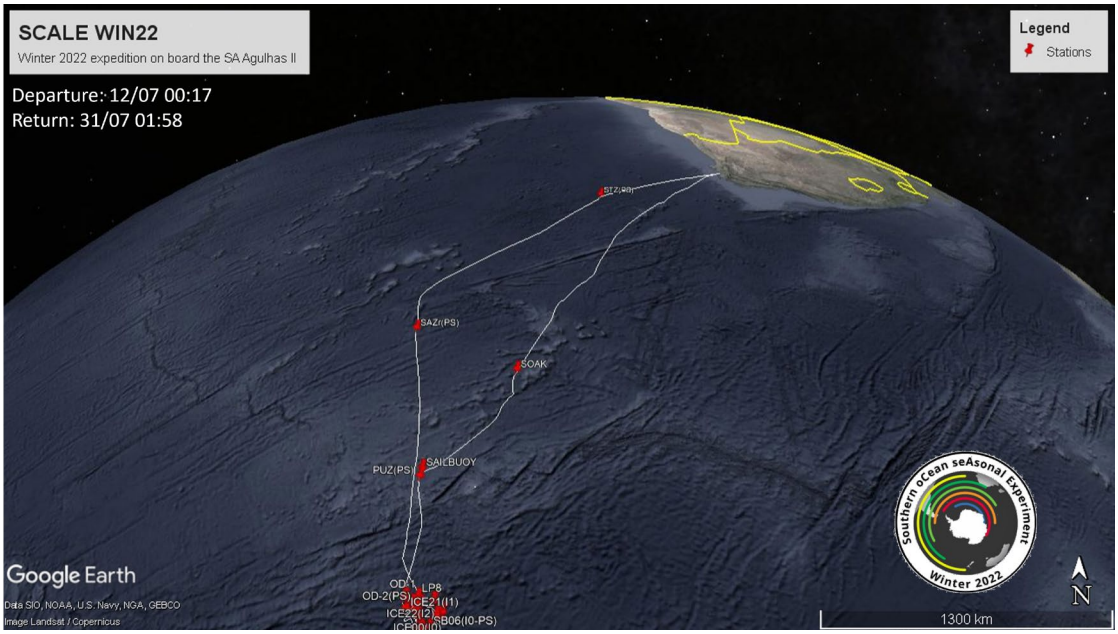

Figure 3 SCALE-WIN22 ship track and stations. Time is South African standard time.

Table 3 General cruise plan and narrative. Refer to the KML file, Table 4 and Figure 4 for activities and weather conditions.

8-Jul-2022	Return of SEAmester. **Ship was treated as a COVID-19 green zone**. People not allowed on board.
10/11-Jul-2022	Quarantine protocol 1. PCR test done by Meiheizen International at the quarantine hotel before checking-in at 2 pm on July 10th. Test results made available at midnight. 2. Participants left the hotel at 11:00 on July 11th for checking-in on the ship. 3. Participants wore K95 masks during loading procedures and immigration **Only participants with negative test results were allowed on board**. Rapid antigen tests have been used during the cruise according to the ship doctor protocol.
11-Jul-2022	The two container laboratories and bigger equipment were loaded before the departure of SEAmester, while smaller equipment and personal belonging were loaded on the departure date. Loading operations were conducted wearing masks and reducing the risks of contact to the bare minimum. Completion of loading operations at 18:00. Ship first moved to the immigration dock for COVID-compliant immigration procedure. One taxi took the crew and passengers to the immigration office from 20:00.
12/15-Jul-2022	Departure: 12th July 2022, 00:17. Beginning of underway sampling. The underway water pump has been irregular for the whole duration of the south leg until sea ice. Initially the water was contaminated but improved over time. Teams had to continuously switch off and on some of the taps to increase the pressure. This procedure has impacted the continuity of the TSG and CO2 systems. Weather at departure was better than forecasted, but waves increased up to 8-10 m on the 13th, when the ship hit the wake of a major storm (see Sec. 2.1). Most of the team's member were sea-sick during this part of the voyage, which affected the underway sampling and the preparation of instruments for the MIZ stations. The doctor treated 52 people with tablets. Sea-ice team performed drills in the cargo hold in preparation to the MIZ stations, while the ice core lab was installed in the ship walk-in freezer. First acquisition of TerraSAR-X (TSX) on the 14th. Sea ice was much further south than expected (58°53'S), in very good correspondence with the forecasted edge location by SAWS. Large floes with extended linear leads indicative of kinematic fracturing but consolidated conditions. Planned MIZ stations moved 1.5° further south and distance between stations also reduced to save on time. XBT sampling and wave buoy deployments proceeded as planned (Sec. 2.2.2.3).
16/18-Jul-2022	Stations 22WIN01-03. First SOAK station was planned on the 15th but cancelled due to issues with one of the bow thrusters. The station was

	done on the 16th after 1107 nm of continuous navigation. ADCP keel was activated on the 17th before the sighting of the SailBuoy, which was safely recovered through crane and net right before a possible sink due to freezing of the sail. PUZ station went on overnight in very good weather conditions. Buoyancy glider was recovered in the morning of the 18th with considerable delay due to the need to wait for daylight. Another TSX acquisition on the 16th revealed large floes close to the sea-ice margin (up to 15 km in length). Between the 16th and 17th July, the sea-ice edge advanced of approximately 25 km, under a strong southerly wind along the wake of a cyclone that transited SE of the ship. High back-scatter streaks are visible in the TSX image. Ice was expected to be further consolidated in a few days due to the cooling associated with winds from Antarctica.
19/20-Jul-2022	MIZ deployment leg: stations 22WIN03-10. The first round of southbound stations was dedicated to the deployment of the ice-tethered buoys, with concurrent sampling of ocean and sea ice properties. The first iceberg was encountered at 16 nm from the ship at 02:40. More persistent open drift conditions were entered at 08:30 and the OD-1 station was initiated. Drop keel ADCP was active during OD-1. A crane problem did not allow to carry out the pancake lifting, which was shifted to ICE21. All buoy deployments were done in sequence, following the outer and inner sectors of the fan shape, although conditions were not fully consolidated due to wave penetration, and coring was only conducted in a reduced set of stations. Given that the time interval had been reduced for time constraints, the GoFlo sampling was only done at a few stations. ICE13 was cancelled due to safety precautions. The southernmost station of the buoy sampling network ICE00 was visited on 20th July at 19:00. Sea ice was in well-consolidated first-year ice conditions at this latitude, with a few elongated kinematic leads as shown in a TSX acquisition from 19:33 that missed the location of the ship for just 3 nm. The ship then inverted the route towards the open-drift process station, to be done during an interval between two cyclones as originally planned in the sailing orders.
21/23-Jul-2022	MIZ retrieval leg: stations 22WIN11-14. PS OD-2 went on for 19 hrs in good sea state with calm wind due to the ship being in an anticyclone. This was a distributed station since the ship had to move for the proper ice or open water conditions. Three SAR images are available for this area. The high-res strip map from TSX at 04:47 (Figure 12) shows the frazil ice drifting northwest along the ship while she is in dynamic positioning for the sampling. The ERA5 reanalysis data (that assimilated the ship data) in Figure 3 show the SE wind at this time. Scattered bands of ice of growing width (3-15 km) are visible to the north of the ship. Cosmo Sky (CSK) was acquired 8 nm from the ship location at 17:36 and another TSX is available at 19:16 on the same day (ship captured in the frame. This was just before the station closing time at 19:27, after the completion of pancake lifting). They document a largely variable region with bands

	modified by the action of wind (rotating clockwise from SE towards WNW) and waves from NW. Given the information on the sea-ice conditions, the team decided to undergo a mapping of the ice cover towards the southernmost process station ICE00 with the EM device (night of the 21-22 July). However, the sea-ice features were very different from deployment, showing clear signs of melting and open drift, apparently not due to the storm action given the presence of the high pressure. All the deployed ice-tethered buoys showed large E/SE drift, and the original shape of the network was disrupted in less than one day. Air temperature was often above freezing, and waves were evident throughout the southward leg. The monitoring had to be interrupted for the lack of level ice, which is visible in the CSK image acquired on the 22nd at 07:02. The new process station was moved south of about 30 nm, at the location of the floe drifting with buoy SB06 (original station ICE00). Process station I0 was distributed in three locations to find the proper conditions (I0A, I0B and at the recovery of SB06). CTD not carroed out at I0B due to wind picking up and difficulty to keep a clear open water area in front of the A-frame. Eventually, sea ice turned out not to be fully safe after a compression test on a core collected in the interstice revealed a ductile structure. Unfortunately, the ship and the CSK image frame were still off of a few nm on 23rd 07:20 right before the starting of the process station. Under the action of a low-pressure system approaching the MIZ (Figure 6), the edge shifted south of 40 km, and the bands were affected by convergence (CSK image acquired at 16:35 farther from the ship location shows a rough margin, difficult to interpret given the angle that invert the backscatter signal between ice and water). This time corresponds to the location of the pancake lifting activity at SB06(I0-PS), which was suspended because of high waves and incident with pulling The retrieval plan continued with the remaining active buoys on the northward leg during the 23rd and 24th July. Operations were extended to allow for the storm to transit north of the ship, while being sheltered by the ice. All buoys were retrieved in conditions very different from deployment (see Chap. 14), with floes reduced to slightly more than 1 m and indications of discoloration possibly due to algal blooms. Sea ice field was very similar to melting spring conditions. There are two more miss of ~5 nm with the CSK acquisitions on the 24th at 07:08 and 16:17, the latter very close to the location where the ship left the open drift conditions with strong wind and waves. Further images from CSK on the next days until the 28th indicated that the sea ice edge remained at approximately 59°S.
24/30-Jul-2022	North Leg: stations from 22WIN15-16. All the monitoring stations had to be cancelled due to the ship struggling to advance under poor conditions (see Sec. 2.1). The CS, in agreement with the team leaders prioritised the process stations, whose locations had to be adjusted to ensure the proper conditions for a long sampling period. A revised sub-Antarctic zone station (SAZr) was carried out on the night between the 26th and 27th July, with the full set of casts, also to resample for some data lost during the south leg.

	XBT sampling and deployment of ARGO and wave buoys along track (Sec. 2.2.2.3). Underway sampling pumps improved with respect to the south leg. The last process station sampled the sub-tropical zone (STZ), and it was conducted under rough sea conditions. All casts were completed safely, although the surface was not sampled, and one bottle had to be removed (see Table 4).
31-Jul-2022	The ship docked at the immigration office of the port of Cape Town a few minutes before 2am local time. Immigration procedures started immediately. The shift to the DFFE dock was completed by 7am and the participants initiated the offloading procedures of personal items and smaller equipment. Ship offload activities continued for the rest of the week until Friday.

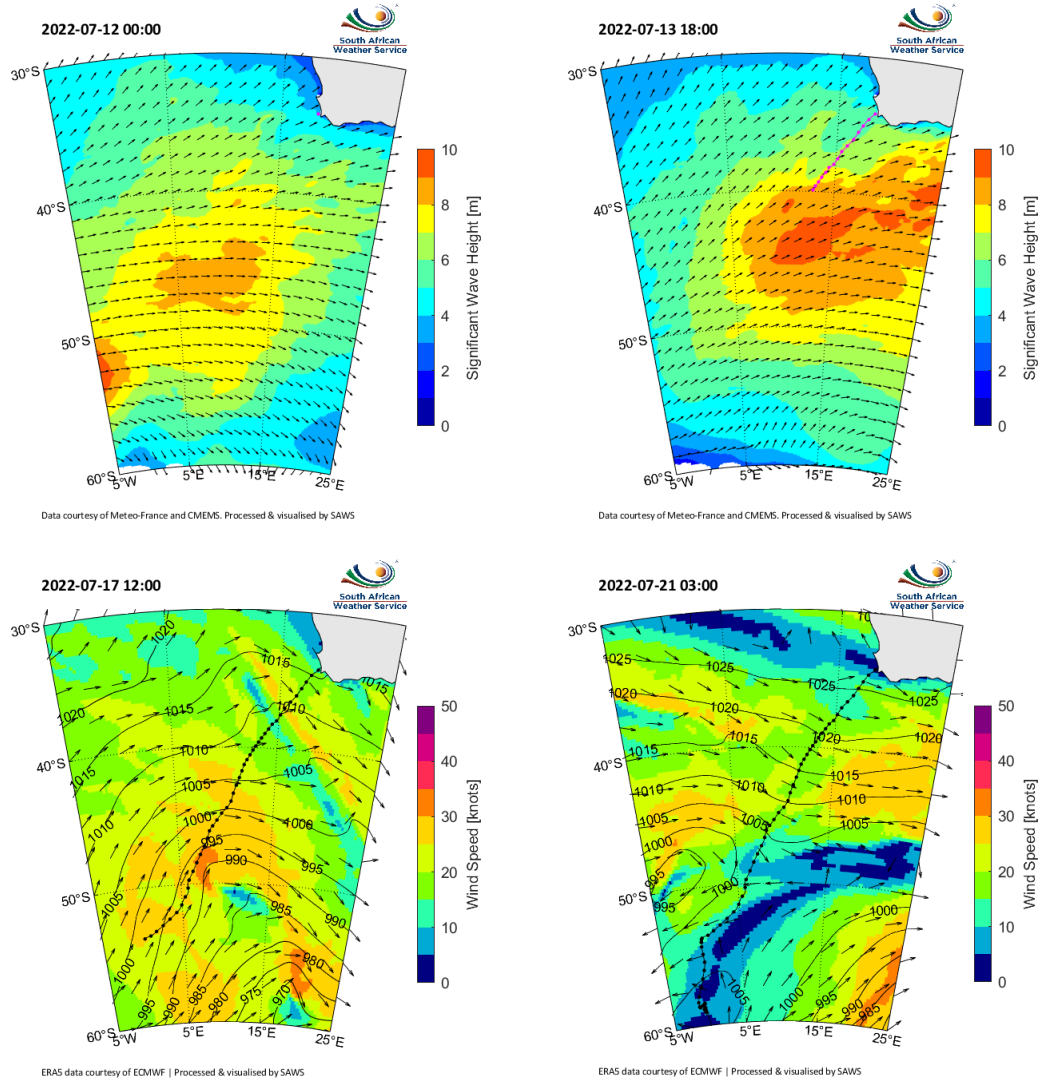

Figure 4 Summary of the met-ocean conditions described in the cruise plan narrative.

1.3 STATIONS AND ACTIVITIES

Table 4 List of stations and activities used throughout the document. The station names in brackets have been used for some of the reports. This table is the only reference for naming conventions

Ship ID	SCALE ID	Station Name	Date (UTC)	Latitude	Longitude	Depth	Activities and notes
AM01308	22WIN01	SOAK	2022/07/16 07:18	-49.7084	5.93338	3571	CTD - GoFlo (1000 m + PAR) Soaking of GoFlo bottles
AM01309	22WIN01.1	SAILBUOY	2022/07/17 14:08	-53.6879	0.1364		Sail Buoy - Retrieval
AM01310	22WIN02	PUZ(PS)	2022/07/17 17:45	-53.999	0.0001	2547	Buoyancy Glider - Retrieval; CTD - Niskin (2000 m, 500 m);

							CTD - GoFlo (2300 m, 130 m); McLane Pump; Marine Snow Catcher; Ship manoeuvres
AM01311	22WIN03	OD-1	2022/07/19 08:32	-58.2949	-1.3424		Frazil Sampler; Wave buoy deployment (LP8); Pancake ice lifting cancelled (5 ton crane not ready)
AM01312	22WIN04	ICE21(I1)	2022/07/19 12:35	-58.6695	-1.2707	4216	Overboard sea ice coring; Sea ice buoy: deployment (SB01); Frazil Sampler; CTD - GoFlo (500 m); Wave buoy deployment (LP4)
AM01313	22WIN05	ICE22(I2)	2022/07/19 17:35	-58.5518	-0.88413	4370	Frazil Sampler; CTD - GoFlo (500 m); Overboard sea ice coring; Sea ice buoy: deployment (SB02); Sea ice buoy: deployment (BB01)
AM01314	22WIN06	ICE23(I3)	2022/07/20 01:52	-58.5839	-0.46742		Sea ice buoy: deployment (SB03); Frazil Sampler; Wave buoy deployment (LP2)
AM01315	22WIN07	ICE13(I6)	2022/07/20 03:56	-58.771	-0.52212		Station cancelled - no activities
AM01316	22WIN08	ICE12(I5)	2022/07/20 08:04	-58.7946	-0.64045		Sea ice buoy: deployment (SB05)
AM01317	22WIN09	ICE11(I4)	2022/07/20 10:40	-58.8556	-0.692	4753	CTD - GoFlo (500 m); CTD - Niskin (500 m); Sea ice buoy: deployment (SB04); Overboard sea ice coring; Notes: issues with CTD oxygen sensor
AM01318	22WIN10	ICE00(I0)	2022/07/20 19:08	-59.0438	-0.50635		Sea ice buoy: deployment (SB06)
AM01319	22WIN11	OD-2(PS)	2022/07/21 01:29	-58.3847	-0.49965	4911	CTD - GoFlo (130 m, 500 m, 4500 m); CTD - Niskin (500 m + PAR and salinity calibration, 2000 m); McLane Pumps; Marine Snow Catcher; Frazil Sampler; Pancake ice lifting; Ship manoeuvres after leaving station and sea ice thickness mapping with EM. Notes: TM container power failure after Deep GoFlo. Bottles stayed on frame in the env hangar longer after retrieval.
AM01320	22WIN12	I0A	2022/07/22 10:56	-59.4047	-0.51032	5188	CTD - Niskin (500 m + PAR); Sea ice conditions not safe for coring
AM01321	22WIN13	I0B	2022/07/22 12:20	-59.4971	-0.41852		Overboard sea ice coring; Ship manoeuvres to next station. Notes: exploratory cores + additional cores on small pancake embedded in larger floe. Also collected consolidated slush in the

							interstitial gap, confirmed to be non-walkable
AM01322	22WIN14	SB06(I0-PS)	2022/07/23 09:47	-59.3973	0.1105	5045	Sea ice buoy retrieval (SB06); CTD - Niskin (500 m); CTD - GoFlo (500 m); McLane Pumps; Marine Snow Catcher; Frazil sampler; Pancake ice lifting. Notes: last 2 activities moved to new position for proper conditions. Incident with pancake hitting on ship side. Structurally compromised pancake but used for bio and chemistry
AM01323	22WIN14.1	SB04	2022/07/24 07:30	-59.1649	0.85777		Sea ice buoy retrieval (SB04); Pancake ice lifting. Notes: additional pancake lifting
	22WIN14.2	LP4	2022/07/24 11:40	-59.0608	0.59938		Wave buoy retrieval (LP4)
	22WIN14.3	SB01	2022/07/24 12:08	-59.1127	0.65782		Sea ice buoy: retrieval (SB01)
	22WIN14.4	SB05	2022/07/24 14:10	-58.9744	1.00705		Sea ice buoy: retrieval (SB05); Wave buoy: redeployment (LP4)
	22WIN14.5	LP8	2022/07/24 17:41	-58.5792	0.46542		Wave buoy retrieval (LP8)
AM01324	22WIN15	SAZr(PS)	2022/07/26 20:31	-46.9997	0.00195	3535	CTD - GoFlo (bottom), CTD - Niskin (500 m, 2000 m, 500 m + PAR); McLane Pumps; Marine Snow Catcher; Ship manoeuvres; Wave buoy redeployment (LP8)
AM01325	22WIN16	STZ(PS)	2022/07/29 11:13	-38.0689	10.9537	5270	CTD - GoFlo (3000 m); CTD - Niskin (500 m + PAR, 2000 m + salinity calibration 50-175-400-1000-2000); McLane Pumps. Notes: very rough seas. Niskin-500: started from 10 m. Niskin-2000: bottle 5 removed, 750 m fired at 995 m.

1.4 CITING THIS REPORT

This report is a collection of cruise reports from the various teams. It contains preliminary results that can be used for referencing purposes in the scientific literature.

Please use the following guidelines when citing this report:

- Expedition, cruise track and overall activities: Vichi M., SCALE-WIN22 Cruise Report, 2023, DOI: 10.5281/zenodo.7901530
- Specific chapters: [Authors], [Chapter title], Chapter [#] in Vichi M., SCALE-WIN22 Cruise Report, 2023, DOI: 10.5281/zenodo.7901530

1.5 ACKNOWLEDGEMENTS

This cruise and the whole SCALE programme would not have been possible without the drive and commitment of the South African polar scientific community. We are grateful to the captain and the fantastic cruise of the SA Agulhas II, without whom none of the science would have been possible. The financial support of the Department of Science and Innovation, the National Research Foundation and the infrastructure support of the Department of Fisheries, Forestry & Environment are greatly acknowledged. The cruise logistics was supported by the South African Polar Research Infrastructure (SAPRI). (Specific acknowledgements to other national and international funding agencies are added to each chapter)

2 METEOROLOGICAL OBSERVATIONS AND OCEAN OBSERVING SYSTEM DEPLOYMENTS

Team name and PI	METEO. Marc de Vos and Tamaryn Morris (SAWS)
Authors	De Vos M., Ramjukadh C-L., Fourie M., Schmitz B., Roberts T., Sulaiman S.

The South African Weather Service (SAWS) conducts activities related to operational marine meteorology as part of SCALE. The project includes operations and research related to the generation, collection, processing and dissemination of marine environmental forecast and observational information, primarily to support safe maritime operations. After being archived, resulting data are also used in support of weather/climate research.

A diverse team was assembled at relatively short notice ahead of the cruise. Marc de Vos, Carla-Louise Ramjukadh and Mark Fourie are employees of the SAWS. Bernhard Schmitz is an employee of Drift and Noise Polar Services and PhD student affiliated to the Alfred Wegener Institute and participated as part of the SAWS team as a scientific exchange. Shaakirah Sulaiman and Taygan Roberts are students of CPUT, studying towards their Diploma: Marine Science, and participated as interns responsible for the deployment of oceanographic instrumentation.

2.1 SUMMARY OF MET-OCEAN CONDITIONS

The predominantly meridional route between Cape Town and the Marginal Ice Zone (MIZ) near the prime meridian results in the vessel's transit being frequently challenged by midlatitude cyclones. These synoptic systems, often associated with strong winds and high seas, propagate from west to east, crossing the intended cruise track. Whilst midlatitude cyclones occur year-round, they are more frequent and intense during winter, posing a significant challenge to navigation and scientific operations. Aside from the magnitudes of winds and waves associated with storms of this nature, their directions are important, with beam seas (relative direction from the side of the vessel) affecting the structure and navigation of the vessel differently to head or following seas (relative direction from ahead of, or behind the vessel). Thus, due consideration of both magnitude and directionality of sea-states is vitally important for science and navigation planning.

During SCALE-WIN22 the sea state was generally poor (averaging Beaufort Scale 6-8) as is typical for research cruises in the Southern Ocean during winter. However, three noteworthy events required particular attention from the science and navigation leadership.

Figure 5.SAWS team for SCALE-WIN22. (L-R): Marc de Vos (Team Leader), Carla-Louise Ramjukadh (meteo analyst/tech), Taygan Roberts (intern), Shaakirah Sulaiman (intern), Bernhard Schmitz (SAR-analyst), Mark Fourie (forecaster).

The first of these occurred prior to departure, resulting in periods of 40-50 knot winds and significant wave heights of 10 m in the vicinity of the intended cruise track. A westerly deviation, aiming to avoid such sea states, was discussed but it was ultimately decided to continue with a direct south-westerly routing. The vessel slowed down at times accordingly, delaying arrival at the MIZ.

The second system which materially affected science and navigation planning occurred around the time of intended departure from the MIZ for the return leg. With 40-50 knot winds and 8-9 m significant wave heights immediately north of the ice edge, the science plan was adjusted such that the vessel remained in the shelter of the ice for longer, allowing the worst of the storm to pass north of the MIZ.

The third system crossed the intended cruise track between latitudes 40 and 50S, with winds of >50 knots and significant wave heights of >10 m at times. In order to avoid the worst impacts from this storm, the science and navigation plan was again adjusted, sailing due north from the MIZ and stopping to sample at 47S, thereby allowing the storm to pass north of the vessel's position.

Figure 1-Figure 3 show snapshot of three aforementioned systems. Figure 4 shows a time-series summary of some basic meteorological variables recorded during the cruise.

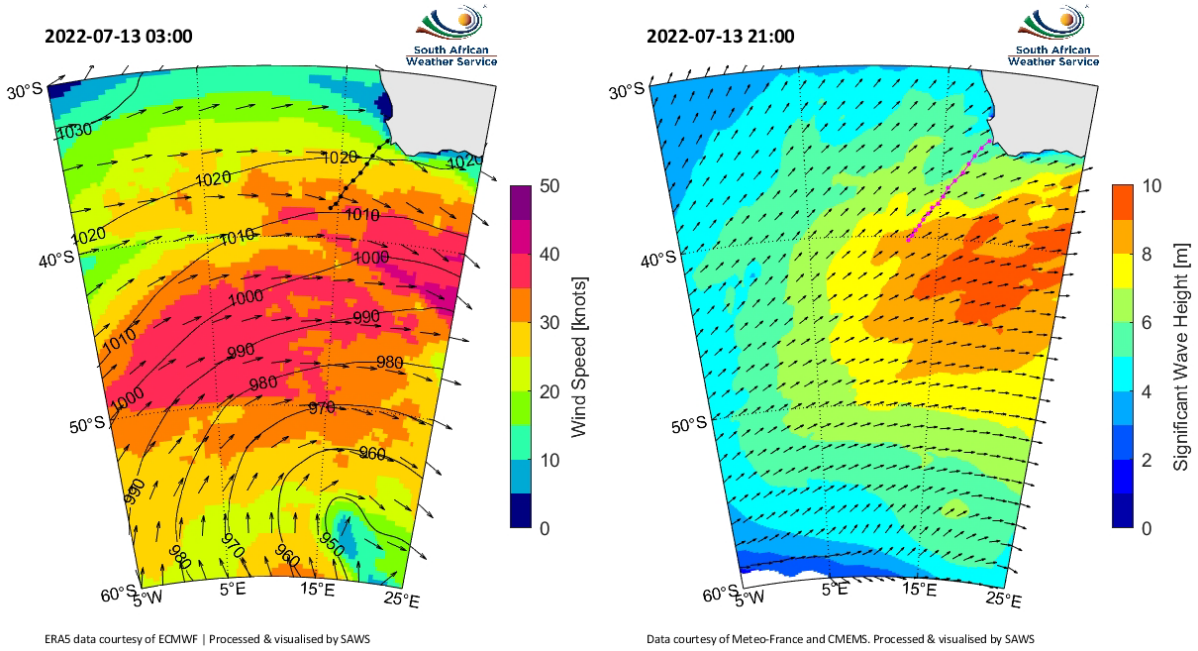

Figure 6. Wind and mean sea level pressure (left) and wave (right) maps showing snapshots, separated by 6 hours, during the occurrence of the midlatitude cyclone which affected the outbound transit. The vessel's track-to-date (line) and 3-hourly positions (dots) are plotted in black and magenta on the wind and wave maps respectively.

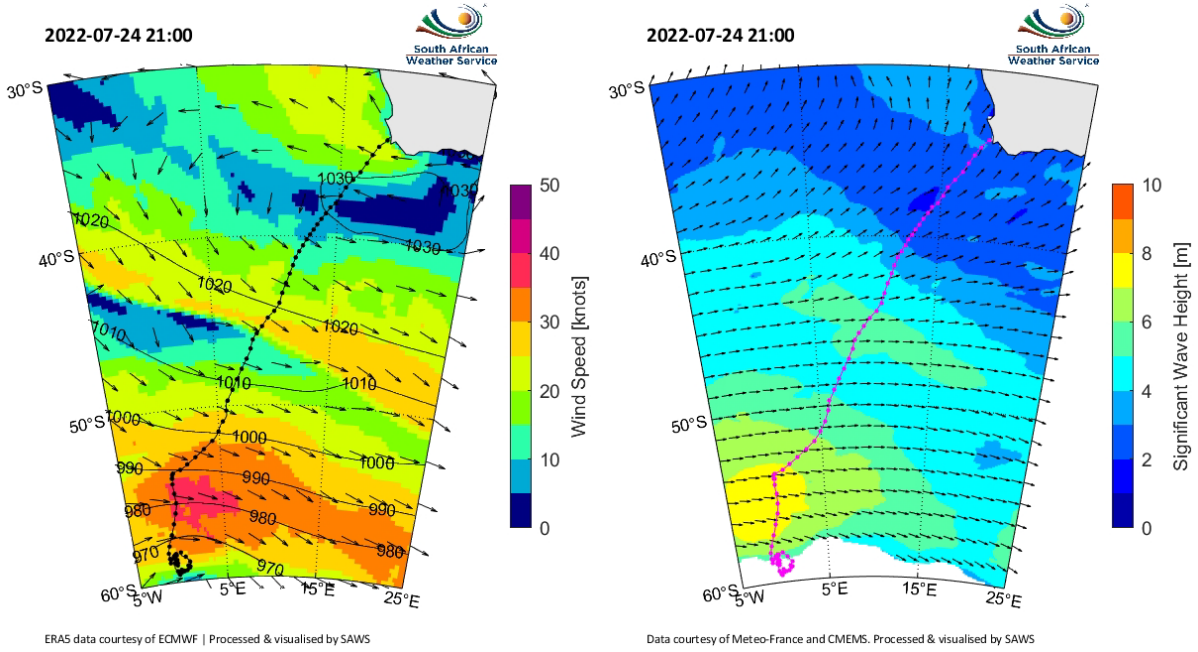

Figure 7. Wind and mean sea level pressure (left) and wave (right) maps showing snapshots during the occurrence of the midlatitude cyclone which affected the timing of departure from the MIZ, ahead of the inbound transit. The vessel's track-to-date (line) and 3-hourly positions (dots) are plotted in black and magenta on the wind and wave maps respectively.

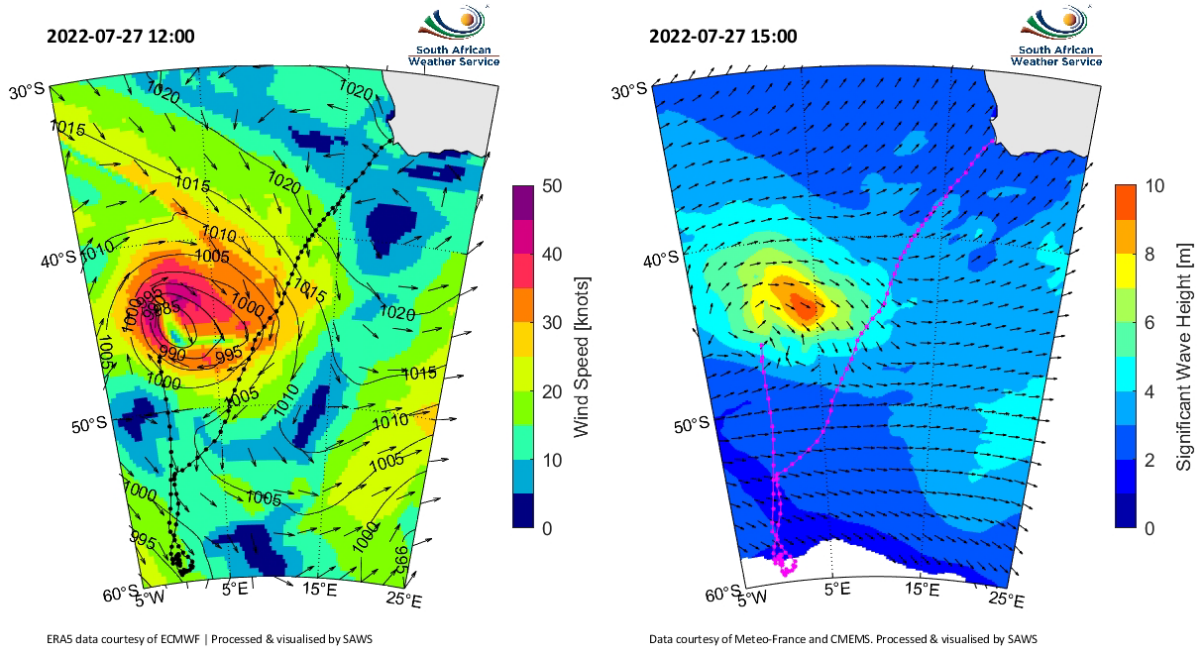

Figure 8. Wind and mean sea level pressure (left) and wave (right) maps showing snapshots, separated by 3 hours, during the occurrence of the midlatitude cyclone which affected the sampling plan during the inbound transit.

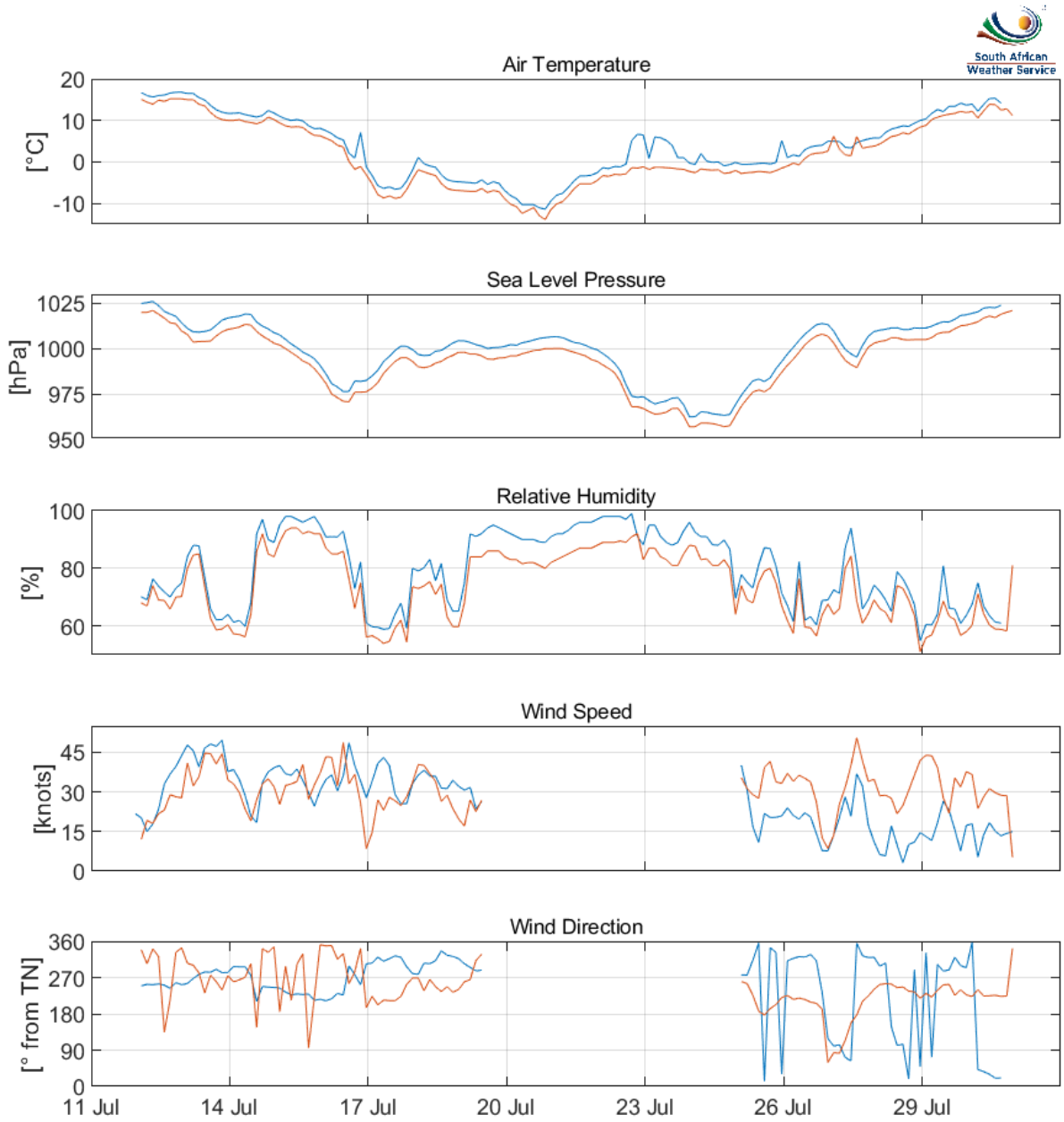

Figure 9. Time series summary of basic meteorological variables recorded by the SAWS (blue) and SDS instrumentation (orange). The data in this figure have not yet been quality controlled and are for display purposes only. However, wind data during the times for which both wind sensors were known to be frozen have been removed.

2.2 WORK PACKAGES

Broadly, the activities conducted on shore and on board by SAWS during the cruise can be classified as belonging to one of three main work packages, each with its own specific intended outcomes:

Operational marine forecasting and analysis	• Provision of relevant and accessible met-ocean forecast information to bridge and science teams to assist navigation 11 and science planning • Training of personnel with respect to marine forecasting and vessel support.
Met-ocean observation	• Production of a set of standard along-track meteorological measurements & observations for the cruise to support decision-making and for supporting use in other research. • Deployment of instrumentation to enhance assimilation of Southern Ocean data into global numerical weather/ocean prediction models (limited w.r.t data denial experiments). • Observations of sea ice related to ground truthing of sea ice edge analysis and forecasting.
Research	• Post-cruise assessment of global NWP performance along cruise track.

2.2.1 WP1. Operational marine forecasting and analysis

A range of global numerical weather and ocean forecasting products were prepared for use onboard. Preparation included the establishment of subset and download protocols to the Cape Town office and scripting for processing and visualisation as required for the expedition. Low bandwidth imagery was then supplied via a custom-built webpage to the vessel to minimize bandwidth requirements. Imagery could also be accessed via direct URL, in order to avoid the requirement of loading an entire page, in the event of severely limited connectivity. SAWS Marine Unit personnel were available in the Cape Town Weather Office to provide support such as the adjustment of operational scripts or download protocols. A summary of the model products, variables acquired, and their producers is given in Table 1.

In addition, the open source XYGrib package, and the Python *Routing Tool* GUI written by SAWS Marine were utilised. This allowed for flexible downloading to the ship of GFS and ICON data, according to variables and areas of interest, and together with the *Routing Tool*, allowed for weather-along-route scenarios to be predicted according to speed/time/distance projections.

This combination of tools proved effective in the research cruise environment, where the science plan must be constantly adapted.

In terms of workflow, the Team Leader would access the latest updated SAWS forecast material via the SAWS SCALE-WIN22 webpage and download the latest GFS and ICON data via XYgrib each

morning. After analysis, a summary would be presented at a briefing with the Chief Scientist and the Captain on the bridge at 09h00 ship time each day. Where possible, this included information about the sea ice, as determined from the Synthetic Aperture Radar data. Thereafter, a text summary would normally be emailed to the Captain and/or Chief Scientist, and if relevant to the science team, it would be disseminated on the science team general Whatsapp group. Further briefings were provided during Team Leader meetings. Any noteworthy developments would also be disseminated to the broader science team on a case-by-case basis.

Throughout the remainder of each day, updated forecast data were downloaded (where necessary; i.e. aside from automatic updating of the webpage) and SAWS personnel monitored forecast models for changes or noteworthy developments, keeping the Chief Scientist updated accordingly. A forecasting Whatsapp group was established for this purpose.

Model	Variables/derived information	Producer	Onboard Use
South African Wave and Storm Surge Forecast System (SWaSS)	Wave parameters, wind speeds and direction, tide and water level.	South African Weather Service Marine Research Unit	Port forecasts prior to departure and arrival at Cape Town. Regional deep sea forecast during transits.
SAWS Free-Drift-Forecast (SAWS-FDF)	Location of sea ice edge	South African Weather Service Marine Research Unit	ETA at MIZ and associated tailoring of science plan.
Global Forecasting System (GFS)	Wave parameters, wind speeds and direction, surface temperature, cloud cover at various levels, rain and snow.	National Oceanic and Atmospheric Administration (NOAA)/National Centers for Environmental Prediction (NCEP)	General forecasting including 2D (map) graphics of a range of variables, and timeseries forecasts for the search area.
Icosahedral Nonhydrostatic Model (ICON)	Wave parameters, wind speeds and direction, surface temperature, rain and snow.	Deutscher Wetterdienst	General forecasting including 2D (map) graphics of a range of variables, and timeseries forecasts for the search area.
Integrated Forecast System (IFS)	Wave parameters, wind speeds and direction, surface temperature,	European Consortium for Medium Range Weather Forecasting (ECMWF)	General forecasting including 2D (map) graphics of a range of variables, and timeseries forecasts for the search area.

Global Ice-Ocean Prediction System (GIOPS)	Sea ice concentration, sea ice drift, sea-ice internal pressure.	Environment and Climate Change Canada (ECCC)	Basic assessment of internal ice pressure to supplement through-ice navigation.

Table 5. The range of forecast products utilised via automated downloading, processing, and visualisation for on board decision support.

Assumptions:

SOG: 16.5 kt avg. from 1030z today (25th) until GT5 (weather should allow).

COG: Generally N'ward (355-005 T)

Overview:

The storm which brought rough seas after departure from the MIZ has passed to the east. Winds veer, becoming light W'ly as we route toward GT5, between a strong cyclone to the north-west and another to the south-west of our track. The left over swell from the MIZ storm have mostly dissipated by 12z on the 16th, hopefully allowing for quick passage to GT5.

Towards the end of the GT5 station, the northerly storm is in the area and we may pick up the SE'ly winds from the SE quadrant (bringing starboard beam-head seas). We may therefore route N, or NW'ly for just a few hours, keeping the sea on out quarter/stern until the storm moves further east, bringing SW winds, and we can turn NW'ward to keep the weather on the stern.

Generally, the routing from GT5 towards GT10 will have to depend entirely on timing as the storm affects the entire general area, and the finally turn to the NE will need to be made as and when conditions allow.

25-07 12h00 UTC 55° 45 S, 000 51 W

Wind: 10 gusting 15 SW

Waves: 4.5 m WNW, swell dominated

Weather: Mostly cloudy, -1 to -2°C

26-07 12h00 UTC 49° 09.8 S, 000 30.3 W

Wind: 20 gusting 25 WSW

Waves: 3-4 m W, swell dominated

Weather: Partly cloudy, -2°C

26-07 20h00 UTC Arrival GT5 47S, 0E

Wind: Light and variable

Waves: 3-4 m WSW, swell dominated

Weather: Partly cloudy becoming overcast, 3°C

During Station: Towards the nd of the 10-12 hour station, the eastern quadrant of the storm arrives in the area. This brings strong NE, E and ultimately SE winds (30 gusting 40 by 09z on the 27th), and rain into the morning of the 27th.

After GT5, the storm propagates directly across the intended track to GT10. We therefore turn NE when it becomes possible to put the seas on the quarter/stern, but this should be possible fairly soon.

Figure 10. An example of a text forecast summary prepared by the Team Leader and disseminated to the Captain and science team.

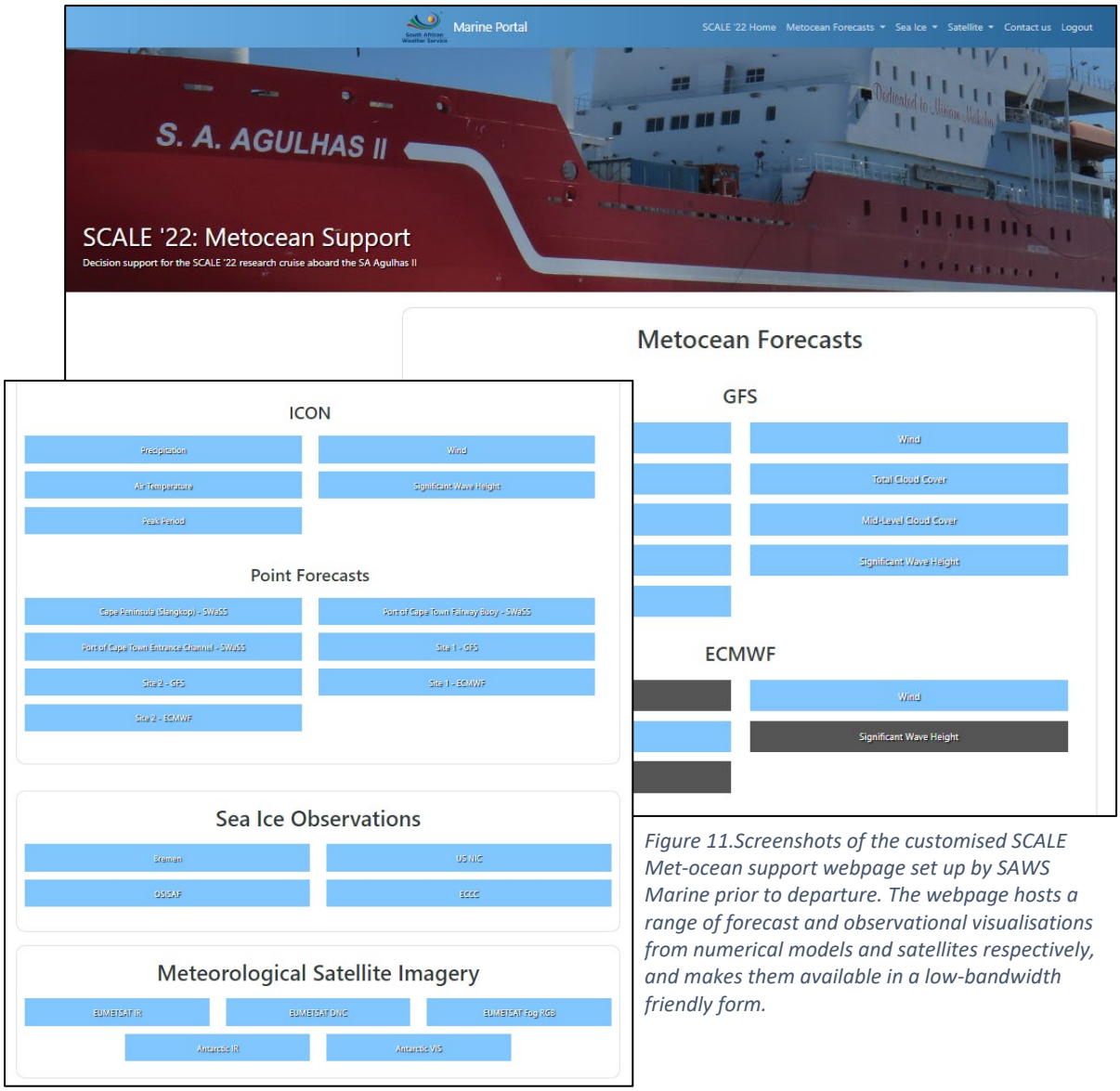

Figure 11.Screenshots of the customised SCALE Met-ocean support webpage set up by SAWS Marine prior to departure. The webpage hosts a range of forecast and observational visualisations from numerical models and satellites respectively, and makes them available in a low-bandwidth friendly form.

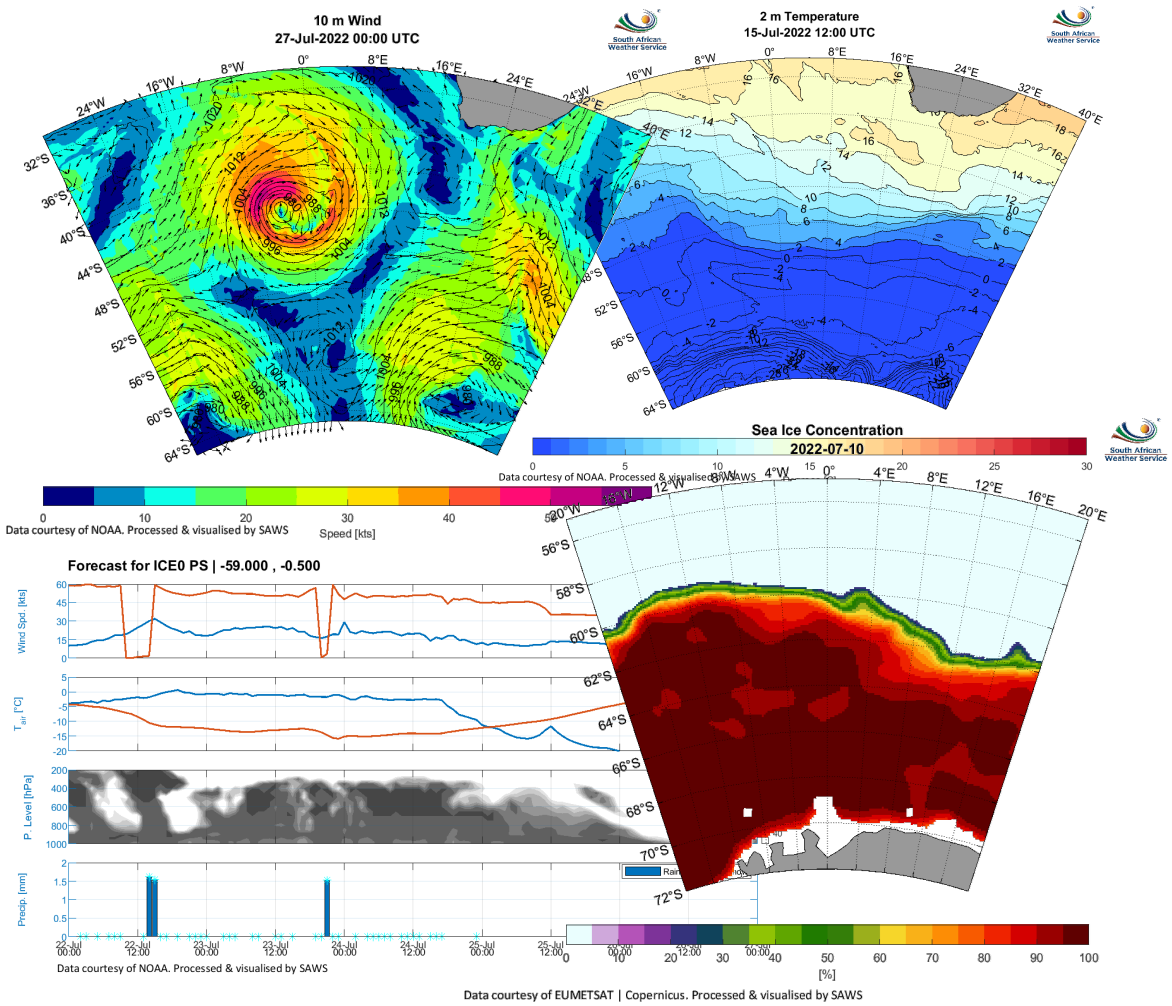

Figure 12.Examples of some of the forecast products available via direct URL or the low-bandwidth SAWS SCALE-WIN22 webpage. Both spatial and time-series (for points of interest) information was available.

2.2.2 WP2. Met-ocean observations

2.2.2.1 Surface synoptic weather observations

Three-hourly surface synoptic observations (SYNOPs) are coded weather messages which are compiled and transmitted from the vessel to the local SAWS office. There, they are quality controlled and transmitted to the World Meteorological Organisation's (WMO) Global Telecommunication System (GTS). Thereafter, they are made available as part of an open-source marine safety information system and accessed in the interest of navigational safety. The messages contain a coded combination of data measured by instrumentation onboard the ship (e.g. temperature, pressure, humidity, wind direction, wind speed) as well as a vast array of visual observations conducted by meteorological personnel (e.g. cloud cover, type and bases, wave conditions, precipitation, visibility etc.). The data they contain are also assimilated into global numerical weather prediction models. This process assists greatly in constraining errors in weather forecasts, and the impact is especially important in otherwise-data sparse regions (such as the one traversed during this cruise). This work also forms part of the VOS programme.

2.2.2.2 Sea ice remote sensing

- Contributed by Bernhard Schmitz. Edited by Marc de Vos.

Synthetic Aperture Radar (SAR) and passive microwave-derived satellite data were used to support navigation in icy waters. This made it possible to react to changed ice conditions and optimize the positions of sampling stations.

By acquiring SAR images via the TerraSar-X satellite, detailed information on sea ice conditions was obtained prior to arrival in the area of interest. As coverage of that area depends on the satellite's orbit, it wasn't always possible to receive two images per day (early morning and evening). For some days, the area of interest wasn't covered at all (with the orbit taking the satellite too far east or west). Tasking was challenged by the continuous adjustment of sampling stations, which is a necessary part of research in the dynamic Antarctic sea ice. The coordinates of the selected areas were transmitted (via email) to the German Aerospace Center (DLR) where the actual tasking was done. Six orders lead to a successful acquisition (2x StripMap, 4x ScanSAR) while some orders got cancelled for technical reasons. For example, on 21st of July it was possible to capture a radar image in the morning (04:47 UTC) and another one in the evening (19:14 UTC) which made it possible to identify how much the ice changed that day (Figure 12).

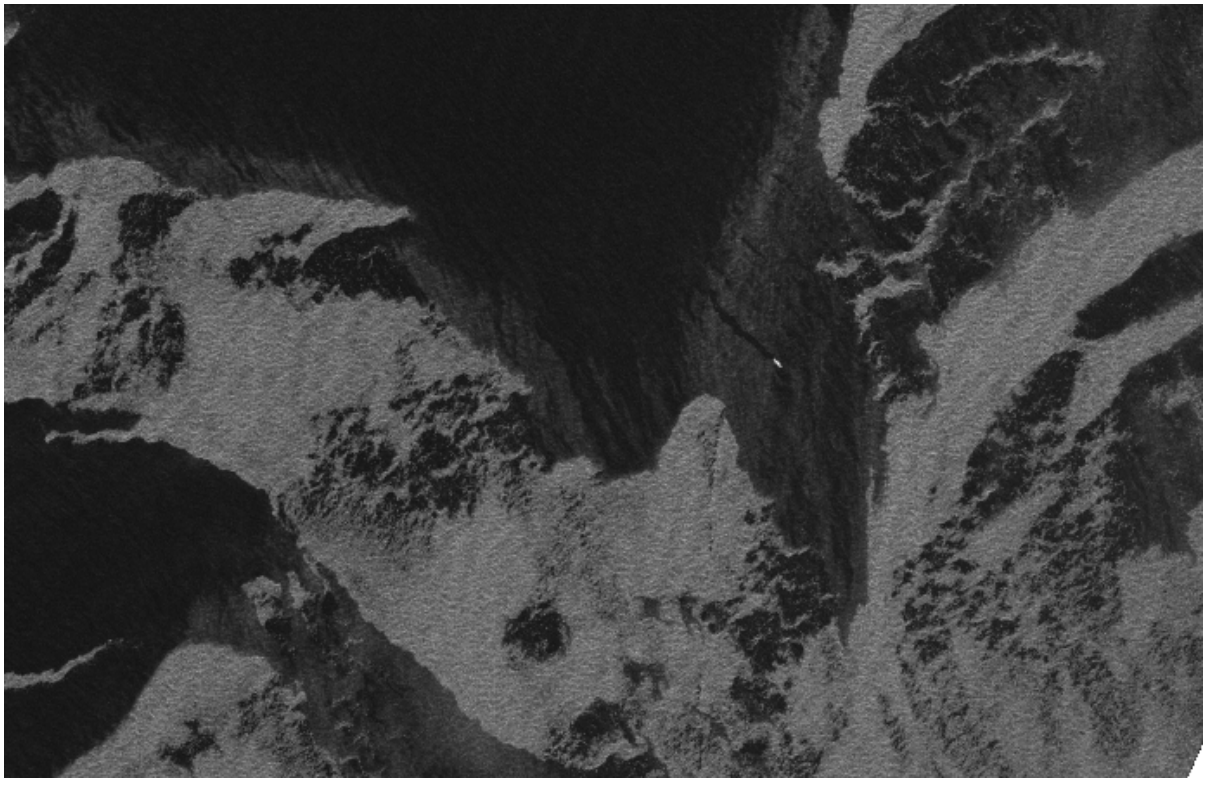

Figure 13. Section of a TerraSAR-X radar image (StripMap) captured on 21st of July 2022, 04:47 UTC. It shows the research vessel S.A. Agulhas II (stationary at that point of time) surrounded by new ice. © DLR 2022.

Between 21st and 30th of July (time of observation) nine radar images from COSMO-SkyMed (CSK) had been provided (see Sec. 3.4). These data fill some data gaps, especially after the 22nd of July,

when it wasn't possible to capture images with TerraSAR-X. These data also enabled monitoring the area of interest after S.A. Angulhas II was on its way back to Cape Town.

Additionally, IcySea was used to download sea ice concentration data derived from the AMSR2 passive-microwave sensor onboard the Japanese Space Agency (JAXA) GCOM-W1 satellite. These data were mainly used as coarser, planning information on the configuration (areas of higher and lower concentration) and location of the MIZ, which assisted in approach planning. They were used less one in the ice for tactical navigation, where SAR is more suitable. During ice observation, the (GNSS) tracking functionality of IcySea has been used to show the expected sea ice concentration for the vessel's current position (on a map, highlighted by a marker). A comparison of the sea ice concentration derived from satellite data and the actual (observed) ice condition was easily possible this way.

QGIS was used to visualize satellite data along with other information like ship position and track or planned sampling stations. It was useful to have a GIS accessible to deal with different file formats and facilitate the organization of rapidly changing geodata (e.g. comparison of ice conditions at a specific location over time). Moreover, it was beneficial to have these classical GIS tools like distance measuring or exporting of maps available.

Finally, a GoPro camera (Hero 9) was set up in a standard position mounted on a railing on the 5th deck, forward of the gangplank, looking down from the starboard side. The camera was set to take photographs every 5 minutes during transit through sea ice. The resulting georeferenced

Figure 14. Example of a photograph taken by the GoPro camera during transit through the sea ice.

photographs will be published for use in research (e.g. satellite ground-truthing or training of automated algorithms)) and are available at: https://doi.pangaea.de/10.1594/PANGAEA.949493

2.2.2.3 Deployment of oceanographic instrumentation

A range of observational met-ocean including Sofar Ocean Spotter buoys (owned by and deployed on behalf of the University of Tasmania), Argo Floats, Surface Velocity Program (SVP) drifting weather buoys and Expendable Bathythermographs (XBTs) was deployed. Data from these platforms is transmitted in real-time to data centres, enabling their use for decision support. They are also archived for weather-ocean-climate research purposes. It should be noted that the XBT system requires a number of hours for installation prior to departure. As with previous voyages on the SA Agulhas II, the system was installed in the Wet Geology lab for SCALE-WIN22. Argo, SVP and XBT data can all be freely accessed via NOAA's Observing System Monitoring Center (OSMC). Table 1 summarises all deployments.

	Latitude	Longitude	Float	Date
Outbound	-39.00	013.70	SPOTTER	13-07-2022
	-41.00	012.04	SPOTTER	14-07-2022
	-42.00	011.55	SPOTTER	14-07-2022
	-44.00	010.61	SPOTTER	14-07-2022
	-46.00	008.45	SPOTTER	15-07-2022
	-50.00	005.80	SPOTTER	16-07-2022
	-56.00	000.04	SPOTTER	18-07-2022
	-56.00	000.04	SPOTTER	18-07-2022
	-56.00	000.04	SPOTTER	18-07-2022
Inbound	-53.49	000.43	ARGO	25-07-2022
	-53.49	000.43	SVP	25-07-2022
	-54.53	000.62	ARGO	25-07-2022
	-54.53	000.62	SVP	25-07-2022
	-50.00	000.21	SPOTTER	26-07-2022
	-46.00	000.16	SPOTTER	27-07-2022
	-44.00	001.62	SPOTTER	28-07-2022
	-43.00	003.77	SVP	28-07-2022

	-42.00	005.72	SPOTTER	28-07-2022
	-41.00	007.56	SPOTTER	28-07-2022
	-39.00	009.86	SPOTTER	29-07-2022

Table 6. Details of instrumentation deployments.

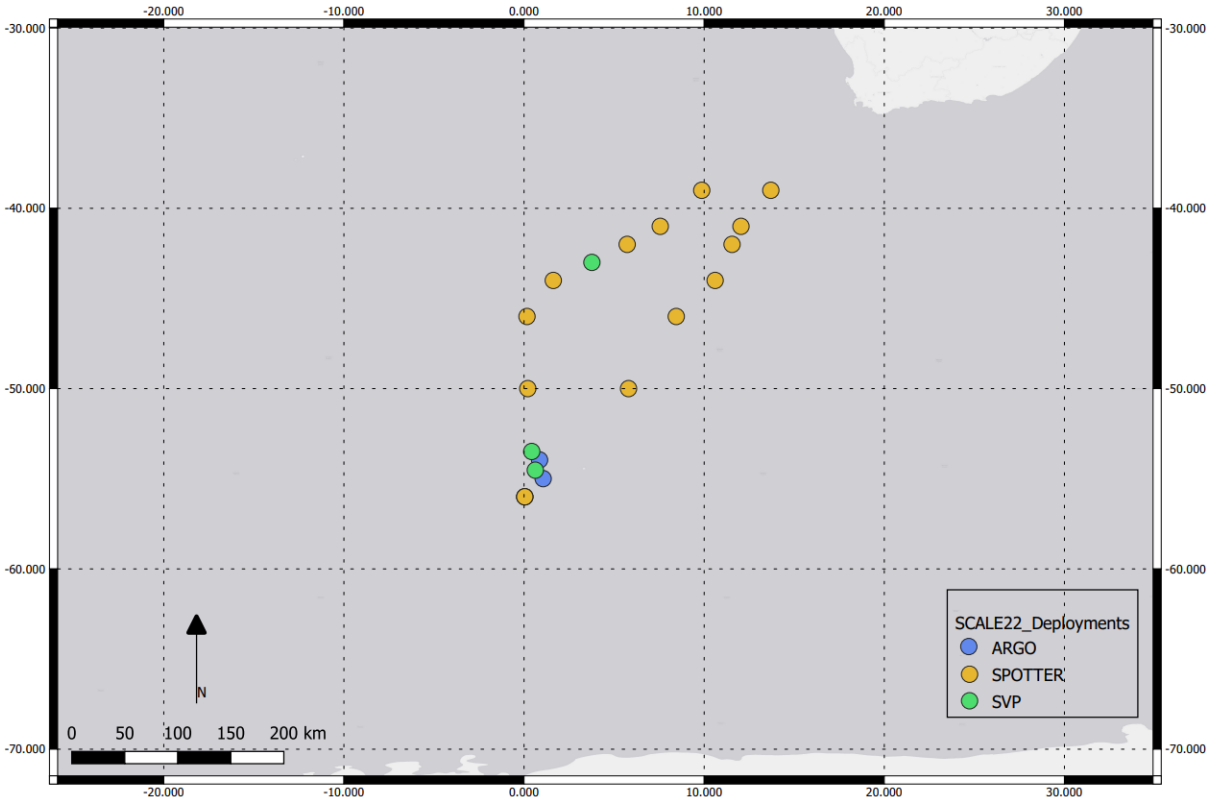

Figure 15. A map of deployment positions for Argo Floats, Spotter Buoys and SVP buoys deployed during the voyage.

2.2.3 WP3. Research

Aside from support to other research groups via data sharing, two main research endeavours are planned by SAWS following data collected during SCALE-WIN22.

The first is an evaluation of the SAWS-FDF sea ice edge forecast and analysis system. Having been operationalised experimentally in 2022, this system should be evaluated against in-situ data collected during SCALE-WIN22.

The second is an evaluation of the global forecast products frequently used by mariners and science teams in the southern ocean sector of METAREA VII. Ideally, a two-pronged approach is to be adopted. First, given the increased deployment effort as a result of the Year of Polar Prediction (YOPP), and plans from global NWP centres to compare free and assimilated simulations, an understanding of the value of instrument deployment and data assimilation in this region should be sought via the relevant research groups. Second, SAWS Marine should conduct a local data denial experiment on a future SCALE cruise, whereby the usual range of observations and instrumentation deployments are not performed whilst at sea. This would allow for global NWP models to be

evaluated without the artificial benefit of SAWS-deployments in the vicinity of the vessel, thereby offering insight into the typical model skill as encountered by non-research vessels.

2.3 CHALLENGES AND RECOMMENDATIONS

2.3.1 Freezing of wind sensors

It was noted that between approximately 19th and 25th July, both the mechanical SDS and ultrasonic SAWS wind sensors located on the mast had frozen completely and were coasted in a thick layer of ice. Consequently, wind data was unreliable, with the SDS sensor (predictably) showing almost-zero wind speeds and the ultrasonic indicating unrealistically high speeds. Due to this problem and the relative inaccessibility of the mast whilst underway, a significant portion of the wind data from the time in the sea ice has been lost. It is recommended that some kind of heating system or other remedial measure be implanted to circumvent this issue on future polar cruises.

Figure 16. SAWS's ultrasonic wind sensor (circled in red) and the SDS mechanical wind sensor (circled in yellow) during the time at which they were frozen.

2.3.2 XBTs

- Contributed by Shaakirah Sualiman and Taygan Roberts. Edited by Marc de Vos

The sampling plan (hourly from the MIZ, every 90 minutes from the ice to Cape Town) was found to be unrealistic for two people (the CPUT interns having been brought onboard for this reason). Especially where both team members are required during rough weather such that one can supervise the other, the resulting disrupted sleep makes maintaining the deployment schedule extremely trying. It is recommended that a team of 3 would be suitable for this. Alternatively, a reduced sampling schedule would be required.

Secondly, numerous profiles appeared unsuccessfully, with unrealistic and spiky data. There are several possible reasons for this but main ones are thought to be unreliable (very old) probes which

have been in storage for many years; rough weather, causing frequent interaction of the copper wire and the ship's hull/superstructure; imperfect installation, with twisted and potentially strained cabling.

2.3.3 SDS Meteorological Sensors

Experience has shown that meteorological sensors frequently malfunction or record spurious values when installed in the harsh environment of the ship. As a result, it is very useful to have two independent sets of meteorological instruments which can be compared, and supplement each other where data gaps arise as a result of technical sensor issues. Unfortunately the SAWS and SDS meteorological sensors show a material level of disagreement. Apart from the wind sensors, errors appear from inspection to be fairly constant and likely an issue of bias due to sensor drift. Wind sensors show frequent, non-linear disagreement. SAWS calibrates its sensors as often as the ship's schedule allows, but it is still possible that these instruments might produce errors. It is unknown when the SDS sensors were last calibrated, but it is strongly recommended that both sets of sensors received (or continue to receive) adequate maintenance and calibration to ensure data quality and continuity during research cruises.

3 LOGISTICS: OCEAN AND ICE OBSERVATIONS, AND AUTONOMOUS DEVICE OPERATIONS

Team name and PIs	LOGISTICS.
Authors	Rogerson J., Hels H., Audh R., Womack A., De Carolis G., de Jager W., Melsheimer C.

3.1 OCEAN OPERATIONS

The LOGISTICS team and collaborators operated the following components during the cruise:

- Conductivity, Temperature and Depth (CTD) operations and maintenance of instrument on board.
- Salinity validation samples for CTD sensors – (Salinometer)·
- Winch operations (CTD, McClane Pumps and Marine Snow Catcher)
- CTD Data processing
- Scientific Data System (SDS)

Activities in the operation room during CTD deployment have been assisted by several volunteers, who gained experience on the various operations. Given the lack of dedicated technicians on board, their role was crucial in the success of the expedition.

3.1.1 CTD

The Geotrace CTD underwater unit and trace metal-free rosette frame with GoFlo bottles were assembled by Sea Technology Services (STS) using a CTD kindly provided by the University of Stellenbosch through SAPRI. Niskin bottles (from CSIR “Miss Daisy” CTD) were used for Niskin CTD casts. The GoFlo bottles used for the Geotrace CTD casts were interchanged with the Niskin bottles therefore using a single underwater unit for all CTD operations and all operated off the Kevlar cable on board the SA Agulhas II.

On inspection, no initial problems were encountered with the CTD and on the 15 July 2022 deck tests as well as a tension test to 1.6 tonnes were conducted. The first deployment at the SOAK station was successful, with all electronic sensors but the fluorometer working as intended (Fig. 1)

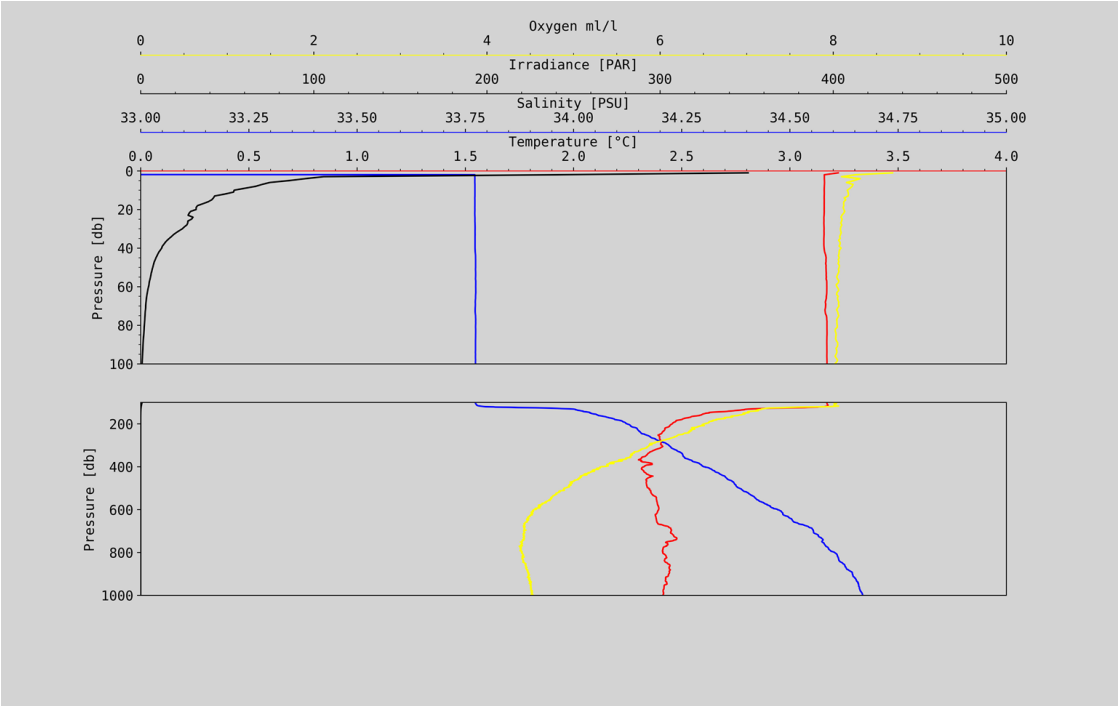

Fig 1: CTD cast at SOAK station showing the performance of the electronic sensors

Interrogating the results of the fluorometer from SOAK, the dark blank value was increased by a factor of 10 for all subsequent casts but this did little in rectifying the anomalous results. In salvaging data, the voltage outputs of the fluorometer were saved for all casts after SOAK, with the intention that fluorescence data could be obtained after the cruise once the instrument has been re-calibrated. An example output is shown in Fig. 2 from the third cast at the PUZ station. Intuitively, the values of fluorescence should not be negative and the inconsistent and erratic oscillating voltage made it difficult, if not impossible to discern any credible signal which could be used to infer the depth of the sub-surface chlorophyll maximum.

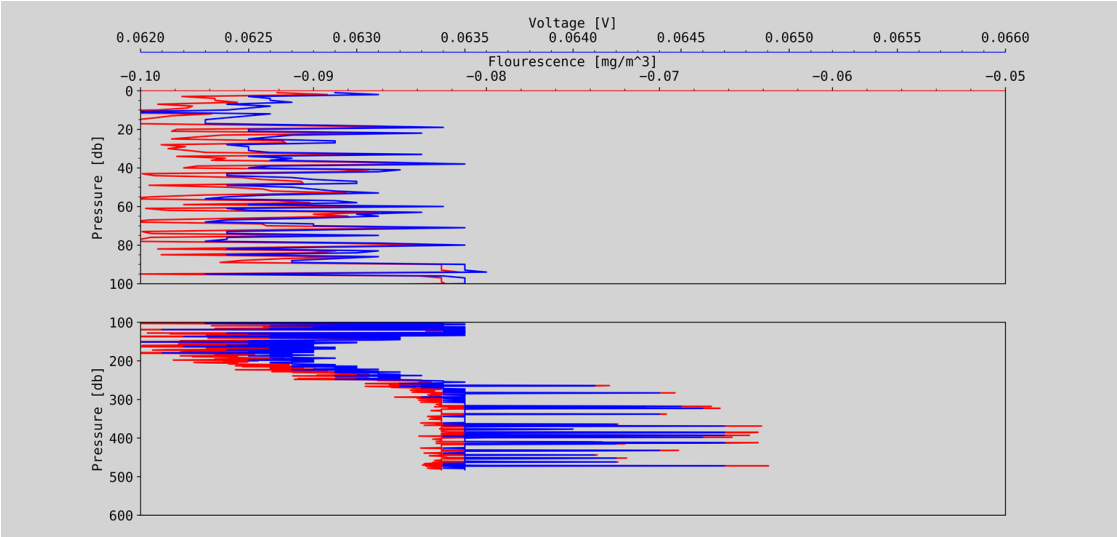

Fig 2: Output of flourescence vs voltage on the third cast of the PUZ station

When conducting the deep CTD casts, the altimeter did not work properly and this limited operational capability in collecting bottom water samples. Though the instrument did respond on the deep cast at the SAZR, it was too unreliable to risk the loss of the CTD. No effort was made to rectify the problem by altering the configuration file. Noteworthy, at the final CTD station, STZ, Niskin bottle 5 sustained damaged being loaded onto the rosette and consequently needs maintenance.

In maintaining the CTD during the cruise, the sensors caps were promptly put on when back on deck after successful deployment and the frame was washed with clean water to prevent salt build-up. The conductivity sensor was cleaned by flushing it with triton-X 0.1% regularly and the PAR sensor was only deployed on casts shallower than 1000 m.

3.1.2 Kevlar cable

The Kevlar cable was used for all CTD operations. During deployment, the cable and compensator were operated according to the standard ship protocols which ensured that all operations were safe for both personnel and equipment. Important to note that CTD operating times were subject to change due to environmental constraints (No CTD operations beyond 30 knot winds with the combination of 4 m-5 m swell as well as the proximity of sea-ice) and limitations of the Kevlar cable. The cable is considerably lighter (18 kg/km in seawater) than the conventional steel cable and the Geotrace CTD frame is fairly light and weighs very little in water. The average speed for the CTD casts were 0.3 m/s – 0.4 m/s on the downcast in rough weather and 0.5 m/s – 0.6 m/s in calmer seas (in ice). The upcast speed ranged between 0.5 m/s – 1.1 m/s dependent on weather conditions influencing the overall tonnage on the cable. The Kevlar cable performed according to its manufacturing specifications and sustained no damage for the duration of this cruise although the crew were cautious on the deep deployments as the cable did not spool properly back onto the drum due to a previous incident.

3.1.3 Processing and calibration of CTD data

All CTD data was processed using SBE Data processing software following the standard filters which were edited to fit the specifications of the configuration file supplied for the GeoTrace CTD. The following data have been used for calibration

- Oxygen: Samples were collected by G. Kiviets and T. Mtshali at 5 stations and measured by titration on board
- Salinity. Samples were taken from 3 depths at the PUZ, SAZr and STZ for calibration purposes
- Chlorophyll: chlorophyll data have been measured as described in Sec. 9.3.

3.1.4 Stations

In total, 10 CTD stations were done. For consistency in the nomenclature the grid numbers were finalised at the end of the cruise which may at times conflict with the file names for the stations. Breaking down the naming convention of the Grid number:

1. 22WIN - the first two numbers indicate the year of the cruise, 2022 and then WIN represents Winter
2. ## - the two proceeding numbers indicate the station number, ie, 03 would be the third station conducted by the ship
3. -SOAK – at the end of the file is the name of the station
4. (PS) or (I#) - the brackets show whether the station was a process station (PS) or an ice station (I#)

3.1.5 Scientific Data system (SDS)

The SDS was switched on at 12:23 on the 12 July 2022 and no issues were reported.

Data were collected on a CSV file at 1 min to 1 hr averages and distributed to the partners

3.2 TECHNICAL INFORMATION FROM THE SEA-GOING TECHNICIAN

The following notes report the activities done by the STS technician, Heino Els.

Day 1 - 2022/07/11 - Monday

15h00	Sorted through all boxes.

Day 2 - 2022-07-12 - Tuesday

00h23	Started the voyage on the SDS server.
02h51	Turned on the valve for the TSG for water flow.
03h07	Turned on the TSG to start log data.
12h20	Turned on the ADCP to start logging data.
12h30	Started with the CTD installed the y cable on the CTD.
13h01	Reconnected the vpn for remote access.
14h00	Changed the instrument config file to Geotrace 2022_par5.

14h05	Had to change the steel cable connection to the Kevlar cable connection on the deck unit.
14h20	Ran a few CTD deck tests.

Day 3 - 2022-07-13 - Wednesday

08h00	Did more deck tests.
15h23	Did some cable management on the CTD cables.
18h00	Checked on the SDS server and heat flux data to see if it is still running.

Day 4 - 2022-07-14 - Thursday

12h38	Made a new log file for the Heat Flux data.
14h54	reconnected the VPN for remote access.

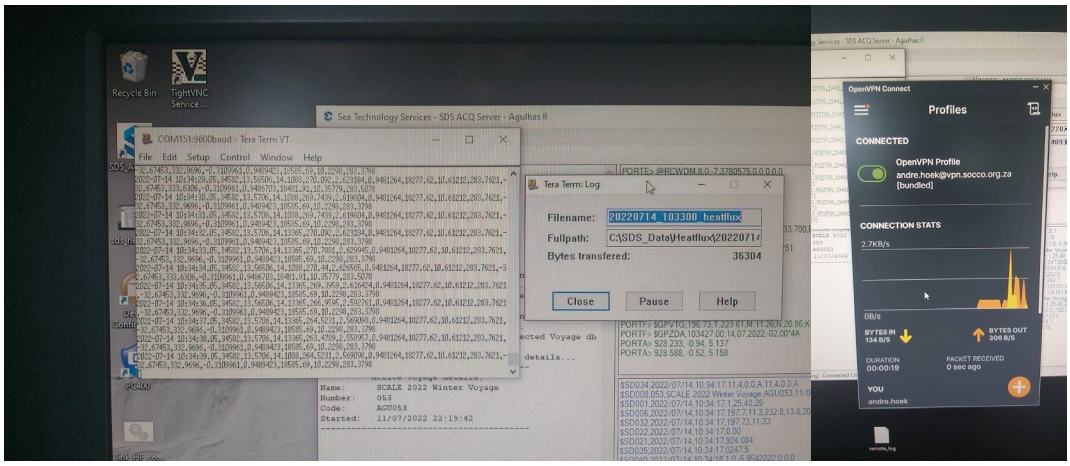

Day 05 - 2022-07-15 - Friday

08h20	Checked on the SDS server and the Heat Flux data.
09h53	Moved the PAR sensor to the outside of the CTD frame (In the way of go-flow bottles).
11h38	reconnected the VPN for remote access.
13h14	Did a tension test on the dead-end went past 1.6 tons.

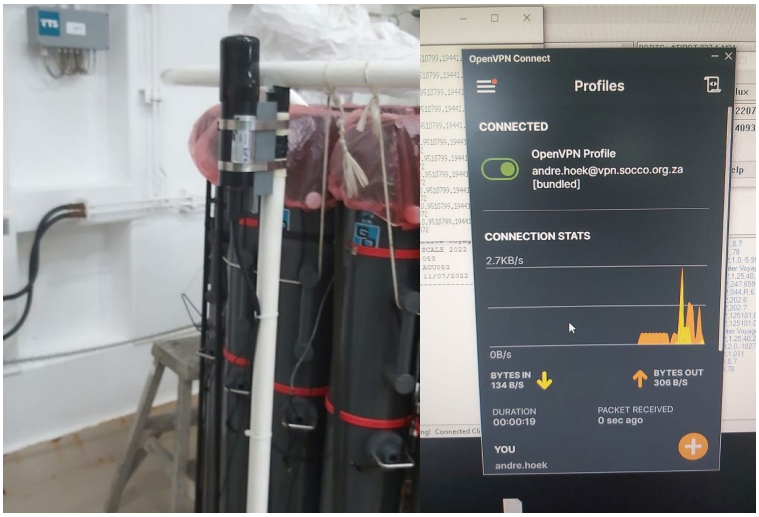

Day 06 - 2022-07-16 - Saturday

09h16	Started with the CTD deployment .
12h39	Cleaned the conductivity sensor with Triton - X 0.1%.
15h00	Checked on the SDS and Heat Flux sensor data.
16h21	Made a new log file for the Heatflux sensor.
22h04	Got the Sailbouy cradle out of the box and ready for tomorrow's recovery.

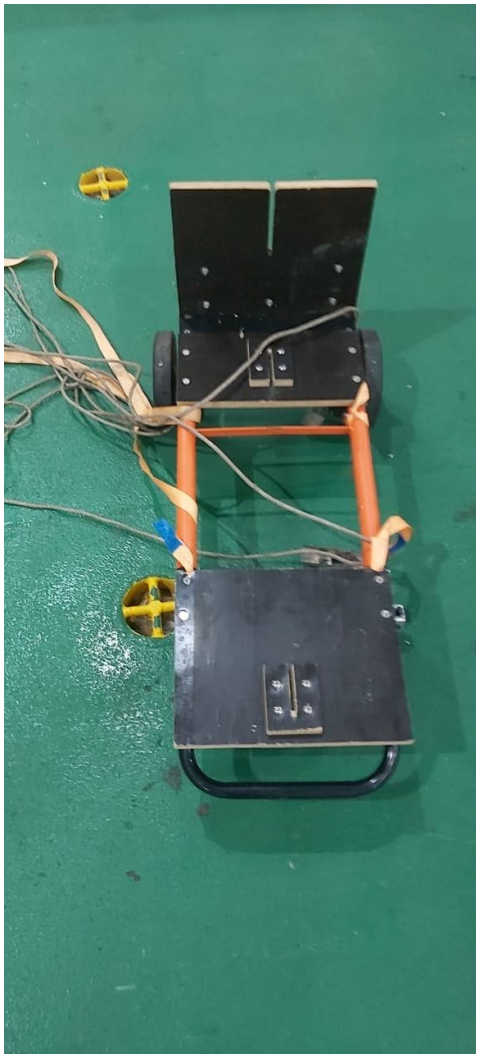

Day 07 - 2022-07-17 - Sunday

08h40	Checked on the SDS server and heat flux sensor data.
13h51	put the net together for Sailbuoy recovery
16h34	recovered the sailbouy .
18h08	rinsed the sailbouy and turned it off.
18h11	restarted the VPN for remote access.

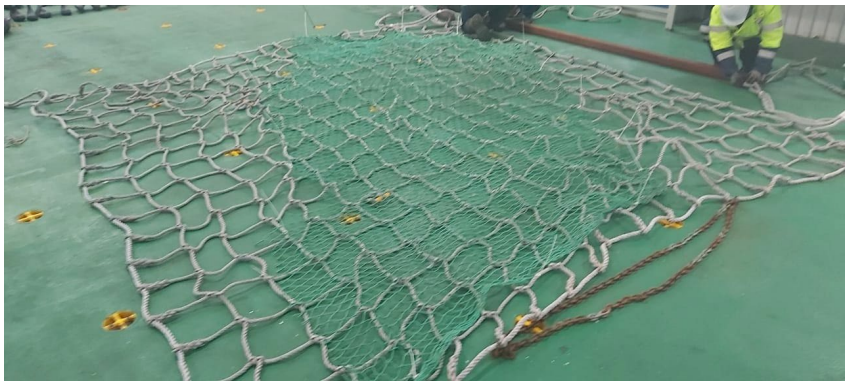

Day 08 - 2022-07-18 - Monday

11h49	Recovered the seaglider.
12h54	Rinsed off the seaglider.
13h00	started working on the Seaglider.
15h54	Started a new log file for the Heat Flux data.
18h07	Flushed the conductivity cells.
18h08	put on the sensor caps on CTD.

18h27	finally got to the menu of the seaglider after struggling to restart the Seaglider used in air can on the connector.
21h23	put lube on the Connector of the Seaglider.
21h37	Stopping working on the Seaglider couldn't turn it off.

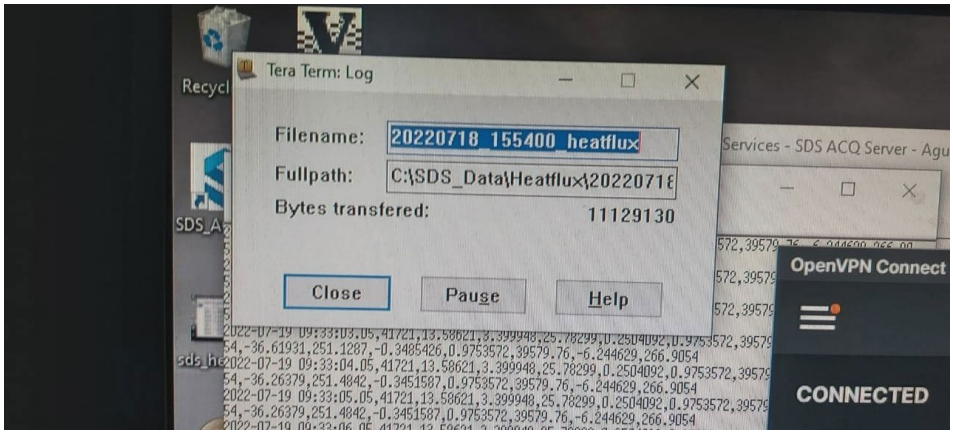

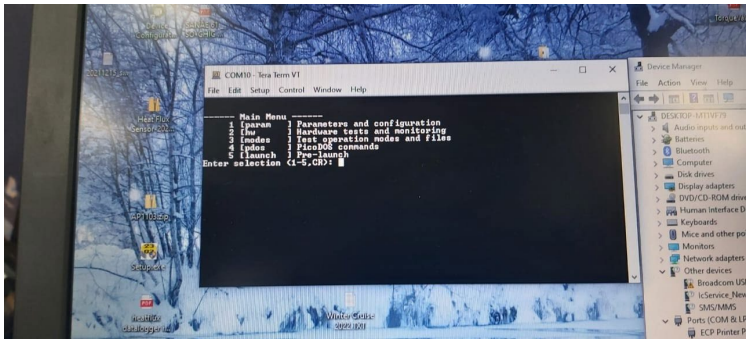

Day 09 - 2022-07-19 - Tuesday

09h40	Started working on the Seaglider.
10h21	put on the sensor cap on the Seaglider.
14h45	Took off the Niskin bottles.
15h05	put on the sensor caps on CTD.
17h31	Started CTD deployment.
18h10	Finished CTD station.

Day 10 - 2022-07-20 - Wednesday

02h20	Flushed the conductivity sensor with triton x and rinsed off the CTD.
14h50	Starting CTD deployment.

15h31	Finished CTD deployment.
19h04	rinsed off the CTD frame and flushed the conductivity sensors.
19h07	Made a new log file for the heat flux sensor.

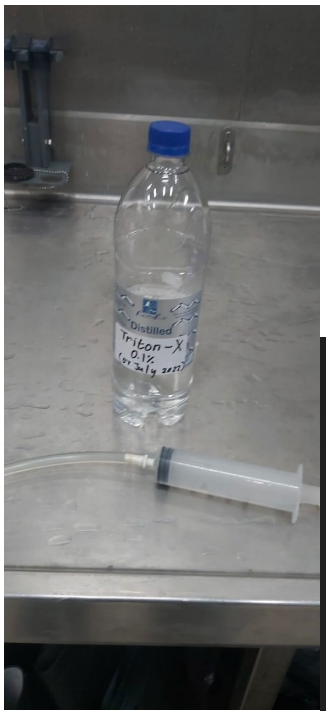

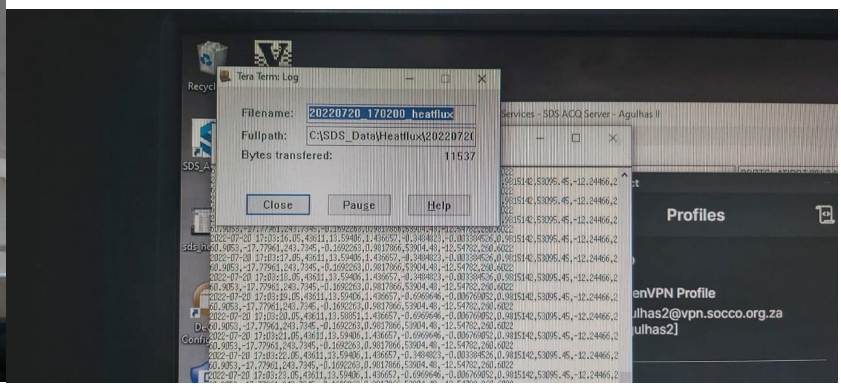

Day 11 - 2022-07-21 - Thursday

02h40	Started CTD deployment .
03h20	Finished the CTD deployment.
04h30	Started a CTD deployment.
06h50	finished the CTD deployment.
06h55	installed the par sensor onto the CTD frame.
16h41	removed the par sensor from the CTD frame.

Day 12 - 2022-07-22 - Friday

10h09	Made a new log file for the heat flux data.
14h00	Checked on the SDS server and heat flux data still logging data.

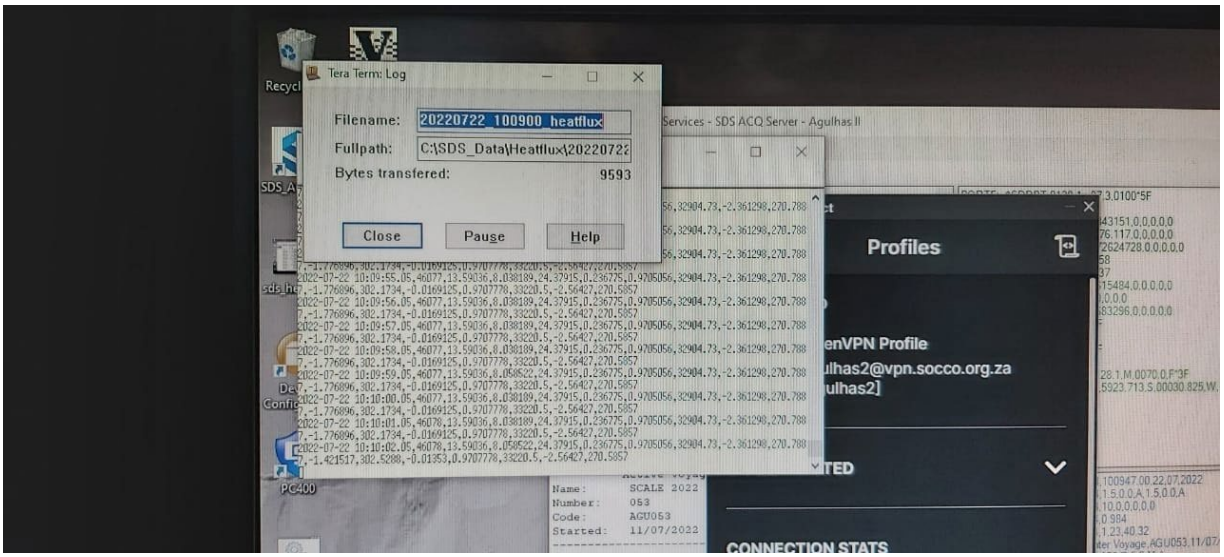

Day 14 - 2022-07-24 - Sunday

10h31	Made a new log file for the Heat flux data.
10h41	Flushed the conductivity sensor with triton x.

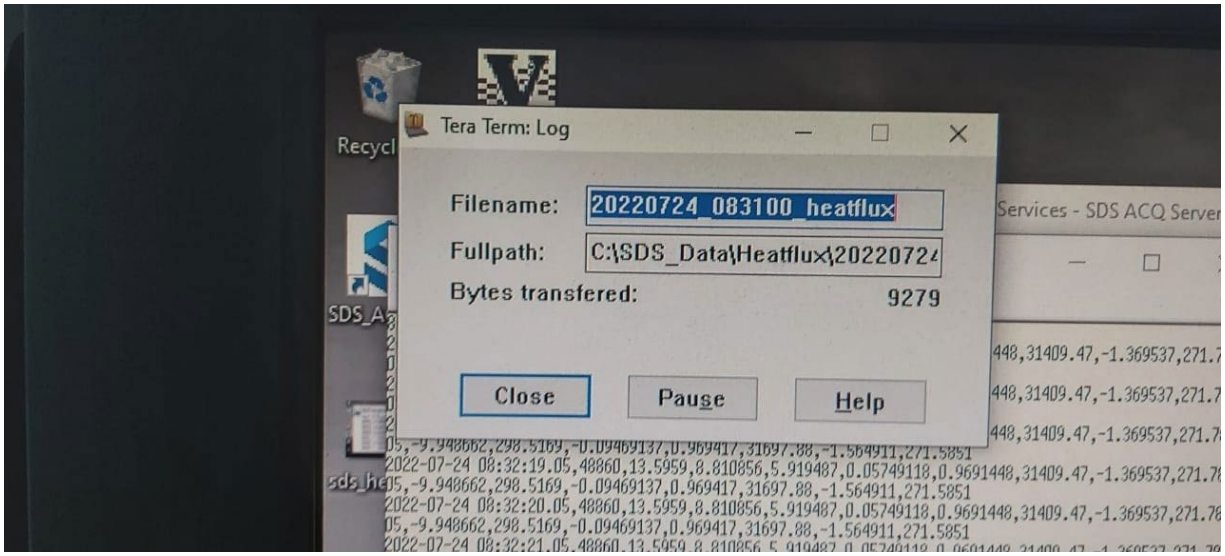

Day 15 - 2022-07-25 - Monday

13h40	Checked on the SDS server and heat flux data still logging data.

Day 16 - 2022-07-26 - Tuesday

20h11	Made a new log file for the heat flux data
22h57	CTD deployment

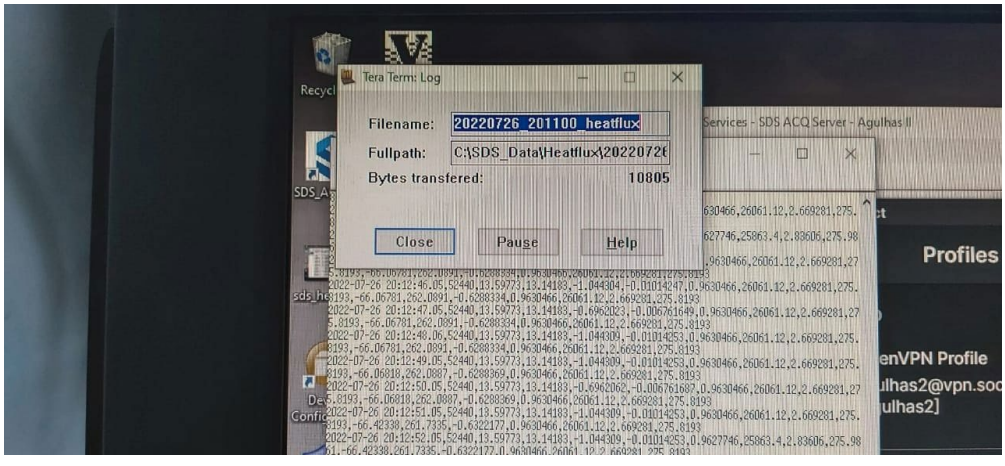

Day 17 - 2022-07-27 - Wednesday

13h45	Checked on the sds server and heat flux data

Day 18 - 2022-07-28 - Thursday

13h30	Put the sailbouy back in its crate.
17h49	Made a new log file for the Heat flux data.
19h59	Flushed the CTD conductivity sensor with triton x

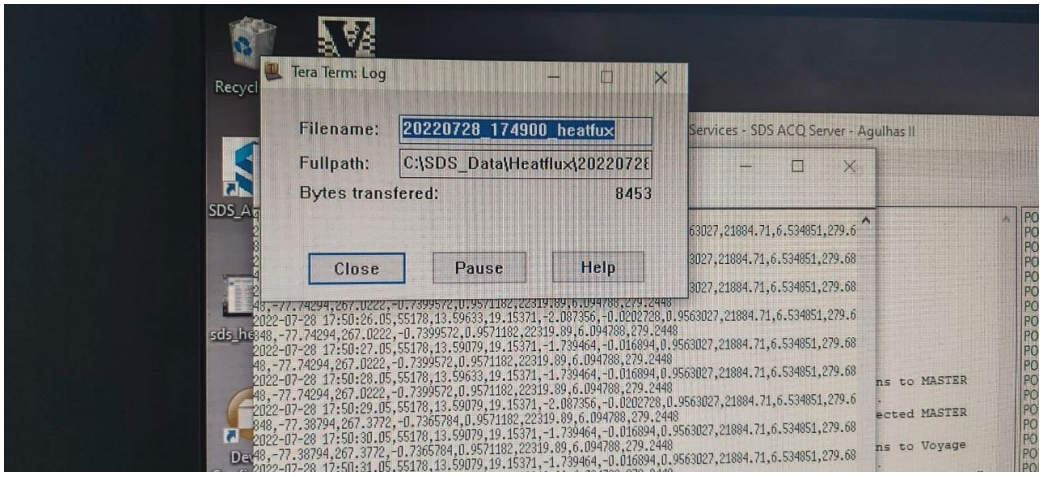

Day 20 - 2022-07-30 - Saturday

20h59	Made a new log file for the Heat flux data

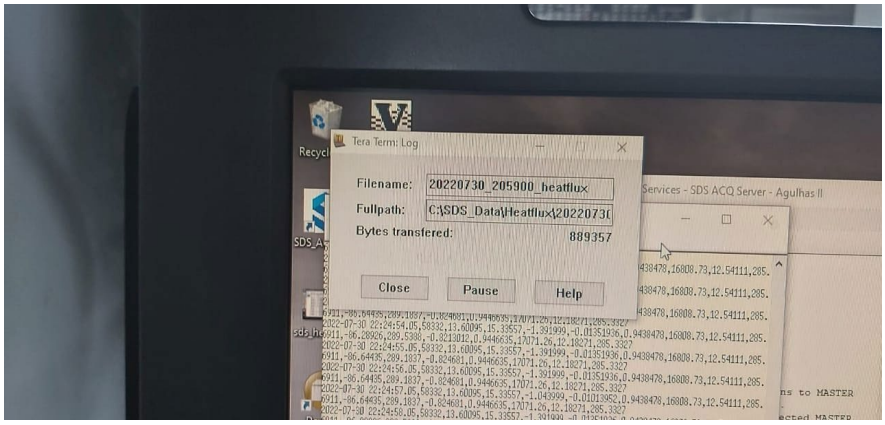

Day 21 - 2022-07-31 - Sunday

00h14	Stopped the adcp and tsg
03h14	Stopped the voyage on the SDS server.

3.3 SEA ICE OBSERVATIONS (ASPECT)

Winter Cruise members: (on the ship) Ashleigh Womack (leader), Alberto Alberello, Giulio Passerotti, Jonathan Rogerson, Francesca De Santi, Taygan Roberts, Agoritsa Spirakis, Dayna Collins, Shaakirah Sulaiman, Bernhard Schmitz, Magata Mangatane, (on land leader) Ehlke Hepworth.

Ship-based sea-ice observations help validate the consistency and accuracy of satellite products in estimating the ice extent and concentration. The Antarctic Sea Ice Processes and Climate (ASPeCt) is the specification of a standard ice observation protocol for ice thickness observations made aboard ships in the Antarctic pack ice. It provides a standardized and quantifiable method for observing sea ice that is now accepted as the international standard. We have taken part in this protocol for a few years now. However, unlike previous years, our sea-ice observations during this winter cruise were done separately to the team VESSEL-4 (previously the VIBRATIONS team), as their requirements for recording the ice observations, in addition to ramming and vibrations needed to be done once per minute, which would have proved difficult for a largely inexperienced team. The ice observation team was largely made up of people from within SEAICE team as well as a few volunteers from other teams, including the SAWS team.

Our sea ice and atmospheric observations were photographed and recorded every 15 minutes according to the ASPeCt protocol. The ice was classified by a total ice concentration – the fraction of the ocean covered by any type of sea ice, estimated to the nearest 10% – and then according to primary, secondary and tertiary concentrations (not the ice types as per the protocol). The estimated concentrations and types were given separately with specific codes (Figure 6.1). The atmospheric variables such as cloud cover and visibility were recorded at the same time as the ice which was additionally complemented by the STS data (including air temperature, water temperature and wind speed) retrieved from the ship at the end of the cruise. The higher frequency observations were eventually combined into the hourly frequency required by ASPeCt. The abridged versions of the forms submitted to the Australian data centre at the University of Tasmania. Unfortunately, this year the TomTom cameras were not used as they had issues with their SD cards; the stereo-cameras described in Sec. 14.2.4 should be used for reference.

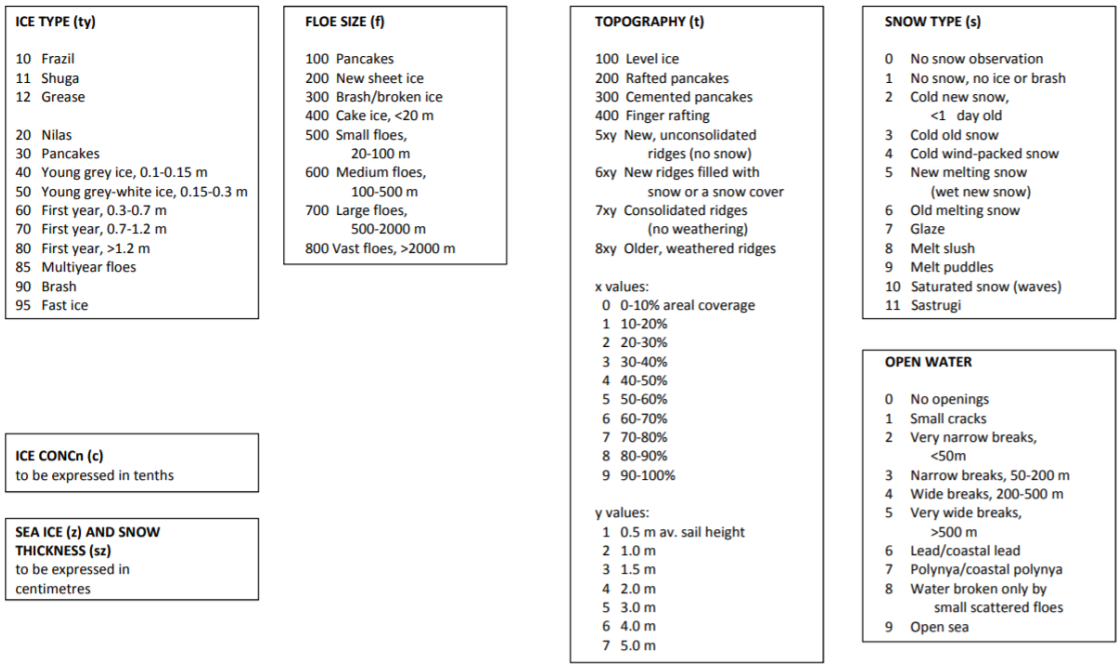

Figure 17 : ASPeCt codes for reporting ice features

Sea ice was found much further south than forecasted for mid-July 2022 and therefore observations started a few days later than expected. The observations began on entering the ice (19.07.2022 at 06h30 UTC) and ended when leaving the ice (25.07.2022 at 17h30 UTC). As it was still dark on the first morning, grease and frazil ice were not initially recorded and the observations only started when small pancake floes were observed. The ice conditions appeared more similar to observed spring conditions (long periods of consolidated floes broken by bands of open water) as we travelled into the ice. Additionally, after colder air temperatures occurred, calm conditions ice types were recorded, including nilas and young grey ice which was not common in previous winter expeditions in the area (Figure 6.2).

The observation site was the portside of the Bridge, which was quiet and calm, thanks to the collaboration with the ship Officers' crew and the VESSEL-4 team. The observations were done continuously while the ship was moving in the ice, with team members switching out every two hours. Besides the team leader and 2 others, the majority of this observation team experienced the ice environment for the first time during this winter 2022 cruise. Therefore, the inexperienced team members were initially paired up with an experienced one. In addition to this, our team attended two seminars held within the ship's auditorium. They were hard working and keen to learn which resulted in them doing well. However, there still will be some subjective biases in these observations.

Nilas Ice (Ty 20)

Pancake Ice (Ty 30)

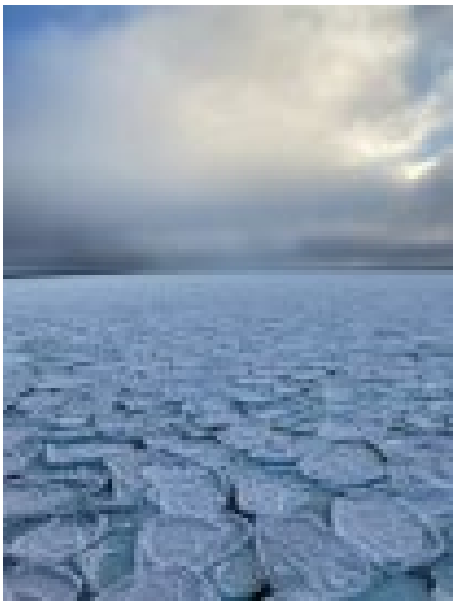

Rafted Pancake Ice (young grey white ice) (Ty 50)

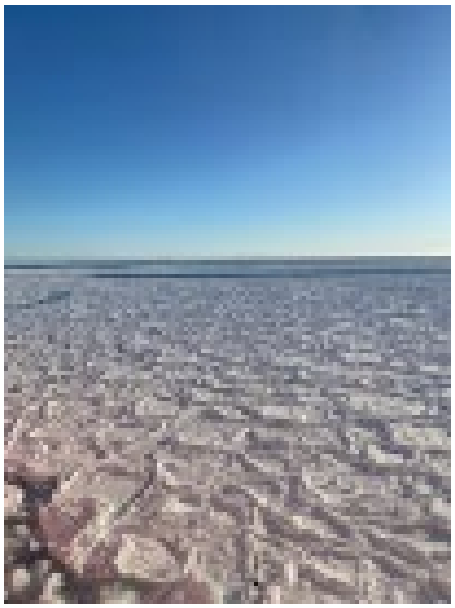

Consolidated ice (first year ice) (Ty 60)

Figure 18 Some ice types observed during this winter cruise

Recommendations for future cruises:

During this winter cruise, the SEAICE team had a highly intense schedule with deployments and coring activities occurring every 5-6 hours when the ship was stationary. However, ice observations needed to be recorded when the ship was moving in-between these stations. This led to a highly stressful and taxing week, often with 24/7 work for members within the SEAICE team. Therefore, it is recommended for future sea-ice expeditions to have two separate teams doing 1. sea-ice activities and 2. ice observations to allow for periods of rest and sleep for both teams.

3.4 AUXILIARY SATELLITE OBSERVATIONS: SAR FROM COSMO-SKYMED

Contributor: Giacomo de Carolis (IREA-CNR)

A survey over the area of campaign operations was carried out with the acquisition of Synthetic Aperture Radar (SAR) images gathered by the Cosmo-SkyMed (CSK) and Cosmo Second Generation (CSG) SAR satellites. CSK consists in a constellation of four low Earth orbit mid-sized satellites, each equipped with a multi-mode, high-resolution SAR operating at X-band; CSG is based on 2 enhanced SAR satellites, placed on the same orbit of the CSK satellites. CSK and CSG instruments are both operated by the Italian Space Agency.

The aim of the survey was to perform an intensive monitoring of the MIZ, at the locations close to the ice edge where buoys were deployed to collect directional wave data and relevant sea ice parameters were measured.

From 21 to 25 of July, a total of 15 SAR images (7 CSK and 8 CSG) were acquired with the support of the ASI User Ground Segment staff who helped us in the selection of the best images fulfilling the objective of the survey. Additional 4 SAR images (3 CSK and 1 CSG) were acquired after the sea-ice campaign ended (28/07 – 03/08) in the area of wave buoys deployment in order to continue monitoring of the sea ice cover.

SAR products were acquired in ScanSAR mode to gather wide-swath images (about 100x100 km^2) to guarantee a synoptic view of the area of operations, including the ice edge and part of open sea. The spatial resolution was about 30 m in both azimuth and range with a pixel spacing of 15 m for CSK and 5 m for CSG products. Finally, VV polarization was selected for both CSK and CGS images to allow the application of SAR wind inversion algorithms with the state-of-the-art X-band semi-empirical geophysical functions.

After geo-referencing the relevant SAR images, the corresponding quick-looks were computed and timely delivered to the ship as support to the in-situ operations for the evaluation of the neighbor sea ice conditions.

A preliminary analysis of the SAR quick-looks shows an excellent discrimination of the ice edge at the available SAR spatial resolution. The wave systems that crossed the ice-covered region were also recognized on the SAR images as typical backscattering modulation produced by the velocity bunching effect. Therefore, it is expected that results of the ongoing analysis aimed at estimating ocean directional wave spectra on full resolution SAR image spectra, will allow comparison with those collected by the wave buoys. Finally, the ice thickness and the rheological properties of the sea ice, such as the equivalent ice viscosity, will be estimated by means of the observation of the wave energy attenuation through the icefield. To this end, a SAR inversion methodology originally developed by our research group will be applied on each SAR image that will be deemed suitable with respect to the incoming open sea wave field.

3.5 AUXILIARY SATELLITE OBSERVATIONS: ECICE SEA-ICE TYPE

Contributors: Wayne de Jager (UCT), Marcello Vichi (MARIS UCT), Christian Melsheimer (Bremen)

Ad hoc satellite observations on sea ice type for given swaths have been made available during the cruise right after the acquisitions. The swath-based sea-ice type estimates are generated from a modified version of the Environment Canada Ice Concentration Extractor (ECICE) algorithm (Shokr et

al., 2008; Shokr and Agnew 2013). The ECICE algorithm utilises a constrained optimisation technique to estimate the probability distributions of radiometric signatures of different ice types using different sets of passive microwave satellite data. Currently an Antarctic ice-type product is made available by the Institute of Environmental Physics (IUP), University of Bremen (Melsheimer et al., 2019). In the standard prototype, daily brightness temperature and backscatter maps are prepared as input data for the ECICE algorithm, resulting in a 24-hr temporal resolution ice type product with full coverage of the Antarctic region. The ECICE algorithm returns five ice concentration values per cell: open water (OW), young ice (YI), first-year ice (FYI), Multi-year ice (MYI) and total ice (a summation of the three different ice types). Correction schemes based on atmospheric reanalyses are also applied to the ECICE output for improving MYI, although this is not done when the product is real time.

During the cruise, we tested the algorithm on individual swaths. The swath-based method applies the ECICE algorithm directly onto brightness temperature swaths retrieved from the AMSR-2 passive microwave sensor on board JAXA's GCOM-W1 platform. This can be advantageous as the timing of the swath-based ice type estimates can be more accurately defined (as opposed to the time ambiguity introduced by merging multiple swaths over a 24-hr window into a single daily map) and potentially less quality degradation caused by the averaging/merging methods but comes at the expense of full spatial coverage and a consistent temporal resolution. Passive microwave input channels used include the 36.5 GHz (horizontal and vertical), 18.7 GHz (horizontal) and 36.5/18.7 GHz vertical polarisation gradient ratio. Unlike the daily product, scatterometer data are not used and no MYI correction schemes are applied, which is of little relevance in the MIZ.

Figure 19 shows an example of the products for the 22nd of July, when the ship was at station I0B. There is a major difference in sea-ice type when considering the instantaneous swath and the daily-averaged product. A dominance of FYI is observed in the swath, while the averaging with subsequent images classifies the ice as YI. This is likely due to the starting of melting conditions observed at the station during that day, which changed the sea ice character in a few hours from FYI to smaller less consolidated floes. Note that the coring at I0B was not deemed entirely safe and confirmed by ductile interstitial ice between pancakes.

References

Melsheimer, Christian; Spreen, Gunnar; Ye, Yufang; Shokr, Mohammed (2019): Multiyear Ice Concentration, Antarctic, 12.5 km grid, cold seasons 2013-2018 (from satellite). PANGAEA, https://doi.org/10.1594/PANGAEA.909054. User guide: https://seaice.uni-bremen.de/data/MultiYearIce/MYIuserguide.pdf

Shokr, M., Lambe, A. and Agnew, T., 2008. A new algorithm (ECICE) to estimate ice concentration from remote sensing observations: An application to 85-GHz passive microwave data. *IEEE Transactions on Geoscience and Remote Sensing*, *46*(12), pp.4104-4121.

Shokr, M. and Agnew, T.A., 2013. Validation and potential applications of Environment Canada Ice Concentration Extractor (ECICE) algorithm to Arctic ice by combining AMSR-E and QuikSCAT observations. *Remote sensing of environment*, *128*, pp.315-332.

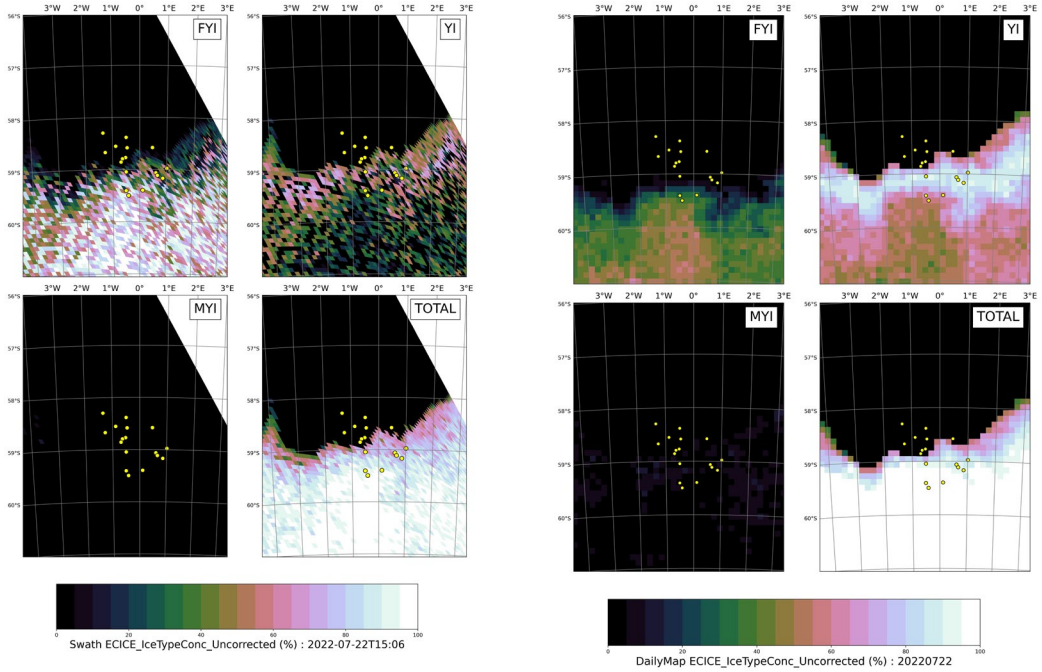

Figure 19 Sea-ice type from the ECICE algorithm for a single swath (left) on July 22nd when the ship was at the southernmost station, and from the daily composite (right).

4 TOP PREDATOR DISTRIBUTION AND ABUNDANCE IN THE SOUTHERN OCEAN

Team name and PI	TOP. Makhado A.
Authors	Masotla MJ, Germishuizen M., Pieters E., Mnyekemfu M.

4.1 OBJECTIVES

The objectives of this project were to:

1. Determine seabird abundance and distribution in the Southern Ocean
2. Determine occurrence and richness of Cetaceans and other marine mammals (i.e. Pinniped) along the transit
3. Collection of eDNA at various stations
4. Collection of acoustics data along the transect
5. Observations of marine debris in the Southern Ocean

4.2 SYNOPSIS

Seabirds and marine mammals are often the early indicators of changes in an ecosystem and display the effects of climate change vividly. Various oceanographic variables, such as ocean currents, physical and chemical forces, are critical to generate nutrients necessary for primary productivity that accumulates biomass, creating hot spots of ecologically important zones for many marine taxa including marine top predators like seabirds and marine mammals. There is a direct linkage of these oceanographic structures to seabed topography, physical water properties and some oceanographic processes, such as fronts, eddies and local upwellings. Prey availability is mostly influenced by these features, therefore it is expected for top predators, to be found in these areas.

The overarching purpose of this expedition was to collect distribution and abundance data on marine megafauna such as seabirds, and marine mammals in relation to a number of different environmental variables (e.g. surface temperature, chlorophyll, fronts, etc.). We aim to do this in order to address the knowledge gap around their at-sea movements in our study area. We envisage several conservation applications using these data, such as defining 'ocean hotspots', where prominent marine life (such as seabirds or cetaceans) congregates in relative abundance and with some degree of consistency. Further objectives are to identify important areas for highly threatened seabird species such as albatross and petrels, to inform on the development of Important Marine Bird Areas or contribute to the designation of Marine Protected Areas, special nature reserves on the high seas, and/or no-take zones to protect sensitive species from commercial fishing.

Over and above there was collection of acoustic data which will help overlay top predator distribution to the Antarctic krill (*Euphausia superba*), a keystone species in the Antarctic ecosystem, to establish predator-prey relationships between marine keystone species. EDNA samples were also collected towards fulfilment of the metabarcoding objective. All observed marine debris was also recorded.

4.3 SIGNIFICANCE

Seabirds spend more than half their lives at sea, foraging or resting. The observations taken are in efforts to maximising key indicators in determining biodiverse hot spots along the transect, for recommendation in areas that requires protection. Furthermore, the obtained data serve as a baseline to understand the effects of climate change on several aspects around the oceans community and how it influences our daily living and the negative impacts of human activities on seabirds at sea and around breeding grounds.

Many cetacean species have undergone a long history of exploitation. It is thus imperative that we continue to monitor their recovery and identify important areas for conservation and protection. Knowledge of the movement of cetaceans as well as changes to their distribution and migratory patterns can also be useful in studying environmental change, and the utility of cetaceans as sentinels for climate change is gaining significant scientific attention (e.g. Seyboth et al., 2016).

The overarching purpose of this expedition was thus to improve the existing database and understanding of these species interaction and to aid in their conservation. Findings from this cruise will contribute to and improve the understanding of the recovery and distribution patterns of these previously over-exploited marine mammals and the dynamics of seabird species interaction.

4.4 SAMPLING

Top predator observations were conducted during day light hours with great visibility from the observation platform (Monkey Island) of the S.A. Agulhas II RV. Observations were done covering an angle of 180° from the port to starboard side and within a 300m distance from the vessel. During oceanographic and sampling stations or during unfavourable weather conditions, effort was paused. Birds were recorded as in-flight or sitting on the water at the time of the sighting. Sightings of seabirds and cetaceans were only recorded while the vessel was steaming between research stations (See table 1).Periods while the vessel was moving were designated as “search effort” and periods when the vessel was still were termed “down time”. For each observation, variables such as directional angle, distance from the ship, behaviour and number of individuals were recorded (Table 2).

Birds that followed the ship from station to station were not recorded. Searching for seabirds was performed with either the naked eye or handheld 10x42 binoculars. A BirdLasser App which is a real-time logging app was used to record the data. Seabirds were identified using their body shape and size, colour patterns and flying behaviour. Digital photographs using a Canon EOS 7D with 100-400 m telephoto lens were taken to further assist in confirming species identification. A seabird field guide, Guide to Seabirds of Southern Africa (Ryan, 2017), was also used to assist with species identification. Same approach was done when identifying cetaceans, blow presence or absence of a dorsal fin, the shape and extent of the dorsal fin relative to the body were some of the key parameters deployed in identifying cetaceans.

Acoustic data were supposed to be collected from three transducers (i.e. 38, 120 and 200 kHz) mounted on the drop keel of the vessel. Unfortunately, the system was not turned due to technical misunderstanding. It is recommended that standard operating procedures are made available prior to departure, to ensure that any technician can operate the instrument.

In total, four stations were sampled for subsequent eDNA analysis (see table 3).

4.5 SEABIRDS

From Cape Town there was low diversity of coastal birds, a few Cape Gannets (adults and a few juveniles) were observed in transit to the west, no plunging was observed, and most of the birds seen were flying high. As we were sailing down the composition of seabirds changed and we started to observe Indian Yellow-nosed Albatross, Shy Albatross and Atlantic Yellow-nosed Albatrosses. No White Chinned Petrels were observed which is usually expected for they are currently in breeding mode and majority of them are in proximity to their breeding sites. In most cases White Chinned Petrel will be observed throughout the year, though during breeding there will mostly be juveniles and non-breeding birds, it was interesting that not a single bird was seen. The same goes for the Spectacled Petrel, although not as numerous as the White Chinned, we were expecting to see at least a few, but none was observed either. Please see observation records on table 1, for to and from the Antarctic ice during the cruise.

Soft-plumaged Petrels started to be observed south of 36°S, we expected to start seeing the high in diversity around the 40th degree mark, perhaps the was more productivity for their prey in the higher latitude than expected. No fishing vessels were observed in proximity to the research vessel, known to attract seabirds and thus possibly biasing results. Throughout the trip there was a very low diversity, and the assemblages were not as pronounced as during the summer months with inference to the SANAE 4 observations, we started to see Antarctic Prions in the 39th degree latitude but their diversity picked around the 42nd latitude where they were soon replaced by Fairy Prions, soft plumaged petrels were fairly consistent and a black morph Soft Plumaged Petrel made an appearance for a short while just when we started to see a high diversity of Great Winged Petrels and a light mantled Albatross (figure 4) also showed up.

Seabird diversity was spaced, and their abundance was also at intervals. He first Antarctic petrel (figure 3) was observed at the 56˚ mark, and they have been constant until we reached the pancake ice where we started to observe the Snow Petrels (figure 2), there was a southern Giant Petrel every now and again, at least one spotted a day, but once at the ice there was virtually no other birds observed except the Antarctic Petrels and snow Petrels.

4.6 CETACEANS

The cruise comprised of 101 hours and 20 minutes of active searching and 13 hours and 49 minutes of down time (search when the vessel was stationary). All the positively identified sightings are listed in table 2. Very few cetaceans were encountered throughout the whole transect. In total, seven sightings were recorded, five of which were identified to species level. Low sightings could be attributed to bad weather conditions in combination with the fact that most Southern Ocean baleen whale species migrate to lower latitudes during the winter for calving (e.g. humpback whales (*Megaptera novaengliae*), southern right whales (*Eubalaena australis*), and fin whales (*Balaenoptera physalus*).

On the 12th of July a large blow was seen on the horizon, however, the distance from the ship and weather conditions made identification impossible. Later that morning a fin whale was seen approximately 200m from the ship. The appearance of the dorsal fin in relation to the blow allowed for a positive identification. Later that afternoon a group of three humpback whales were photographed moving rapidly and blowing regularly (Figure 5). The next cetacean sighting occurred

on the 27th of July, with a group of approximately eight long-finned pilot (*Globicephala melas*) whales which were seen porpoising in a tight group moving in a southerly direction passed the starboard side of the ship (Figure 6), On the 29th of July at 10:35 On the 30th of July a pod three of grey beaked whales (*Mesoplodon grayi*) were seen breaching and later that afternoon and a brydes whale (*Balaenoptera edeni*) was seen moving in a south westerly direction (Figure 7 and 8).

Table 7 Seabird abundance and diversity observed in transit to and from the Antarctic ice during the SCALE winter cruise. July 2022.

	Transect to	**Transect from**
Date	12 – 23/07/2022	24 – 30/07/2022
Observations	361	285
Species	24	27

Table 8 Positively identified sightings of cetaceans along transect. During the SCALE winter cruise. July 2022.

Date	Time	Species	Coordinates	Number of Individuals	Behaviour
12/07/2022	10:10	Fin Whale	35,2596S; 16,5493E	1	Blow
12/07/2022	10:35	Humpback whale	36,2333S; 16,0727E	3	Blowing and moving
27/07/2022	13:25	Long-finned pilot whale	46,5287S; 0.0018E	8	Porpoising
29/07/2022	10:35	Grey Beaked whale	35,5011S;14,5625E	2	Breached
29/07/2022	16:44	Brydes whale	34,5908S; 16,3343E	1	Blow

Table 9 eDNA sample data

Station	**Date**	**Latitude**	**Longitude**	**Depth**	**Filter size**
22WIN02-PUZ	2022/07/17	-53,9989	0,0001	20m;500m	0,45
22WIN10-I0	2022/07/20	-59,0437	-0,5063	20m;500m	0,45
22WIN09-I4	2022/07/20	-58,8556	-0,6920	20m;500m	0,45
22WIN11-SAZR	2022/07/26	-46,9997	-0,0019	300m;500m	0,2

Figure 20 Snow petrel treading water for take-off next to a crawler during the SCALE winter cruise. July 2022

Figure 21 Antarctic Petrel skimming the water surface searching for prey during the SCALE winter cruise. July 2022.

Figure 22 Light-mantled Albatross soaring around the southern Ocean, with visible moulting feathers flew by during the SCALE winter cruise. July 2022.

Figure 23 Humpback whale blowing and displaying small, curved dorsal fin. During the SCALE winter cruise. July 2022.

Figure 24 Long-finned pilot whales displaying distinctive greyish white saddle behind the curved dorsal fin. Observed during the SCALE winter cruise. July 2022.

Figure 25 Grey's beaked whale breaching. During the SCALE winter cruise. July 2022.

Figure 26 Bryde's whale displaying dorsal fin observed during the SCALE winter cruise. July 2022.

Figure 27 Top Predator team for seabirds and marine mammal observations during SCALE cruise 2022: Matthew Germishuizen, Mpumalanga Mnyekemfu, Makhudu Masotla, and Estefan Pieters.

References

Ainley, D.G., Ribic, C.A., Fraser, W.R., 1992. Does prey preference affect habitat choice in Antarctic seabirds? Mar. Ecol. Prog. Ser. 90, 207–221.

Ainley, D.G., Ribic, C.A., Spear, L.B., 1993. Species-habitat relationships amongst Antarctic seabirds: a function of physical or biological factors? Condor 95, 806–816.

Begon, M., Townsend, C.R., Harper, J.L., 2006. Ecology – from individuals to ecosystems. Blackwell Publishing Ltd, United Kingdom.

Bost, C.A., Cotté, C., Bailleul, F., Cherel, Y., Charrassin, J.B., Guinet, C., Ainley, D.G., Weimerskirch, H., 2009. The importance of oceanographic fronts to marine birds and mammals of the southern oceans. J. Mar. Syst. 78, 363–376. doi: 10.1016/j.jmarsys.2008.11.022

Fraser WR, Ainley DG (1986) Ice edges and seabird occurrence in Antarctica. BioScience 36:258–263.

Genin, A., 2004. Bio-physical coupling in the formation of zooplankton and fish aggregations over abrupt topographies. J. Mar. Syst. 50, 3–20. doi: 10.1016/j.jmarsys.2003.10.008

Grecian, W.J., Witt, M.J., Attrill, M.J., Bearhop, S., Becker, P.H., Egevang, C., Furness, R.W., Godley, B.J., González-Solís, J., Grémillet, D., Kopp, M., Lescroël, A., Matthiopoulos, J., Patrick, S.C., Peter, H.-U., Phillips, R.A., Stenhouse, I.J., Votier, S.C., 2016. Seabird diversity hotspot linked to ocean productivity in the Canary Current Large Marine Ecosystem. Biol. Lett. 12, 20160024. doi: 10.1098/rsbl.2016.0024

Hunt, G.L., 1990. The pelagic distribution of marine birds in a heterogeneous environment. Polar Res. 8, 43–54. doi: 10.3402/polar.v8i1.6802

Olson, D.B., Backus, R.H., 1985. The concentrating of organisms at fronts: a cold-water fish and a warm-core Gulf Stream ring. Journal of Marine Research. 43, 113–137. doi: 10.1357/002224085788437325

Ribic CA, Ainley DG (1988/89) Constancy of seabird species assemblages: an exploratory look. Biol Oceanogr 6:175–202.

Scales, K.L., Miller, P.I., Embling, C.B., Ingram, S.N., Pirotta, E., Votier, S.C., 2014a. Mesoscale fronts as foraging habitats: composite front mapping reveals oceanographic drivers of habitat use for pelagic seabird. J. R. Soc. Interface 11, 20140679. doi: 10.1098/rsif.2014.0679

Scales, K.L., Miller, P.I., Hawkes, L.A., Ingram, S.N., Sims, D.W., Votier, S.C., 2014b. On the front line: frontal zones as priority at-sea conservation areas for mobile marine vertebrates. Journal of Applied Ecology. 51, 1575–1583. doi: 10.1111/1365-2664.12330

Seyboth, E., Groch, K.R., Dalla Rosa, L., Reid, K., Flores, P.A. and Secchi, E.R., 2016. Southern right whale (Eubalaena australis) reproductive success is influenced by krill (Euphausia superba) density and climate. *Scientific reports*, *6*(1), pp.1-8.

Sournia, A., 1994. Pelagic biogeography and fronts. Prog. Oceanog. 34, 109–120. doi: 10.1016/0079-6611(94)90004-3

Stroud, J.T., Bush, M.R., Ladd, M.C., Nowicki, R.J., Shanz, A.A., Sweatman, J, 2015. Is a community still a community? Reviewing definitions of key terms in community ecology. Ecol. Evol. 5, 4757–4765. doi: 10.1002/ece3.1651

Weimerskirch, H., 2007. Are seabirds foraging for unpredictable resources? Deep-Sea Research. Part II 54, 211–223. doi: 10.1016/j.dsr2.2006.11.013

5 CO2 AND HEAT STORAGE AND FLUXES

Team name and PI	CO2-HEAT. Sarah Nicholson (SOCCO/CSIR)
Authors	Hamnca S, Mdokowana B, Rasmeni B, Nicholson S.

5.1 INTRODUCTION

The contemporary Southern Ocean mitigates the effects of anthropogenic climate change through its disproportional uptake of carbon and heat. However, it is not well understood how this role will evolve under different emission and mitigation scenarios. The Southern Ocean also remains the largest source of global ocean uncertainty in the global estimates of CO_2 and heat fluxes. While much has been achieved globally and regionally in constraining the variability and some of the mechanisms that drive Southern Ocean CO_2 and heat fluxes separately, we propose that a significant part of the challenge lies in the lack of research on CO_2 and heat together to better understand the feedback and the mechanisms that drive those feedbacks. This SANAP-NRF project aims to examine the changing role of the Southern Ocean in global climate by looking at the two main drivers CO_2 and heat, in an integrated way using an unprecedented 10-year high resolution glider dataset from the 2012-2022 SOSCEx experiments, prognostic biogeochemical models, and new observational experiments planned in partnership with CSIR and DFFE as well as the SO-CHIC EU H2020 project. This collaboration is undertaken as part of the emerging National Ocean CO2 Facility, a research infrastructure integration between CSIR and DFFE within SAPRI and hosted at DFFE.

This project aims to gain a better understanding of how the interaction of atmospheric synoptic cycles (storms) and fine-scale (0.1-100 km) ocean processes influence seasonal-decadal variability of CO_2 and heat fluxes. This will include the extent to which they feedback on each other and ultimately contribute to a better understanding of the role of the Southern Ocean in the global carbon-climate system.

The expected three outcomes are

1. Improved observational constraints for the contemporary seasonal-interannual variability of CO_2 and heat fluxes.

2. Understanding of how storms and their interaction with fine-scale dynamics influence the seasonal and interannual variability of CO_2 and heat fluxes.

3. Identify the potential mechanisms that could explain the decadal anomaly in CO2 fluxes at the end of the 20th century.

The SCALE Winter-2022 cruise provides an important opportunity to address a key source of uncertainty in annual Southern Ocean CO_2 and heat observations - the dearth of winter time observations. During the SCALE Winter -2022 cruise, the CO2 and heat team measured four parameters of the carbonate system during the voyage. Underway surface observations of continuous surface pCO_2 (equilibrator based), underway pH measurements, Dissolved Inorganic Carbon (DIC) and Total Alkalinity (AT).

5.2 CONTINUOUS pCO_2 MEASUREMENTS

Sea surface pCO_2 measurements were carried out using a General Oceanics underway pCO_2 system with a Licor-LI7000 Infra-red gas detector (Pierrot D., et al, 2009). The underway pCO_2 system was calibrated using 4 reference gases (0 ppm, 284.22 ppm, 399.15 ppm, 410.03 ppm), certified against reference standards traceable to NOAA central calibration laboratory. The instrument was sequenced to cycle between reference standards, atmospheric air, and seawater roughly every 4 hours. Data was logged through a computer interface using propriety LABVIEW software, which also controlled the mechanical operation of the instrument. Measurements were carried out from Cape Town to the marginal ice zone in the Southern Ocean and back to Cape Town.

The two figures below show preliminary results of intake temperature, sea surface pCO_2 and salinity of the southward leg (Figure 1) and the northward leg (Figure 2). The intake temperature and salinity data were obtained from the TSG. The pCO_2 values during the southward leg ranged from 373-782 µatm whereas values falling between 363 – 708 µatm where observed during the northward leg. The water content fluctuated between 0 and 14 µm/m throughout the voyage.

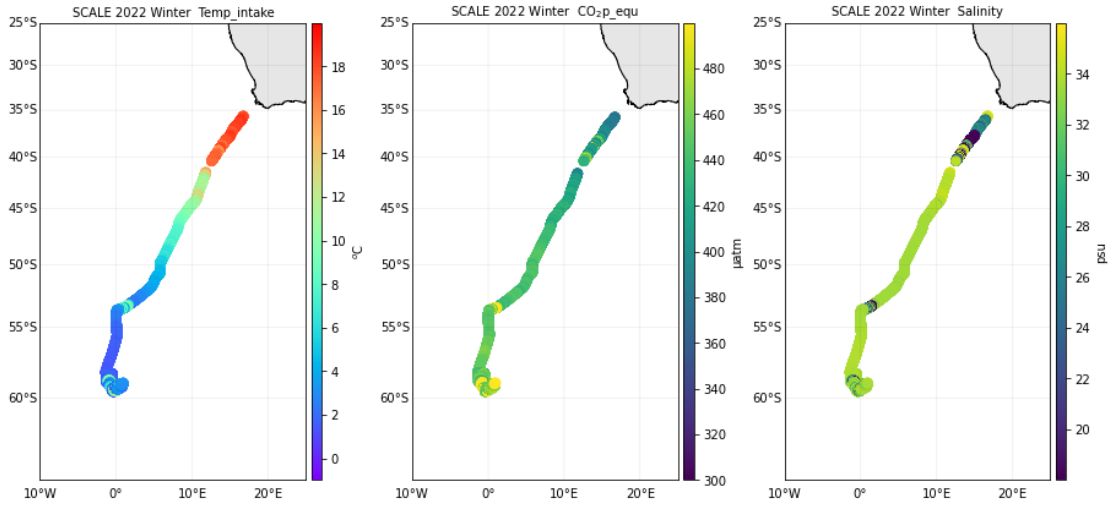

Figure 28 Preliminary sea surface pCO2 data from Cape Town to the marginal ice zone.

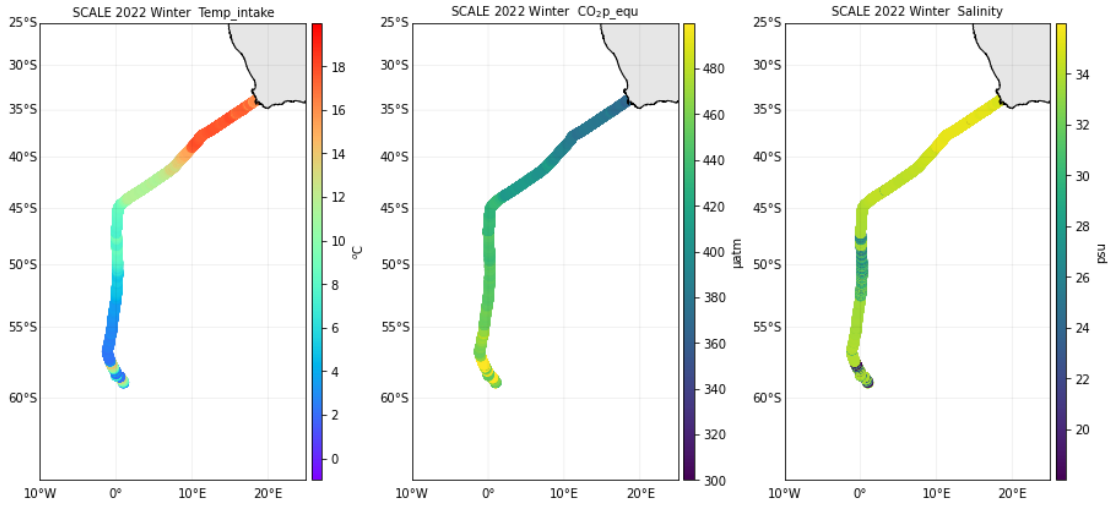

Figure 29 Preliminary sea surface pCO2 data from the marginal ice zone to Cape Town

5.3 DISSOLVED INORGANIC CARBON (DIC) AND TOTAL ALKALINITY (AT) MEASUREMENTS

DIC/AT samples were every four hours collected from the underway surface seawater supply in the underway lab where the pCO_2 system is placed. Samples were also collected from CTD stations; SAZ 2, PUZ, the marginal ice zone (MIZ) transect and the Good Hope (GT) transect. The CTD was deployed to a maximum depth of 500 m on the MIZ transect, to a depth of 1500-2000 m on SAZr , PUZ and GT transect. A total of 52 underway DIC/AT samples and a total of 148 samples were collected from the CTD niskin bottles. Samples were collected in a 500 ml bottle and spiked with 120 µL of concentrated HgCl2 (Mercuric Chloride) to prevent any further biological modification of the sample. The DIC/AT samples were analysed on board using Marianda's VINDTA 3C (Versatile Instrument for the Determination of Titration Alkalinity). The VINDTA determines total alkalinity by potentiometric titration and also coloumetrically measures CO2 from the same sample.

5.4 CONSTRAINING THE PCO2 BIAS ON SA AGULHAS II

The pCO2 bias of a ship is the difference between the pCO2 observed by the instrument on the ship and the water at the intake. This arises from the bacterial growth in the pipes of the Scientific Water Supply and it is highly temperature sensitive. It needs to be carried out spanning a range of temperatures that are representative of the cruise track. The essence of the protocol is that water samples are collected with near surface (±5-7m), representative of the depth of the intake.

This protocol was conducted by triggering three separate Niskin bottles from the same depth but 5 seconds apart. Simultaneously with triggering the Niskin bottles, 3 replicates from the water supply in the underway lab were collected. From each Niskin bottle This protocol was repeated 3 times during the cruise in warm (38 degrees South), cool (48 degrees South, and cold (54 degrees South). waters to obtain a good confidence in the temperature dependence of the bias correction. This was done to provide a useful mean to overcome the uncertainty that comes from the ship roll.

5.5 MARINE PH MEASUREMENTS

SeaFET™ from Sea-Bird Electronics was used for the continuous pH measurements. The primary sensor element of the SeaFET™ is the ISFET, a solid-state sensor that senses pH in marine environments. The ISFET has two reference electrodes: an internal reference and an external reference, that give separate reference potentials to the ISFET and show separate pH values (pH Internal and pH External). After the corrections for temperature and salinity are applied, the values from the internal and external are similar, and allow us to verify the validity of the sensor's measurements.

5.6 CONTINUOUS HEAT FLUX MEASUREMENTS:

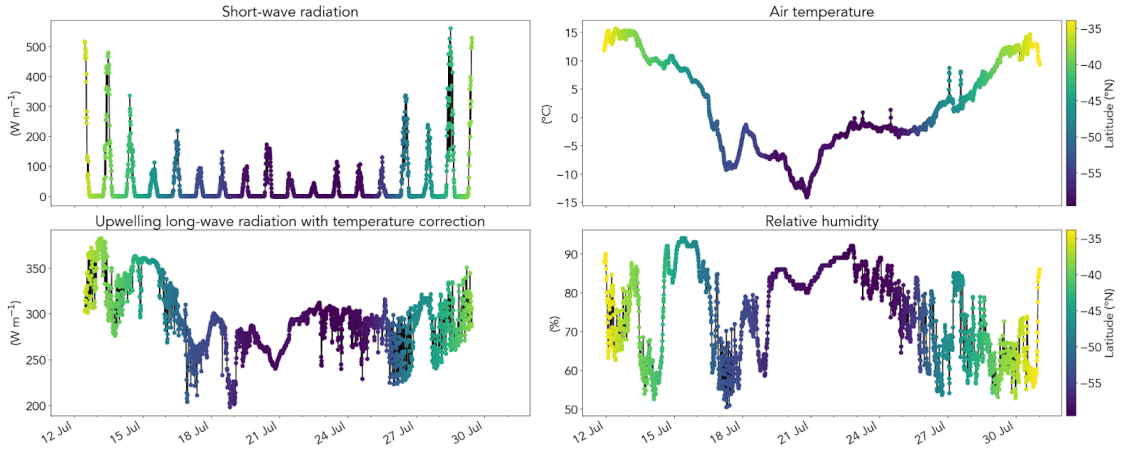

Figure 30 Preliminary time series of the heat flux data resampled to 10 min bins for the entire winter cruise, colored according to Latitude.

References

Dickson, A. G., C. L. Sabine, and J. R. Christian (2007), Guide to best practices for ocean CO2 measurements, edited, p. 173, North Pacific Marine Science Organization (PICES), Sidney, British Columbia.

Feely, R.A., Wanninkhof, R., Milburn, H.B., Cosca, C.E., Stapp, M. and Murphy, P.P., 1998. A new automated underway system for making high precision pCO2 measurements onboard research ships. Analytica Chimica Acta, 377(2-3), pp.185-191.

Pierrot, D., Neill, C., Sullivan, K., Castle, R., Wanninkhof, R., Lüger, H., Johannessen, T., Olsen, A., Feely, R.A. and Cosca, C.E., 2009. Recommendations for autonomous underway pCO2 measuring systems and data-reduction routines. Deep Sea Research Part II: Topical Studies in Oceanography, 56(8-10), pp.512-52.

Wanninkhof, R. and Thoning, K., 1993. Measurement of fugacity of CO2 in surface water using continuous and discrete sampling methods. Marine Chemistry, 44(2-4), pp.189-204.

6 MICROBIOME RESEARCH

Team name and PI	MICROBIOME. Thulani Makhalanyane (UP)
Authors	Mogase O, Nair G, Mafumo N, Mtshali T, Abraham B, Buthelezi M, Makhalanyane TP

6.1 UNRAVELLING THE ROLE OF IRON AND MANGANESE CO-LIMITATION ON MICROBIAL COMMUNITIES FROM THE SOUTHERN OCEAN

Contributors: Girish Nair, T Mtshali, TP Makhalanyane

6.1.1 Introduction and Rationale

The role and quantitative contribution of chemoautotrophic microbial (picoplanktonic) communities in ocean systems is largely unknown. Previous studies have shown that iron fertilization results in increased productivity of marine phytoplankton. However, little work has been done to elucidate the effect of iron on deep-sea microbes. While the chemical form of iron in high nutrient low chlorophyll (HNLC) regions such as the Southern Ocean remains unknown, it is well established that molecular speciation affects microbial competition for iron uptake. The importance of iron and manganese for marine ecosystems and its role in the fixation of CO_2 makes the study of this trace metal of great interest as trace metals like Fe, Mn and others are important micronutrients that form an integral part of metalloenzymes, which take part in various cellular processes essential for the survival of microorganisms.

6.1.2 Aims and Objectives

This experiment aims to assess how the co-limitations of trace metals, specifically iron (Fe) and Manganese (Mg), influence microbial community composition and functionality using an omics approach combined with a trace metal profile.

6.1.3 Research approach and methodology

The effect of nutrient-colimitation (Fe and Mn) was studied on bacterial and phytoplankton communities of the sub-Antarctic waters using an on-board mesocosom experiment. Seawater samples (260 L in total) were collected at two depths (50 m and 500 m) at station OD2 using GoFlo – trace metal free bottles.). Unincubated controls were prepared using 2 X 10L bottles to measure the initial iron and manganese concentrations in water samples. Subsequent to this, 10 L water samples were incubated in 24 X 10 L acid washed carboys for a total duration of 168 hours for both depths (50 m & 500 m). The incubated mesocosms were spiked with $FeCl_3$ (2nM/L), $MnCl_2$ (4nM/L) and FeCl3 + MnCl2 combined for each depth. The mesocosms were exposed to light during incubation at 4°C, with sub-sampling taking place after 1 hour, 120 hours and at the termination point of the experiment (168 hours). 125 mL of the seawater samples were collected from each mesocosm in order to measure dissolved iron and manganese. Seawater samples from each mesocosm were further aliquoted for Flow cytometry (10 ml sample + 2.5 ml formaldehyde), Microscopy (5 ml sample + 5 ml glycerol), Single cell genomics (10 ml sample + 1 ml TE-Gly Buffer), Enzyme assays (100 ml sample), Nutrient analysis (150 ml sample) and stored at -20°C and 3X 15 ml for phytoplankton

analysis. Remaining water up to a volume of 9.5 L (per bottle) was filtered via a dual filtration mechanism and vacuum pump through 0.22 µm Polyethersulfone (PES) filters, and filters were subjected to flash freezing (Liquid N2) and stored at -80°C for meta-omics.

6.2 2. ELUCIDATING THE EFFECTS OF OCEANOGRAPHIC VARIABLES ON THE DISTRIBUTION OF VIRUSES IN THE SOUTHERN OCEAN

Contributors: Nyasha Mafumo, Oliver Mogase, TP Makhalanyane

6.2.1 Introduction and Rationale

Virio- and pico-plankton are very small (<2.0 µm), abundant and diverse life forms in the ocean, that facilitate essential marine biogeochemical cycles. Marine viruses (i.e. virus-like particles; VLPs), are estimated to have a global ocean abundance of 10^{30}, making them the most abundant life form in the ocean. Viral induced lysis via infection, contributes significantly to the cell death of autotrophic and heterotrophic plankton, and results in a process called a "viral shunt". This ecological event occurs when cellular contents are expelled into the environment, diverting organic material (e.g. carbon, nitrogen and phosphorus) into dissolved pools rather than it being channeled along trophic levels. About 6-26% of the photosynthetically fixed carbon is "shunted" to the dissolved organic matter pool by viral lysis in the pelagic zone. Viruses infect autotrophic picoplankton (Prochlorococcus, Synechococcus and picoeukaryotes), which are the most abundant and ubiquitous primary producers in the epipelagic zone, and they account for >50%, and at times >80%, of the marine primary production. In addition, these infect heterotrophic picoplankton communities which carry out most of the extant ecological processes. Viral dynamics are influenced by environmental and biological factors which modify infectivity, degrade or remove virus particles, adversely affect adsorption to host and proliferation in the host cell, e.g. temperature, UV, nutrients, host physiology. Nutrients for example, have been shown to directly impact viral community structure and distribution, with higher abundances of viruses in nutrient replete sites compared to limited sites. However, the mechanism behind how physico-chemical factors regulate virus dynamics and host–virus interactions is poorly characterised, particularly with regard to seasonality that is likely to influence the microbial ecology.

6.2.2 Aims and Objectives

This study aims to examine the influence that environmental variables, specifically nutrients have on the distribution of viruses in the Southern Ocean. The natural nutrient concentrations between the different stations and water depths will be used as a proxy to determine the influence of nutrient concentrations on viral abundances. We will further assess how these differences affect viral infection and thus biogeochemical cycling. Results from this study will potentially allow better understanding of viral driven processes in different environments and thus better predictions of biogeochemical consequence.

6.2.3 Research approach and methodology

During the cruise water samples (20 L at each depth) were collected using Niskin bottles from variable depths (50 m, 250 m, 500 m, 1000 m, and 2000m – depths vary per station) at stations PUZ, I4, OD-2, SB06(ICE0), and SAZr. These were treated with Fe_2Cl_3 for viral fraction enrichment and

subsequently filtered (on-board) using 142 mm 0.8 µm pore size filters and stored at 4°C for downstream meta-omic work.

6.3 EXPLORING THE CHEMICAL ECOLOGY OF MARINE FUNGI AND DISCOVERY OF IMPORTANT BIOSYNTHETIC PATHWAYS INVOLVED IN THE BIOLOGICAL CARBON PUMP

Contributors: Benjamin Abraham, TP Makhalanyane

6.3.1 Introduction and Rationale

Marine fungi are under studied in marine microbial ecology research and their role in the biological carbon pump has only recently been investigated. A relatively new term called the 'mycoloop' has been used to describe the process of diverting carbon supplies to parasitic fungi and thus upsetting the biological carbon pump. Metals play a crucial role in fungal parasitism as they serve as co factors for both enzymes and analytes. This is because they have the redox and catalytic ability necessary in many important biological processes. However, there is insufficient understanding on how this parasitic process works biochemically and previously it has been difficult to identify metal binding compounds using standard untargeted metabolomic techniques. However, novel native metabolomics procedures allow for the identification of metal bound compounds in complex biological samples which can be appropriated for the identification of key analytes involved in the parasitic process.

6.3.2 Aims and objectives

This project aims to understand the role played by metal co factors towards fungal virulence as well as the discovery of novel metallo-based compounds that are affected by various nutrient limitations using novel metabolomic approaches. Using metagenome assembled genomes (MAGs) and ultra-high pressure liquid chromatography, high-resolution mass spectrometry (LC-MS), novel metal bound analytes will be characterized as well as their associated biosynthetic gene clusters required for metabolite production. This, along with stable isotope assisted metabolomics (SIMS), will be used to explain how marine fungi are able to redirect carbon flow in the biological carbon pump.

6.3.3 Research approach and Methodology

Water samples (20 L at each depth) were collected using Niskins from variable depths (50m, 250 m, 500 m, 1000 m, and 2000 m – depths vary per station) at stations PUZ, I4, OD2, ICE00, SaZr and STZ. Samples filtered using 142 mm filters (3µm, 0.2µm), flash frozen in liquid N2, and stored at - 80°C for further meta-omic analysis. 1L samples were also taken from each depth for LC-MS using solid phase extraction (SPE). Samples were filtered through a C8 column to remove contaminants and eluted using methanol.

6.4 INVESTIGATION OF MICROBIAL GENOMICS TO UNDERSTAND BIOGEOCHEMICAL FATES OF DIMETHYLSULFONIOPROPIONATE IN THE SOUTHERN OCEAN

Contributors: M Buthelezi, TP Makhalanyane

6.4.1 Introduction and Rationale

Dimethylsulfoniopropionate (DMSP) is an organosulfur compound known to be ubiquitously available up to eight billion tons in the global oceans. This compound is primarily produced in large amounts by marine eukaryotic microorganisms including phytoplankton and some bacteria. This serves as an important source for carbon and reduced sulfur and has been indicated to further be utilized by microorganisms as an osmoprotectant, antioxidant, and cryopotectant. Its biosynthesis in *alphaproteobacteria* has been observed to be through the methionione transanimation related pathway which involves a methyltransferase gene *dysB*. This gene has been reported to get upregulated under conditions that relate to increased salinity, low temperature, and nutrient limitations. However, despite the developments around the DMSP research, we still lack insight towards the roles played by diverse bacterial phyla towards (i) DMSP-carbon use and assimilation pathways; (ii) and how these processes, phyla, as well as pathways differ across variable depths.

6.4.2 Research aims and objectives

This study aims to analyse DMSP cycling genes and concentrations in the Southern Ocean waters to provide an understanding towards the variable microbial physiological responses towards DMSP degradation. Using meta -omics and GC-FPD approaches variable taxa, and their associated metabolic processes will be determined and further linked to variable depth profiles.

6.4.3 Research approach and methodology

Water samples (20L at each depth) were collected using Niskins from variable depths (50m, 250m, 500m, 1000m, and 2000m – depths vary per station) at stations PUZ, I4, OD2, ICE00, SaZr and STZ. Samples filtered using 142mm filters (3µm, 0.2µm), flash frozen in liquid N2, and stored at - 80°C for further meta-omics analysis. For DMSP samples collection: 20 ml of sea water samples were collected using umber bottles and let it overflow to avoid bubbles. 10 ml of water was subsequently transferred into two headspace crimp vials and topped up with milliQ water (with some room left towards the headspace). The samples were treated with single pallet of sodium hydroxide to cleave DMSP into DMSP and DMS. Vials were subsequently closed with headspace crimp cap and crimp seal using crimping tool. These were then stored in room temperature until DMSP analyses. This experiment was conducted in a low light environment.

6.5 Closing Remarks

We would firstly like to thank the Chief Scientist, Prof. Marcello Vichi for leading the expedition as well as the deputy Chief Scientist, Dr. Thato Mtshali for his guidance and assistance towards setting up our on-board mesocosm experiments. The team would further like to thank SANAP, the organisers, SA Agulhas II & crew, and our PI for the amazing opportunity afforded to us via SCALE.

Due to time constraints and unpleasant weather conditions, our team did not manage to collect water from all stations and depths as initially planned (see tables 1 and 2, and Figure 1). However, the team is grateful for the experience and look forward to further process the samples and generate data and new knowledge that will inform their research.

7 SEASONAL IRON (FE) SPECIATION IN THE SOUTHERN OCEAN

Team name and PI	FE. Thato Mtshali (DFFE), Thomas Ryan-Keogh (SOCCO/CSIR), Hanna Whitby and Pascal Salaun (ULIV)
Authors	Thato Mtshali, Natasha van Horsten, Gareth Kiviets and Gemma Portlock

7.1 INTRODUCTION

The importance of dissolved iron (dFe) in regulating ocean primary production and the carbon cycle is well established (Tagliabue et al., 2012). However, a lack of winter sampling in the Southern Ocean (SO) has resulted in large gaps in our understanding of seasonal variability of productivity and the consequently of the carbon biological pump (Tagliabue et al., 2012; Mtshali et al., 2019). To our knowledge, there is only two reported wintertime studies of dFe (0.2 – 0.45 m fraction) (Ellwood et al., 2008; Mtshali et al., 2019), an essential micronutrient that limits primary productivity in this oceanic region. This deficiency in seasonal observations restricts our understanding of how Fe is supplied to the surface ocean waters in spring, when it fuels primary production. More than 99% of the dFe has been reported to be complexed by organic ligands but no winter-time measurements of organic Fe ligands measurements have been reported in the SO (Wu et al., 2001). The identity of these organic ligands remains largely elusive. It has been recently proposed that humic substances may account for up to the entire ligand pool in certain oceanic regions (Whitby et al., 2020). Despite their potential to be a major player in the Fe cycle, very few measurements of these ligand types exist in the SO (Whitby et al., 2020). Furthermore, very few and no wintertime soluble Fe (SFe) has been reported in the SO (especially in the marginal ice zone (MIZ)).

7.2 AIMS AND OBJECTIVES

The final understanding of the SCALE winter 2022 cruise was that the cruise will depart on the 11th of July 2022 for 3 weeks and be back on the 31st July 2022. Initial ideas suggested that the ship will steam south and be available for scientific work at the winter MIZ stations and at 5 process stations (PS) along GIPY04 transect (see cruise track figure). This will provide an opportunity to address two key questions (highlighted above and our aims below), with the goal of producing publications and facilitating human capital development (HCD). Building from our previous SCALE winter and spring 2019 cruises, the overarching goal of the winter cruise was to improve our understanding of the complex biogeochemistry of Fe and Mn cycling in terms of sources and internal cycling on a seasonal scale in the SO, in both the open ocean and at the winter MIZ. Three aims were proposed for this work:

Aim 1: Focuses on quantifying the bio-physico-chemical processes that control the distributions of dFe pool (physical speciation; soluble and colloidal Fe) and organic speciation (humics), together with other bioactive trace metals (such as manganese (Mn)) in the open ocean and the MIZ.

Aim 2: Focuses on closing the seasonal gaps in the sources, partitioning and distribution of Fe and other trace metals in the SO.

Aim 3: To understand how SO phytoplankton community adapt and response to Fe and Mn co-limitation by conducting 48hrs incubation bioassay experiment

7.3 METHODOLOGY

7.3.1 Sampling Facilities

Trace metal sampling facilities (GEOTRACES CTD rosette equipped with 24 x 12L GoFlo bottles, Kevlar rope with conducting wires, trace metal clean sampling (GoFlo) and sample analysis (FIA) containers) are available at CSIR (Stellenbosch) and on-board the ship.

7.3.2 Sampling and preservations

7.3.2.1 Dissolved Fe (dFe)

Dissolved Fe samples were collected by filtering seawater through a 0.2µm pore size filter (Sartobrun; Separations SA) into acid washed 60ml LDPE bottles (Nalgene, Thermoscientific SA) and immediately acidified with 250µl of 30% Hydrochloric acid ultrapure (HCl; Merck SA) to pH < 1.7. Samples were then preserved at room temperature for further analysis on land using a Flow Injection Analyser with Chemiluminescence detection (FIA-CL; CSIR) or Inductively Coupled Plasma Mass-spectrophotometry (ICP-MS; SUN).

7.3.2.2 Soluble Fe (SFe)

Seawater samples for SFe measurements, we firstly filtered through a 0.2µm pore size filter (similar collection to dFe sampling, but un-acidified) into an acid washed 60ml LDPE bottles and filled to the brim. These samples were then transported to another laboratory (FIA container) for further filtration of SFe through a 0.02µm pore size filter (Whatman Anotop syringe filter; Merck) into a second acid washed 60ml LDPE bottles and immediately acidified to pH < 1.7 using 30% HCl ultrapure (Merck, SA). The samples were stored at room temperature for further analysis on land.

7.3.2.3 Humics

Seawater samples for humics measurements, were collected by filtering seawater through a 0.2um pore size filter (Sartobrun; Separations, SA) into acid washed 125ml LDPE bottles (Nalgene, Thermoscientific, SA) and stored frozen at -20°C until further analysis on land using cathodic stripping voltammetry (CSV).

7.3.3 Fe and Mn addition incubation experiments

Two 48 hour incubation experiments were conducted in the polar upwelling zone (54°S) and in the MIZ at the OD2 station. The GEOTRACES CTD was used to sample seawater within the upper mixed layer (~ 50m) for the incubation experiments. Once the GoFlo bottles were in the trace metal clean sampling container, the exterior of the GoFlo bottles were rinsed with ultra-pure Milli Q water and then inverted three times to ensure a homogenous sample. Water was passed through a 200µm mesh filter to remove grazers from the incubation water sample. Seawater was collected into 250ml acid washed polycarbonate bottles (PC; Armersham; SA), after the bottles had been rinsed three times with seawater. Four treatments were conducted in triplicate; control, +Fe, +Mn, +Fe and Mn, in order to assess the possible Fe and Mn co-limitation of SO phytoplankton during winter. Fe and Mn spike solutions were prepared in 0.01 mol. L^{-1} Ultrapur Hydrochloric acid. To determine initial

conditions samples were collected for trace metals (Fe and Mn), flow cytometry, macronutrient, chlorophyll, and photo-physiology analyses.

All treatments were incubated in customized Minus40 Specialized Refrigeration^{TM} units (MINUS40, SA), equipped with adjustable time- and intensity-controlled LED strips, as well as a temperature control thermostat. Treatments were incubated in clear polyethylene back to minimize exposure to contamination, at in situ temperature and the lowest light levels achievable in the incubators (to be determined on land due to there not being a handheld PAR sensor onboard), under in situ day - night cycle.

Incubation experiments were terminated after 48 hours, sampling for macronutrient, photo-physiology, chlorophyll, and flow cytometry analysis, to determine the effects of the added Fe and Mn on the phytoplankton community sampled.

	PUZ incubation	**OD2 incubation**
Start date and time (GMT)	18/07/2022 10:06	21/07/2022 8:01
Termination	20/07/2022 10:33	23/07/2022 8:15
In situ temperature (°C)	-0.6	-1.6

7.4 PRELIMINARY RESULTS

No preliminary results are currently available. The sampling stations for dFe pool and humics (log-sheets) are presented under TracEx cruise report (Dr. Susanne Fietz)

7.5 FUTURE RECOMMENDATIONS

Trace metal GoFlo sampling container electrical wiring box need to be serviced. Broken GoFlo bottles need to be repaired for spares. Trace metal FIA container need to be serviced. GEOTRACES CTD rosette sensors needs to be calibrated.

References

Ellwood, M., P. Boyd, and P. Sutton, Wintertime dissolved iron and nutrient distributions in the Subantarctic Zone from 40–52S; 155–160E. Geophysical Research Letters - GEOPHYS RES LETT, 2008. 35.

Mtshali, T., et al., Seasonal Depletion of the Dissolved Iron Reservoirs in the Sub-Antarctic Zone of the Southern Atlantic Ocean. Geophysical Research Letters, 2019. 46(8): p. 4386-4395.

Tagliabue, A., et al., A global compilation of dissolved iron measurements: focus on distributions and processes in the Southern Ocean. Biogeosciences, 2012. 9(6): p. 2333-2349.

Wu, J. and E. Boyle, Iron in the Sargasso Sea: Implications for the processes controlling dissolved Fe distribution in the ocean. Global Biogeochemical Cycles, 2002. 16(4): p. 33-1-33-8

8 BIOLOGICAL CARBON PUMP

Team name and PI	BGC-PUMP. Sandy Thomalla (SOCCO/CSIR)
Authors	Lain L, Naicker A, Biyela A, Ruiter L, Mpapane S, and Thomalla S

8.1 INTRODUCTION

The Southern Ocean is a well-established CO_2 sink and plays an essential role in the global carbon cycle, but knowledge of the capacity of the SO to act as a long-term sink will only be revealed upon a better understanding of the impacts of various forcing mechanisms on phytoplankton physiology and community structure.

The measurements undertaken and experiments performed on this SCALE winter 2022 cruise fall generally into addressing the following two (overlapping) aims:

1. A better determination of regionally specific relationships between water optical properties and biogeochemistry for the Southern Ocean, in turn informing on a better estimation of phytoplankton functional types from marine reflectance (i.e. satellite data).
2. Characterizing the response in the phytoplankton community (biomass, carbon content, community structure) to event, seasonal and inter-annual variability in ecosystem physical drivers, facilitating an improved understanding of the interconnectedness between phytoplankton biomass, production, community structure, export potential and CO2 fluxes.

Together, these aims are directed towards an improved ability to predict the long-term responses of the Southern Ocean biological carbon pump to global warming and climate change.

Four student projects, 2 MSc and 2 PhD, were the foci for the Process Stations which provided the opportunity to acquire water samples from different depths via the deployment of both Niskin and Go-Flow bottles on the CTDs, as well as large volumes of water acquired from the deployment of the Marine Snow Catchers. Sample collection for these projects went ahead as planned despite some equipment setbacks which will be detailed in the relevant sections. Samples for the routine biogeochemical measurements of Chl a concentration, Particulate Organic Carbon, Dissolved Organic Carbon, particle size distribution, particulate absorbance and High Performance Liquid Chromatography (HPLC) pigment analysis were also collected, also with some shortcomings as will be described.

However, the suite of under way optical and biogeochemical measurements originally planned for this cruise for linking the optical properties to carbon content, size distribution and taxonomic composition of algal communities, were not made due to the malfunctioning of the under way scientific water supply, effectively rendering this part of the measurement campaign impossible. Measurements accounted for in the pre-cruise planning of the CTD water budget went ahead at stations, unfortunately no backscatter measurements could supplement the station measurements as the water requirement for the BB3 (minimum 3 litres) exceeded the water budget constraints.

8.2 Routine Measurements (all stations)

8.2.1 Chlorophyll a concentration

A fluorometric method was used to measure [chl *a*] as per Welschmeyer *et al*., (1994). 500 ml water samples from each available CTD depth were filtered through a Whatmann 0.7 µm 25mm glass fibre (GF/F) filter, extracted in 8 ml 90 % acetone at -20°C for 12-24 h. Fluorescence was measured on a Turner Trilogy Benchtop Fluorometer (non-acidification module) and converted to chl *a* using a standard dilution calibration.

Chl a concentration was measured at each deployment of the CTD, at the top 6 CTD depths of 5, 20, 50, 75, 100, 125 and 150 m. Given the lack of functioning fluorometer on the CTD, these data will be made available for use by all Teams.

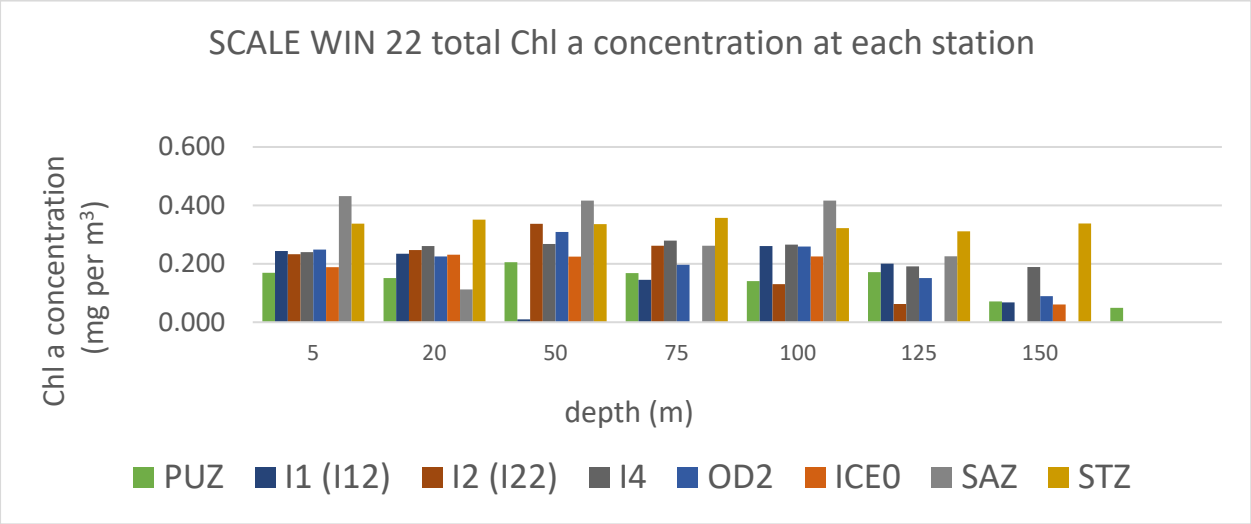

8.2.2 Particulate & Dissolved Organic Carbon

Seawater was collected from the top 6 CTD depths at each station. Approximately 2 L seawater was filtered through 25 mm ashed (pre-combusted) GF/Fs (0.7 µm nominal pore size). The ashed filters were combusted in a muffle furnace at 400°C overnight, prior to the cruise. Following filtration, filters were placed into petri-dishes and incubated at 50°C for 24 h. Filters were then placed in a fume hood, in a desiccation chamber that contained a beaker of concentrated HCl, at room temperature for 24 h. Filters were then stored for punching and folding into tin cups, for analysis on land. The filtrate was also filtered onto pre-combusted GF/Fs and followed the same treatment to give an approximation of the dissolved inorganic carbon (DOC) that is adsorbed onto the filter during the filtration process.

8.2.3 Particulate Absorbance

Seawater was collected from the top 6 CTD depths at each station. Approximately 2 L seawater was filtered through 25 mm GF/Fs (0.7 µm nominal pore size). Filters were placed in petri-dishes, flash frozen in liquid nitrogen, wrapped in tin foil and stored at -80°C for analysis on land.

8.2.4 Particle Size Distribution

Unfortunately, a catastrophic malfunction of the Coulter Counter was discovered immediately prior to the cruise, leaving no time for repair before departure, so this instrument was not brought on

board. Size distribution and community characterisation data will instead be shared by L. Haraguchi (SYKE) for the samples that were processed as part of her own data campaign. It is not yet clear for which stations and depths these data will be available following processing, but it is understood that as a minimum, surface (5 m) measurements were performed at each station. These data will give an indication at least of broad scale changes in community composition with latitude.

8.2.5 HPLC

Seawater was collected from the top 6 CTD depths at each station and filtered through 25 mm GF/Fs (0.7 µm nominal pore size). Filters were placed in cryo-vials before being flash frozen in liquid nitrogen and stored at -80°C, for shipment to France and further analysis.

Figure 31 25 mm filtration unit set-up & training, Wet Lab. Photo credit: L. Ruiters

8.3 Student Projects

8.3.1 Optical effects of photophysiological changes in Southern Ocean phytoplankton (S. Mpapane, for MSc)

8.3.1.1 Background & Rationale

The Southern Ocean is a well-established CO_2 sink and plays an essential role in the global carbon cycle. The in situ examination of the influence of seasonal cycles and physical drivers on biological production is often spatially and temporally limited.

Remote sensing has allowed for regional characterisation by providing routine, synoptic and cost-effective observations at a high frequency and over decadal time scales. Most often remotely sensed data are the only systematic observations available for chronically under-sampled marine environments (e.g. the polar oceans), and there is thus a need to maximise the value of these observations by developing ecosystem-appropriate, well-characterised products.

Phytoplankton absorption spectra in the Southern Ocean (SO) is observed to be distinctively depressed compared to other oceans. These unique phytoplankton optics in the SO are attributed to it being a highly dynamic light and nutrient environment. Changes in growth conditions invites a photophysiological response in phytoplankton – where the intracellular chlorophyll density (ci) in phytoplankton cells is altered to best suit the new growth environment. A greater understanding of SO phytoplankton inherent optical properties (IOPs) is required to improve characterization of the optical variability observed in the SO. To address this, a series of in situ experiments are needed to assess the range of variability of the above mentioned IOPs and ci across different growth conditions. Furthermore, an Equivalent Algal Populations (EAP) model for phytoplankton optics will be used to systematically illustrate the impact of a dynamic growth environment on phytoplankton optical properties.

8.3.1.2 Measurements

In order to address the in situ aspects on the above mentioned, several station filtrations were performed in the SO during the SCALE 2022 winter cruise. These experiments included measurements of size fractionated chlorophyll a concentrations, where analysis was carried out using fluorometry on board and other samples were collected for further pigment analysis to be done using (High Performance Liquid Chromatography) HPLC on land. In addition, samples were also collected for size fractionated particulate absorption (PAB), dissolved organic carbon (DOC), and particulate organic carbon (POC).

Furthermore, incubation experiments were also performed on seawater samples obtained at each process station. These experiments were designed to investigate the impact on phytoplankton optical properties when growth stress is relieved, either by increasing light levels to reduce photoacclimation, and/or by relieving iron stress on phytoplankton growth. 4 scenarios were investigated following the measurement of initial conditions:

1. Light levels increased, iron stress relieved
2. Light levels increased, ambient iron maintained
3. Ambient light maintained, iron stress relieved
4. Ambient light maintained, iron stress maintained

Each scenario was incubated for 24 - 48 hours. Upon termination of each incubation, filtration experiments were once again performed to measure the resulting chlorophyll a concentration, and PAB. It is theorised that will sufficient cell counts so as to ensure measurements larger than the standard deviation of measurement error, changes in the chl a concentration and phytoplankton absorption spectra following each incubation may be observed. However, in conditions displaying such low chl a concentrations, it remains to be ascertained if these changes were of sufficient magnitude to be observable.

It should be noted that the experiments for the first two Process Stations were completed using trace metal clean water from the Go-Flow. The remainder of the incubations were performed with Niskin water.

Figure 32 Niskin water collection: S. Mpapane (left) & A. Biyela (right). Photo credit: L. Lain

8.3.2 Analysis of the sources of variability in photophysiological parameters derived from phytoplankton fluorescence in the Southern Ocean (L. Ruiters, for MSc)

8.3.2.1 Background & Rationale

There is an increasing necessity to better understand and quantify primary production in the Southern Ocean due to the disproportionate importance of this ocean in carbon cycling (drawing down 33% of the annual global organic carbon flux). Active chlorophyll fluorescence techniques can be used to accurately estimate rates of primary production in marine phytoplankton through the derivation of electron transport rates which are a measure of photosynthetic capacity. Fast repetition rate fluorometry can be used to measure active chlorophyll fluorescence and is autonomous, instantaneous, *in vivo*, non- destructive, and has high spatial and temporal resolution. However, in the absence of standardisation and agreed upon best practices in the field of fluorescence research, comparing measurements of primary production is not straightforward. This hampers the goal of having a global inter-comparable dataset which would enable the identification of large-scale patterns in primary production and limits our ability to accurately predict and model future changes in primary production. Given that there are many uncertainties in the derivation of the photophysiological parameters needed to quantify rates of primary production, this work aims to identify the drivers of variability through: 1) a statistical comparison of various algorithms to determine the degree of variability resulting from mathematical differences, and 2) determining the dominant ecological drivers of variability.

8.3.2.2 Methodology

Variable chlorophyll fluorescence measurements of the parameters Fv/Fm, σPSII and ETRs were performed using a Chelsea Scientific Instruments FastOceanTM FRRf integrated with a FastActTM laboratory system. Seawater was collected from six different depths at all CTD stations. Samples were acclimated at *in situ* temperatures before measurement, undergoing dark acclimation for 30 minutes. Triplicates were conducted for each sample with corresponding blanks using 0.2 µm filtrates (Cullen & Davis 2003). FRRf measurements used a single turnover (ST) protocol with a saturation sequence (100 x 2 µs flashlets with a 2 µs interval) and a relaxation sequence (25 x 1 µs flashlets with an interval of 84 µs), with a sequence interval of 100 ms repeated 32 times, therefore total acquisition times was 3.2 s. The excitation LED (λ450 nm) power was adjusted between samples in order to saturate the observed fluorescence transients (following manufacturer specifications), but was kept constant during FLCs.

Co-located ancillary data will be used to determine the potential ecological drivers of variability in phytoplankton community structure, using HPLC and Chl a concentration data.

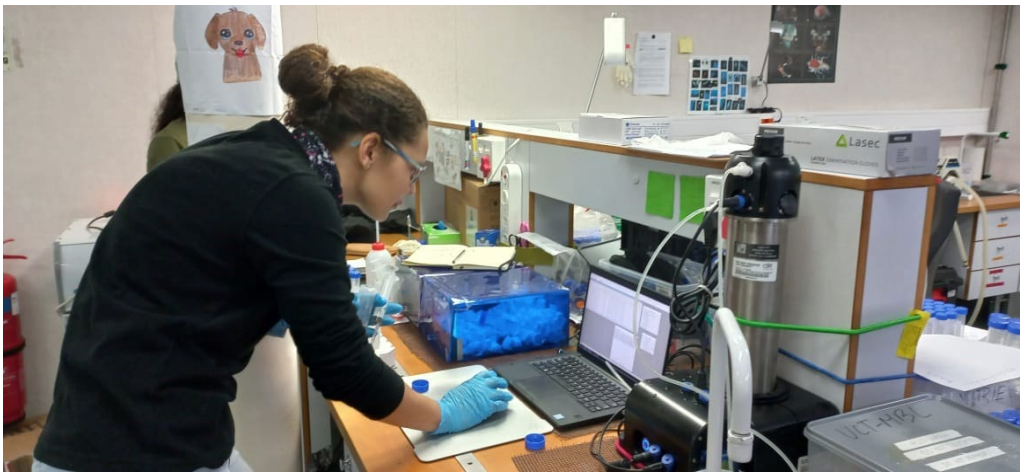

Figure 33 L. Reuters & the Fast Repetition Rate Fluorometer (FRRF). Photo credit: L. Lain

8.3.3 Investigating the Dominant Controls of Carbon Export in the Southern Ocean (A. Naicker, for PhD)

8.3.3.1 Background & Rationale

In the Southern Ocean, the biological carbon pump (BCP) is driven by phytoplankton productivity and is an effective organic matter sink. There is evidence showing 1) particle composition impacts carbon export 2) there is a relationship between particle size and sinking rates and 3) sinking particulate organic matter sustains microorganisms with different ecological strategies, but there is a paucity of mechanistic insights with regards to these factors, the variability due to seasonal and regional changes and the influence these factors have on the efficiency of the BCP and microbial carbon pump (MCP).

When phytoplankton die and sink they remove carbon from the surface waters driving a partial pressure gradient at the ocean-atmosphere interface, which drives the uptake of more atmospheric CO2 (Henley et al, 2020). Sinking particles (or aggregates), are considered the primary component of the BCP responsible for transporting carbon from the upper ocean to the deep ocean (Durkin et al, 2021). The transported amount of carbon is difficult to quantify in part due to the complex

ecological interactions that generate particles and the variety of pathways that carbon can take on its way to the deep ocean (Durkin et al, 2021). Each of these factors varies seasonally and regionally (Henson et al, 2019) and it is not known how they interact to drive carbon export in the relatively understudied Southern Ocean (Henson et al, 2019). To further complicate the process, carbon can transition from one particle pool to another as it sinks through the mesopelagic and interacts with grazers and microbes. These particles are thought to transport carbon with differing efficiencies through the mesopelagic zone. As we understand more regarding the types of particles and the sinking process through the water column, we will be able to better predict the magnitude of carbon flux and its attenuation with depth (Durkin et al, 2021).

In the marine environment, most organic material that results from photosynthesis in the surface ocean is, more often than not, biologically labile and acts as substrate that supports vast prokaryotic populations. Microbes degrade POC to Dissolved Organic Carbon (DOC) and simple DOC to Dissolved Inorganic Carbon (DIC). This process reduces the amount of Particulate Organic Material being exported to the depth. Although labile DOC is produced in great abundance, it has a very short life time ranging from hours to days, being rapidly consumed by heterotrophic prokaryotes and is quickly respired back to CO_2 in support of the microbial loop (Azam et al, 2016), therefore limiting its contribution to the global inventory of DOC.

Even though the greater majority of NPP passes through the labile DOC fraction, a small fraction of the labile DOC is transformed, either biotically (by microbes) or abiotically, to resistant material that accumulates as residual biologically recalcitrant dissolved organic carbon (RDOC) or refractory DOC (rDOC) (Ogawa et al, 2001). Due to the degradation resistance, RDOC can be maintained in the ocean for decades to millennia (Ogawa et al, 2001; Jiao et al, 2014) thus contributing to the large ocean inventory of DOC. Both structural recalcitrance and huge molecular diversity of DOC compounds present below microbial uptake thresholds of picomolar or subpicomolar concentrations, that evade further consumption (Mentges et al, 2017; Jiao et al, 2018; Zark and Dittmar, 2018; Noriega-Ortega et al, 2019). Current estimates suggest that carbon stored over long time scales through the MCP is approximately 0.4% of the annual oceanic Primary Production, while the amount of carbon exported by the BCP over 2000 m depth ranges from 0.6% to 1.3% of annual primary production (Legendre et al, 2015).

Notwithstanding the great research efforts, neither the BCP or MCP has achieved full understanding regarding their respective quantitative contribution to climate modulation and the environmental and biological factors that may control their contributions and dynamics (Boyd et al, 2015; Robinson et al, 2018). Any trajectory in the efficiency of the Southern Ocean's BCP and MCP would necessarily reflect the integrated impact of a complex suite of concurrent physical, chemical and biological processes (Caron and Hutchins, 2013). The rationale for the research conducted is to develop a better understanding of the role of particle size, ballasting and the activity of microbes in dictating carbon export efficiency and transfer efficiency in the Southern Ocean.

This will be achieved by addressing the following key research questions:

1) Does the composition of the particles produced through Primary Production aid in more effective carbon export and transfer specifically with regards to ballasting by measuring how much Biogenic Silica (BSi) and Particulate Inorganic Carbon (PIC) there is in settling material?

2) How does particle size impact sinking rates?

3) How does microbial community composition and functional activity impact carbon export efficiency and transfer efficiency?

4) Do we observe regional and seasonal changes in the role of particle content, sinking rates and microbes in dictating carbon export and transfer efficiency?

8.3.3.2 Methodology: MSC Deployment

The Marine Snow Catchers were deployed at 10 m below the MLD and at 100 m below the MLD as per the method described by Riley et al (2012). After 2 hours of settling a suspended sample was collected from the top of the MSC, while a sinking sample was collected from the bottom of the MSC. These samples (suspended and sinking) were subdivided into aliquots for Particulate Organic Carbon (POC)/ Particulate Organic Nitrogen (PON), Particulate Inorganic Carbon (PIC), Biogenic Silica (BSI) and metagenomics using a Folsom splitter. Samples for POC/PON analyses (~2 l) were filtered onto pre-combusted (450°C. 12h) glass fibre filters (47 mm diameter GF/F Whatman) using a vacuum filtration pump. The resultant filters were placed in sterile petri-dishes and oven dried overnight at 25°C. An acid fumigation using concentrated hydrochloric acid was conducted overnight to remove inorganic carbon. Filters were then stored for punching and folding into aluminium tin cup foils on land. Samples for BSi (~1 L) and PIC (~1 L) were filtered through 10 µm and 0.4 µm filters respectively (47 mm (diameter) polycarbonate membrane) placed in sterile petri-dishes, oven dried overnight at 25°C, wrapped in tin foil and stored in zip lock bags with silica balls for later analysis.

It was noted on the first deployment of the MSCs that one of the support stands was warped out of alignment and the instrument could no longer be safely secured upright. With the assistance of technicians from DFFE, a makeshift stand was improved and the first deployment was undertaken without incident. During the retrieval of the MSC during the second deployment however, the full cartridge was unstable on its stand and toppled over onto the supporting crew, fortunately without serious injury. Following some discussion the deployments did continue, but with a lot of additional strapping and support which took additional time at each deployment. This is a considerable safety issue and needs attention and remedy before any future deployment of the MSCs.

Figure 34 Prepping the Marine Snow Catcher for deployment. The messenger trigger mechanism requires careful handling. Photo credit: L. Lain

8.3.4 The impacts of ocean acidification and increasing temperatures on phytoplankton primary productivity, physiology, and nutrient uptake (Attang Biyela, for PhD)

8.3.4.1 Background & Rationale

With climate change being an imminent threat to the functioning of marine ecosystems and biogeochemical cycling, it is important to try and elucidate the potential effects that warming and an increase in CO_2 could have on important processes. It is anticipated that with an increase in the amount of CO_2 in the ocean from the current ~400ppm to ~900ppm, the acidity of the ocean will drop to a pH of 7.8 by the end of the century from a current pH of 8.1, this is known as ocean acidification (OA). OA has the potential to bring about changes that could possibly affect the efficiency of the biological carbon pump, which has been instrumental in controlling the level of CO_2 in the atmosphere on glacial/interglacial timescales (Sigman and Boyle, 2000). It is currently uncertain how increasing temperature and OA will affect the BCP. The availability of macronutrients that phytoplankton use to photosynthesise may also be affected by OA, and with phytoplankton being the drivers of the BCP, it is important to try and understand the potential effects to decrease uncertainties.

There have been multiple studies that have looked at the effects of single drivers (e.g., OA alone) on either biogeochemical cycling, phytoplankton physiology or phytoplankton productivity. Although insightful, it is difficult to extrapolate the findings of these studies and apply them generally to entire ocean ecosystems because of their specificity. This then brings about the need for studies that test the effect of multiple drivers on entire phytoplankton communities and biogeochemical cycling. The main aim of this PhD research project is to assess the impacts of OA on phytoplankton physiology, productivity and biogeochemical cycling using multiple driver manipulations on Southern Ocean phytoplankton communities.

There is a need to increase the number of multiparameter studies in the Southern Ocean because most analyses use single parameter studies. Multiparameter studies are important because the changes in ocean factors associated with climate change will be acting on the ocean and phytoplankton communities simultaneously. Multiple stressors acting across a range of climate change scenarios will help us better understand changes in the Southern Ocean. Moreover, most data collected in the Southern Ocean is collected over summer, there is a lack of year-round data which will aid in better understanding the dynamics of phytoplankton biology and biogeochemical cycling all year-round.

The solubility of carbon dioxide in the ocean increases with a decrease in temperature. Consequently, the rise in sea surface temperatures will reduce the solubility of carbon dioxide, and lead to a decrease in the DIC pool which supplies the biological carbon pump (BCP). It is estimated that this positive feedback alone will reduce the ocean's carbon sequestering ability by as much as 15% by the end of the 21st century (Riebsell et al, 2009). These perturbations to the solubility pump will ultimately affect the BCP, which is responsible for the remainder of the surface to depth DIC gradient (Riebsell et al, 2009).

The main aim of this research project is to examine the combined effects of temperature and ocean acidification on phytoplankton primary production, nutrient uptake, physiology, and community structure in the Southern Ocean using multiple driver manipulation experiments. This will be achieved through the following objectives:

1) Manipulating temperature and pH in seawater samples to projected RCP future levels.

2) Measuring phytoplankton productivity under increased temperature and pH levels.

3) Measuring phytoplankton nutrient uptake under increased temperature and pH levels.

4) Assessing phytoplankton physiology and community structure under future temperature and pH levels.

8.3.4.2 Methodology

Seawater was collected at each station and was filled into a series of polycarbonate bottles after being filtered through a 200µm net.

Temperature and pH treatment

The pH level was adjusted in line with the projected pH for the year 2100, which is approximately 7.9. The seawater pH was adjusted through the addition of equimolar HCl and $NaHCO_3$. For the temperature and combined temperature and pH treatments, bottles were placed in an incubator set to +2℃ more than the in-situ temperature. All experiments were incubated in light-controlled fridges which simulate surface light levels. Initial pre-conditioning incubations were run for approximately 24 - 48 hours before radioisotopic tracers were added (see next section) to determine primary production and nitrate uptake. To determine whether pH levels were achieved separate samples were collected after initial manipulation and at the end of the incubations to measure DIC and total alkalinity.

Primary production and nutrient uptake

To measure primary production, nutrient uptake, and nitrification, a series of radioisotopic tracers were used, namely $^{15}NO_3^-$, $^{15}NH_4$ and $^{13}NaHCO_3$. Primary production and nutrient uptake were measured following 24 hours of incubation and termination by size fractionated filtration onto ashed GF/F filters. The size fractions include >20 µm, 20 - 2.7 µm and 2.7 - 0.3 µm. These samples were oven dried and acid fumed before being stored until analysis on land using an elemental analyser at the University of Cape Town. Nitrification was assessed by filling 50 mL tubes after initial spiking with the radiotracers and again after 24 hours of incubation. The samples were frozen at -20℃ to be analysed using a mass spectrometer at the University of Cape Town.

Chlorophyll a

Chlorophyll-a was measured by size fractionation using the same size filters as above, with the filters placed into 90% acetone for 24 hours in a freezer at -20℃. Samples were then analysed using a Turner Designs Trilogy fluorometer which has been calibrated using standards.

Community Structure

Community structure was assessed using an imaging flow cytometer (cf L. Haraguchi, Chap. 10).

Phytoplankton Physiology

Phytoplankton physiology was assessed using active chlorophyll fluorescence measured by a Fast Repetition Rate fluorometer. Samples were taken from each treatment and placed into a low light (~10 µmol photons m-2 s-1) for 30 minutes before being measured using a single turnover protocol. Blanks were measured following careful filtration through a 0.2µm syringe filter. All data will be

processed using the Python package Phytoplankton Photophysiology Utilities (Ryan-Keogh & Robinson, 2021).

References

Azam F, Smith DC, Hollibaugh JT (2016). The role of the microbial loop in Antarctic pelagic ecosystems. *Polar Res* **10:** 239-244.

Boyd PW, Lennartz ST, Glover DM, and Doney SC (2015). Biological ramifications of climate-change-mediated oceanic multi-stressors. Nat. Clim. Change 5, 71–79. doi: 10.1038/nclimate2441

Caron DA, Hutchins DA (2013). The effects of changing climate on microzooplankton grazing and community structure: drivers, predictions and knowledge gaps. *J Plankton Res* **35:** 235-252.

Cullen, J.J. and Davis, R.F., 2003. The blank can make a big difference in oceanographic measurements.

Durkin CA, Buesseler KO, Cetinić I, Estapa ML, Kelly RP, & Omand M (2021). A visual tour of carbon export by sinking particles. Global Biogeochemical Cycles, 35, e2021GB006985. https://doi.org/10.1029/2021GB006985

Figure 35 Geotraces work: A. Biyela. Photo credit: L. Ruiters

Henley SF, Cavan EL, Fawcett SE, Kerr R, Monteiro T, Sherrell RM, Bowie AR, Boyd PW, Barnes DKA, Schloss IR, Marshall T, Flynn R and Smith S (2020). Changing Biogeochemistry of the Southern Ocean and Its Ecosystem

Henson S, Le Moigne F, & Giering S (2019). Drivers of carbon export efficiency in the global ocean. Global Biogeochemical Cycles, 33, 891–903. https://doi.org/10.1029/2018GB006158

Jiao NZ, Robinson C, Azam F, Thomas H, Baltar F, Dang H, *et al* (2014).Mechanisms of microbial carbon sequestration in the ocean – future research directions. Biogeosciences 11, 5285–5306. doi: 10.5194/bg-11-5285-2014

Jiao, NZ, Cai RH, Zheng Q, Tang K, Liu JH, Jiao FLE, *et al* (2018). Unveiling the enigma of refractory carbon in the ocean. Natl. Sci. Rev. 5,459–463. doi: 10.1093/nsr/nwy020

Legendre L, Rivkin RB, Weinbauer MG, *et al* (2015). The micro- bial carbon pump concept: potential biogeochemical significance in the globally changing ocean. Prog. Oceanog., 134, 432–450.

Mentges A, Feenders C, Seibt M, Blasius B, and Dittmar T (2017). Functional molecular diversity of marine dissolved organic matter is reduced during degradation. Front. Mar. Sci. 4:194. doi: 10.3389/fmars.2017. 00194

Noriega-Ortega BE, Wienhausen G, Mentges A, Dittmar T, Simon M, and Niggemann J (2019). Does the chemodiversity of bacterial exometabolomes sustain the chemodiversity of marine dissolved organic matter? Front. Microbiol. 10:215. doi: 10.3389/fmicb.2019.00215

Ogawa H, Amagai Y, Koike I, Kaiser K, and Benner R (2001). Production of refractory dissolved organic matter by bacteria. Science 292, 917–920. doi: 10.1126/science.1057627

U. Riebsell, A. Kortzinger, and A. Oschlies. (2009). Sensitivities of Marine Carbon Fluxes to Ocean Change. *Proceedings of the National Academy of Sciences of the United Statesof America*. 106:49, 20602-20609. https://doi.org/10.1073/pnas.0813291106

Riley JS, Sanders R, Marsay C, Le Moigne FAC, Achterberg EP, Poulton AJ (2012). The relative contribution of fast and slow sinking particles to ocean carbon export. *Global Biogeochem Cycles* **26**.

Robinson C, Wallace D, Hyun JH, Polimene L, Benner R, Zhang Y, *et al* (2018). An implementation strategy to quantify the marine microbial carbon pump and its sensitivity to global change. Natl. Sci. Rev. 5, 474–480. doi: 10.1093/nsr/nwy070

T.J. Ryan-Keogh and C.M. Robinson. (2021). Phytoplankton Photophysiology Utilities: A Python Toolbox for the Standardization of Processing Active Chlorophyll-a

D.M. Sigman and E.A. Boyle. (2000). Glacial/interglacial variations in atmospheric carbon dioxide. *Nature* 407, 859-869. https://doi.org/10.1038/35038000

Welschmeyer, N.A., 1994. Fluorometric analysis of chlorophyll a in the presence of chlorophyll b and pheopigments. *Limnology and oceanography*, *39*(8), pp.1985-1992.

Zark M, and Dittmar T (2018). Universal molecular structures in natural dissolved organic matter. Nat. Commun. 9:3178. doi: 10.1038/s41467-018-05665-9

9 NITROGEN CYCLE: NITROGEN CYCLING IN THE UPPER SURFACE SOUTHERN OCEAN

Team name and PI	N-CYCLE. Sarah Fawcett (UCT) and David Walker (CPUT)
Authors	Mdutyana M, Deary A, Yapi S, Monteiro C, Rawat S, Esau A, van Balla V, Maholobela N, Kalyan B, Walker D, and Fawcett S

9.1 INTRODUCTION

Biological carbon production in surface waters followed by organic carbon export to depth (i.e., via the "biological pump") is a major contributor to the Southern Ocean's carbon dioxide (CO_2) sink, removing an estimated 3 Pg of carbon from surface waters south of 30°S annually (~33% of the global ocean's organic carbon flux) (Schlitzer, 2002; Takahashi et al. 2002). This mechanism, combined with physico-chemical processes, makes the Southern Ocean the most important oceanic region for natural and anthropogenic CO_2 removal (Sabine et al. 2004; Devries 2014; DeVries, Holzer, and Primeau 2017; Frölicher et al. 2015). My recent work has shown that the seasonal cycle of primary production in the Southern Ocean is separated between regenerated production in winter and new production in summer – in other words, nitrate uptake by phytoplankton is dominant in summer while winter is dominated by nitrification (Mdutyana et al. 2020). An important implication of this is that, because some fraction of the nitrate regenerated in the winter mixed layer is supplied to phytoplankton in the following spring and summer, its consumption cannot be equated with export.

Iron is the primary limiting micronutrient across most of the Southern Ocean (e.g., de Baar et al. 1990; Moore et al. 2013). It is required during photosynthesis for the functioning of photosystem I and photosystem II (Raven et al. 1999; Shi et al. 2007) and the nitrate and nitrite reductase enzymes require iron to reduce nitrate to ammonium during assimilation (de Baar et al. 2005). The role of iron during nitrate uptake has been examined fairly extensively in the Southern Ocean (e.g., (Van Leeuwe et al. 1997; Ryan-Keogh et al. 2017), but nothing is known about how iron affects other N cycle processes like ammonium oxidation. Although there is reasonable consensus among current biogeochemical and ecosystem models that Southern Ocean primary productivity will increase in future, largely as a function of increased iron supply, along with increased light availability and warming (Bopp et al. 2013; Leung et al. 2015; Moore et al. 2018; Boyd et al. 2019), no models

integrate the iron response of other biogeochemical processes that can affect primary production and carbon export, such as nitrification.

As the substrate for ammonium oxidation, the supply of ammonium should exert a strong control on the rate of nitrification. The ammonium concentration in the upper Southern Ocean is relatively high and accumulates southwards during winter (to >1.6 µM). For ammonium to accumulate to such high concentrations, the rate of its production must far outpace the rate of its removal by assimilation and oxidation. Under these conditions, the Southern Ocean mixed layer is likely net heterotrophic and a CO_2 source to the atmosphere (Mdutyana et al. 2020; Mdutyana et al. 2022). Mdutyana et al (2022) has shown that ammonium oxidation does not increase in response to increasing ambient ammonium concentrations or to changes in temperature, light, macronutrients, or ammonium uptake rate (i.e., competition with phytoplankton for ammonium). This has led to the hypothesis that the dominant control on ammonium oxidation may be iron availability given recent culture work showing that ammonium oxidation by *Nitrosomopumilus maritimus* requires elevated iron concentrations (Shafiee et al. 2019). However, the effect of dissolved iron on ammonium removal processes like nitrification and uptake by phytoplankton has not been examined in the Southern Ocean. Systematically examining the effect of iron on ammonium oxidation is an important step towards fully understanding the role of iron in the Southern Ocean's N cycle. As the iron supply to the Southern Ocean increases with climate change (IPCC, 2019), nitrification may become more favourable in the winter mixed layer, particularly given the apparently non-limiting ammonium concentrations (Mdutyana et al. 2020). This has implications for carbon export since nitrate produced in the winter mixed layer supports some phytoplankton growth in summer.

The ammonium uptake can be affected by the co-occurring process of ammonification of unlabeled particulate organic N that causes dilution ^{15}N of the ammonium pool (Glibert et al. 1982). The occurrence of this process leads to underestimation of rates either uptake or oxidation rates and eventually affects the application of the new production paradigm (Glibert et al. 1982). This process occurs in significant amounts in much of the global ocean, the Southern Ocean only has a single study to date (Goeyens et al. 1991). Therefore, quantifying this process in the open Southern Ocean will present a good measure to account for under and/or over estimation of export production in the future.

Nitrifying organism community composition and distribution in the open ocean has been widely documented and AOA generally dominates over AOB (Beman, Popp, and Francis 2008; Lam et al. 2009; Newell et al. 2011; 2013; Buchwald et al. 2015) although the depth distribution of these

organisms appears to vary depending on the region (Mincer et al. 2007; Church et al. 2010;Beman et al. 2012; Newell et al. 2013; Shiozaki et al. 2016). However, in the Southern Ocean, while limited direct measurements of nitrification have been conducted (Olson 1981; Bianchi 1997; Cavagna et al. 2015; Mdutyana et al. 2020), there are no data on nitrifier community composition and distribution. It is possible that the composition of the AOA/AOB community will affect the response of nitrification to iron, which argues for examining in situ Southern Ocean community composition and distribution in conjunction with biogeochemical rate measurements.

9.2 NITROGEN SPECIES SAMPLING

9.2.1 Field collections

Seawater samples: Several stations were sampled across the different frontal zones of the Southern Ocean to fully represent the changing biogeochemical conditions of the Southern Ocean. Seawater samples were collected from the underway system and CTD casts (see Figure 36). Various parameters were collected from the underway system and CTD casts; from the underway system samples for NH_4^+ concentration analysis were collected from 34°S until 58°S every four hours, while from the CTD casts seawater samples to measure nutrients (NO_3^-, NO_2^-, phosphate (PO_4^{3-}), silicate and NH_4^+), NO_3^- isotopes, NH_4^+ isotopes, and particulate organic nitrogen (PON) were collected from either Niskin or Go-Flo cast (see table 1). NH_4^+ concentration samples were analysed onboard the *SA Agulhas II*, while the rest of the samples will be analysed at the Marine Biogeochemistry Lab at the University of Cape Town.

Ammonium (NH_4^+) and nitrite oxidation in the upper water column: ^{15}N-tracer experiments were collected to measure the rates of NH_4^+ and NO_2- oxidation from 7 depths (20 m to 500 m). Samples were collected from each depth through a 200um shower into a 2 L HDPE bottle and filled to 1.5 L volume which were then spiked with either $^{15}NH_4^+$ or $^{15}NO_2^-$, then each 1.5 L bottle was dispensed into 4 x 250 mL dark HDPE bottles then incubated for 24 hours, 50 mL subsamples were removed at different timepoints (0 hours (immediately after the addition of the ^{15}N tracer (NH_4^+ or NO_2^-)), 12 hours, and 24 hours) during incubation. Samples were filtered through a 0.2 um filter to remove possible bacterial presence and stored in a -20°C freezer.

Ammonium (NH_4^+) oxidation: ^{15}N-tracer experiments were conducted to measure the rates of NH_4^+ oxidation at different iron concentrations *(*Figure 37*)*. The ^{15}N-tracers were treated with Chelex-100 resin to remove trace metal (TM) contaminants (Price et al. 1989). Experiment samples were collected from the MLD at each station. The experiments had four iron concentrations: zero (via the

addition of a chelator, desferrioxamine B (DFB), seawater DFe was made biologically unavailable), ambient (no iron added or removed), intermediate (ambient+0.2 nM), high (ambient+2.0 nM).

Seawater was collected in teflon-coated GoFlo bottles attached to a TM-clean CTD rosette (epoxy coated aluminium frame with titanium bolts. All 14 x 500 mL clear HDPE bottles from each treatment (Zero, Seawater DFe, ambient+0.2 nM and ambient+2 nM) were amended with iron (or iron-chelator) to yield low, ambient, intermediate, and high iron, as outlined above and incubated for 24 hours (for nitrifiers to acclimatization to the new DFe concentrations). After the initial 24 hours incubation, each iron concentration at each, triplicate 500 mL transparent polycarbonate bottles were amended with $^{15}NH_4^+$. $^{15}NH_4^+$ tracer was added at ~10% of the ambient concentration, estimated based on past measurements (e.g., Mdutyana et al. 2020). Prior to incubation immediately after the addition of $^{15}NH_4^+$, 40 mL subsamples (zero hours: T_1) were collected from all NH_4^+ oxidation bottles and frozen at -20°C. Bottles were incubated for 36 hrs in order to capture a full diurnal cycle and subsamples were collected at different timepoints (12 hours: T_2, 24 hours: T_3, and 36 hours :T_4). All samples were incubated inside the walk-in 5°C fridge

Nitrogen oxidizing organism gene abundance: Seawater for AOA and AOB community composition were collected CTD and GoFlo casts. Water samples (2 L collected in dark bottles) were collected from the same depths as the nitrification samples. Samples were filtered onto 0.2-µm-pore Sterivex filters. Samples were then be frozen immediately in liquid nitrogen and stored at -80°C until analysis ashore.

$^{14}NH_4^+$dilution of the $^{15}NH_4^+$ during NH_4^+ removal processes: Seawater samples were collected from the underway system. Two 20 L of seawater were collected from the underway system into 2 X 25 L carboys, one 20 L seawater was spiked with $^{15}NH_4^+$ tracer according to Mdutyana et al. 2022 kinetic parameters of NH_4^+ oxidation in the wintertime Southern Ocean and the other 20 L was not spiked with anything. From each 20 L 15 x 1 L clear HDPE bottles were collected immediately after the addition of the $^{15}NH_4^+$ tracer to the spiked 20 L carboy. The carboys were incubated for 5 days and sampled every 24 hours from the time of incubation. A variety of subsamples (1 X 50 mL centrifuge tube for NH_4^+ oxidation analysis, 2 X 40 mL HDPE bottles for NH_4^+ concentration analysis, 250 ml dark HDPE bottle for NH_4^+ isotope analysis, and a GF/F filter was collected by filtering 400 mL of) were collected at time zero (i.e., immediately after the addition of $^{15}NH_4^+$). Every at 24 hours three 1 L bottles from each treatment (Carboy with $^{15}NH_4^+$ added and Control (carboy without addition of $^{15}NH_4^+$)) from each 1 L bottle the same subsamples were collected as mentioned above.

McClane Pump: The pump was deployed at all process stations around the mixed layer depth.

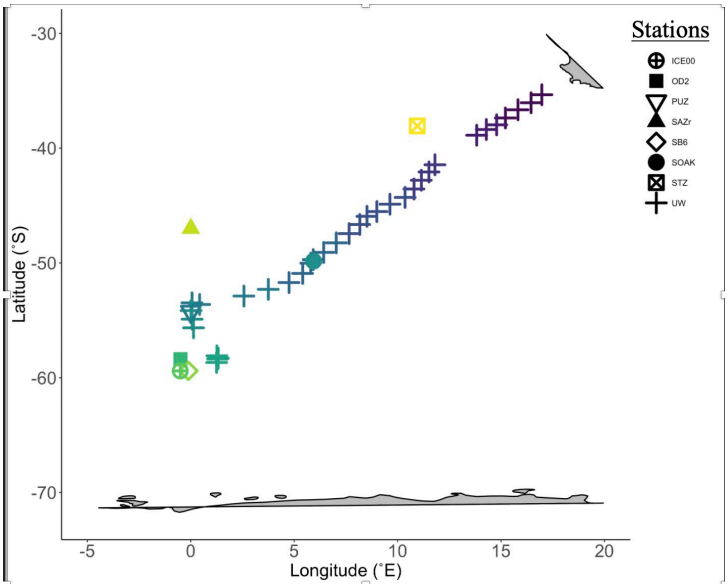

Table 1: List of parameters collected from selected CTD casts							
Station	**Nutrients**	**d15N-Nitrate**	**PON isotopes**	**Ammonium**	**d15N-NH4**	**Nitrification**	**Nitrif. comm. Comp**
PUZ(PS)	X	X	X	X	X	X	X
ICE22(I2)	X	X	X	X	X	X	X
OD-2	X	X	X	X	X	X	X
SB06(I0-PS)	X	X					
SAZR(PS)	X	X	X	X	X	X	X
STZ(PS)	X	X	X	X	X	X	X

Figure 36 Position of stations sampled and the transect of the underway sampling

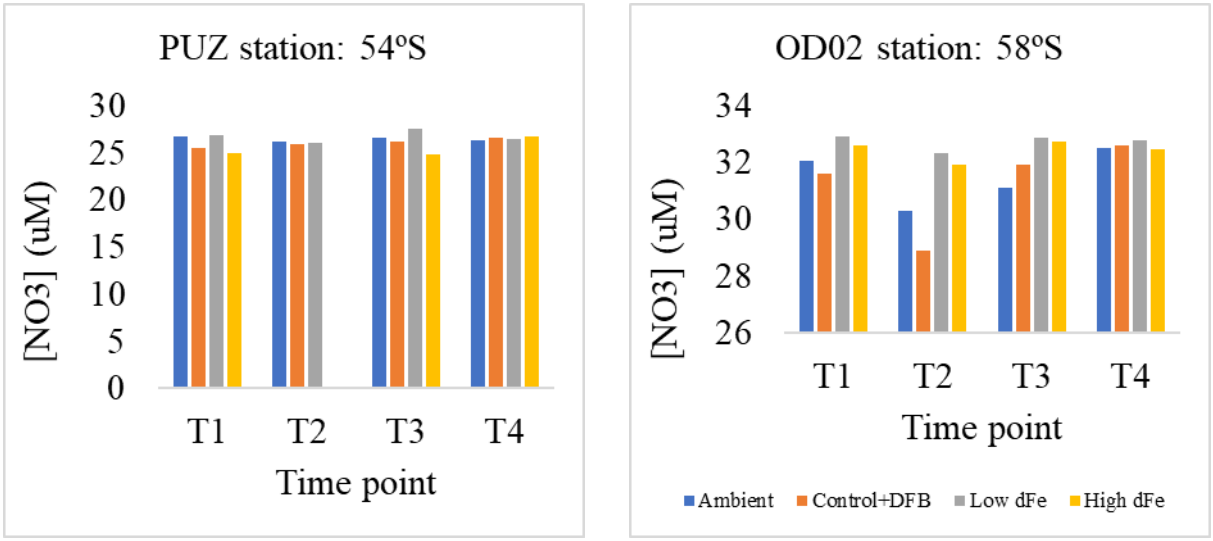

Figure 37 Nitrate concentrations at different timepoints subsampling, showing all the different treatments of dissolved iron.

9.2.2 Recommendations

There was one big problem during the duration of the cruise: the underway system was unreliable especially in open waters. The system kept losing pressure, and we could not pump water from the underway system to the deck for our *in situ* incubation. It is recommended that the whole system design is checked and fixed/improved before any future research cruises.

9.3 CHLOROPHYLL SAMPLING

The CPUT students were part of the Nitrogen Cycle team. Overall, the activities included participation with the University of Cape Town and The Council for Scientific and Industrial Research (CSIR) teams. The activities included were CTD, go-flow, underway and ice sampling. The students assisted the two mentioned teams regularly with incubation analysis for productivity in the water as well as nitrogen experiments. The main focus of the CPUT team was to collect water and ice samples and measure for chlorophyll-a, this was inclusive of collecting water samples that underwent Lugols preparation for later microscopic analysis. Eight (8) stations were sampled in total, as denoted by Table 11 below.

Table 10 Stations sampled for chlorophyll

Station number	Station name	Latitude	Longitude	Type of sample
1	PUZ(PS)	-53,99895	0,0001	Niskin
2	ICE22(I2)	-58,5518	-0,88413	Go-flow, Frazil ice
3	ICE22(I2)	-58,5518	-0,88413	Niskin
4	ICE11(I4)	-58,85563	-0,692	Niskin
5	OD-2	-58,38472	-0,49965	Niskin, Ice cores
6	ICE00(I0)	-59,04377	-0,50635	Niskin
7	SAZR(PS)	-46,99972	0,00195	Niskin
8	STZ(PS)	-38,06888	10,9537	Niskin

9.3.1 Methodology

9.3.1.1 Filtering for Chlorophyll-a

The water was collected from Go-flo, and Niskin CTD bottles, at 5m, 20m, 50m, 75m, 100m, 125m and 150m. The water was collected using 1L and 2L bottles from the assigned bottles associated with the desired depth. The water was kept in the dark (in a black container), immediately after collection and throughout in the lab, with each bottle taken out at a time for filtering, this was done to prevent further biological activities from taking place after the water was collected and awaiting filtration.

The workstation was cleaned with 70% ethanol before filtering. The water was size fractionated using 0.3, 2.7 and 20-micron filter paper, at different volumes of water depending on water availability. The volume aimed at filtering was 500ml. The water filtered was recorded and the samples were put in assigned vials which were recorded in association with depth and filter paper size and 8ml of acetone was added to the vial containing the filter paper for extraction and placed the freezer for 24 hours before reading could take place.

9.3.1.2 Ice Core and frazil ice filtering

For the ice frazil, this sample was collected in buckets and allowed to melt completely before filtering. The bucket was closed to avoid exposure to light. 1L of the melted frazil was filtered per 0,3, 2.7 and 20-micron filter paper. The filter papers were then placed in appropriate vials, preserved with 8 ml acetone and stored in the freezer for 24 hours to allow for extraction. The Ice cores were collected and cut in the ice lab by the ice team. Only 2 cores were collected and were cut into 10cm slices. Each slice was put in ziploc bags with 2545ml of filtered seawater (FSW) to melt before further processing. The volume of FSW was calculated using a 4:1 ratio of FWS to ice. The section of each slice was recorderd appropriately. The filtration process was the same as for the frazil ice. The same volume of 1L was filtered per size fraction.

9.3.1.3 Fluorescence reading

After the samples had been left for 24 hours in the freezer, they were read on a fluorometer. A blank reading was done as the first reading and after every four readings. The blank was done using acetone, which was also used to rinse the test tube after every reading. The samples were read using a fluorometer with the module Chlorophyll-NA. All readings were electronically recorded immediately after a batch of readings wre complete.

9.3.1.4 Lugol's

Lugol samples were collected in amber bottles for 5m, 50 and 100m at each station sampled. 150ml were collected. 2.5ml of Lugols solution was added using a pipette to each of the samples to preserve them and was stored in a dark place for later on-land microscopic analysis.

9.3.1.5 Additional work

- Assisted with washing bottles for the UCT team
- Assisted with water sample collection
- Assisted UCT with underway water collection and filtration
- Assisted CSIR with filtering and fluorescence reading

References

Baar, Hein J.W. de, Philip W. Boyd, Kenneth H. Coale, Michael R. Landry, Atsushi Tsuda, Philipp Assmy, Dorothee C.E. Bakker, et al. 2005. "Synthesis of Iron Fertilization Experiments: From the Iron Age in the Age of Enlightenment." *Journal of Geophysical Research C: Oceans* 110 (9): 1–24. https://doi.org/10.1029/2004JC002601.

Baar, HJW de, AGJ Buma, RF Nolting, GC Cadee, G Jacques, and PJ Treguer. 1990. “On Iron Limitation of the Southern Ocean: Experimental Observations in the Weddell and Scotia Seas.” *Marine Ecology Progress Series* 65: 105–22. https://doi.org/10.3354/meps065105.

Beman, J. Michael, Brian N. Popp, and Christopher A. Francis. 2008. “Molecular and Biogeochemical Evidence for Ammonia Oxidation by Marine Crenarchaeota in the Gulf of California.” *ISME Journal* 2 (4): 429–41. https://doi.org/10.1038/ismej.2007.118.

Bopp, L., L. Resplandy, J. C. Orr, S. C. Doney, J. P. Dunne, M. Gehlen, P. Halloran, et al. 2013. “Multiple Stressors of Ocean Ecosystems in the 21st Century: Projections with CMIP5 Models.” *Biogeosciences Discussions* 10 (2): 3627–76. https://doi.org/10.5194/bgd-10-3627-2013.

Boyd, Philip W., Hervé Claustre, Marina Levy, David A. Siegel, and Thomas Weber. 2019. “Multi-Faceted Particle Pumps Drive Carbon Sequestration in the Ocean.” *Nature* 568 (7752): 327–35. https://doi.org/10.1038/s41586-019-1098-2.

Buchwald, Carolyn, Alyson E. Santoro, Rachel H.R. Stanley, and Karen L. Casciotti. 2015. “Nitrogen Cycling in the Secondary Nitrite Maximum of the Eastern Tropical North Pacific off Costa Rica.” *Global Biogeochemical Cycles*. https://doi.org/10.1002/2015GB005187.

Cavagna, A. J., F. Fripiat, M. Elskens, P. Mangion, L. Chirurgien, I. Closset, M. Lasbleiz, et al. 2015. “Production Regime and Associated N Cycling in the Vicinity of Kerguelen Island, Southern Ocean.” *Biogeosciences* 12 (21): 6515–28. https://doi.org/10.5194/bg-12-6515-2015.

Church, Matthew J., Brenner Wai, David M. Karl, and Edward F. DeLong. 2010. “Abundances of Crenarchaeal AmoA Genes and Transcripts in the Pacific Ocean.” *Environmental Microbiology*. https://doi.org/10.1111/j.1462-2920.2009.02108.x.

Devries, Tim. 2014. “The Oceanic Anthropogenic CO2 Sink: Storage, Air-Sea Fluxes, and Transports over the Industrial Era.” *Global Biogeochemical Cycles* 28 (7): 631–47. https://doi.org/10.1002/2013GB004739.

DeVries, Tim, Mark Holzer, and Francois Primeau. 2017. “Recent Increase in Oceanic Carbon Uptake Driven by Weaker Upper-Ocean Overturning.” *Nature* 542 (7640): 215–18. https://doi.org/10.1038/nature21068.

Frölicher, Thomas L., Jorge L. Sarmiento, David J. Paynter, John P. Dunne, John P. Krasting, and Michael Winton. 2015. “Dominance of the Southern Ocean in Anthropogenic Carbon and Heat Uptake in CMIP5 Models.” *Journal of Climate* 28 (2): 862–86. https://doi.org/10.1175/JCLI-D-14-00117.1.

Lam, Phyllis, Gaute Lavik, Marlene M. Jensen, Jack De Van Vossenberg, Markus Schmid, Dagmar Woebken, Dimitri Gutiérrez, Rudolf Amann, Mike S.M. Jetten, and Marcel M.M. Kuypers. 2009. "Revising the Nitrogen Cycle in the Peruvian Oxygen Minimum Zone." *Proceedings of the National Academy of Sciences of the United States of America* 106 (12): 4752–57. https://doi.org/10.1073/pnas.0812444106.

Leeuwe, M. A. Van, R. Scharek, H. J.W. De Baar, J. T.M. De Jong, and L. Goeyens. 1997. "Iron Enrichment Experiments in the Southern Ocean: Physiological Responses of Plankton Communities." *Deep-Sea Research Part II: Topical Studies in Oceanography* 44 (1–2): 189–207. https://doi.org/10.1016/S0967-0645(96)00069-0.

Leung, S., A. Cabre, and I. Marinov. 2015. "A Latitudinally Banded Phytoplankton Response to 21st Century Climate Change in the Southern Ocean across the CMIP5 Model Suite." *Biogeosciences* 12 (19): 5715–34. https://doi.org/10.5194/bg-12-5715-2015.

Michael Beman, J., Brian N. Popp, and Susan E. Alford. 2012. "Quantification of Ammonia Oxidation Rates and Ammonia-Oxidizing Archaea and Bacteria at High Resolution in the Gulf of California and Eastern Tropical North Pacific Ocean." *Limnology and Oceanography* 57 (3): 711–26. https://doi.org/10.4319/lo.2012.57.3.0711.

Mincer, Tracy J., Matthew J. Church, Lance Trent Taylor, Christina Preston, David M. Karl, and Edward F. DeLong. 2007. "Quantitative Distribution of Presumptive Archaeal and Bacterial Nitrifiers in Monterey Bay and the North Pacific Subtropical Gyre." *Environmental Microbiology*. https://doi.org/10.1111/j.1462-2920.2007.01239.x.

Moore, C. M., M. M. Mills, K. R. Arrigo, I. Berman-Frank, L. Bopp, P. W. Boyd, E. D. Galbraith, et al. 2013. "Processes and Patterns of Oceanic Nutrient Limitation." *Nature Geoscience* 6 (9): 701–10. https://doi.org/10.1038/ngeo1765.

Moore, J. Keith, Weiwei Fu, Francois Primeau, Gregory L. Britten, Keith Lindsay, Matthew Long, Scott C. Doney, Natalie Mahowald, Forrest Hoffman, and James T. Randerson. 2018. "Sustained Climate Warming Drives Declining Marine Biological Productivity." *Science* 359 (6380): 113–1143. https://doi.org/10.1126/science.aao6379.

Newell, Silvia E., Andrew R. Babbin, Amal Jayakumar, and Bess B. Ward. 2011. "Ammonia Oxidation Rates and Nitrification in the Arabian Sea." *Global Biogeochemical Cycles* 25 (4): 1–10. https://doi.org/10.1029/2010GB003940.

Newell, Silvia E., Sarah E. Fawcett, and Bess B. Ward. 2013. “Depth Distribution of Ammonia Oxidation Rates and Ammonia-Oxidizer Community Composition in the Sargasso Sea.” *Limnology and Oceanography* 58 (4): 1491–1500. https://doi.org/10.4319/lo.2013.58.4.1491.

Raven, John A., Michael C.W. Evans, and Rebecca E. Korb. 1999. “The Role of Trace Metals in Photosynthetic Electron Transport in O2-Evolving Organisms.” *Photosynthesis Research* 60 (2–3): 111–50. https://doi.org/10.1023/A:1006282714942.

Ryan-Keogh, Thomas J., Sandy J. Thomalla, Thato N. Mtshali, and Hazel Little. 2017. “Modelled Estimates of Spatial Variability of Iron Stress in the Atlantic Sector of the Southern Ocean.” *Biogeosciences* 14 (17): 3883–97. https://doi.org/10.5194/bg-14-3883-2017.

Sabine, Christopher L, Christopher L Sabine, Richard A Feely, Nicolas Gruber, Robert M Key, Kitack Lee, John L Bullister, et al. 2004. “The Oceanic Sink for Anthropogenic CO 2.” *Science* 367 (2004): 2–7. https://doi.org/10.1126/science.1097403.

Schlitzer, Reiner. 2002. “Carbon Export Fluxes in the Southern Ocean: Results from Inverse Modeling and Comparison with Satellite-Based Estimates.” *Deep-Sea Research Part II: Topical Studies in Oceanography* 49 (9–10): 1623–44. https://doi.org/10.1016/S0967-0645(02)00004-8.

Shi, Tuo, Yi Sun, and Paul G. Falkowski. 2007. “Effects of Iron Limitation on the Expression of Metabolic Genes in the Marine Cyanobacterium Trichodesmium Erythraeum IMS101.” *Environmental Microbiology*. https://doi.org/10.1111/j.1462-2920.2007.01406.x.

Shiozaki, Takuhei, Minoru Ijichi, Kazuo Isobe, Fuminori Hashihama, Ken-ichi Nakamura, Makoto Ehama, Ken-ichi Hayashizaki, Kazutaka Takahashi, Koji Hamasaki, and Ken Furuya. 2016. “Nitrification and Its Influence on Biogeochemical Cycles from the Equatorial Pacific to the Arctic Ocean.” *The ISME Journal*, 1–14. https://doi.org/10.1038/ismej.2016.18.

Takahashi, Taro, Stewart C. Sutherland, Colm Sweeney, Alain Poisson, Nicolas Metzl, Bronte Tilbrook, Nicolas Bates, et al. 2002. “Global Sea-Air CO_2 Flux Based on Climatological Surface Ocean PCO_2, and Seasonal Biological and Temperature Effects.” *Deep-Sea Research Part II: Topical Studies in Oceanography* 49: 1601–22. https://doi.org/10.1016/S0967-0645(02)00003-6.

10 IMICROBE PROJECT

Team name and PI	With N-CYCLE. Kaartokallio H (SYKE, Finland)
Authors	Tedesco L and Haraguchi L

IMICROBE (Iron limitation on primary productivity in the Marginal Ice Zone of the Southern Ocean – unravelling the role of bacteria as mediators in the iron cycle) is an Academy of Finland project (2021-2024) that aims to:

i) investigate bacterial iron scavenging capacity and iron transfer into the autotrophic production in the food web over the different Southern Ocean (SO) habitats, and

ii) combine enhanced biogeochemical modelling with observational data to better understand the large-scale consequences of bacterial iron uptake and transfer for SO primary productivity patterns.

In particular, the work done during the SCALE winter cruise 2022 aimed to:

i) collect samples for metagenomics, in order to characterize communities and asses the presence of genes involved in the iron cycle in different SO habitats, which present distinct biogeochemistry (e.g., nutrient concentrations, communities) conditions;

ii) perform incubations with iron manipulations and collect samples for transcriptomics, aiming to highlight pathways associated with iron availability and depletion at stations representing conditions of the main SO habitats;

iii) evaluate the grazing by nanoflagellates in different SO habitats;

iv) provide background data on bacterial abundances and phytoplankton community structure in the water column and sea ice;

v) better describe the sea-ice environment, in particular for improved model parameterisations of the heat and salt fluxes at the sea ice-ocean interface and of the light transmission through and underneath sea ice.

10.1 METHODS

IMICROBE methods include:

i) state-of-the-art metagenomic and -transcriptomic tools for 16S- and 18S rRNA gene amplicon sequencing;

ii) mixo- and heterotrophic nanoflagellates quantification and grazing assays;

iii) phytoplankton community characterization using pulse-shape recording and imaging flow cytometry;

iv) refining of iron limitation parameterizations in bacterial acquisition, and adding mixotrophy as an alternative route into biogeochemical models;

v) develop and test ocean biogeochemical models in assessing production capacity and limitation dynamics of the Southern Ocean ecosystem.

During the SCALE winter cruise 2022, our activities included:

i) deployment of a Valeport mini-CTD for high-resolution data of temperature and salinity under sea ice and up to 20 m deep;

ii) deployment of a TriOS RAMSES spectral radiometer with an under-ice arm;

iii) collection and processing of sea ice cores following the standard protocol for metagenomics analysis;

iv) collection of metagenomic filters in the water column of the process stations;

v) incubations with iron manipulation for transcriptomics carried out in the process stations;

vi) phytoplankton community characterization in the water column and sea ice using live pulse-shape recording and imaging flow cytometry (conducted in all stations and IMICROBE ice cores);

vii) sample collection for quantification of bacterial abundances in the water column and sea ice (conducted at all stations and IMICROBE ice cores);

viii) nanoflagellates grazing essays using the acidophilic stain Lysotracker combined with live pulse-shape recording and imaging flow cytometry at the process stations;

ix) heterotrophic respiration assessment using PyroScience dissolved oxygen sensors;

x) teaching students on board the principles of flow cytometry and demonstration of pulse-shape recording and imaging flow cytometry.

xi) a seminar onboar on 28 of July on the sea ice biome

10.2 MINI CTD

Under-ice and shallow seawater temperature and salinity profiles are not available from the regular CTD coupled to the rosette. The miniCTD was deployed between pancakes from the ship for testing purposes and through holes in larger ice floats for data collection at high temporal and spatial resolution and with high accuracy. The miniCTD is fitted with a conductivity sensor, a PRT temperature sensor, and a strain gauge pressure transducer. In addition, salinity and density values are also calculated by the software (DataLogX2). The unit operates autonomously, with setup and data extraction performed by direct communications with the PC and is fitted with a solid-state, non-volatile flash memory, that can store over 10 million lines of data. The software DataLogX2 is used for instrument setup, data extraction and display. The miniCTD was deployed under sea ice at all ice stations (Figure 38).

Figure 38 miniCTD deployed under sea ice at ice stations

10.3 UNDER-ICE LIGHT MEASUREMENTS

Under-ice light measurements were carried out using a spectral radiometer (TriOS RAMSES) attached to a custom-built beam for under-ice measurements. RAMSES radiometers are spectral imaging radiometers to measure radiance, irradiance, or scalar irradiance in the UV, VIS and UV/VIS ranges. The sensor is small size and weight, so it is especially suitable for hand-held and autonomous applications, such as installation on ships, handheld usage or autonomous measurements in remote places, like the Southern Ocean.

The sensor was first deployed at one of the ice station where the ice conditions were safe enough to allow the deployment. However, the extreme weather conditions (cold and windy) made the custom battery run out of energy shortly. The following measurements (all triplicates) were taken on deck over and under lifted pancakes at different time of the day (from sunrise to sunset) with the sensor directly connected to an electricity plug. Additionally, several measurements of incoming shortwave solar radiation were taken next to the PAR sensor installed on the ship on Monkey island (on the 8th deck) for sensor calibration.

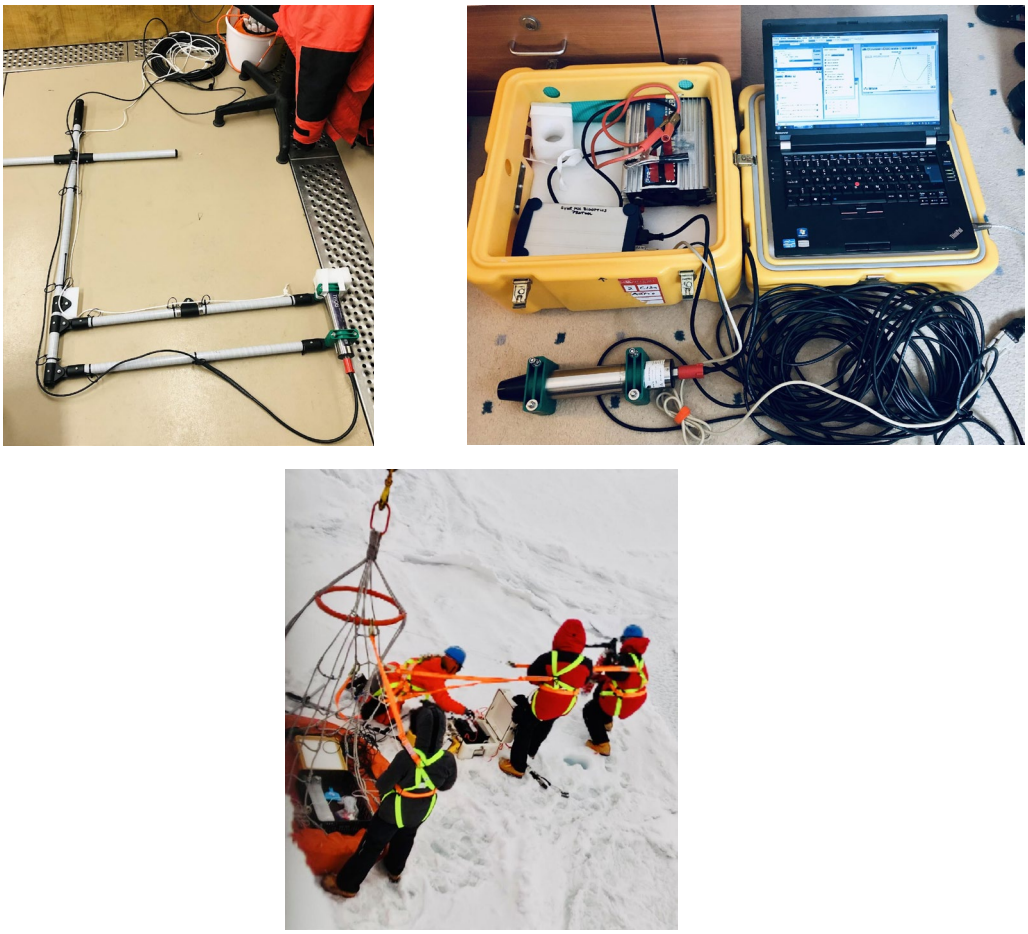

Figure 39 Spectral radiometer (TriOS RAMSES) with the custom-made beam and testing in the field

10.4 Sea Ice work

Ice cores were retrieved from larger ice floats using baskets or from pancakes lifted on the ship deck (Figure 40). The cores were handled with nitrile gloves, placed in clean bags and kept in darkness until processed. The ice cores from larger ice floats were transported to a -10 °C freezer and cut with an electric saw the following day. The cores from pancakes were immediately cut with a hand saw. For all ice cores, the top and bottom 15 cm were cut first. If the core was shorter than 30 cm, the core was cut into two horizons of the same thickness. For cores longer than 40 cm, a middle horizon was processed separately. If the middle section was longer than 30 cm, it was divided into two horizons. Once cut, each horizon was placed in a clean bag and immediately crushed with a hammer. Once crushed they were left in darkness at room temperature to melt. When processing of the horizons was not possible due to conflicts with other activities, they were placed into +4 °C fridge and protected from light until processing (within 24 hours).

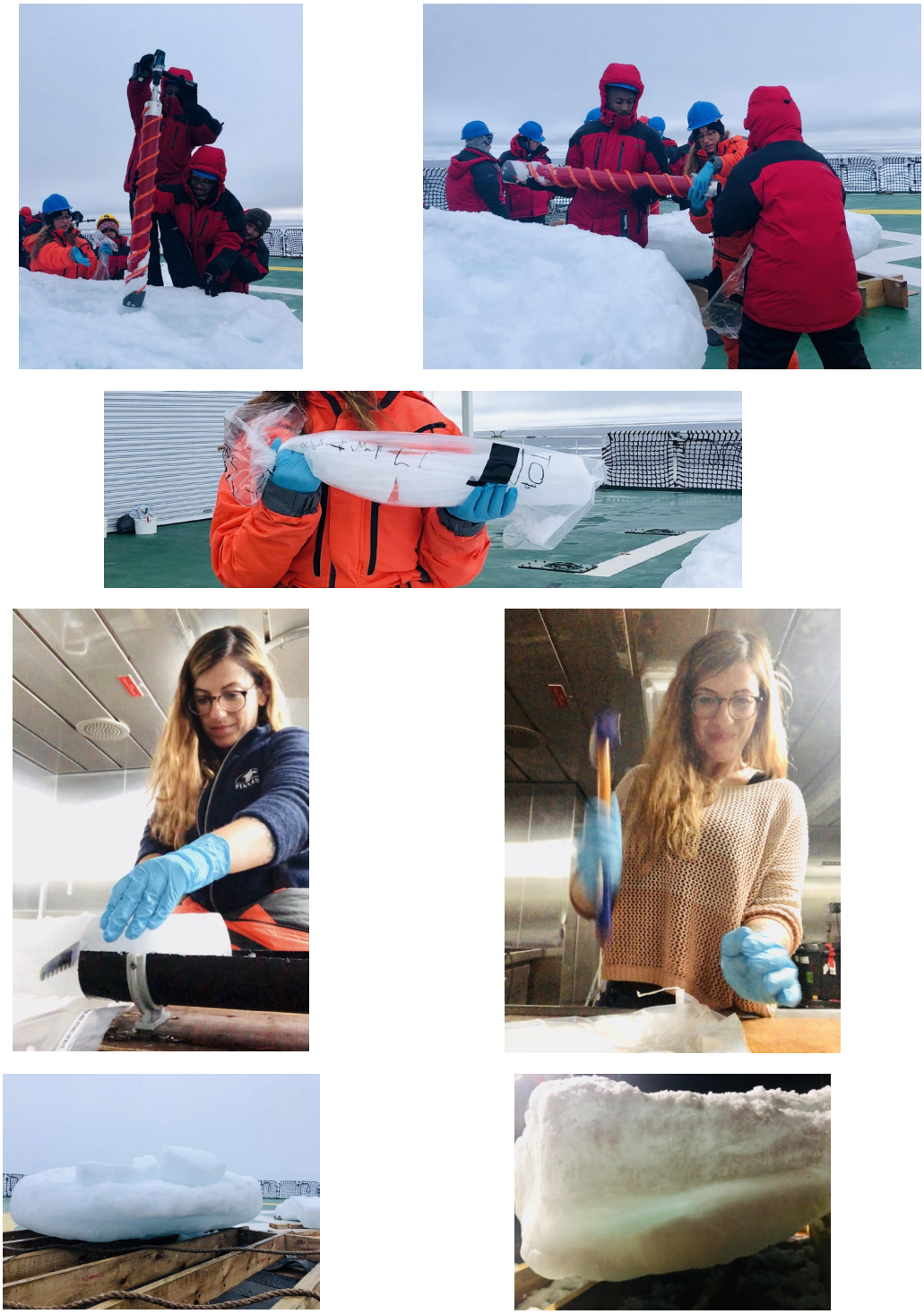

Figure 40 Various phases of the core collection from pancakes. The last 2 pictures show the shape of the pancakes and a possible gap layer

10.5 METAGENOMIC SAMPLES

Filters for metagenomics were collected at three depths (surface, 50 m and base of the mixing layer) in all process stations. Water samples were collected either from the GoFlos (PUZ and MIZ) or Niskins (SB06-ICE0, SAZr and STZ) in sterile plastic bags and processed as soon as possible. While

waiting for processing, samples were kept in the dark at +4 °C. Water was gently filtered through 47 mm PC membranes with a nominal pore size of 0.2 µm using a peristaltic pump (Figure 41). Each sample was filtered for a maximum time of 30 minutes to avoid any degradation of the material. Filters were folded and placed into MP vials and flash-frozen in liquid nitrogen, after that filters were stored at -80 °C. DNA will be extracted at SYKE facilities in Helsinki and material will be sequenced in the University of Helsinki Institute of Biotechnology sequencing center.

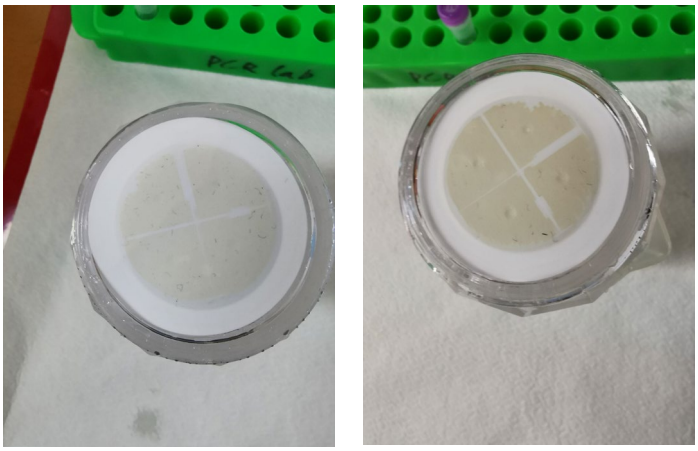

Figure 41 Filters for metagenomics analyses showing different concentrations of biogenic material

10.6 Fe manipulation incubations

Iron manipulation experiments were conducted in three depths (surface, 50 m and base of the mixing layer) at the process stations PUZ and MIZ. Our treatments were: a control, iron removal (using the chelator DFB), + 0.2 nM Fe and + 2 nM Fe. As those experiments required trace metal clean conditions, the water was collected in the Go-Flos and experimental units (trace metal clean 2 L PC bottles) were filled in the environmental trace metal clean container. Two replicates were used for each treatment and depth, totalling 24 bottles for each incubation. After being filled, the bottles were moved to another trace metal clean container, where they were spiked according to the treatments described above. Bottles were then incubated in the dark at in situ temperature (using fridge-style incubators) for approximately 24 hours. After that period, filters for metatranscriptomics were processed in the same way as described above (the only difference is that for those RNA will be the genetic material extracted). Note that due to the larger sample volume required by transcriptomes the two replicates were combined. After the incubation, aliquots were also taken for bacterial abundances and phytoplankton community characterization. Experiments were not conducted at the remaining process stations due to issues with the trace metal clean container.

10.7 Phytoplankton characterization

Phytoplankton communities were characterized in the water column (5-200 m) in all water column stations and for all IMICROBE cores horizons, using a CytoSense pulse-shape recording and imaging flow cytometer. This flow cytometer was designed for phytoplankton analysis, being able to detect a broad size range (0.5-1000 µm) and different types of pigments (chlorophyll a; phycocyanin and phycoerythrin), while scattering properties reflect cell morphological features (e.g. size, coverage). By analyzing different combinations of the particles' optical characteristics, it is possible to define populations that represent different components of the community. Additionally, high-resolution

imaging allows for further classification of some of the populations identified based on the optical properties. The relatively fast processing capacity allows it to process live samples on board (Figure 42), preserving delicate organisms and cell characteristics that might be lost during fixation. Below is an example of:

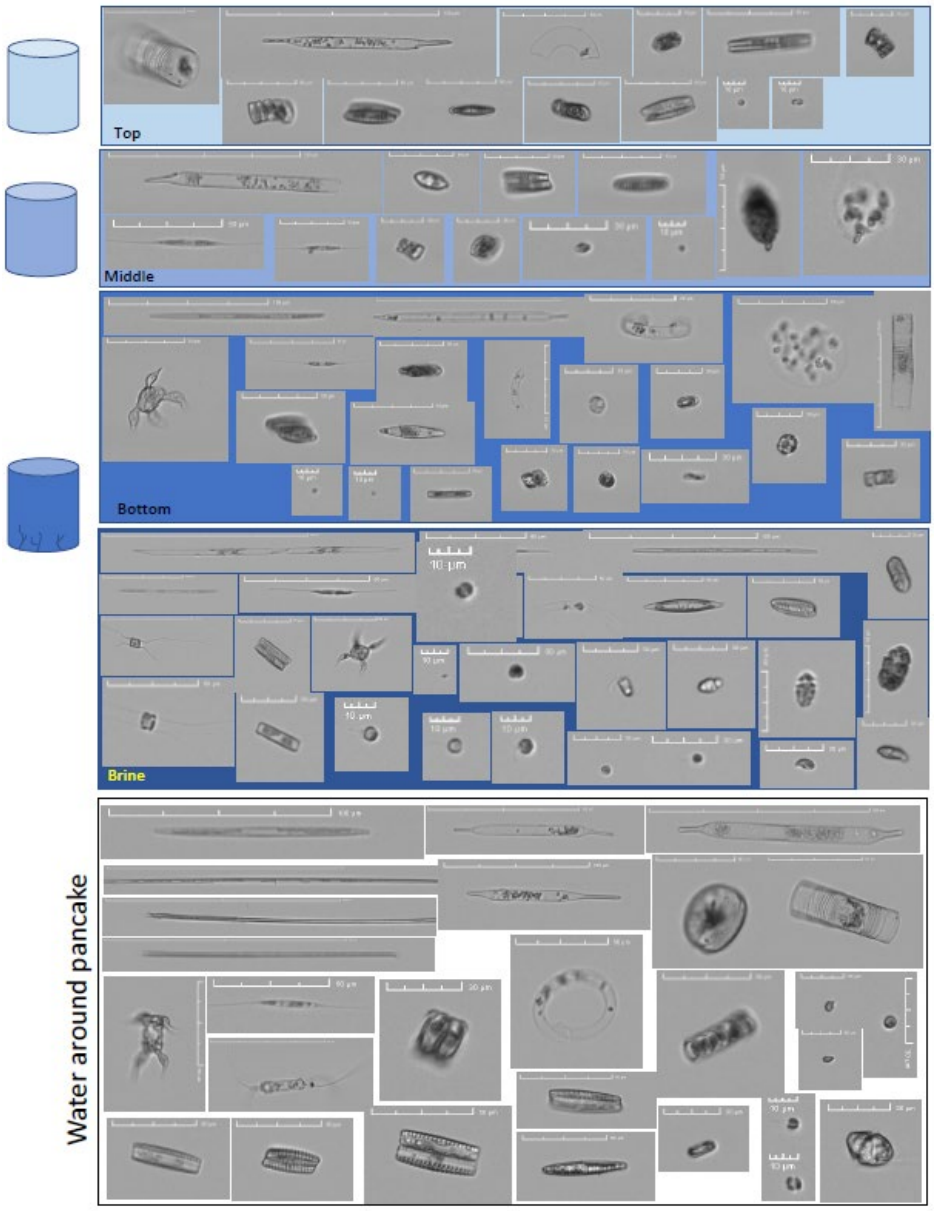

Figure 42 Selected images taken at station SB04 (internal label OD3), showing examples of organisms found in different sea ice portions, brines and surrounding water.

10.8 BACTERIAL ABUNDANCES

Samples for bacterial abundances were collected in the water column (5-200 m) in all water column stations and for all IMICROBE cores' horizons. Samples (1.8 mL) were collected in 2 mL cryovials and fixed with paraformaldehyde and glutaraldehyde (1% and 0.5% final concentration, respectively). Samples were then flash-frozen and stored at -80 °C. Samples will be analyzed at SYKE facilities in Helsinki using a Guava EasyCyte flow cytometer and SYBR Green nucleic acid stain.

10.9 NANOFLAGELLATES GRAZING

Mixo- and heterotrophic nanoflagellates were identified by using the acidophilic stain LysoTracker green, which stains food vacuoles and can be detected (as well as cell autofluorescence) with CytoSense. Auto-, mixo- and heterotrophic organisms were enumerated in all water column stations and IMICROBE ice cores. In all process stations, essays were conducted at three depths (surface, 50 m and base of the mixing layer). For each depth, duplicate 500 mL PC bottles were filled with water filtered through 200 µm mesh (to remove large grazers) and incubated in the dark and at + 4 °C (except for the STZ, which was 16 °C and were incubated at room temperature). During a 3-hour interval, each bottle was subsampled three times, stained with Lysotracker green and analyzed with CytoSense. Expected results are both the quantification of the standing stocks of different functional groups of nanoflagellates as their grazing activity under different light and nutrient regimes in different SO habits. Figure 43 shows some examples of autotrophic, heterotrophic, and mixotrophic organisms stained with LysoTracker green and recorded by CytoSense. Note that the green line represents the Lysotracker fluorescence and red lines the chlorophyll fluorescence; a heterotroph will display only green fluorescence, an autotroph will only display red fluorescence and a mixotroph will display both green and red fluorescence.

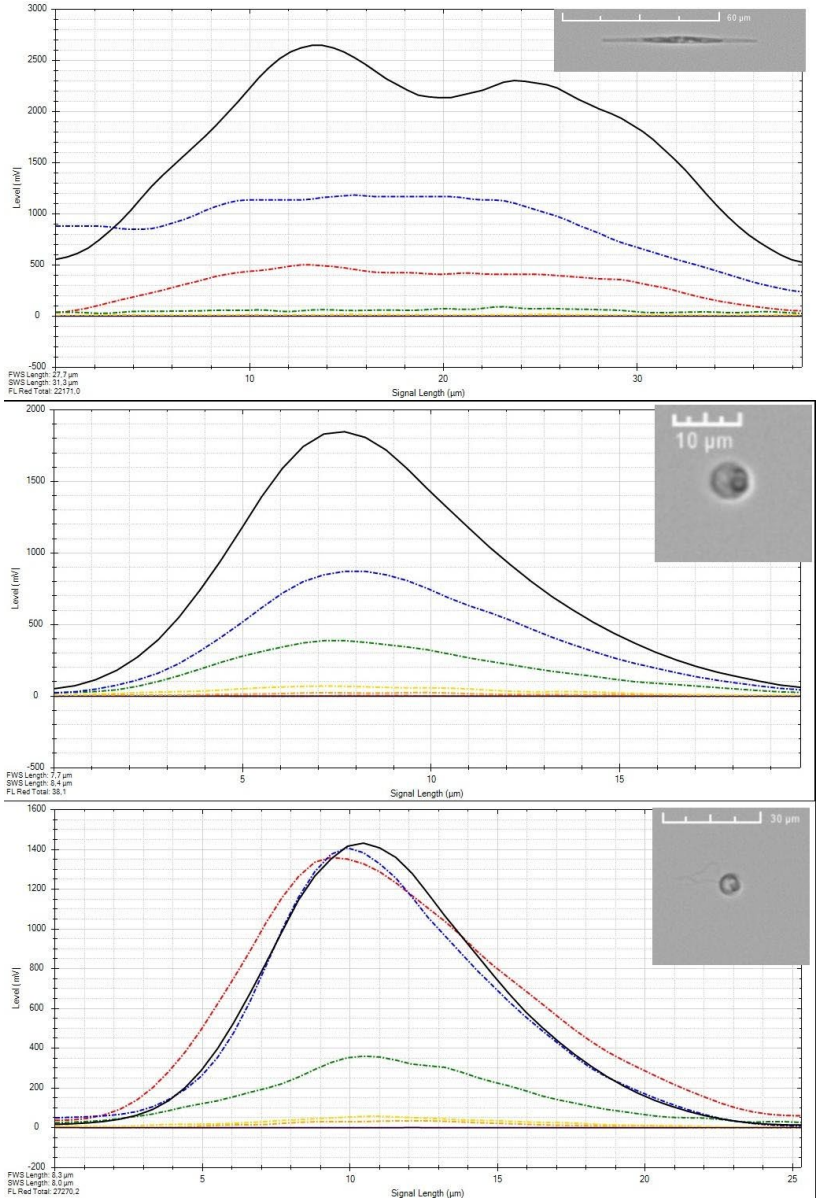

Figure 43 Autotrophic, heterotrophic, and mixotrophic organisms stained with LysoTracker green and recorded by CytoSense (optical profiles and images)

10.10 HETEROTROPHIC RESPIRATION

Heterotrophic respiration assays were planned for all process stations (surface, 50 m and base of the mixing layer), following the dissolved oxygen dynamics over 24 hours. Such information would provide information on the heterotrophic activity of the communities in distinct habitats of the SO. For this, PyroScience vials and sensors were filled with water from the Niskins and incubated in the dark and at in situ temperatures (temperature was controlled by a water bath). Due to issues in the walk-in fridge those assays had to be suspended.

10.11 FCM DEMONSTRATION

Basic principles of flow cytometry and a live demonstration of the CytoSense (pulse-shape recording and imaging flow cytometer) were conducted to different groups of students and researchers on board. As such technology is still not widely available in South Africa and given the teaching aspect of the cruise, it was a great opportunity to teach and share our expertise with South African colleagues and students.

10.12 SEMINAR ON SEA ICE BIOME

During the expedition we were given the possibility to talk about the extraordinary biome that sea ice is to the wide audience of scientists onboard. During the seminar, sea ice as a habitat was presented, the controlling factors for biological growth were described, differences between Arctic and Antarctic sea ice and food webs were highlighted, the IMICROBE project was presented as well as the IMICROBE sea ice work during the cruise. The seminar gave the opportunity to all the scientists with a different background to learn about the sea ice biome and importance.

10.13 ACKNOWLEDGEMENTS

We acknowledge the financial support from the Academy of Finland project IMICROBE and the logistic support from FINNARP. We would like to thank the Chief scientist Marcello Vichi and PI Sarah Fawcett for the opportunity given to join the expedition. We would also like to thank UCT N-cycle and Sea Ice teams, Natasha van Horsten, as well as Captain Knowledge Bengu and the crew of the R/V *S.A. Agulhas II* for their tech

11 THE DIGITAL SA AGULHAS II

Team name and PI	VESSEL4.0. Anriëtte Bekker (SUN) and Jukka Tuhkuri (Aalto)
Authors	Taylor N, Muchow M, Gilges M., van Zijl C, Tuhkuri J, and Bekker A

11.1 PROJECT DETAILS

Team Vessel 4.0 performed research during the Southern oCean seAsonaL Experiment (SCALE) Winter Cruise of 2022 coordinated by the Sound and Vibration Research Group (SVRG) at Stellenbosch University in collaboration with the MarTERA HealthProp consortium and Aalto University. The details of the associated research projects are as follows:

Name of Institution or Consortium	**Project Details**
Stellenbosch University	The Digital SA Agulhas II – Flagship for Vessel 4.0 funded by the South African National Antarctic Programme (SANAP)
Aalto University	ANTGRAD funded by the Academy of Finland that is part of Finnish Antarctic Research Programme (FINNARP) and supported by the Department of Forestry, Fisheries and the Environment (DFFE) of South Africa
MarTERA HealthProp Consortium	HealthProp funded by the MarTERA partners, including Research Council of Norway, South African Department of Science and Innovation, and German Federal Ministry of Economic Affairs and Energy, and supported by the South African DFFE

Team Vessel 4.0 performed full-scale measurements and environmental observations on board the SA Agulhas II during the SCALE Winter Cruise of 2022. Instrumentation was installed prior to vessel departure to ready vessel-wide measurement systems for the voyage. Full-scale measurements were recorded continuously by various instrumentation systems throughout the voyage, sea state observations performed in open water and sea ice observations during ice traversal. The installation, measurement systems, data captured, and environmental observations performed are reported on in this section.

11.2 PRIOR TO VESSEL DEPARTURE

Representatives from Stellenbosch University instrumented the vessel with accelerometers, strain gauges and additional sensors while the SA Agulhas II was docked at East Pier in the weeks preceding SCALE Winter Cruise. This included measurement setups in the port shaft line, voids in the hull structure, and other locations vessel-wide for an extensive sensor network, as detailed in Section 11.3.

11.3 Ship Structural Response and Propulsion System Measurements

Full-scale measurements from SCALE Winter Cruise 2022 include structural responses of the hull and superstructure, along with various measurements from the ship propulsion system. Three separate measurement systems, which are described in this section, were installed for the purpose of acquiring these measurements, including:

- a primary full-scale measurement system,
- an acoustic emission measurement system in the port shaft line, and
- a hull stress monitoring system.

11.3.1 Primary Full-Scale Measurement System

11.3.1.1 Description of Full-Scale Measurement Infrastructure

An overview of the primary measurement infrastructure, including the number of channels and sample rate, are presented in Table 3. Measurements from a total of 46 channels were captured by four Siemens Supervisory Control and Data Acquisition Systems (SCADAS). Two SCADAS units in the Engine Store Room, along with another unit in the Steering Gear Room captured the structural ship response measurements. The remaining SCADAS unit was located at the port-side shaft line and captured the propulsion measurements. The four SCADAS units were connected in a Master-Slave configuration and all data was collected and recorded at a centralised location by Simcenter Testlab Turbine Testing data acquisition software. Measurements were continuously recorded and stored as five-minute records in raw ".ldsf" format. Over the whole voyage, a total of 5583 five-minute records were captured, resulting in approximately 607 GB of raw data.

Table 11: Full-Scale Structural Response and Propulsion Measurements on the SA Agulhas II (Adapted from Bekker et al., 2018).

Measurement	Variables	Equipment	Number of Channels	Sample Rate
Ship structural response (hull and superstructure)	Acceleration (Rigid body motion and flexure)	DC accelerometers	10	2048 Hz
		ICP accelerometers	16	2048 Hz
	Strain (wave bending and flexure)	Strain gauges	2	2048 Hz
Ship propulsion measurements	Thrust, Torque	Strain gauges, V-links and Quantum data acquisition units	3	2048 Hz
	Propulsion motor acceleration	ICP accelerometers	2	2048 Hz
	Bearing acceleration	ICP accelerometers	7	2048 Hz

Shaft rotational speed	Tachometer	1	20480 Hz
Bearing temperature	Temperature probes	5	2048 Hz

11.3.1.2 Ship Structural Response Measured Through Acceleration

For SCALE Winter Cruise 2022, structural ship responses were captured with an accelerometer network consisting of 26 accelerometers. Measurements are referenced to a vessel-centric coordinate system, where the respective axes, x-y-z refer to longitudinal (fore-aft), lateral (starboard-port), and vertical acceleration. The sensor network consists of 16 Integrated Circuit Piezoelectric (ICP) accelerometers and 10 Direct Current (DC) accelerometers. A schematic of the accelerometer network is presented in Figure 45, which provides the unique IDs for each degree of freedom (DOF) and the corresponding measurement locations. Specific sensor details are provided for each DOF in Table 14, including the measurement direction, accelerometer type and sensitivity. Signals from the accelerometers are received by the SCADAS units indicated in Table 14 by an existing network of BNC cables.

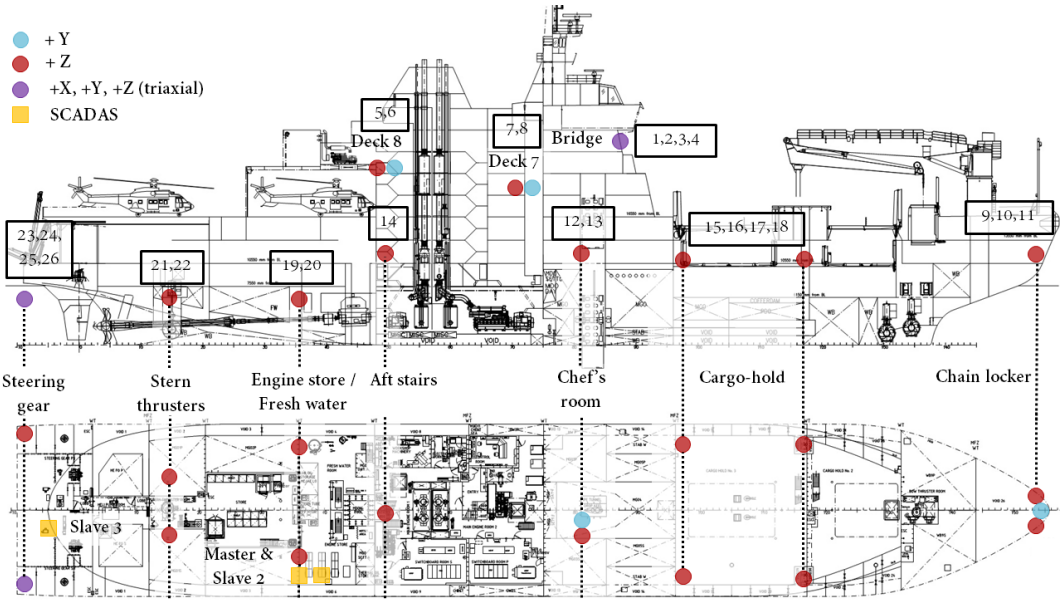

Figure 44: A Diagram of the Accelerometer Network Used to Measure Structural Responses of the SA Agulhas II.

The accelerometer network in Figure 45 is suitable to capture both rigid body and flexural motion. Low-frequency rigid body responses can be accurately reconstructed using the 10 DC accelerometers that are capable of measuring frequencies down to 0 Hz. Further, the low-frequency characteristics of the DC accelerometers are useful for studying motion sickness of passengers, which typically occurs around 0.2 Hz (Soal, 2015; Bekker *et al*., 2017). Sensors located in the superstructure, closer to accommodation areas, recreational spaces and the Bridge, are specifically used to monitor human responses to vibration. The global flexural responses of the ship include lateral and vertical bending, and torsion (Soal *et al*., 2015; Soal, 2018; Van Zijl, 2020). Lateral motion is measured by two sensors, one on the starboard side of the stern and the other on the centre line in the bow chain locker. Vertical motion and torsion are captured by six pairs of accelerometers on the port and starboard sides of the vessel hull.

Table 12: A List of Sensor Locations, Sensors and Measurement Specifics for Full-Scale Acceleration Measurements.

DOF ID	DAQ	Cable ID	Location	Side	Deck	Axis	Type	Sensitivity $[\mathbf{mV/m/s^2}]$
1	Master	V14	Bridge	STBD	9	X	DC	19.97
2	Master	V15	Bridge	STBD	9	Y	DC	19.94
3	Master	V16	Bridge	STBD	9	Z	DC	20.01
4	Master	V17	Bridge	PORT	9	Z	ICP	9.98
5	Master	V18	Deck 8	PORT	8	Y	ICP	10.4
6	Master	V19	Deck 8	PORT	8	Z	ICP	9.83
7	Master	V12	Deck 7	STBD	7	Y	ICP	9.87
8	Master	V13	Deck 7	STBD	7	Z	ICP	10.36
9	Master	V1	Bow	STBD	4	Z	DC	19.9
10	Master	V2	Bow	CTR	4	Y	DC	19.61
11	Master	V3	Bow	PORT	4	Z	DC	198.4
12	Master	V8	Chef's room	STBD	4	Y	ICP	9.99
13	Master	V9	Chef's room	STBD	4	Z	ICP	9.51
14	Master	V10	Aft stairwell	CTR	4	Z	ICP	10.23
15	Slave 2	V5	Cargo-hold	STBD	3	Z	ICP	10.19
16	Slave 2	V6	Cargo-hold	PORT	3	Z	ICP	10.16
17	Slave 2	V7	Cargo-hold	STBD	3	Z	ICP	10.52
18	Slave 2	V4	Cargo-hold	PORT	3	Z	ICP	9.93
19	Slave 2	BNC	Engine store	STBD	2	Z	ICP	9.82
20	Slave 2	RG5 84	Fresh water	PORT	2	Z	ICP	10.01
21	Slave 2	V20	Stern thruster	STBD	2	Z	ICP	9.64
22	Slave 2	V21	Stern thruster	PORT	2	Z	ICP	9.68
23	Slave 3	-	Steering gear	STBD	2	X	DC	19.86
24	Slave 3	-	Steering gear	STBD	2	Y	DC	19.78
25	Slave 3	-	Steering gear	STBD	2	Z	DC	19.83
26	Slave 3	-	Steering gear	PORT	2	Z	DC	19.74

11.3.1.3 Ship Structural Response Measured Through Strain

Low frequency wave-bending (hogging and sagging), along with wave-induced slamming vibrations are captured using two strain sensors. Each sensor consists of four strain gauges connected in a full Wheatstone bridge configuration, which allows for temperature compensation and common mode rejection. The strain measurements are relayed via four-core, twisted, shielded-pair cables along cable trays and watertight penetrations to the Master-Slave SCADAS units located in the Engine Store Room.

The sensors were installed at Frame 98 on longitudinal bulb stiffeners, on both the port and starboard side, as shown in Figure 2. Frame 98 is located 17.6 m fore of midship and coincides with an abrupt decrease in section modulus at the intersection of the superstructure and strength deck. Cracks have been observed, an example shown in Figure 2, and repaired at this location and is, therefore, believed to be provide an accurate measurement of the maximum global stress.

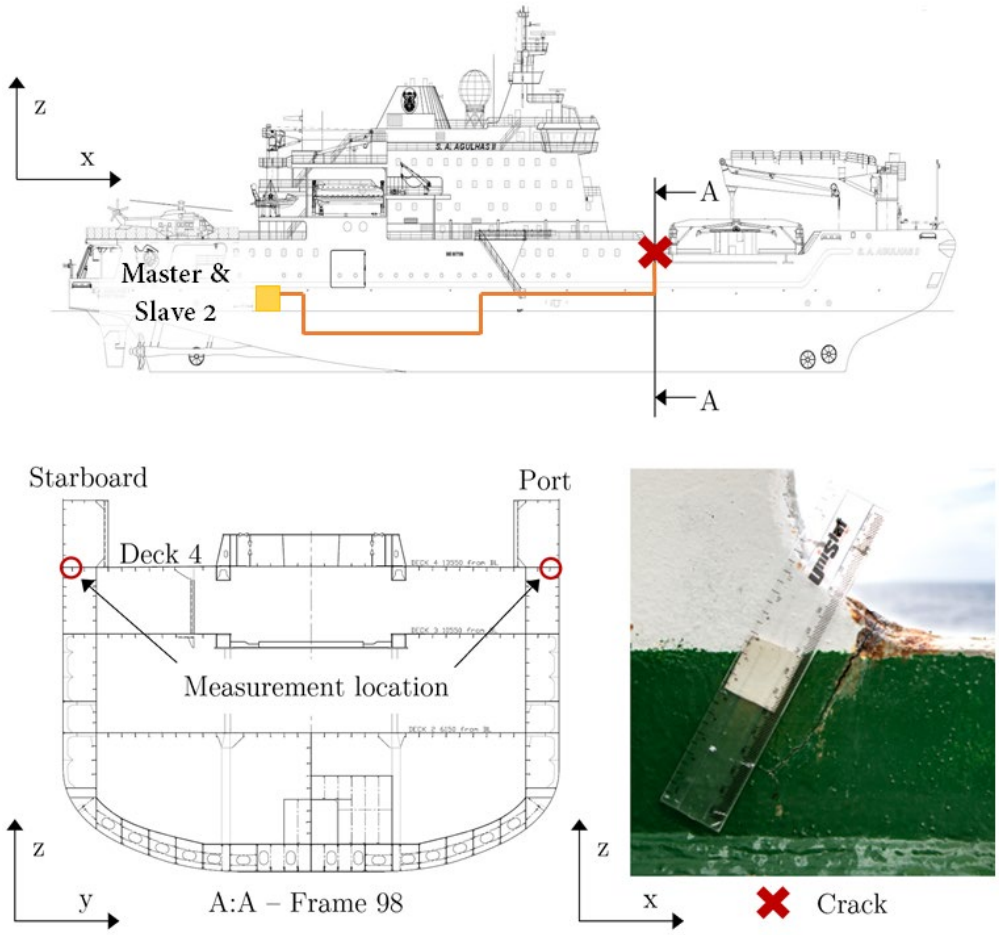

Figure 45: Strain Measurement Locations and Nearby Cracking (Adapted from Pferdekamper, 2022).

11.3.1.4 Propulsion System Measurements

Full-scale propulsion system measurements from SCALE Winter Cruise 2022 are captured for the EU MARTERA project, Life Prediction and Health Monitoring of Marine Propulsion System under Ice Impact (HealthProp). The propulsion measurement system is comprised of multiple sensors, including strain gauges, accelerometers, temperature probes and a tachometer. The sensor locations in the port-side shaft line are shown in Figure 47. Two sets of accelerometers on two different bearings measure acceleration in the lateral (starboard-port) and vertical directions, respectively.

Another accelerometer is mounted on the aft bearing to measure acceleration in the longitudinal (aft-fore) direction. Further, two accelerometers are mounted on the port-side propulsion motor to measure acceleration in the lateral and vertical directions, respectively.

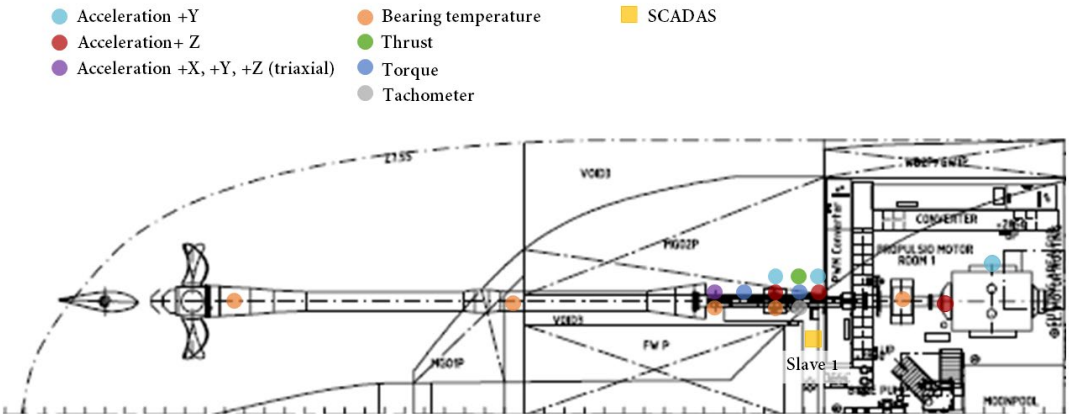

Figure 46: A Diagram of the Instrumentation Used for Propulsion System Measurements in the Port-Side Shaft Line of the SA Agulhas II.

Strain measurements on the port-side shaft line are used to determine shear and axial strain, which enables calculation of instantaneous torque and thrust in the shaft. The measurement setup used during SCALE Winter Cruise 2022 effectively measures internal thrust and torque at one location, and internal torque only, at another location. Furthermore, high resolution shaft speed is captured by zebra tape and a tachometer. The purpose of these measurements is threefold (Bekker *et al.*, 2018; De Waal, 2017):

1. Internal torque stress cycles, which are obtained from shear strain measurements, can be used to estimate fatigue damage using rainflow counting.
2. Transient torque, along with shaft speed measurements, enable the estimation of ice-induced propeller moments.
3. Global resistance forces can potentially be estimated through concurrent analysis of the thrust measurements and ship speed.

11.3.2 Shaft Line Acoustic Emission Measurement System

As part of the project HealthProp, the Institute of Machine Elements and System Engineering (MSE) of the RWTH Aachen University investigates the influence of propeller-ice contact on the wear and fatigue behavior of the stern tube bearings on the SA Agulhas II. Stern tube bearings are hydrodynamic journal bearings. This bearing type is characterised by a carrying oil film, which separates shaft and bearing bush and is generated by a relative movement between these components (Muhs *et al.*, 2003). The resulting fluid friction condition, in combination with a stationary radial load, is the desired condition of journal bearings since neither wear nor fatigue occur. When the gap between shaft and bearing reaches a value smaller than the minimum lubrication gap, determined by the surface roughness, metallic contact occurs. This lubrication regime is commonly known as mixed friction and can cause bearing damage. Usual causes for mixed friction are low speeds, overload, start/stop cycles, insufficient oil supply or oil contamination (Mokhtari and Gühmann, 2018).

During standard operation of the ship, the propeller shafts always run at a minimum rotational speed, which means that start/stop cycles barely occur outside the port. Insufficient oil supply, as well as oil contamination, is not likely under standard conditions as each stern tube is a “closed system” filled with 3000 litres, which was recently purified (dry dock 2021) to remove any contaminating particles. Low speeds, however, are possible during standard operation, as the operational parameters can be almost freely set by the ship operators. Also, overloads may occur quite frequently during harsh turning manoeuvres in open water (Sethumadhaven, 2018) and propeller-ice interactions in the Marginal Ice Zone (MIZ).

The influence of propeller-ice loads on the contact conditions of stern tube bearings is barely investigated yet. Ice contact leads to dynamic, eccentrical propeller loads and thus cause bending moments on the propeller shaft, which result in high radial loads on the journal bearings. The amount of these loads is unknown. A direct measurement of the bearing loads would, however, be extremely time and cost intensive as the stern tube is almost entirely submerged under water. To still detect and classify the influence of propeller loads on the bearings, representatives from the MSE and Stellenbosch University installed an Acoustic Emission (AE) measurement system on the port shaft line. AEs are transient elastic waves that are generated by suddenly released elastic energy, for example due to material deformation or damage. Therefore, friction also generates AE, which can be detected by a sensor when it is transferred within the material or on the surface. There are already several publications of AE systems detecting mixed friction conditions in journal bearings on a component level. Typical frequency ranges of AEs are between 50 kHz–2 MHz (Albers and Dickerhof, 2010).

To measure AEs from the stern tube bearings, a *Qass Optimizer4D*, shown in Figure 48 (a), was positioned and operated at the port shaft line, as shown in Figure 48 (b). Two sensor positions were identified to measure AE coming from the middle and forward stern tube bearing, as shown in Figure 49.

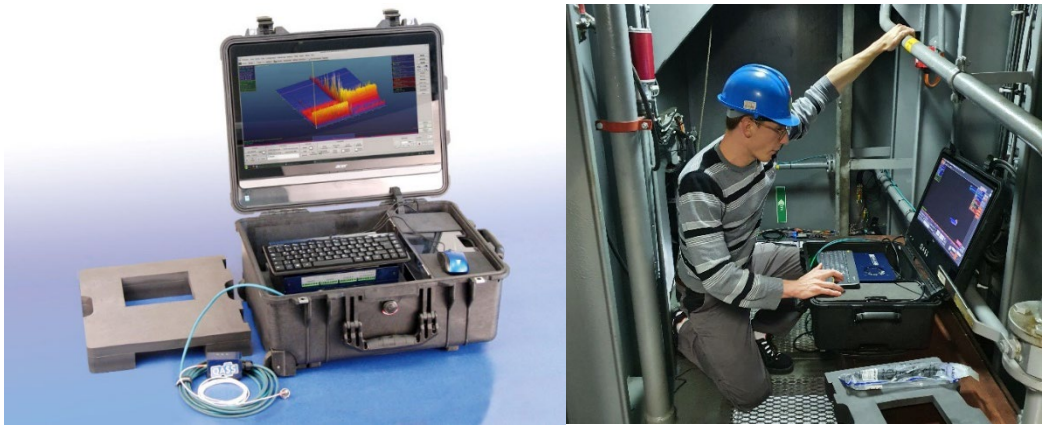

(a) **(b)**

Figure 47: (a) Qass Optimizer4D; (b) AE System Installed at Shaft Line of the SA Agulhas II.

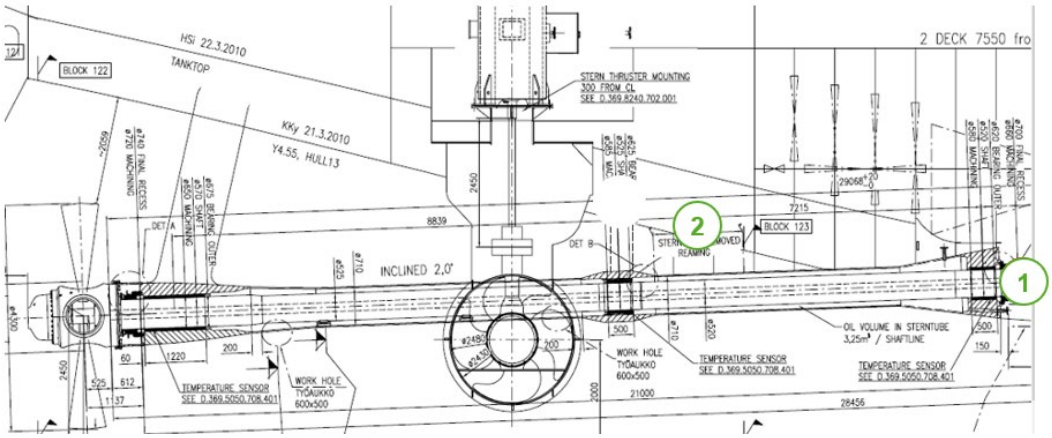

Figure 48: Port Shaft Line Arrangement of SA Agulhas II Showing AE Sensor Positions 1 and 2.

To compare different operational conditions of the ship, AE measurements were conducted in both ice and open water. An exemplary AE signal of a reference measurement in open water is shown in Figure 50 (a) and in ice in Figure 50 (b) over a measurement duration of one second. The occurrence of sea ice is clearly noticeable and appears as stochastic energy outbursts in the signal. A more detailed analysis of the measurements is planned.

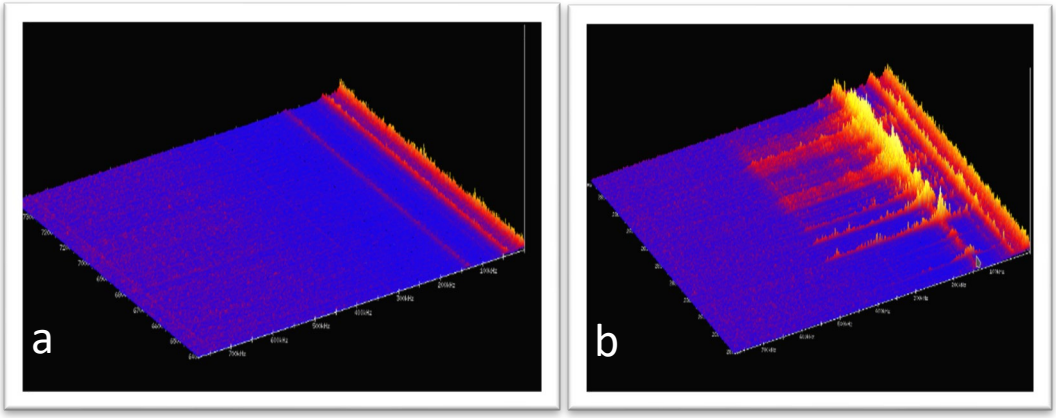

Figure 49: AE Measurement of Ship Going Through (a) Open Water and (b) Sea Ice with an Ice Concentration of 100 %.

11.3.3 Hull Stress Monitoring System

Aalto University (Finland) and Stellenbosch University (South Africa) jointly measured ice loads on the hull of SA Agulhas II and conducted parallel ice condition observations, discussed further in Section 11.4, to accompany the analyses of the ice loads. The hull stress monitoring system installed during ship construction in Rauma, Finland, was used to record the ice loads through strain gauge measurements on the hull. The three strain gauge measurement locations are shown with red rectangles in Figure 51. The strain measurements are recorded by the central measurement unit of this system located in the Engine Store Room, which was regularly monitored by the Aalto University and Stellenbosch University representatives.

Data was recorded continuously through this hull stress monitoring system when the ship was in sea ice. The 5-minute-maxima of the measured loads on the hull of the ship during SCALE Winter Cruise are presented in Figure 52, which includes the ice loads between the two vertical dotted lines and the loads from waves on the open ocean outside of the dotted lines.

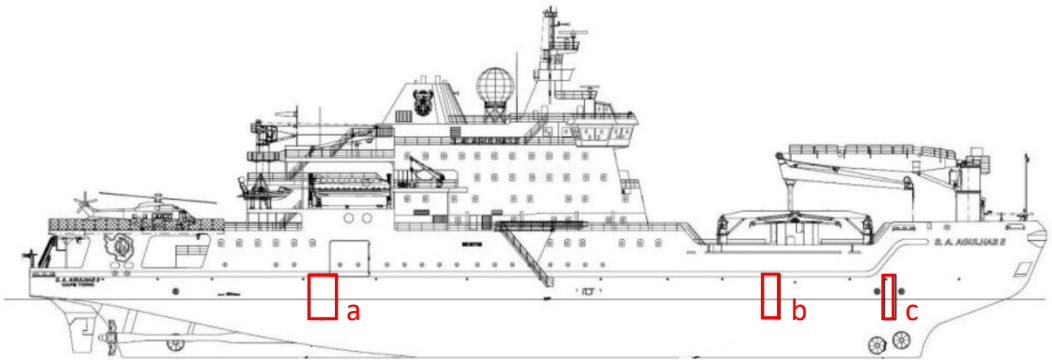

Figure 50: A Diagram Showing the Strain Gauge Locations for Ice Load Measurements on the Hull. (a) Stern Shoulder; (b) Bow Shoulder; (c) Bow Area.

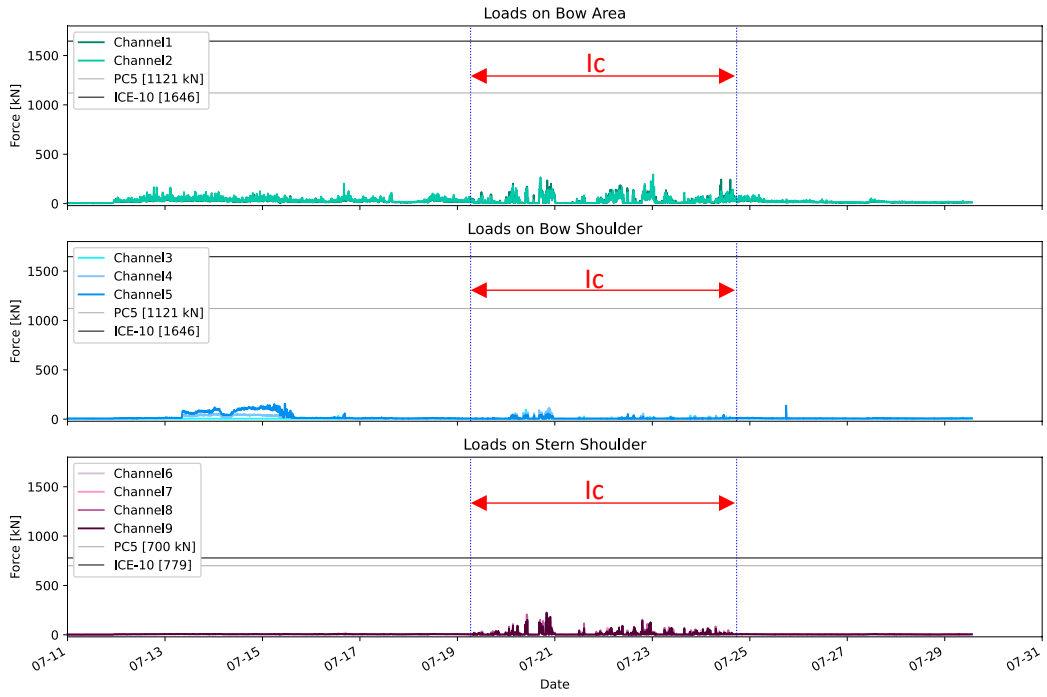

Figure 51: 5-Minute-Maxima of the Measured Loads on the Bow Area, Bow Shoulder and Stern Shoulder During SCALE Winter Cruise 2022.

In Figure 52, loads recorded during open water travel are found to be of a similar order of magnitude as for ice traverse on the bow of the ship, while the loads on the stern appear notably higher when traversing ice. The data displayed is preliminary and without in-depth quality control yet. Fourteen values in total from channel 3 to 5 (Bow Shoulder) from the 16th of July were removed as they displayed non-physical peaks probably originating from sensor malfunction.

This system was installed on board the SA Agulhas II in 2011 and has been operating since. Thus, the data collected about winter sea ice conditions in the MIZ during SCALE Winter Cruise 2022 will extend the over 10-year long time series containing ice loads that the SA Agulhas II has encountered during different sea ice conditions. This contributes to the most extensive ship ice load data set that exists.

11.4 Sea Ice and Sea State Observations

Team Vessel 4.0 members recorded the environmental conditions that the SA Agulhas II encountered throughout SCALE Winter Cruise 2022 to supplement the ship response and propulsion system measurements. The sea state conditions were notated through visual observations only, and sea ice conditions were recorded through visual observations (by team members), machine vision (by a camera) and an electromagnetic (EM) device.

11.4.1 Visual Sea State Observations

Variables describing the sea state that the SA Agulhas II encountered while travelling through open water were recorded in an Excel spreadsheet by Stellenbosch University representatives. Metrics notated included wave height, wave encounter frequency, relative wave incidence, and more. Sea state observations were performed through visual observation of the sea state in three-hourly intervals during daylight from the Deck 7 Passenger Lounge windows and balcony, with reference to the Scientific Data System (SDS) display on the computer screen in the lounge. In total, the available daylight hours allowed for 24 sea state observations during the leg from Cape Town to the MIZ, and 18 from the MIZ to Cape Town.

11.4.2 Visual Sea Ice Observations

Throughout the time of the cruise when the SA Agulhas II was in ice-covered areas, the Vessel 4.0 Team conducted visual observations of the sea ice state from the Bridge. A team member was standing on the port-side of the Bridge, recording the ice conditions every minute in an Excel spreadsheet on a laptop that created 10-minute averages. Metrics including sea ice concentration, thickness and floe size were monitored continuously when in ice and the ship was moving. The number of hours that the ship was moving through various sea ice concentrations as noted in the sea ice observations, recorded from the morning of 19 July to the evening of 24 July, is shown in Figure 53. In Figure 53, a sea ice concentration of 0 (in the range [0, 10]) also includes the time recorded travelling through open water, such as polynyas, while in the MIZ. In total around 51 hours of sea ice observations were conducted.

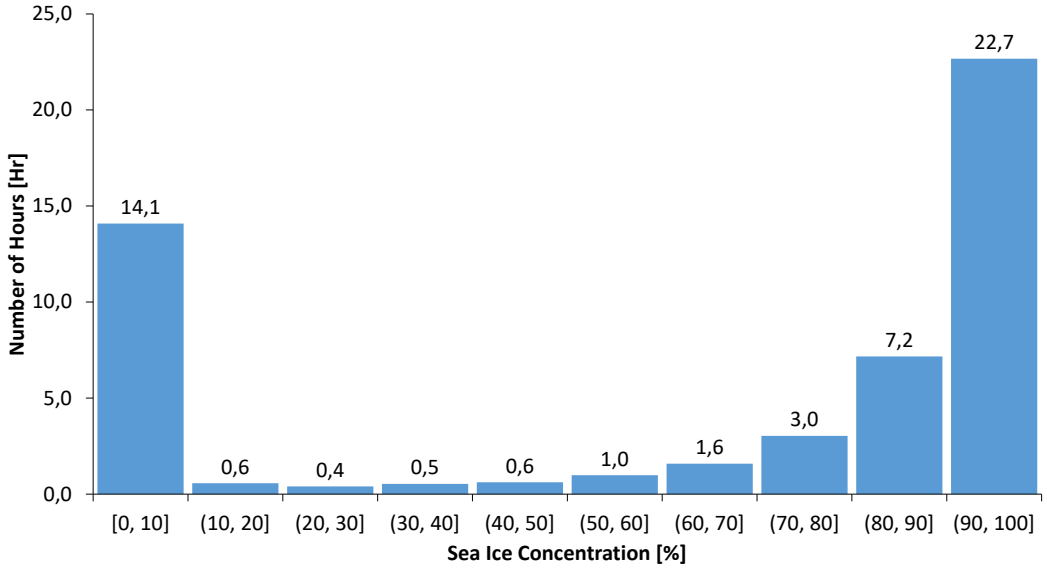

Figure 52: Number of Hours Recorded in Different Sea Ice Concentrations.

For an estimate of the ice thickness, a yardstick with a total length of 1.5 m and markings in 10 cm intervals, fixed to the railing on the port side of the main deck, was utilised. The views from the port-side of the Bridge when doing sea ice observations in daylight and with ship spotlights on when it was dark are shown in **Figure 54** (a) and (b), respectively, which includes the location of the yardstick. The observations also included additional comments on the ice conditions, ship movement and operational test sequences, and possible events that could influence the ship.

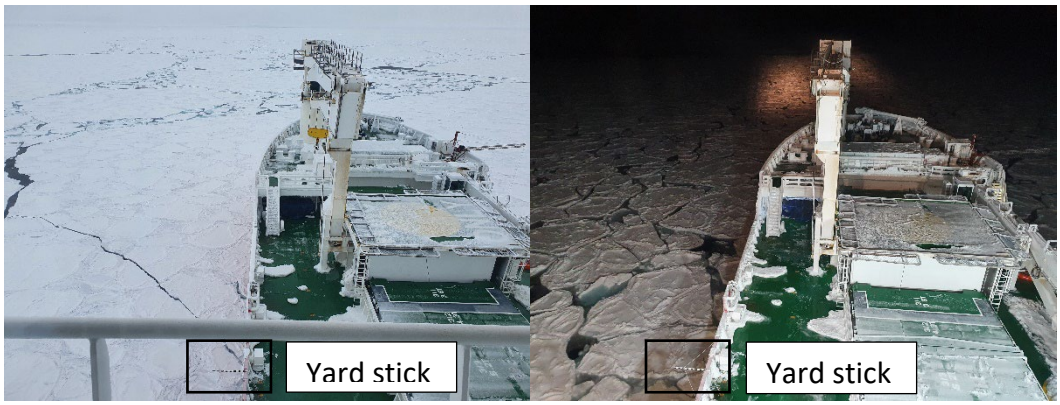

Figure 53: View from the Port-Side of the Bridge While Doing Ice Observations. (a) During Daylight; (b) With Spotlights on at Night.

11.4.3 Sea Ice Observations with Machine Vision

A machine vision system was placed at the Crow's Nest on Deck 10, watching over the front of the ship and the environment around it. The system consisted of a camera, which was located outside on a frame, a laptop for data collection, which was placed inside the Crow's Nest, and a GPS tracker, which was located behind the Crow's Nest. The camera was set to time-lapse mode taking an image every 5 seconds during daytime. The raw images were transformed into jpg-images every 30 seconds. Two pictures taken by the camera are shown in Figure 55. The frame on which the camera gets mounted remains stowed on board in the Science Store Room on Deck 2 for future use.

Figure 54: Two Pictures Taken by the Camera Located at the Crow's Nest of the Ship During Different Sea Ice Conditions. (a) 20th July 2022 Around 14h00 (UTC); (b) 21st July 2022 Around 14h00 (UTC).

11.4.4 Ice Thickness Measurements

Team Vessel 4.0 supported the measurement of sea ice thickness by installing and operating a crane, custom-developed by Stellenbosch University representatives, during ice traversal. The crane is comprised of a beam and winch system that was set up at the bow on the starboard side, as shown in Figure 56 (a). The crane suspended an EM device and laser housed in a kayak just above the ice, as shown in Figure 56 (b). The computer logging data retrieved from the EM device and laser through a wired connection, shown in Figure 56 (c), was housed in the Bosun and Chippy Store. Additionally, a GPS module was placed in the Bosun and Chippy Store and logging location data to the same computer. The EM device, laser, GPS module and data acquisition computer were provided by the Finnish Meteorological Institute, who post-process the raw data captured to compute the measured ice thickness.

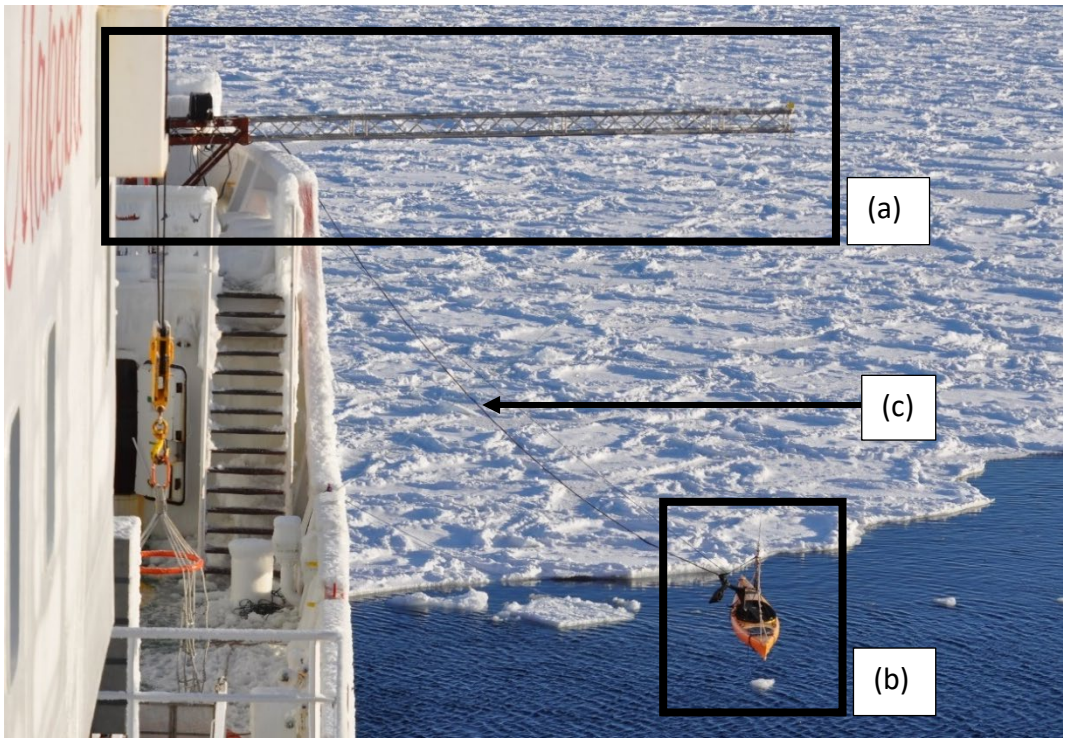

Figure 55: Crane and EM Device Setup. (a) Crane; (b) EM Device; (c) Cables Connecting Devices in the Kayak to the Data Acquisition Computer.

11.5 Operational Test Sequences

Multiple vessel operational test sequences were requested to be performed in sea ice and open water during SCALE Winter Cruise 2022. Descriptions and notations relating to the sets that were performed are documented in this section, and those that could not be performed are included in Appendix A.

11.5.1 Varying Incident Wave Angles in Open Water

A set of open water sequences that make up a single full test is completed by holding the vessel stationary at various headings to investigate the ship response to varying incoming wave directions, as shown in Table 15. The test set is preferred to be repeated in different sea states (wave heights between 1 m and 4 m, as the captain determined it was safe) to enable comparison of ship response to varying incident waves in different wave heights.

Table 13: Requested Incoming Wave Directions.

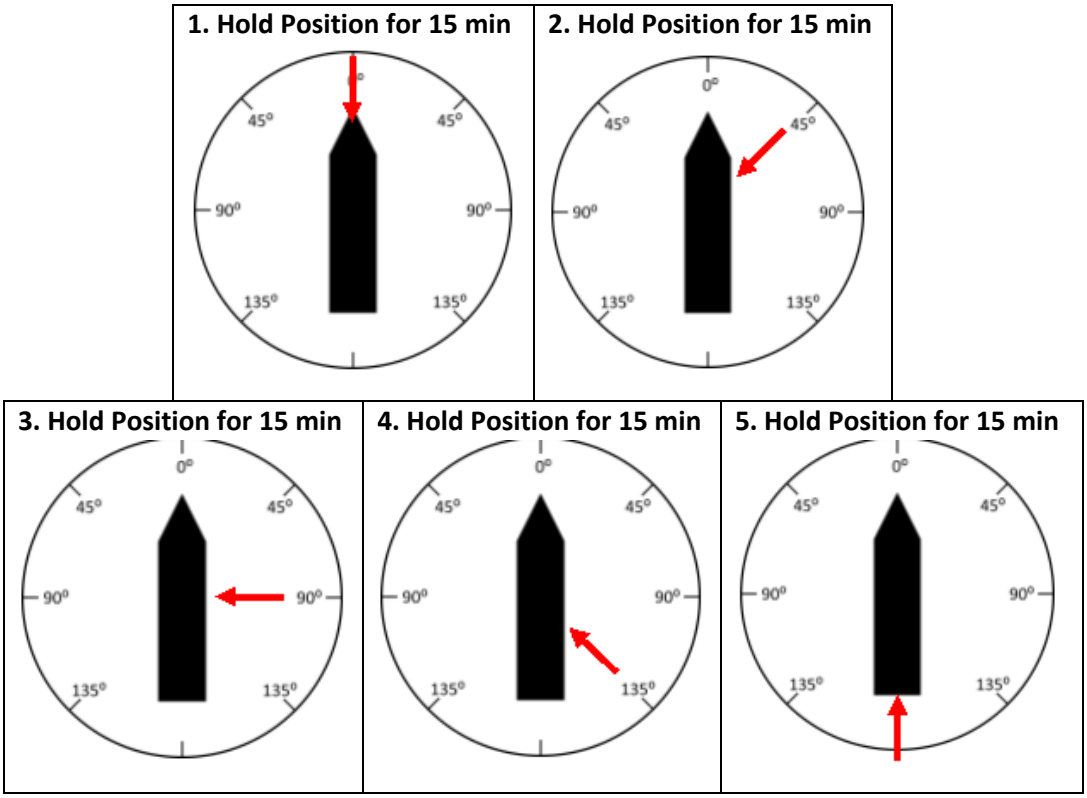

This test set was requested to be repeated twice during SCALE Winter Cruise 2022. The first set scheduled to be performed on 18 July 2022 was cancelled due to sea states being too rough. One full test set was performed on 27 July 2022 on the leg from the MIZ to Cape Town, as described by the details recorded in

Table 16. Four participants recorded subjective slamming notes during the test sequence, which is described further in Section 11.6.3.

Table 14: Details of Full Test Set Performed (Times Indicated are UTC).

Date of Test	27 July 2022
Location of Participants During Test	Bridge
Wave Height (m)	1 to 1.5 m (Amplitude)
Time to Count 10 Periods (s)	68,86 to 76,53
Ship Speed (kt)	0 to 0,1
Comments at Start	Wave state is confused – using wind waves to coordinate ship position, but there is a sea swell 40 degrees relative to the ship with a wave height of 1 m (Amplitude)
Position 1 (0°) Start Time	09h15
Position 1 (0°) End Time	09h30
Comments	None
Position 2 (45°) Start Time	09h38
Position 2 (45°) End Time	09h53
Comments	None
Position 3 (90°) Start Time	09h58
Position 3 (90°) End Time	10h13
Comments	Thrusters causing noticeable vibration
Position 4 (135°) Start Time	10h18
Position 4 (135°) End Time	10h33
Comments	None
Position 5 (180°) Start Time	10h39
Position 5 (180°) End Time	10h54
Comments	None
Wave Height (m)	1.5
Time to Count 10 Periods (s)	85,18
Ship Speed (kt)	0

11.5.2 Breaking Ice at Constant Speed

The first requested test sequence (called scenario 1) to be performed in ice was going straight through ice at specified speeds for set durations of time, as detailed in Figure 57 and

Table 17. While the ship was travelling straight through ice to map ice conditions in the MIZ on 22 July 2022, this set of sequences was performed, as recorded in Table 18.

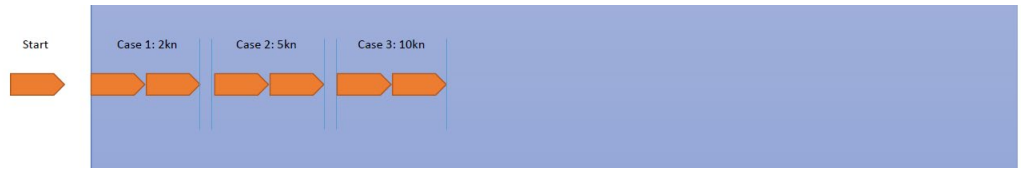

Figure 56: Scenario 1 of Operational Test Sequences Requested to be Performed in Ice (Breaking Ice at Constant Speed).

Table 15: Parameters Requested While Breaking Ice at Constant Speed.

Duration	15 minutes per speed
Preferred Speeds	2 kt, then 5 kt, then 10 kt (or 3 kt, 6 kt and 9 kt)
Power Levels	Low, then medium, then high
Preferred Ice Conditions	Level new ice floe, 2000 m to 5000 m wide, 0.5 m to 1.0 m thickness
Parameters to Note Down	Ship draught, starting and stopping time of each speed, propeller pitch, shaft RPM, ship speed achieved

Table 16: Details of Breaking Ice at Constant Speed (Times Indicated are UTC).

Date of Test	22 July 2022
Start 3 kt	02h25
Stop 3 kt	02h40
Start 6 kt	02h45
Stop 6 kt	03h00
Start 9 kt	03h05
Stop 9 kt	03h20
Start 10 kt	04h05
Stop 10 kt	04h20 (maintained 10 kt until 04h38 to maintain course)
Notes	• Ship is in sea mode • Aft draught is 6.5 m • Fore draught is 7.1 m • It is dark outside – ship spotlights on to see conditions • Air temperature is -3.4°C • See ice observation sheet for ice conditions • 10 kt was recorded opportunistically while steaming straight to a station

11.5.3 Turning in Ice Without a Channel

The third requested test sequence (called scenario 3) to be performed in ice was turning in ice without a channel, as detailed in Figure 58 and Table 19. This test sequence was performed on the night of 22 July 2022, as detailed in Table 20. At times while performing these operations, the speed of the ship fluctuated as she turned. Manual control from the officer on duty was required to maintain as constant a speed as possible, but the varying magnitudes of speed noticed were also recorded in Table 20. The resulting ship track of this set of movements, extracted from the SDS, is shown in Figure 59.

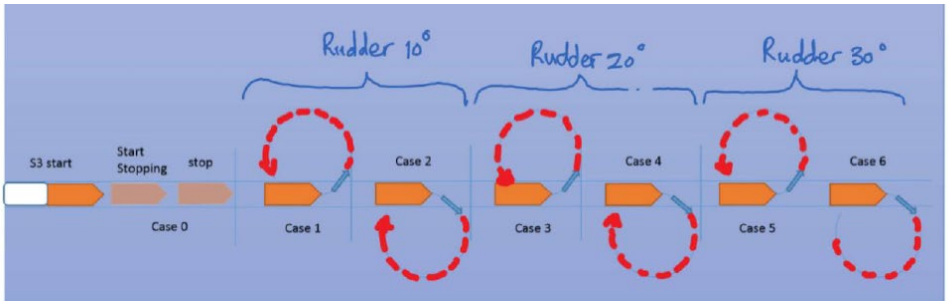

Figure 57: Scenario 3 of Operational Test Sequences Requested to be Performed in Ice (Turning in Ice Without a Channel).

Table 17: Parameters Requested While Turning in Ice Without a Channel.

Duration	Record for 20 minutes per circle (if can't do for full circle)
Preferred Speed	6 kt (constant for all cases)

Rudder Angles	Case 1 and 2 is 10° Case 3 and 4 is 20° Case 5 and 6 is 30°
Preferred Ice Conditions	Level new ice floe, 2000 m to 5000 m wide, 0.5 m to 1.0 m thickness
Parameters to Note Down	Ship draught, starting and stopping time of each circle, propeller pitch, shaft RPM, ship speed achieved

Table 18: Details of Turning in Ice Without a Channel (Times Indicated are UTC).

Date of Test	22 July 2022
Start 10° Port	**21:20**
Comments	Port: 80% pitch, 78 rpm, torque 28%, 705kW Stbd: 76% pitch, 77 rpm, torque 22%, 548kW 21:22 6.7 kt, 21:24 6.5 kt, 21:26 6.1 kt, 21:28 5.8 kt, 21:30 5.5 kt, 21:33 5.0 kt, 21:34 4.8 kt, 21:41 7.1 kt
Stop 10° Port	**21:43**
Start 10° Stbd	**20:55**
Comments	Port: 78% pitch, 77 rpm, torque 23%, 570kW Stbd: 75% pitch, 77 rpm, torque 22%, 544kW
Stop 10° Stbd	**21:13**
Start 20° Port	**22:15**
Comments	Port: 79 % pitch, 77 rpm, torque 26 %, 666 kW Stbd: 74 % pitch, 77 rpm, torque 18 %, 451 kW 22:15 6.0 kt, 22:19 6.1 kt, 22:23 5.8 kt, 22:27 6.3 kt
Stop 20° Port	**22:29**
Start 20° Stbd	**21:53**
Comments	Port: 76 % pitch, 76 rpm, 21 % torque, 522 kW Stbd: 71 % pitch, 75 rpm, 20 % torque, 491 kW 21:53 5.8 kt, 21:56 5.2 kt, 21:58 5.5 kt, 22:00 5.9 kt, 22:02 6.7 kt, 22:04 6.6 kt
Stop 20° Stbd	**22:05**

Start 30° Port	**22:36**
Comments	Port: 80% pitch, 78 rpm, 26 % torque, 660 kW. Stbd: 72 % pitch, 76 rpm, 23 % torque, 558 kW. 22:37 5.6 kt, 22:44 6.0 kt
Stop 30° Port	**22:45**
Start 30° Stbd	**22:53**
Comments	Port: 80% pitch, 78 rpm, 28 % torque, 710 kW. Stbd: 74 % pitch, 77 rpm, 20 % torque, 488 kW. 22:56 5.8 kt, 22:58 5.9 kt, 23:02 6.2 kt
Stop 30° Stbd	**23:03**
Notes	• Ship is in sea mode • Aft draught is 6.5 m • Fore draught is 7.1 m • It is dark outside – ship spotlights on to see conditions • Air temperature is -2.0°C • See sea ice observation sheet for ice conditions

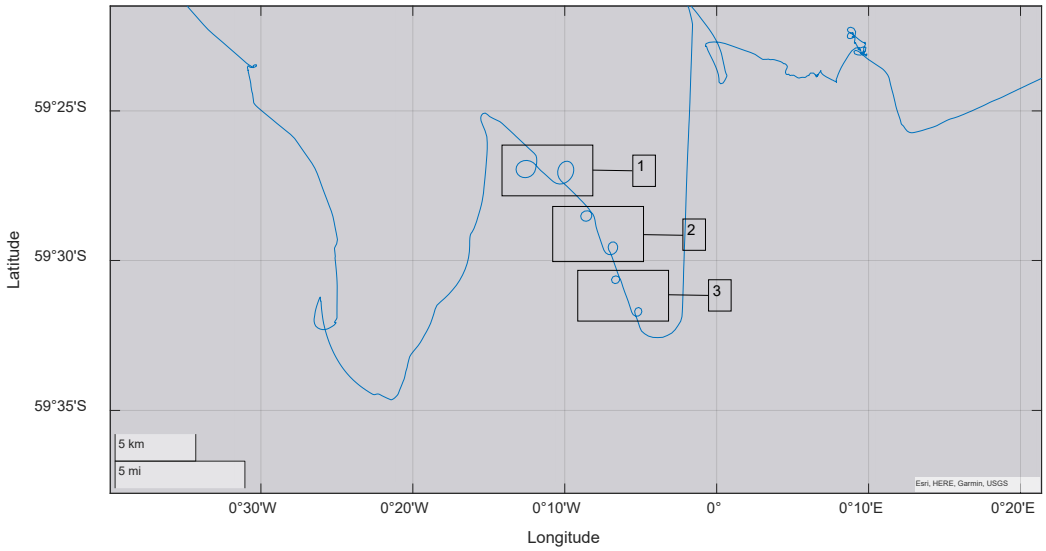

Figure 58: Ship Track After Turning in Ice Without a Channel; (1) Rudder Angle at 10°, (2) Rudder Angle at 20° and (3) Rudder Angle at 30°.

11.5.4 Fixed Shaft RPM and Propeller Pitch Test Sequences

The propeller loads, caused by direct contact of the propeller with sea ice, are mainly dependent on the kinematics of the ice entering the propeller, depth of cut of the propeller going through the ice,

and the mechanical and physical features of the sea ice. The kinematics of a propeller are often described by the advance coefficient *J*,

$$J = \frac{V}{nD},$$

where *V* describes the velocity of the incoming ice, which can be approximated by the vessel speed over ground (SOG), *n* describes the rotational speed of the propeller and *D* the outer diameter of the propeller. A certain value of advance coefficient always results in a corresponding nominated thrust and torque of the propeller. To investigate the influence of these parameters on the AE signal, and thus on the contact conditions in the bearings, two dedicated ice test sequences were performed using a vessel operation system mode that allowed separately setting propeller pitch and rotational speed of the propeller shaft (RPM). The first test sequence included keeping a fixed propeller pitch, and the second a fixed RPM. The resulting SOG from setting the pitch and RPM parameters, and influence of the current ice and sea conditions, cannot be set independently.

During the fixed-pitch test sequence, the pitch of both port and starboard (STBD) propellers were set to 88 %. This pitch setting equals the pitch of a model propeller designed to carry out small scale ice-contact experiments at MSE. The rotational speed was then increased gradually from 45 RPM (minimum rotational speed) to 120 RPM, as shown in Figure 60. The rudder angle was set to 0° to create a symmetrical wake field around the propeller and thus to keep hydrodynamic influences on the propeller loads to a minimum. During the fixed-pitch test sequence, a pitch setting of 88 % could not exactly be maintained. Both propellers show a maximum pitch deviation of 5.7 %. The port propeller nearly settles at a pitch of 91 % and the STBD propeller at 86 %. Both propeller pitches dropped significantly at 120 RPM. This was caused by the generators reaching their power limit even though the theoretical rotational speed limit is 140 RPM.

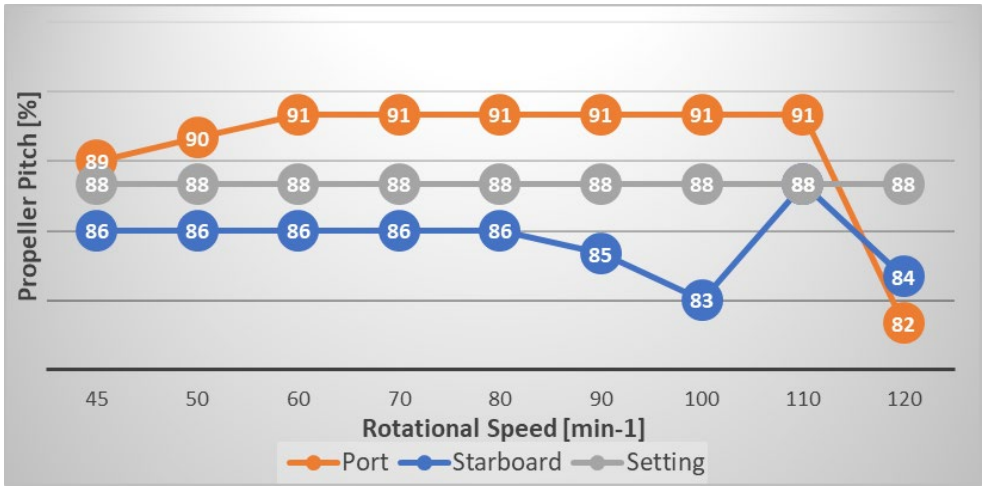

Figure 59: Fixed-Pitch Test Sequence Where Pitch of Both Propellers (Port and STBD) Was Set to 88 % and RPM Was Gradually Increased.

During the fixed-RPM test sequence, a constant RPM of 140 was set for both propellers and the pitch setting was gradually increased, as shown in Figure 61. In contrast to the pitch, the RPM of both propellers stayed constant over the entire sequence and only dropped at a pitch setting of 75 %. This is again due to the power limit of the generators. Both propellers show a maximum deviation between pitch setting and actual pitch of 8.6 %. The operational parameter curves can

now be compared to the AE signal to analyse the influence of propeller pitch and RPM on the contact conditions in the stern tube bearings.

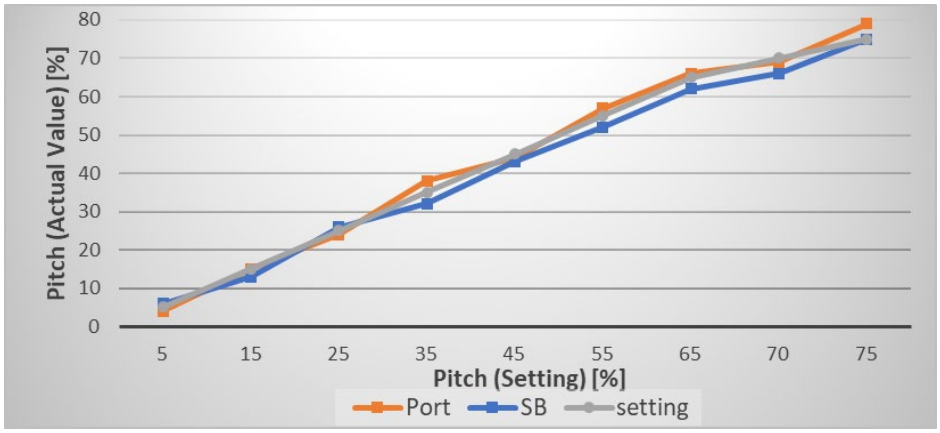

Figure 60: Fixed-RPM Test Sequence Where RPM Was Set to Maximum Speed (140 RPM) and Pitch of Both Propellers (Port and STBD) Was Gradually Increased.

11.6 Human Responses to Slamming and Motion Sickness

In addition to studying the structural responses of the ship, passengers were recruited to participate in the study of human responses to slamming and rigid body motion experienced during the voyage. The recruitment procedure and incentive scheme to motivate participation is outlined in Section 11.6.1. Passengers were invited to participate in three activities; namely completing paperbound daily diary booklets, submitting daily responses through a mobile application, called Mariner 4.0, and dedicated slamming observation sessions, reported in Sections 11.6.2 and 11.6.3.

11.6.1 Participant Recruitment and Incentive Scheme

A recruitment presentation was performed by the primary investigator in the auditorium of the SA Agulhas II on the evening of 11 July 2022 before departure for SCALE Winter Cruise 2022. All passengers (84 on board) were invited to attend the recruitment presentation. The daily diary booklets, consent forms, and complimentary pens were distributed in the auditorium before the meeting, as shown in Figure 62, so that prospective participants could view them while the primary investigator was providing questionnaire completion guidelines. Passengers interested in using the Mariner 4.0 application were invited to install the application at an installation station (the primary investigator facilitated installation through Android Studio) after the presentation.

Figure 61: Daily Diaries, Consent Forms and Pens Distributed Before Recruitment Presentation.

The presentation content included information regarding the research background, where participants fit into the research, expectations of participants and ethical considerations. Guidelines for completing the daily diary booklets, using the Mariner 4.0 application and information regarding the participation incentive scheme were also provided in the presentation.

Previous studies and experience have shown that participation is positively influenced by an incentive scheme. In efforts to encourage sustained participation throughout the voyage, the SCALE Winter Cruise 2022 was partitioned into three legs with a participation check point at the end of each leg. Participants that fully completed entries for each leg received a coupon that they could redeem from the passenger lounge bars for a beverage of their choice. The leg names with number of participants that completed daily diary entries and Mariner 4.0 application submissions during each leg are shown in Table 11. Based on the check point results, the average participation rate observed throughout the voyage was 56 %. Upon preliminary daily diary processing, the number of daily diaries that contained usable data revealed the true participation rate to be closer to 75 %.

Table 19: Research Activity Participation Summary Throughout Winter Cruise.

Leg Name	Cape Town to MIZ	MIZ	MIZ to Cape Town
Date of Check Point	18 July 2022	24 July 2022	30 July 2022
Daily Diary Participation	65 %	57 %	45 %
Mariner 4.0 Participation	12 %	17 %	15 %

11.6.2 Daily Diary Distribution and Mariner 4.0 Application Deployment

The daily diary and Mariner 4.0 participation opportunities related to the study of human factors during SCALE Winter Cruise included:

Completing daily diary booklets that contained a one-page long questionnaire repeated for every day of the voyage, as shown in Figure 19, requested to be completed each day throughout the voyage. At the start of the booklet was a once-off questionnaire to record background and demographic information unique to the participant, as shown in Figure 20.

Installing the Mariner 4.0 application on smartphones of participants that had Android operating systems. Participants were requested to submit feedback via the Mariner 4.0 application at least three times a day around mealtimes and at the onset of motion sickness symptoms.

The Mariner 4.0 application facilitated a digitized means of capturing data relating to passenger motion sickness and location on board. Near-Field Communication (NFC) tags were installed vessel-wide as an enabling technology for monitoring passenger location using the Mariner 4.0 application. NRF tags were placed in strategic positions on board for the duration of the voyage.

Data transfer from the Mariner 4.0 application on the smartphones to a computer that hosted custom-developed data acquisition software relied on the onboard WiFi network and required a static IP address. The Electrical Technical Officer on board assisted the Stellenbosch University representative by allocating a static IP address on the local network. The computer hosting the human response data acquisition software was located in the Business Centre. Additionally, a dedicated ethernet access point in the Dry Biology Laboratory was allocated to Stellenbosch University to enable communication between the primary full-scale measurement system and the human response data acquisition system on the local network. This enabled the real-time integration and analysis of ship motion measured by the full-scale measurement system and feedback captured through the Mariner 4.0 application for a participant.

1. Encountered slamming: ○ No ○ Occasionally ○ Regularly

2. If you consider slamming on what scale do you experience:

	0 - Comfortable	1	2	3 - Uncomfortable	4	5	6	7 - Extremely Uncomfortable	8	9	10
2.1. 24 – Hour ***average*** slamming rating	○	○	○	○	○	○	○	○	○	○	○
2.2. Rating for slamming induced ***vibration***	○	○	○	○	○	○	○	○	○	○	○
2.3. Rating for slamming induced ***noise***	○	○	○	○	○	○	○	○	○	○	○

3. Which is the main source of your discomfort and/or activity disturbance?

○ Slamming (vibration and sound when ship hits waves) ○ Rigid body motion (roll, pitch or yaw of the ship) ○ Both ○ N/A

4. Activities affected:

	Sleeping	Typing/Writing	Visual Tasks	Equipment Use	Equipment Damage
Slamming	○	○	○	○	○
Rigid Body Motion	○	○	○	○	○
Both	○	○	○	○	○
None	○	○	○	○	○

	Rate (Frequentness)	Magnitude
4.1. **Reason** for activity disturbance: Yes	○	○
No	○	○

5. In case of sleep disturbance indicate:

	0 - Comfortable	1	2	3 - Uncomfortable	4	5	6	7 - Extremely Uncomfortable	8	9	10
5.1. Disturbance ***rating***:	○	○	○	○	○	○	○	○	○	○	○

5.2. How often did slamming ***wake*** you up? ○ None ○ Once ○ More than once

	Noise due to slamming	Vibration due to slamming
5.3. ***Why*** did slamming ***wake*** you? Yes	○	○
No	○	○

5.4. Shift ***worked***: ○ 08:00 - 12:00 ○ 12:00 - 18:00 ○ 18:00 - 00:00 ○ 00:00 - 08:00

5.5. ***Time*** of disturbance:

08	09	10	11	12	13	14	15	16	17	18	19
○	○	○	○	○	○	○	○	○	○	○	○
20	**21**	**22**	**23**	**00**	**01**	**02**	**03**	**04**	**05**	**06**	**07**
○	○	○	○	○	○	○	○	○	○	○	○

5.6. Comment(s):

6. Indicate three locations where you encountered the most slamming in order of most (1) to the least (3):

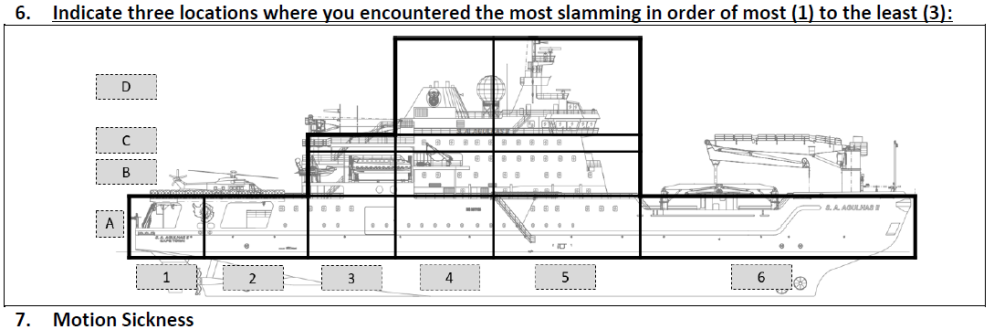

7. Motion Sickness

Did you get motion sick?		Did you vomit?		What is your illness rating on a scale of 0-3?			
Yes	No	Yes	No	0 - Nothing	1 - Slight	2 - Moderate	3 - Dreadful
○	○	○	○	○	○	○	○

Figure 62: Example of a Daily Questionnaire.

1. Personal voyage duration

What date did you embark?		*What date will you disembark?*	

2. Demographics

Please enter your age		*Sex*	Male	Female
Please circle the most appropriate term that describes you:				
Ship based scientist	Land based scientist	Other (please specify)		

3. Previous experience at sea

Time spent at sea	Days		Weeks		Months		Years	
Number of voyages (a voyage = longer than a week at sea)	1st	2nd	3rd	4th	5th	6+		

4. Susceptibility to motion sickness

Have you ever had motion sickness on ships?	Yes	No
Have you ever had motion sickness on cars?	Yes	No
Have you ever had motion sickness on buses?	Yes	No
Have you ever had motion sickness on coaches?	Yes	No
Have you ever had motion sickness on small boats?	Yes	No
Have you ever had motion sickness on aeroplanes?	Yes	No

5. Motion sickness prevention

Have you taken any motion sickness medication prior to the voyage?		Yes	No
Did you use any other means to prevent motion sickness?		Yes	No
Please detail the type of medication or means you use(d) to try combat motion sickness, if any. Please also include the dosage.	*Type*		
	Dosage		

Figure 63: Questionnaire to Capture Background and Demographic Information.

11.6.3 Slamming Observations During Operational Test Sequence

A slamming observation session involved participants logging subjective measures of slams experienced at a given time through a user interface. A single slamming observation session was conducted during the varying incident wave angles test sequence described in Section 4.4.1 (on 27 July 2022). An average of 167 slams were noted among the four participants who stood on the port-side of the Bridge throughout the duration of the procedure.

11.7 Requested Operational Test Sequences Not Performed

During SCALE Winter Cruise 2022, test sequences requested to be performed in ice that could not be performed included reversing in ice and breaking out of an existing ice channel. In the channel created by breaking ice at constant speed, called scenario 1 in the requested test sequences and detailed in Section 4.4.2, it was requested to reverse straight out of the channel through ice debris and perform the scenario detailed in Figure 22, considering parameters in Table 12, in the channel. During SCALE Winter Cruise 2022, consolidate ice that formed a level sheet of ice large enough to perform the full scenario in was not encountered. Additionally, opportunistic reversing could not be performed due to bad weather present when the research schedule allowed for it.

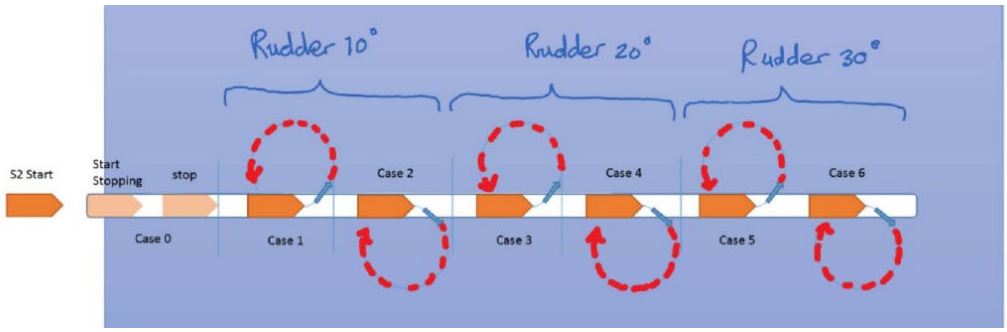

Figure 64: Scenario 2 of Operational Test Sequences Requested to be Performed in Ice (Breaking Out of an Existing Channel).

Table 20: Parameters Requested While Breaking Out of an Existing Channel.

Duration	Record for 20 minutes per circle (if can't do for full circle)
Preferred Speed	6 kt (constant for all cases)
Rudder Angles	Case 1 and 2 is 10° Case 3 and 4 is 20° Case 5 and 6 is 30°
Preferred Ice Conditions	Level new ice floe, 2000 m to 5000 m wide, 0.5 m to 1.0 m thickness
Parameters to Note Down	Ship draught, starting and stopping time of each circle, propeller pitch, shaft RPM, ship speed achieved

11.8 Acknowledgements

Team Vessel 4.0 would like to express their sincerest thank you to the following groups of people. The captain and crew of the SA Agulhas II who skillfully supported and enabled the research that was performed on board. The crew members are held in very high esteem among research members for consistent supportive aid towards the success of research on board, which is appreciatively recognised.

The passengers that participated in the human response research. Participation from passengers is an invaluable part of the research success that required a sustained commitment of time and effort throughout the duration of SCALE Winter Cruise 2022, which is gratefully acknowledged.

The National Research Foundation (NRF) that provided financial assistance, through the South African National Antarctic Programme, towards this research. Opinions expressed and conclusions arrived at are those of the authors and are not necessarily to be attributed to the NRF.

The South African Department of Science and Innovation through the MarTERA ERA-NET Cofund Scheme of Horizon 2020 of the European Commission.

The South African DFFE for their consistent support that contributes to the success of research conducted on board the SA Agulhas II.

The work by Aalto University was funded by the Academy of Finland and the Finnish Antarctic Research Program, FINNARP. This support is gratefully acknowledged.

References

Albers, A. and Dickerhof, M., 2010. *Simultaneous Monitoring of Rolling-Element and Journal Bearings Using Analysis of Structure-Born Ultrasound Acoustic Emissions*. Proceedings of the International Mechanical Engineering Congress and Exposition. Vancouver, British Columbia, Canada.

Bekker, A., Soal, K. I. and McMahon, K. J., 2017. Whole-Body Vibration Exposure on Board a Polar Supply and Research Vessel in Open Water and in Ice. *Cold Regions Science and Technology*, Volume 141, pp. 188-200. DOI: 10.1016/j.coldregions.2017.06.008.

Bekker, A., Suominen, M., Kujala, P., de Waal, R. J. O. and Soal, K. I., 2018. From Data to Insight for a Polar Supply and Research Vessel. *Ship Technology Research*, Volume 66, Issue 1, pp. 57-73. DOI: https://doi.org/10.1080/09377255.2018.1464241.

De Waal, R. J. O., 2017. *An Investigation of Shaft Line Torsional Vibration During Ice Impacts on PSRVS*. Stellenbosch: Stellenbosch University.

Mokhtari, N. and Gühmann, C., 2018. Classification of Journal Bearing Friction States Based on Acoustic Emission Signals. *Technisches Messen*, Volume 85, Issue 6, pp. 434-442.

Muhs, D., Wittel, H., Jannasch, D. and Voβiek, J., 2003. *Roloff/Matek Maschienelemente*. Wiesbaden: Springer. ISBN 978-3-8348-0262-0.

Pferdekamper, K., 2022. *Full-Scale Measurement and Quantification of Hull Fatigue on a Slamming-Prone Polar Vessel*. Stellenbosch: Stellenbosch University.

Sethumadhaven, A., 2018. *DNV GL Tackles Shaft Bearing Challenges.* [Online]. Available at: https://www.dnv.com/expert-story/maritime-impact/DNV-GL-tackles-shaft-bearing-challenges.html. [Accessed: 25 August 2022].

Soal, K. I., 2015. *Vibration Response of the Polar Supply and Research Vessel The S. A. Agulhas II in Antarctica and the Southern Ocean*. Stellenbosch: Stellenbosch University.

Soal, K., Bienert, J. and Bekker, A., 2015. Operational Modal Analysis on the Polar Supply and Research Vessel The S.A. Agulhas II. Proceedings of the 6th International Operational Modal Analysis Conference. Gijon, Spain.

Soal, K., 2018. *System Identification and Modal Tracking of Ship Structures*. Stellenbosch: Stellenbosch University.

Van Zijl, C.M., 2020. *Operational Modal Analysis on the SA Agulhas II*. Stellenbosch: Stellenbosch University.

12 WAVES FROM VESSEL MOTION

Team name and PI	VESSEL-waves. Butteur Ntamba-Ntamba (CPUT)
Authors	Senda P and Ntamba-Ntamba B

12.1 INTRODUCTION

The stochastic phenomenon of waves at sea is best described by its directional spectrum depending on frequency and direction. In coastal regions data from wave buoys are routinely recorded while, in the open sea, data from remote sensing satellites are available. The latter, however, lack directional information and the time and spatial resolution is not always satisfactory. In nautical practice the watch officer is required to enter the sea state regularly into the ship's log. This is usually done by visual estimation of characteristic height, period and direction.

Ship oscillations, in particular roll, are, of course, generated by waves and the avoidance of dangerously high amplitudes is of the utmost importance. Since the reaction of a ship to a particular wave system depends on course and speed, there are decision support systems which rely on the officer's estimate as input. However, the recommendations given by such systems are highly doubtful, as long as the sea state spectrum is reduced to a single point and that depending on the officer's experience. There is a necessity to carry out extensive studies of dynamic stabilities to provide shipmasters with a decision support tool to prevent large amplitude motions in different encounter conditions. This can be done by reconstruction of the sea state from the motion of the vessel. Thus the importance of a full-scale measurement of ship motions with the objectives of developing an autonomous method on board of a vessel underway, which, will enable to estimate full directional wave spectrum. Once the system works, the ship can therefore be used as a sensor for the prediction of the sea state in which it travels. The measurements are done using sensor box (it is a small self-contained strap-on system and records the time series of roll, pitch and heave.

12.2 EXPERIMENT DETAILS

During the SCALE Winter Voyage 2022, Team Vessel – Wave conducted a full-scale measurement on board the SA Agulhas II. The measurements were performed using three sensor boxes installed at different position on the SA Agulhas II. Two of the sensors were installed near the centre of gravity of the vessel in the engine room, the other sensor was installed at the observation deck (monkey deck).

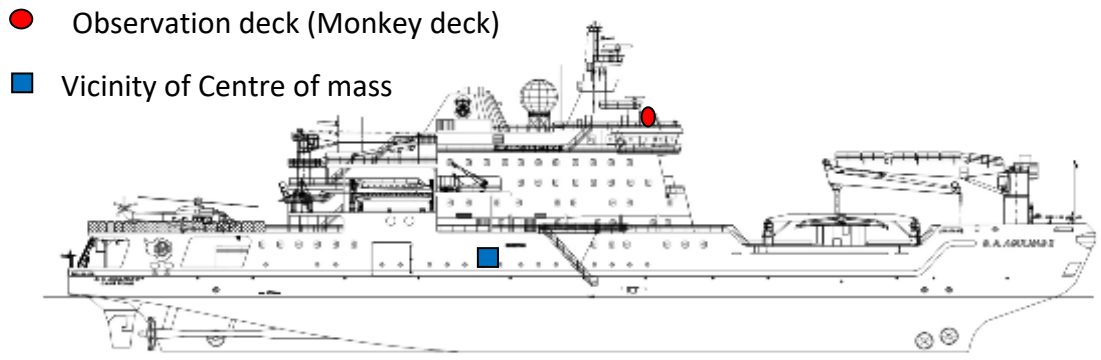

Figure 65 Location of sensors

There are two generation of sensors. The two sensors (first generation) in the engine room are without a GPS, it measures accelerations in three dimensions and the rate of roll and pitch. It consists of a 3d acceleration sensor and two gyros for the pitch and roll angle. The acceleration sensor is used to calculate the angle of roll and pitch from the direction of the gravitational force. All sensors are sampled synchronously at 400 Hz, applying appropriate filtering the data are down sampled to a rate of 10 Hz. The down sampled data are optionally sent to a serial interface (38400 Baud, 8 bits, no parity, 1 stop bit) and/or recorded on a micro SD card.

The second-generation sensor has a GPS reception connected to its that provides accurate time and position tags of the vessel this sensor gives a 3d-information on both acceleration and angular rates. This sensor was placed at the monkey deck as mentioned previously. After successful boot the display shows roll and pitch angle and symbols in the upper line, time and date are shown below. There are three symbols: the left one is for GPS (the icon should resemble a flying satellite). With an "x" show below, no GPS device is found. If there are three dots, a GPS is attached but has no fix. A check mark appears, once a fix is achieved,

Power to both types of sensors can be supplied through the USB port; it can be connected to the power supply for autonomous operation or to a computer which will give a serial connection as well. The box requires a DC power between 8V and 12 V on the barrel jack on the rear. Positive voltage is on the inner pin, the negative pole is the ground potential and to be connected to the outer pole. A noisy power supply may degrade the function of the box, it is recommended to use my AC power device. A FTDI driver is needed for the serial link.

12.3 SENSOR OPERATION

The major difference between the two generations of sensors is the insertion on the GPS in the second generation. Other than that, the sensors operate the same way as follow:

Menu: The button on the very right unlocks the other keys and brings you into the menu. The left and right button below the display move to the previous or next menu point. The up and down buttons right to the display usually start actions. Let's step through the menu:

Display to bow or aft: is just a reminder of the sensor orientation with respect to the ship. The value is logged in the output data, the output of the sensor data is not affected by this.

SD Logfile: well opens and closes logfiles. I would recommend to close a logfile before turning power off or removing the card.

SD Dir: once the card is mounted you may step through the card's directory using the up- and down key. Again, a mounted card should be ejected before removing the card or turning power off. This can be accomplished in the SD Logfile menu.

USART: the serial port can be turned on and off here. A file header is included into the data each time the on-button is pressed.

Light: it is about the display's backlight. Pressing a key keeps the backlight on for a while.

GPS Position, GPS (UTC) just display the corresponding data. The next menu point shows the number of satellites with a signal strength of more than 20dB (arbitrary unknown units) and the maximum signal strength. This is to help placing the gps antenna somewhere. Usually a fix is achieved if there are more than 3 satellites > 20 dB. Since gps reception depends on reflections as well, this is not a safe indicator.

RTC: there is an internal clock with a battery backup. Sampling is synchronized with this clock. The down key will bring you into the settings menu, within this menu the left and right key move the cursor to the previous or next item. Finally, the option to set the clock or to cancel the process are offered. The new date-time is copied into the RTC at the moment of pressing the ok button.

With the next menu points the RTC may be synchronized with the GPS clock if a fix is available. Possible time zones are UTC, UTC+1, UTC+2. The synchronization is not very precise, a difference of about one second might occur.

The expert menu has a collection of debugging information. For experts (or to put it in different words: the stupid programmer) as the name says.

Data: Data are filtered with a 6 db-frequency of 3.5 Hz and a group delay of 242 ms which is not compensated in the output. On the SD-card there is a file "readSensor.m" which reads data files into Matlab.

Both sensors use the same right-handed coordinate system with the x-axis pointing through the display and the z axis upwards. The columns in the data are date, time as given by the internal rtc.

Data were recorded every 3 hours.

Figure 66 Image of the sensor box with GPS antenna

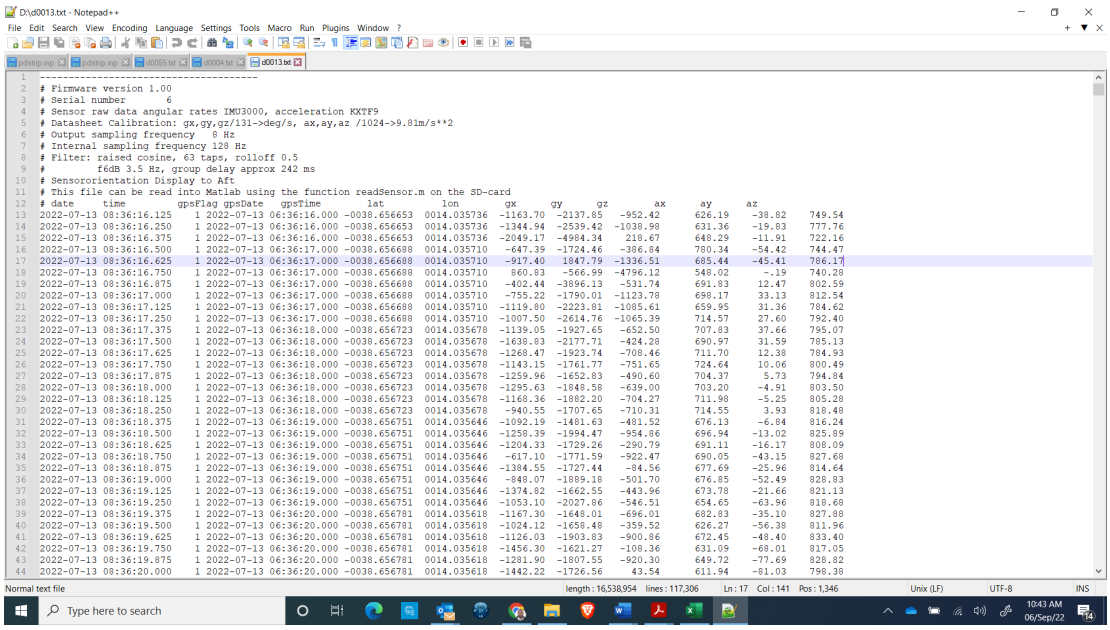

Figure 67 Sample of data recorded

12.4 ACKNOWLEDGEMENTS

- The team would like the express their gratitude to entire SA Agulhas crew, the captain, the chief engineer, the second mate and the second engineer for their availability and support we received during this voyage.
- Our gratitude goes to the South African DSI and DFFE for their continuous support in sponsoring the Southern oCean seasonal Experiment (SCALE).
- We will not finish if we don't recognise the friendly and amicable collaboration from all the researchers onboard the SA Agulhas II during SCALE Winter 2022.

13 SEA ICE SAMPLING

Team name and PI	SEAICE. Tokoloho Rampai, Sarah Fawcett and Marcello Vichi (MARIS UCT)
Authors	Audh R, Johnson S, Paul F, Moos S, Keche T, Swait H, Mangatane M, Kumadiro L, Collins D, Rampai T, Fawcett S, and Vichi M

During the winter cruise, the SA Agulhas II entered the Marginal Ice Zone on the 19/7/2022 and exited on the 25/7/2022. Figure 68 shows an overview of all the stations completed during the sea ice leg of the expedition. Due to time constraints and unexpected sea ice conditions, the order of stations and sampling conducted differ from the original station plan.

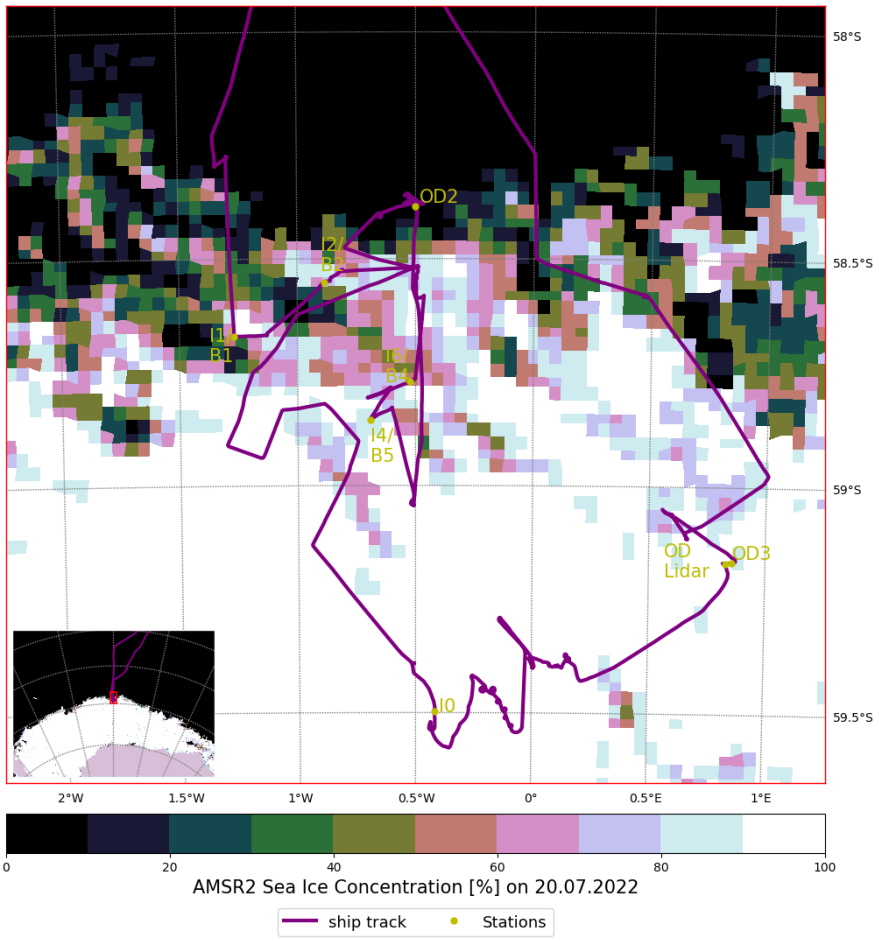

Figure 68 Map of the sampled stations. Station names are only used for internal referencing of the sample labels. Not to be used in scientific publications. Please refer to the official station names given in brackets in Table 21, as given in Table 4.

Table 21 List of sea ice stations. Station names are only used for internal referencing of the sample labels. Not to be used in scientific publications. Please refer to the official station names in brackets as given in Table 4.

Station name	Date	Time	Location	Sea Ice Type	Notes

I1/B1 (ICE21)	19/7/2022	12:35 UTC	-58.66952 S, -1.2707 W	Consolidated, very young ice	
I2/B2 (ICE22)	19/7/2022	17:35 UTc	-58.5518 S, -0.88413 W	Partly consolidated, very young ice	Deemed unsafe to core, no cores collected.
I6/B4 (ICE13)	20/7/2022	03:30 UTC	-58.771 S, -0.52212 W	Consolidated, very young ice	Team member injury, station abandoned. No cores collected.
I4/B5 (ICE11)	20/7/2022	11:00 UTC	-58.85563 S, -0.692 W	Consolidated, very young ice	Bags were labelled B2 and B3.
OD2 (OD-2)	21/7/2022	09:00 UTC	-58.38472 S, -0.49965 W	Pancake	Two pancakes were collected and fully processed.
I0 (I0B)	22/7/2022	12:30 UTC	-59.49713 S, -0.41852 W	Consolidated, young ice	Deemed unsafe for a full consolidated process station. Limited cores taken.
OD Lidar (SB06)	23/7/2022	20:00 UTC	-59.16803 S, 0.8298 E	Pancake	Pancake was prioritised for LIDAR imaging. Cores were taken approximately 2 hours after collection
OD3 (SB04)	24/7/2022	07:30 UTC	-59.16485 S, 0.85777 E	Pancake	Two pancakes were collected. However, the first pancake was not safely placed on beams thus only ALGAE cores were taken. Second pancake was fully processed.

13.1 SAMPLE COLLECTION

The aim of sampling sea ice during SCALE22 was to characterise the physical, mechanical, and biogeochemical properties of the ice in the marginal ice zone. This was done in two ways - onboard and overboard.

13.1.1 Onboard - Pancake Stations

Since this ice type is too small to core overboard, they are fished out of the ocean using a net contraption attached to the helideck crane. The pancake lifting operations during SCALE22 were conducted at 3 stations, with a total of 5 pancakes being collected across the stations.

During pancake ice stations, the crane was operational and used to lift the pancakes floes from the water to the deck, using the net seen in Figure 69. Hard hats were necessary to be worn at all times

along with the necessary cold gear PPE outlined. Pancakes floes were chosen based on their size and approximate weight; the specimen must not be larger than 3 m in diameter and thus be not more than 5 tonnes in weight. Additionally, use of the crane and net was only advised in wind speeds of below 20 knots, as wind speeds greater than this may cause the specimen to sway with the wind while in the air and become uncontrollable and dangerous to lower onto the deck. Guide ropes were attached to the net to assist in guiding the specimen to the deck as well as to control it from swaying with the wind. Once the pancake floe was safely on the wooden grids on the deck, a black bag was placed over one half of the pancake to avoid surface contamination for TracEx and snow was collected. Afterwards, coring commenced on the exposed half of the pancake. Coring whilst standing on the pancake was prohibited to maintain the integrity of the pancake during the coring process. As a result, a step ladder next to the specimen was used to core samples in the centre of the specimen.

During coring, each core was logged, and an illustration was drawn (Figure 70) to show where that core was taken from within the pancake, relative to the others. The first cores to be taken were always the PHY and BGC cores, as they are time-sensitive and were needed for immediate temperature measurement. The subsequent cores were taken for other research groups; I-Microbe, CPUT, Microbiome and Tracex. The cores dedicated for Tracex were taken from the half of the pancake covered by the black bag. Each team had a dedicated team member present to collect their cores. The remaining cores taken were assigned for structural analysis and sent to the processing laboratory for further testing.

Station OD1

Station OD1 was scheduled for the 19th July 2022 upon entering the Marginal Ice Zone. This station was a training experience whereby team members would learn how to core, take temperature measurements, process the samples in the lab and the general work environment of a typical station. Upon arrival at the station, the aft crane began malfunctioning and had a hydraulic problem thus the station had to be cancelled.

Station OD2

Station OD2 took place on the 21st July 2022 at approximately 09:00 UTC. Two pancakes were successfully collected using the aft crane. Both pancakes were fully processed. As this was the first pancake station that most team members experienced owing to the cancellation of sea ice operations at OD1, the workflow was slow to compensate for learning and training.

Station OD Lidar

The station named OD Lidar (called SB06 in master station list) took place on the evening of the 23rd July 2022 at approximately 21:00 UTC. Owing to the night-time conditions and strong winds, only one pancake was successfully collected. The pancake was left on deck for approximately an hour and a half before coring commenced to allow for LIDAR imaging to take place. Once completed, coring commenced and the pancake was fully processed. This delay in the start of coring should be noted for the temperature measurements.

Station OD3

Station OD3 (called SB04 in master station list) took place on the morning of the 24th July 2022. Owing to the strong winds, two pancakes were collected. The first pancake was not fully processed as it was not positioned on the beams correctly because of the strong winds. This pancake was only cored for the four ALGAE cores. The second pancake was fully processed. However, conditions

became dangerous towards the end of the coring activities owing to strong winds, large waves and the onset of the ship moving.

Figure 69 Pancake lifting operations

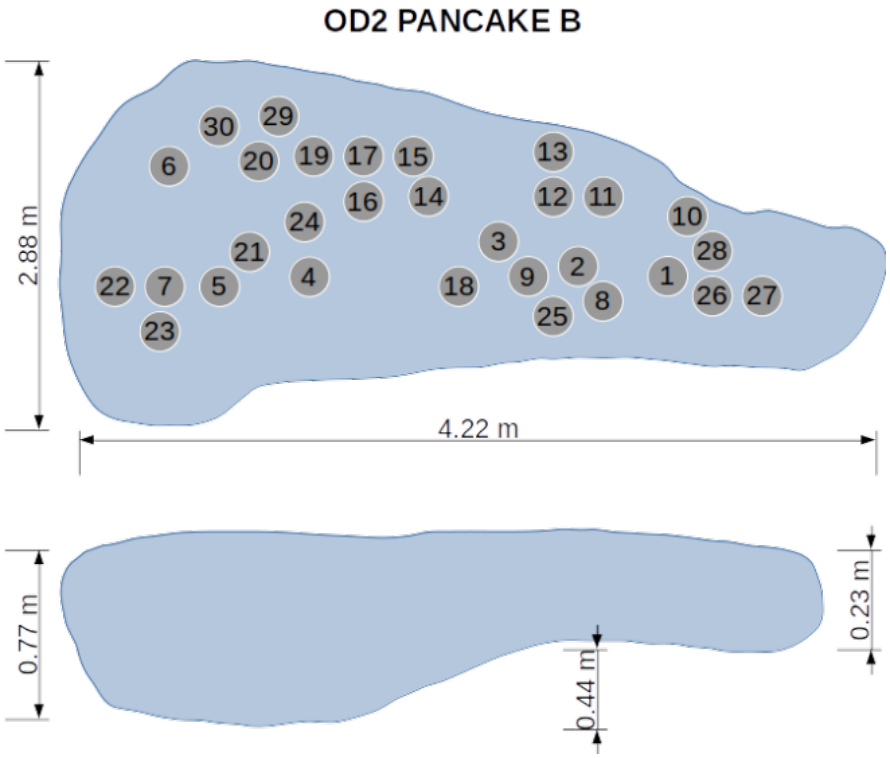

Figure 70 Schematic representation of the pancake and location of the cores collected as per log sheet.

13.1.2 Overboard - Consolidated stations

Several overboard stations took place using the forward crane and orange personnel basket. These stations required full cold gear PPE with hard hats and harnesses. A maximum of four people can be

carried overboard using the personnel basket at a time. Upon reaching the station, a suitable location was first scouted for coring. Signs of overwashing, flooding, loose frazil conglomeration or thin ice were deemed not suitable for overboard coring.

Once the basket was resting on the ice, all personnel remained on the basket while the first core was being taken for assessing the ice's safety. The first core was inspected for its length and texture to assess whether it is safe to step off the basket. Upon agreement of the ice's integrity, coring re-commenced. The PHY and BGC cores were taken last before returning to the ship's deck, and upon arrival were immediately taken for temperature measurement and subsequent laboratory processing.

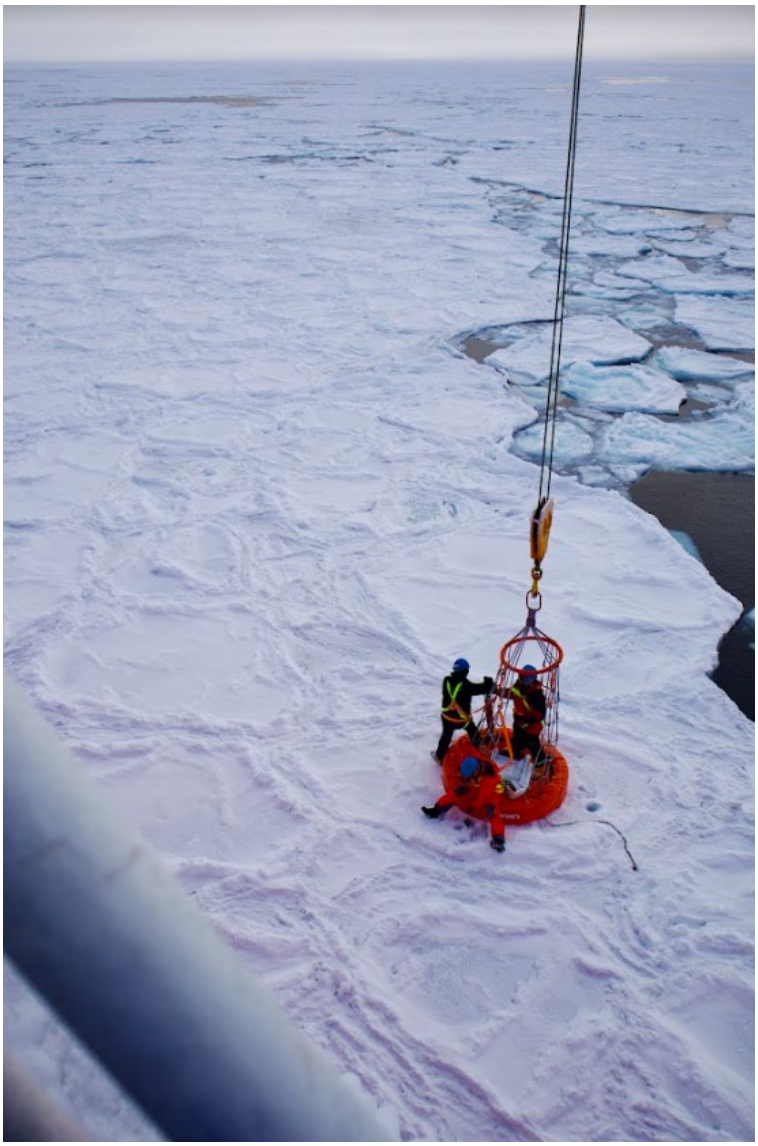

Figure 71 Overboard coring operations

Station I1/B1

Station I1 took place on the afternoon of the 19th July 2022. The sea ice was very young consolidated ice and conditions were favourable to coring. Three personnel were overboard during coring and four cores were collected. A mini CTD was deployed in the first core hole while the remainder of the cores were being taken. Upon arrival back on deck, only one core was used for temperature measurement as the team was still in training.

Station I2/B2

Station I2 took place in the late evening of the 19th July 2022. Upon arrival of the station, the sea ice conditions were assessed and was deemed not suitable for overboard coring activities. The sea ice was not consolidated, showed signs of flooding and loosely packed frazil and had large bodies of water nearby.

Station I6/B4

Station I6 took place in the early morning of the 20th July at approximately 03:00 UTC. The sea ice conditions were deemed suitable for overboard activities. Three personnel were craned overboard and coring commenced. The sea ice was difficult to core and was 'hard', with the corer blades struggling to catch the ice. After a few attempts, a team member lost consciousness and all operations were cancelled. The basket was lifted back onboard and the respective team member was taken to see the doctor.

Station I4/B5

Station I4 took place in the afternoon of the 20th July 2022. The sea ice conditions were favourable for overboard coring and this station was used for overboard and coring training for team members. Three shifts of team members were craned overboard on the personnel basket. A total of 12 cores were collected over the three shifts.

Station I0

Station I0, on the 22nd July 2022, was planned to be a fully consolidated process station with unharnessed personnel overboard. However, the safety assessment of the ice deemed that the ice floes were not large enough or consolidated enough for a full process station. Four personnel were craned overboard. A total of 7 cores were taken at various locations around the floe; some being taken along the cementing region between two floes.

13.1.3 Sea ice sampling methods

The sea ice at all stations were cored using the Kovacs Mark II coring system (Figure 72). The coring barrel was the primary component that was used to shape the ice core. At the top of this barrel, can be attached a T-bar, battery-powered drill or petrol motor which drove the barrel downwards. Attached to the bottom of the barrel, were a pair of cutting blades that rotate with the barrel and cut into the ice. The barrel was 1 m in length and thus created a core of 1 m in length. If the depth of the ice was greater than 1 m, an extension pole was attached between the barrel and power source. The inner diameter of the barrel and thus the resulting diameter of the core produced was 9 cm. During operation, it was imperative to be aware of safety at all times. Careful handling of the corer was vital as the blades can cause injury if handled inappropriately. As the barrel was driven vertically downwards, a core of ice was cut and inserted into the barrel. Once the depth of ice had been exceeded or the barrel was full, the drill or motor was stopped, the barrel was lifted out of the ice and rested horizontally. The T-bar, drill or motor was removed and the core was slid out of the barrel, and placed inside a marked plastic sleeve. It was then transported to the appropriate location depending on the core's allocation

Figure 72 Kovacs Mark II Corer apparatus

13.2 SEA ICE CORE PROCESSING

Processing of sea-ice samples was conducted at -10 ℃ in the SA Agulhas II's forward cargo hold freezer. Both freezers were used; one was set to -10 ℃ for sample processing, whilst the other was set to -20 ℃ for sample storage back to land.

The freezer dedicated to sample processing was used for several activities as detailed below. A Makita M2401B 2000W cut-off saw was used for sectioning samples with a stainless steel blade. For long cores, several 3-D printed holders were used to hold the sample off the platform edge.

Figure 73 Makita M2401B 2000W cut-off saw in use

13.2.1 Uniaxial compressive strength- constant stress

PI: Dr Tokoloho Rampai; Winter Cruise members: Tamuka Keche

Sea ice cores were collected at different stations during the Scale Winter Cruise 2022. In total 9 cores of them were used for testing with a uniaxial compression jig (Figure 4.2). Each sea-ice core was photographed and cut into sections of a length of 15 cm. The uniaxial compression test that was used was electronically driven using a chosen strain rate of 4E-04/s. The uniaxial compression device recorded the pressure measured in the system and data from two displacement sensors. The test results in stress-strain curves and allows one to calculate the Young's modulus.

Figure 74 Electronically driven uniaxial compression device

Figure 4.2

13.2.2 Uniaxial compressive strength- constant strain

PI: Dr Tokoloho Rampai, Prof. Doru Lupascu; Winter Cruise members: Felix Paul

Sea ice cores were collected at different stations during the Scale Winter Cruise 2022. In total 13 cores of them were used for testing with a stress-controlled hydraulic uniaxial compression jig (Figure 75). Each sea-ice core was photographed and cut into sections of either a length of 22.5 cm or 14 cm. The length of 22.5 cm was chosen, as this leads to samples with a length-to-diameter ratio of 1:2,5 which is best suited for uniaxial compression tests. The 14 cm samples were used to maximize the data output of the cores, as most cores had a limited size and did not allow two sections of 22.5 cm. Each sample was weighed, and the size was measured precisely to calculate the density. The uniaxial compression test that was used was hydraulic driven. The uniaxial compression device records the pressure measured in the system and data from two displacement sensors. The test results in stress-strain curves and allows one to calculate the Young's modulus.

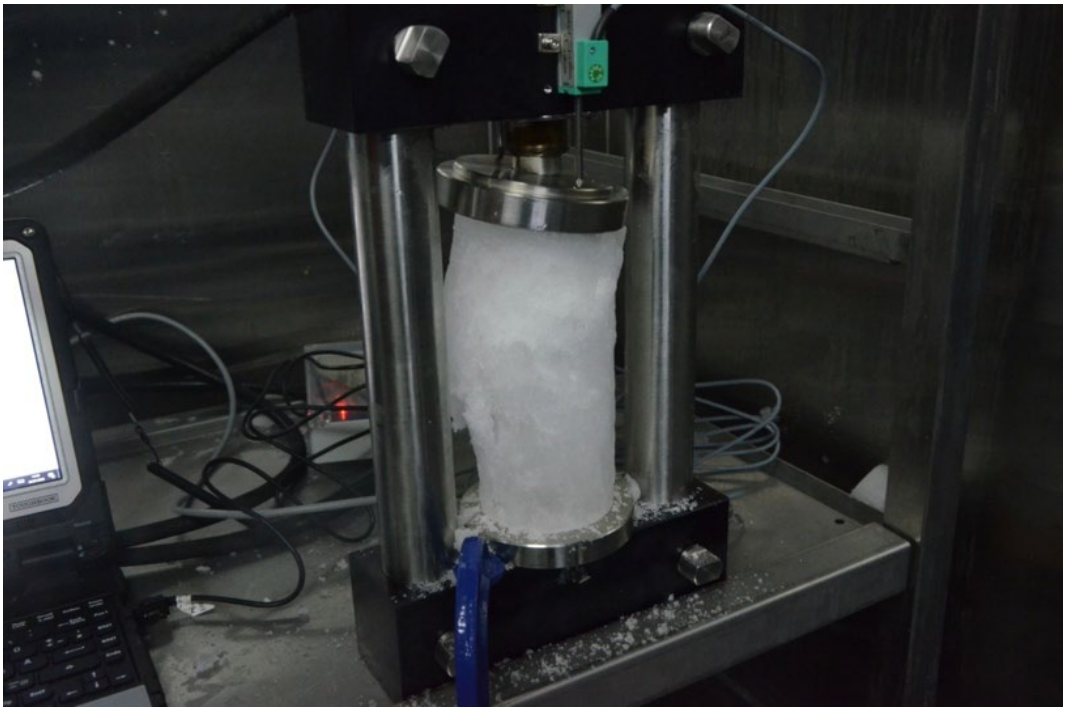

Figure 75 Hydraulic Uniaxial Compression Test

13.2.3 Cross polarisation

PI: Dr Tokoloho Rampai; Winter Cruise members: Safiyyah Moos, Hayley Swait

Cross polarization cores were obtained from 5 process stations (I1, I4, OD2, I0, OD3). A total of 17 cores were collected during the cruise for cross-polarization.

Using the Makita cut-off saw, the cores were cut into 10 cm sections from the bottom. From the 10 cm segment, slices of 1 cm thickness were cut vertically through the centre. A 1 mm thin slice was further cut using a thermal macrotome and the slice was placed on a lightbox between polarized sheets. The polarized sheets were crossed to allow the individual crystal grains within the sea ice to be observed. Subsequently, images were taken and will be further processed at UCT.

13.2.4 Temperature and salinity processing

PI: Dr Tokoloho Rampai and Prof Marcello Vichi;

Winter Cruise members: Riesna Audh, Siobhan Johnson, Justin Pead, Ashleigh Womack, Safiyyah Moos, Hayley Swait, Lisa Kumadiro, Dayna Collins, Tamuka Keche, Magata Mangatane, Felix Paul, Jonathan Rogerson, Jacques Welgemoed

Cores dedicated for physical property testing were first to be processed from all stations. All cores were handled with lab gloves to prevent contamination. A total of 15 cores were taken.

The cores were tested for temperature, immediately after coring the sample. Using a Ryobi drill with a 4mm drill bit, holes were drilled into the ice to place a GMH 3700 Series PT100 temperature probe for temperature measurement. The holes were drilled 2.5 cm from the bottom, 5 cm from the bottom, and 5 cm thereafter until the top of the core was reached. Each temperature recording was logged accordingly.

After temperature measurement, the core was transported to the laboratory for immediate processing for salinity. Each core was measured for length then cut into 5 cm segments from the bottom of the core and placed in labelled tupperware containers or zip-lock bags. The enclosed segments were placed into large black boxes and stored in the -20 ℃ freezer in the dark. All segments were transported back to UCT. Segments will be melted, filtered for chlorophyll and measured for salinity accordingly.

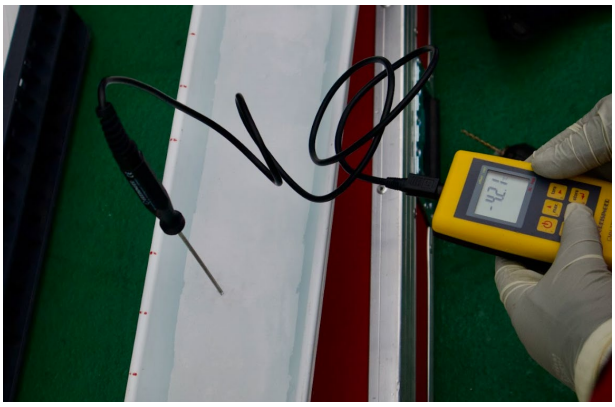

Figure 76 temperature measurements on deck after the collection of a pancake ice core

13.2.5 Biogeochemistry

PI: Prof Marcello Vichi, Dr Sarah Fawcett
Winter Cruise members: Riesna Audh, Dayna Collins

A total of 12 cores were taken for immediate biogeochemical processing (named BGC). The cores were handled and treated in the same manner as the cores marked for temperature and salinity processing. Segments, once stored at -20℃, were transported back to UCT for further processing for nutrient profiles within the sea-ice samples.

13.2.6 Algae Incubation

PI: Dr Tokoloho Rampai, Dr Susanne Fietz, Dr David Walker, Dr Sarah Fawcett
Winter Cruise members: Lisa Kumadiro

A total of four cores were collected at station OD3 from a single pancake and processed for algae incubation experiments. Three 3 litre clear, perspex tanks were filled with surface seawater and set up in the -10℃ processing laboratory. The seawater was collected at the same station (OD3) that the cores were collected. The filled tanks were wrapped in insulation as seen in Figure 77. Heating cable and LED light strips were wrapped around the tanks underneath the insulation padding. Additionally, PAR sensors were placed underneath the tanks to measure the light below the surface.

With the collection of the four cores, the bottom 15 cm of each core was cut.. Three of the bottom segments were placed in a tank each and secured with a lid to prevent water spillage. The remaining

segment was cut in half lengthwise, where one half was stored in darkness for transport back to UCT, whilst the other half was melted and analysed by microscopy for the existing algae community.

The heating cables on the tanks were set to maintain their temperature at -1.8 ℃; the freezing point of seawater. This prevents the underlying water in the tank from freezing and killing the algae community within it. LED lights were switched on for 6-7 hours every day, and the tanks were kept in darkness as far as possible for the remainder of each day. One week after collection, each tank was dosed with nutrients and vitamins for the algae community by drilling a hole into the ice and using a pipette to distribute the nutrients. The tanks were transported back to UCT where further experimentation and analysis will be conducted.

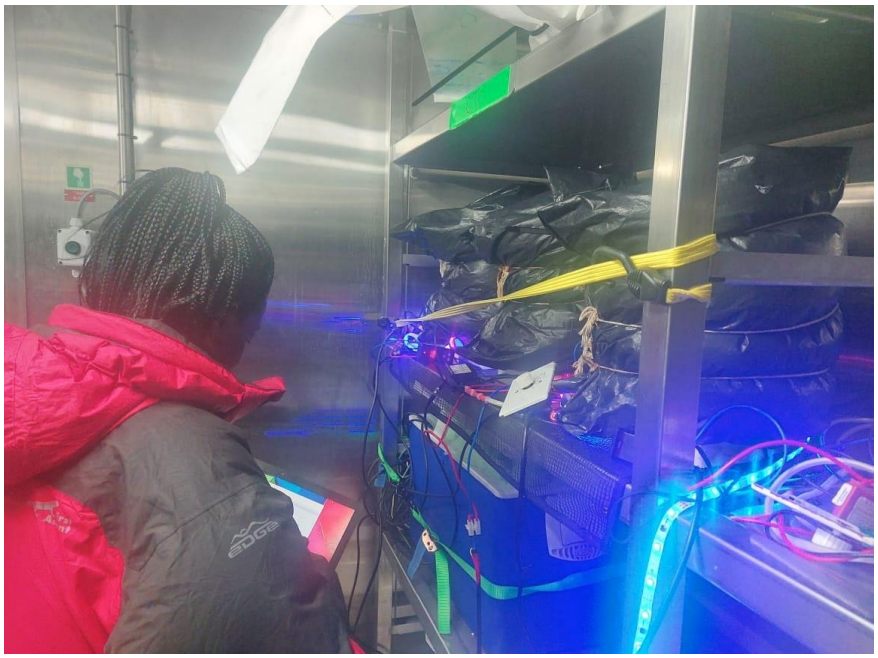

Figure 77 Algae Incubation Tank Set-Up in Processing Laboratory Freezer

13.2.7 CT scanning

PI: Dr Tokoloho Rampai
Winter Cruise members: Hayley Swait

X-ray Computer Tomography (CT) scanning cores were obtained from 2 process stations (OD2 and OD3). A total of 9 cores were collected during the cruise for CT-scanning.

The cores were transported to the processing laboratory and processed further within a week of collection. The Makita cut-off saw was used to cut the cores into 5 cm sections from the bottom. The sections were further cut into 2 cm x 2 cm x 5 cm cuboids which will be imaged and processed further at UCT.

13.2.8 Storage biogeochemical processing

PI: Prof. Marcello Vichi, Dr Sarah Fawcett
Winter Cruise members: Riesna Audh, Dayna Collins

A total of twelve cores were collected for biogeochemical storage experiments from one pancake at station OD3. All cores were handled with laboratory gloves and were measured immediately after collection for temperature. Three cores were marked for immediate processing, three were for

marked processing after one day of storage, three were marked for processing one week after storage and the remainder was to be processed one month after storage. Processing of these samples were in a similar manner to the PHY and BGC cores, whereby they were cut into 5 cm segments and stored in air tight bags in the dark. These samples will be melted and analysed for nutrients, salinity and chlorophyll. Each core was stored at -20 ℃ in the dark until it was ready to be cut.

13.3 Frazil Ice sampling

PI: Prof Doru Lupascu; Winter Cruise members: Felix Paul, Hayley Swait, Ashleigh Womack, Dayna Collins, Jonathan Rogerson

Frazil ice was collected from five different stations during the cruise. Three samples were collected at each station. Samples were collected using the frazil collector that was suspended above the ocean by the A-frame. After sampling the frazil ice (Figure 78), the sample height and temperature was measured immediately.

Figure 78 Frazil ice sample

The rheometer was then placed into the samples to measure the viscosity of the sample. The viscosity measurements took place one minute after collection. The viscosity measurement was repeated for each sample. The sample was then separated into solid ice crystals and sea water. The two components were weighed to determine the ratio of frazil ice to the sample volume. The procedure was repeated twice for each station.

14 A NETWORK OF AUTONOMOUS SEA ICE OBSERVATION PLATFORMS IN SUPPORT OF SOUTHERN HEMISPHERE CLIMATE PREDICTIONS

Team name and PIs	BUOY. Robyn Verrinder and Marcello Vichi (MARIS UCT); Alessandro Toffoli (UniMelb), Alberto Alberello (UEA), Mikko Lensu (FMI)
Authors	Verrinder R, Noyce M, Spirakis A, Stanton L, Pead J, Alberello A, Tersigni I, Passerotti G, Mangatane M, Welgemoed J, de Santi F, Björkqvist J-V, Toffoli A, Lensu M, and Vichi M.

14.1 OVERVIEW AND SCIENTIFIC OBJECTIVES

This section describes the activities undertaken by the BUOY team during the cruise.

A variety of synoptic, seasonal and interannual drivers influence the forms, types and concentration of sea ice in the Marginal Ice Zone (MIZ) in the Southern Ocean. The temporal and spatial distribution of the ice and its physical, mechanical and biological properties are directly related to the natural variability of the oceans and atmosphere, but also anthropogenic climate change. Climate and Earth System Models have limited sea ice variable parameterisations due to the scarcity of spatially distributed high resolution measurements from the region, specifically during winter/spring. To better understand atmosphere-ice-ocean MIZ processes and to improve future prediction of seasonal sea ice coverage and extent, three main approaches are available: (i) in situ measurements, (ii) area-wide satellite data, and (iii) numerical and experimental modelling. The meaningful connection of these is essential for enhancing understanding of this region.

Improved use of technology and autonomous devices, capable of persistent in situ sampling at finer spatial resolutions over the winter/spring seasons in the Antarctic MIZ, are key to obtaining the datasets needed to improve Earth System Models (ESMs) and to validate remote-sensing products. This requires a multidisciplinary approach including engineering, oceanography and climate science. The SCALE expedition BUOY team comprised researchers and students from several institutes including the **University of Cape Town** (UCT), **Nelson Mandela University** (NMU), **University of Melbourne** (UNIMELB), **University of East Anglia** (UEA) and the **Finnish Meteorological Institute** (FMI). During the expedition we aimed to collect high-frequency wave and ice drift data using ice-tethered buoys designed and built by the UCT team as well as open water buoys developed by **Tallinn University of Technology** and **WiseParker OÜ**. These measurements were complimented by advanced ship-based imaging of ice floes and waves using LiDAR, stereo and thermal cameras. These unique high resolution data sets will be used to better characterise wave drivers of Antarctic sea ice formation during winter and to inform Southern Hemisphere climate predictability.

14.1.1 Stations

Scientific activities were conducted by the BUOY team at the following stations in the MIZ and are outlined below (naming convention according to Table 4):

Station name	Date	Activities
OD-1	2022/07/19	**Buoy deployment:** • FMI open water wave buoy (**LP8**)
ICE21 (I1)	2022/07/19	**Buoy deployment:** • FMI open water wave buoy (**LP4**) • UCT SHARC buoy (**SB01**) **Imaging:** • Go-Pro stereo imaging of UCT SHARC buoy deployment
ICE22 (I2)	2022/07/19	**Buoy deployment:** • FMI box buoy (**BB1**) • UCT SHARC buoy (**SB02**) **Imaging:** • Go-Pro stereo imaging of UCT SHARC buoy deployment
ICE23 (I3)	2022/07/20	**Buoy deployment:** • FMI open water wave buoy (**LP2**) • UCT SHARC buoy (**SB03**) **Imaging:** • Go-Pro stereo imaging of UCT SHARC buoy deployment
ICE12 (I5)	2022/07/20	**Buoy deployment:** • UCT SHARC buoy (**SB05**) **Imaging:** • Go-Pro stereo imaging of UCT SHARC buoy deployment
ICE11 (I4)	2022/07/20	**Buoy deployment:** • UCT SHARC buoy (**SB04**) **Imaging:** • Go-Pro stereo imaging of UCT SHARC buoy deployment
ICE00 (I0)	2022/07/20	**Buoy deployment:** • UCT SHARC buoy (**SB06**)
OD-2 (PS)	2022/07/21	**Imaging:** • Ondeck LiDAR and Intel Realsense imaging of the two collected pancake ice floes after coring activities had taken place.
SB06 (I0-PS)	2022/07/23	**Buoy retrieval:** • UCT SHARC buoy (**SB06**) **Imaging:** • Go-Pro stereo imaging of UCT SHARC buoy deployment • One ice pancake was scanned using the thermal camera before all other activities took place. • Ondeck LiDAR and Intel Realsense imaging of one collected pancake ice floe before coring activities had taken place.
SB04	2022/07/24	**Buoy retrieval:** • UCT SHARC buoy (**SB04**) **Imaging:** • Ondeck LiDAR and Intel Realsense imaging of one collected pancake ice floe after coring activities had taken place.
LP4	2022/07/24	**Buoy retrieval:** • FMI open water wave buoy (**LP4**)

SB01	2022/07/24	**Buoy retrieval:** • UCT SHARC buoy (**SB01**) **Imaging:** • Go-Pro stereo imaging of UCT SHARC buoy deployment
SB05	2022/07/24	**Buoy retrieval:** • UCT SHARC buoy (**SB05**) **Buoy redeployment:** • FMI open water wave buoy (**LP4**)
LP8	2022/07/24	**Buoy retrieval:** • FMI open water wave buoy (**LP8**)
SAZr (PS)	2022/07/26	**Buoy redeployment:** • FMI open water wave buoy (**LP8**)

14.2 SHIP-BASED IMAGING

14.2.1 Scientific background

Antarctic sea ice is one of the largest and most dynamic ecosystems on Earth (Arrigo et al., 1997) and plays a pivotal role in the Earth's climate system by influencing the state of the atmosphere, the global thermohaline circulation, and the life cycle of the polar marine microbial communities (Eayrs et al., 2019). Its extent varies on average from 3.1 million km^2 in February to 18.5 million km^2 in September (Parkinson et al., 2014) following a seasonal cycle of freezing and melting. In contrast to the significant decrease of Arctic sea ice due to global warming from the late 1970s up until 2014, the Antarctic sea ice extent has increased (Meehl et al., 2016). This increasing trend puzzles researchers. However, after 2014 the annual mean Antarctic sea ice extent dropped rapidly from 12.8 million km^2 to 2.1 million km^2 in 2017 (Eayrs et al., 2021), and reached an historic minimum in 2022.

Sea ice covers the upper layer of the ocean and controls heat, moisture, and momentum fluxes at the interface between the ocean and atmosphere (Dieckmann et al., 2010). Over the Southern Ocean the estimated annual average heat flux can be as high as 30 W/m^2 (Llytle et al., 2000), against 3-4 W/m^2 in the Arctic Ocean (Krishfield et al., 2005). Nevertheless current climate models struggle to represent the extremely dynamic Marginal Ice Zone (MIZ) processes and interactions at the sea-ice ocean-atmosphere interface (Sun et al., 2021).

Interactions between ocean waves, which get modified by the ice cover, and the sea ice cover itself create an inhomogeneous environment difficult to monitor through large scale (temporal and spatial) remote sensing products (Gryschka et al., 2008). Ocean models are unable to accurately describe the sea ice floe melt, growth and thickness, dynamic floes collisions and, new ice formation in the MIZ (Rasmussen et al., 2018; Hall et al., 2015; Worby et al., 2015). The scarcity of field measurements, particularly in the winter season, contributes to the lack of knowledge of the physical mechanisms that govern heat and momentum exchanges in the MIZ.

One of the withstanding unknowns is the heat fluxes through the MIZ, which are governed by the sea ice surface temperature (IST). IST drives the upper-ocean circulation and thermal structure on daily, seasonal, decadal and climatic timescales (Rasmussen et al., 2018; Allan et al., 2014; Hall et al., 2004), and the associated thermodynamics governs sea ice extent, thickness and drift (Horvat et al., 2018).

Here we report underway measurements of sea ice surface temperature with high-definition infrared (IR) camera and concurrent acquisitions of waves and sea ice properties with a stereo camera system during the SCALE 2022 winter cruise. We also outline LiDAR acquisition of the ocean and sea ice surface.

14.2.2 Activity report

The main activities undertaken by the imaging group during SCALE 2022 winter cruise were: (i) thermal imaging of the ocean and sea ice surface temperature (**IT**, **FdS**)); (ii) LiDAR measurements of the ocean and sea ice surface (**AS**, **GP**, **JW**); (iii) LiDAR measurement of single pancake ice floes on deck (**AS**, **FdS**); (iv) stereo imaging of the ocean and sea ice surface to reconstruct wave and sea ice properties (**AA**, **MM**, **GP**) and (v) GoPro stereo imaging of buoy deployments and retrievals (**AS**, **JR**, **AA**, **GP**). The thermal imaging follows successful trials during the SCALE 2019 winter and spring cruises. LiDAR measurements were intended as a trial to retrieve information on ocean waves in the open ocean and the ice morphology (elevation and thickness) in ice covered waters.

14.2.3 Thermal imaging

14.2.3.1 Method and equipment

Open ocean and sea ice skin temperature were recorded using an infrared camera (IR) **Telops FAST M350 TEL-5115**, equipped with a 13 mm lens, which returns images of the temperature at the ocean surface in Kelvin. This instrument allowed acquisition of high-speed thermal imaging at a temporal resolution up to 44 Hz and at a 640x512 pixels resolution. For our purposes it was found (following trials during SCALE 2019) that the optimal frame rate is 2 Hz. This provides a good tradeoff between the amount of data generated during scans, while still maintaining statistically independent scenes.

The camera lens was left exposed not to deteriorate the acquisition and accuracy of the measurements. To protect the lens and camera from the harsh environment (e.g. sea spray) it was mounted and unmounted every 2 hours during daylight on the portside of the vessel at deck 7 (approximately 16–17 m from the waterline; Figure 79). Acquisition lasted approximately 20 minutes per sampling session. The acquisition protocol was designed following experience gained during the previous voyages and subsequent post-processing.

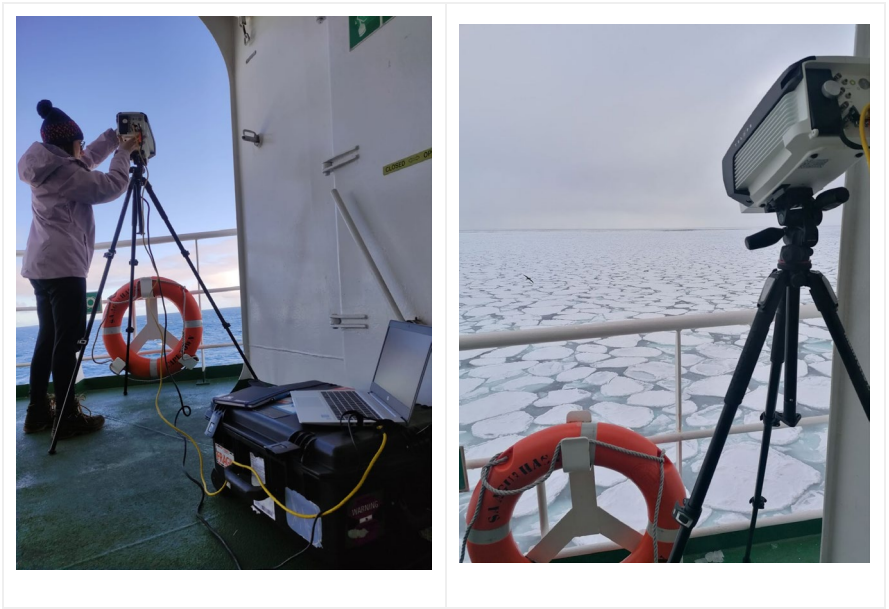

Figure 79 Setup for open ocean and sea ice surface temperature measurements from deck 7.

14.2.3.2 Preliminary results

The thermal camera returned IR images, in ***.hcc** format, which are processed in Mathworks MATLAB to generate ***.mat** files. Each pixel provides the IST of the sea ice and the IR images clearly show the sea ice composition. An example of the IR acquisition is shown in Figure 80 (left). The frame shows a patch of the sea ice dominated by compact ice. The IR image clearly highlights pancakes frozen together that create a consolidated pack ice with ice fractures. The IST difference between different sea ice conditions, clear from the IR images, indicates that the IST of the pack ice is approximately 2 ºC colder than brash ice and nilas in between.

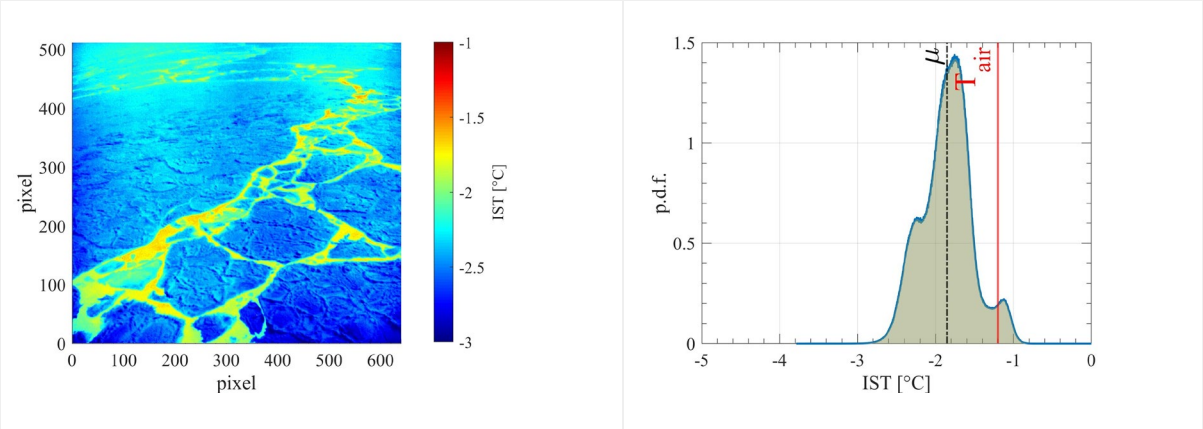

Figure 80 Example of thermal imaging over consolidated pancake floes (colder) and cracks in between (warmer) and probability density function (p.d.f.) of IST computed over the frame and over a 20-minute interval. Mean value and air temperature are also reported

From the data matrix, the probability density function (pdf) in Figure 80 (right) is extracted from 204 statistically independent frames over a 20-minute time interval because the ship is moving during acquisition. A strip equivalent to 7.5 km is therefore covered during the acquisition interval. The IST distribution shown in Figure 80 is obtained from an entire recording session in compact ice conditions. The pdf indicates a non-normal distribution denoting the predominance of the pack ice IST with the highest peak at -1.7 ºC and another peak at -2.2 ºC. A statistically significant smaller peak at -1.2 ºC indicates the presence of brash ice (or nilas) IST in the ice fractures. The pdf also shows the mean of the distribution at -1.8 ºC and the air temperature at -1.2 ºC measured with an on-board sensor during the recording time. The air temperature is warmer than the IST of the pack ice, therefore suggesting that the consolidated ice is in a melting phase (IST < Air Temp). Heat flux is from the warmer air to the colder ocean (Talley, 2011) during the shown example.

Data collected during the cruise will also provide a benchmark for remote sensing products. Due to the high frequency of the thermal camera measurements (at least 3 times a day), we are able to perform an accurate match with the orbits of the satellites with IR sensors that measure the IST such as Terra and Aqua Satellite (MODIS sensor), SUOMI NPP and NOAA_20 (VIIRS sensor). The fusion of the IST data, together with other variables measured on board (air temperature, relative humidity, surface salinity, wind speed and Photosynthetically Active Radiation) will also enable an evaluation of the surface energy fluxes over the Antarctic marginal ice zone.

The thermal camera was also used to scan pancake ice floes lifted onboard the helideck (Figure 81).

Station name	Date	Activity start time (UTC)	Location	Notes
SB06 (I0-PS)	2022/7/23	19:00	-59.38258, 0.1575	Pancake was prioritised for thermal and LiDAR/Realsense imaging. One ice pancake was scanned using the thermal camera before all other activities took place.

The main objective of the measurements was to characterise the thermal properties of a typical floe. Measurements of the same floe before and after the snow cover was removed show that the snow, in contact with the air, is approximately 0.5 ºC warmer than the underlying ice which remained thermally insulated.

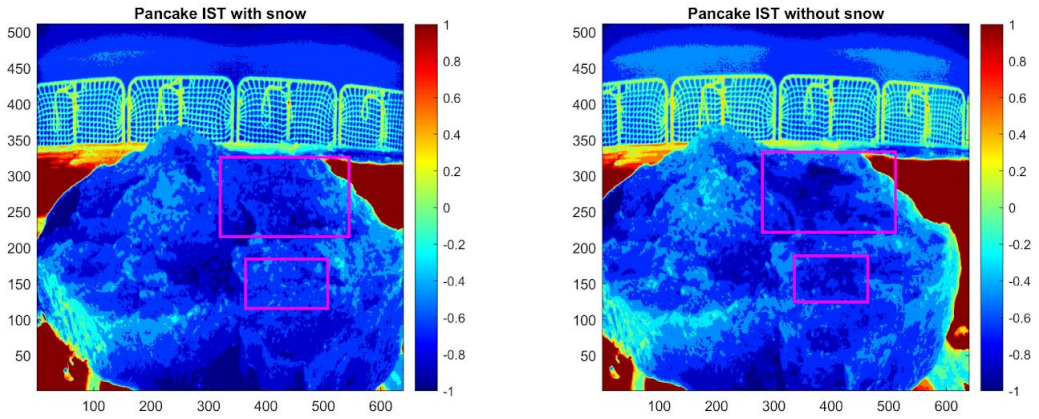

Figure 81 Example of thermal imaging of the pancake on deck before snow on top was removed (left) and after (right), the zones where snow was removed are highlighted by the pink rectangle box.

14.2.3.3 Recommendation

The system needed to be set up on deck 7 at regular time intervals. This proved to be the most effective way of operating the system, but it is not optimal as it always requires 1-2 operators.

14.2.4 Stereo camera system

14.2.4.1 Method and equipment

The Wave Acquisition Stereo System technique developed by Benetazzo (2006) and successfully employed on previous voyages (Alberello et al., 2022) has been used to measure waves (in the open ocean and in ice). Two industrial cameras record a video sequence of synchronised and largely overlapping images of the ocean surface. By applying binocular photogrammetry techniques, post processing of the image pair allows the reconstruction of the 3D ocean surface.

The camera system comprises two **DMK 333GX264e GigE Monochrome Industrial Cameras** (2/3" Sony CMOS Pregius sensor (IMX264), Global Shutter, 1920 x 1080) equipped with 5 mm F1.8 C-mount lens with angle of view of ~120º. The cameras were installed on the port side of the monkey bridge of the *SA Agulhas II* at a distance of about 4 m from each other and with their longitudinal axes parallel to each other (Figure 82). The cameras were angled ~20°. Considering that the height of the monkey bridge is about 25 m from the waterline, this configuration allowed observations of a footprint of the ocean extending up to 200 m from the ship.

The cameras were controlled by a desktop computer which greatly improved the reliability and speed of the system compared to similar installations during 2019 voyages. Synchronised pairs of images were acquired at a sampling frequency of 1 Hz (1 frame per second). Acquisitions in open water were conducted during daylight hours only, in ice the system was operated during the night as well because the vessel spotlights, operated only in sea ice, illuminated the camera field of view (Figure 83). The cameras were operated with the open source software IC Capture that controlled acquisition, trigger, and the frame rate. In addition, a Python script automatically transfers the files in 1-hour sequences.

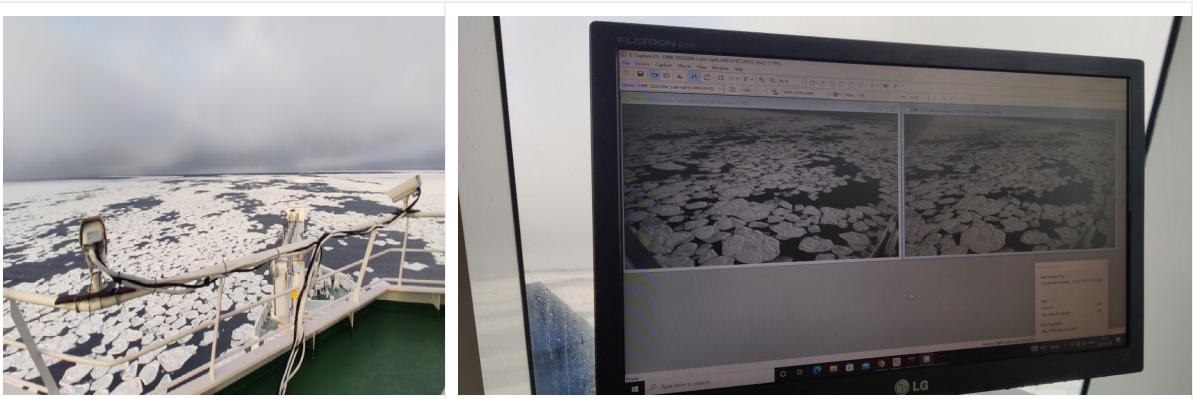

Figure 82 Stereo camera on the monkey bridge (left) and desktop computer (right).

A motion sensor unit (IMU; Yost https://yostlabs.com/) synchronised with the camera acquisition was also controlled via the desktop computer and operated at a sampling frequency of 10 Hz. This sampling frequency minimises the error in the computation of ship displacements and rotations from the IMU observations (i.e. accelerations and rotational velocities), which are then used to project the reconstructed ocean surface in the frame of reference of the ship into a common horizontal plane.

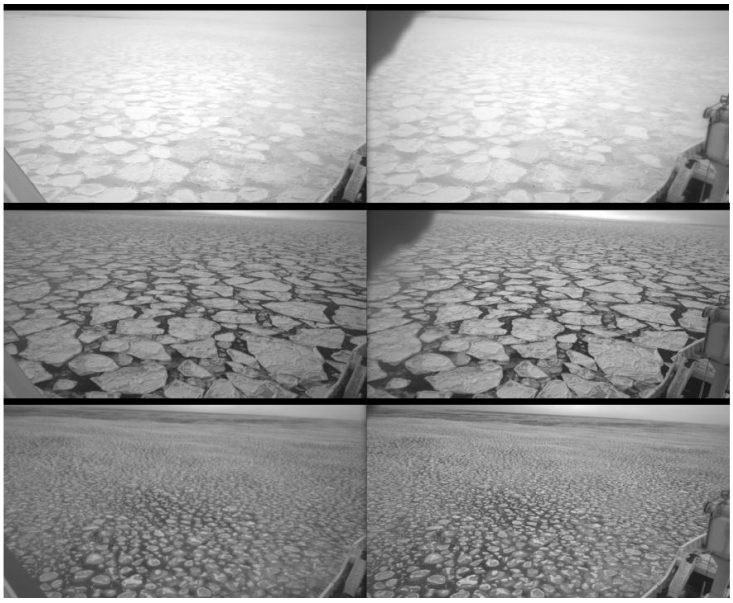

Figure 83 Example of acquisitions in ice with the stereo camera system in various sea ice conditions. Left and right camera field of view are shown

14.2.4.2 Preliminary results

The processing pipeline for the sea surface reconstruction has been tested in previous voyages (see results in Alberello et al., 2022 and Figure 84).

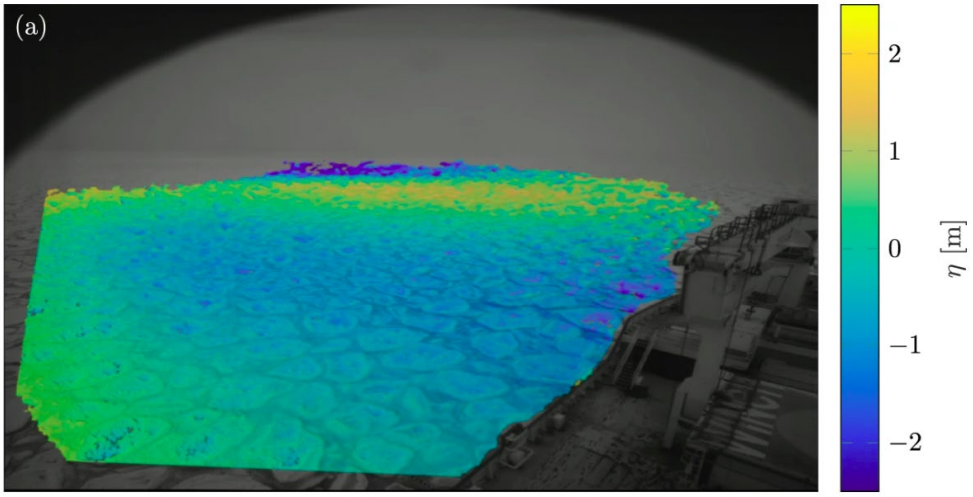

Figure 84 Example of reconstructed surface elevation (from Alberello et al., 2022).

Camera images are also used to monitor sea ice properties (Figure 85). The first step is to orthorectify the camera image field of view to account for lens distortion and the angle of view. The floe detection algorithm is then based on the gradient vector flow (GVF) snake algorithm (Xu and Prince, 1998). The GVF snake algorithm, successfully employed by Zhang et al. (2015), is the evolution of the traditional snake or active contours algorithm (Kass et al., 1988). In the classic algorithm a given initial contour can move under the influence of internal and external forces until it matches the boundary of the object of interest. However, this requires a high computation time. The initial contour has to be quite close to the real boundary and the edge detection in presence of concavities is limited. The new method introduced the dense vector field (GVF) to overcome these limitations. To start the algorithm, a proper initial contour detection is still required. This approach improves the accuracy of floe reconstruction compared to Alberello et al. (2019; used to analyse images during the winter cruise 2017). The methodology complements ASPeCT observation by providing objective measurements of the floe size distribution.

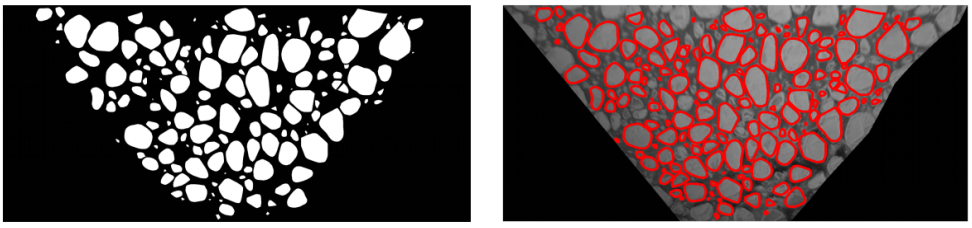

Figure 85 Example of binary image and identified floes

The imaging techniques will provide a new extended database of combined waves and floe size in the marginal ice zone.

14.2.4.3 Recommendation

The right camera suffered from freezing at night due to issues with the heater connection inside the camera. A heater on the screen would be recommended for future installations. The power and

communication cables to the camera housings should be detachable at the camera case to ease installation, maintenance, and repairs.

14.2.5 LiDAR imaging for ocean and sea ice elevation monitoring

14.2.5.1 Method and equipment

Ocean and sea ice elevation were monitored using a Livox Avia LiDAR (905 nm, 240 000 points/s, 450 m range, 70.4º (horizontal) x 4.5º (vertical) FOV, 2 cm precision) mounted on a platform attached to a tripod. The Livox Avia LiDAR was connected via an ethernet connection to an ASUS Zenbook 14X OLDED UX5400 (Intel® Core™ i7-1165G7 Processor 2.8 GHz, 16 GB RAM, 512 GB SSD, NVIDIA GeForce MX450) running Ubuntu 20.04 with ROS Noetic using the Livox ROS driver for data acquisition. The system was powered off an extension cord connected to the ship's 220V AC power supply. The launch file included live feedback from the LiDAR via rviz, a ROS 3D visualisation tool. The data captured are saved in a **.bag** file format, including topics of the LiDAR point cloud and the built-in IMU data on the Livox.

Similarly to the thermal camera system the front of the LiDAR was exposed so as to not deteriorate the acquisition and accuracy of the measurements. To protect the LiDAR from the harsh environment (e.g. sea spray) it was mounted and unmounted 3 times per day on the portside of the vessel at deck 7 (approximately 16–17 m from the waterline; i.e. same location of the thermal camera acquisition; Figure 86). Acquisition lasted 10 minutes per sampling session.

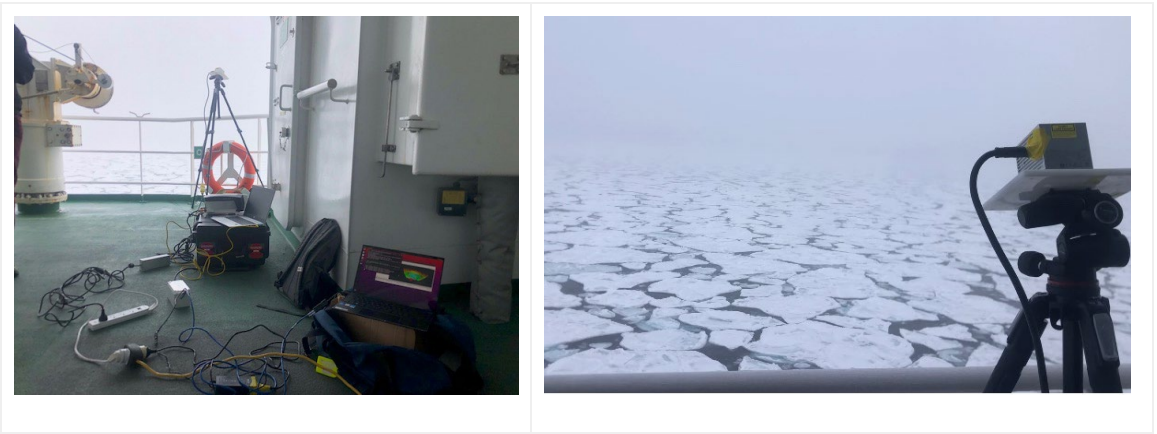

Figure 86 Full Livox Avia LiDAR setup installed on deck 7 for ocean and sea ice elevation monitoring. (left) installed on deck 7 alongside the thermal imaging rig; (right) the Livox Avia LiDAR attached to a tripod with a view of the sea ice field. Photos by AS.

14.2.5.2 Preliminary results

Upon brief inspection, the Livox Avia data collected are promising as they have a high point density, provide a good reconstruction of the reflectivity and show the motion of the waves. The marginal ice zone scans are slightly clearer than those taken in the open ocean. The pancake ice provided distinct shapes easily detected by the LiDAR therefore the wave behaviour can be extrapolated from the 3D displacement of the pancakes shown in the scans. In the open ocean scans, there was interference by the wake created by the ship's motion so the wave motion is less clear to the naked eye.

Data (example shown in Figure 87) will be compared with established stereo collected techniques (Alberello et al., 2022) for the reconstruction of water waves and sea ice properties both in the open ocean and in the marginal ice zone.

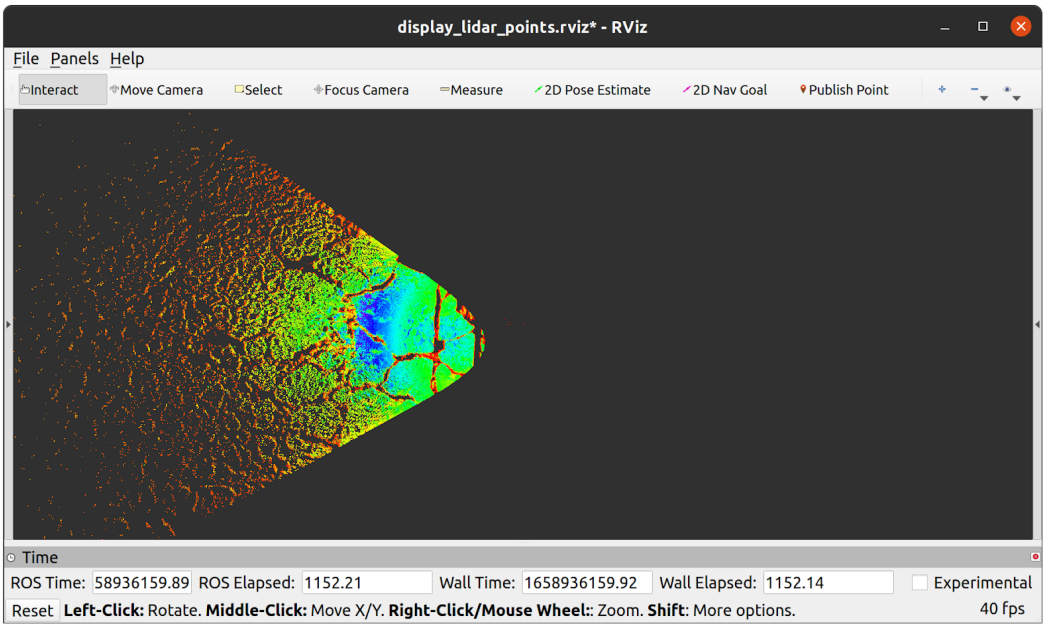

Figure 87 Example of a Livox Avia LiDAR acquisition taken from deck 7 in consolidated pancake ice conditions. Pancake floes are clearly visible in the scan.

14.2.5.3 Recommendation

The system needed to be set up on deck 7 at regular time intervals. If trials during the SCALE 2022 winter voyage prove to be successful an easy to install physical configuration should be designed for future voyages.

14.2.6 Imaging of individual ice pancake floes on deck

14.2.6.1 Method and equipment

Individual pancake ice floes were scanned on the deck 5 helideck during ice pancake collection activities using the Livox Avia LiDAR connected to the ASUS Zenbook (described previously) and an Intel Realsense D455 depth camera (1280 x 720 stereo depth resolution, 1280 x 800 RGB resolution, 6 Degree of Freedom Inertial Measurement Unit), which was linked via USB to a Raspberry Pi4 8 GB RAM powered off a Romoss power bank (5 V, 3 A). A Wave 7" touchscreen, external keyboard and mouse was used to interact with the Intel Realsense through the Raspberry PI. The Realsense acquisitions were made using the Realsense Viewer running on a Raspberry Pi 4, which was running Ubuntu 20.04 and Realsense data are saved in a **.bag** file format. The system design is outlined in Figure 88.

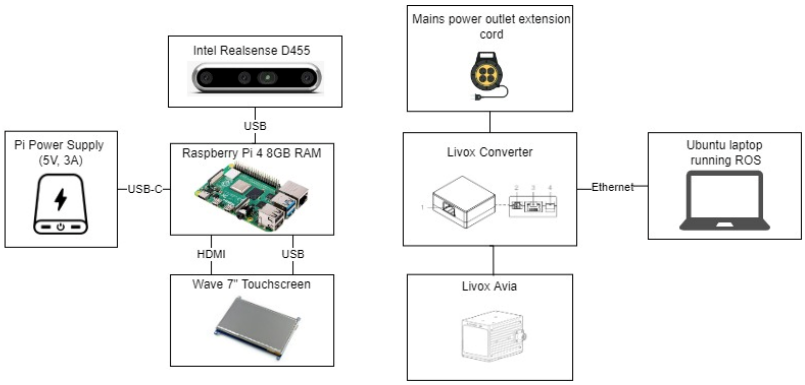

Figure 88 A block diagram illustrating the system used to image individual pancake ice floes. The system comprises an Intel Realsense D455 and Livox Avia LiDAR sensors used to collect LiDAR point-cloud and RGB-D data.

These data will be used in 3D reconstruction of individual floes, which will be used to characterise ice floe geometry and surface roughness (Landy et al., 2015). Individual sea ice pancake floes were collected as part of the larger sea ice coring activities (see SEAICE team section), which were conducted during the SCALE WIN2022 expedition. The pancakes were collected by the *SA Agulhas II* crew using the aft crane fitted with a pancake collection net (Figure 89).

Figure 89 Pancake ice floe collection stations on the helideck on deck 5. (left) Four wooden lattices were constructed on the helideck and ice floes were placed on top of them for coring and imaging. (right) A pancake floe being lowered at OD-2. Photos by RV.

Ice floes were collected in open drift (**OD**) conditions during three sampling sessions (21, 23, and 24 July 2022) and placed on wooden lattices on the deck 5 helideck (see Sec. 13.1.1). Although every effort was made to keep the pancakes intact, they were often damaged during collection, altering their geometric shape (Figure 90). A list of the stations and activities related to imaging is provided below. Note that the naming convention may differ from the one used in Sec. 13.1.1.

Station name	Date	Activity start time (UTC)	Location	Notes
OD-2	21/7/2022	15:30	-58.40125, -0.64933	Two pancakes were collected (**Pancake 1** and **Pancake 2**). Pancake imaging took place after coring activities occurred. Both ice pancakes were damaged during collection but were scanned.

SB06 (I0-PS)	2022/7/23	19:10	-59.38213, 0.15668	Pancake collection was prioritised for thermal and LiDAR/Realsense imaging. Two pancakes were collected and one (**Pancake 3**) was scanned before coring activities took place.
En route scanning	2022/07/25	13:00	-55.41653, -0.6067	Two pancakes were collected. However, the first pancake was not safely placed on beams and was damaged and therefore not imaged. The second pancake was fully scanned (**Pancake 4**).

Figure 90 Four pancake ice floes were scanned during the SCALE WIN2022 cruise. The condition of the floes varied with some scans happening after coring activities (Pancake 1, 2 and 4) or before coring (Pancake 3).

The sensor setup described in Figure 88 was housed in an enclosure that could be attached to a tripod. The tripod rig was placed in positions A-H (Figure 91) surrounding the extracted pancake and at each of these points, separate LiDAR and Realsense acquisitions were made for approximately 10 seconds each. The distances between the tripod and the wooden stands were measured with a measuring tape and logged. Camera footage of the activities on the helideck were recorded to further aid in the 3D mapping processing. Scans were taken of all four retrieved pancakes.

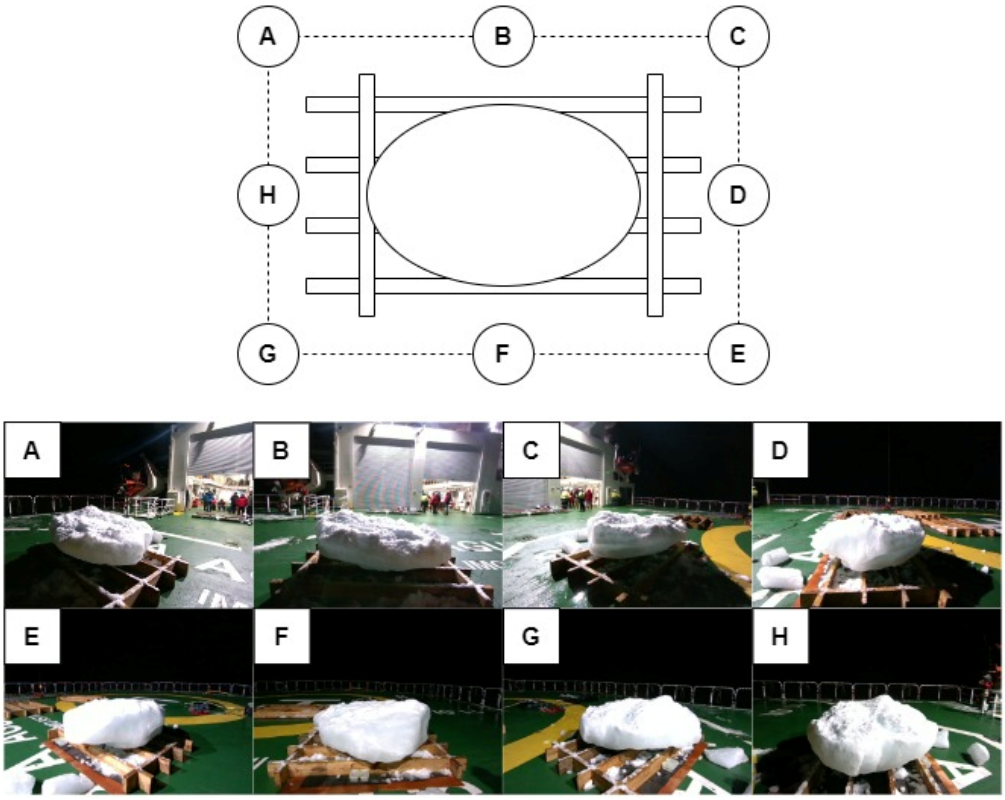

Figure 91 Scan positions around a pancake floe placed on the wooden lattice on the helideck. LiDAR and Realsense acquisitions were taken at each position and the distance from the floe was recorded.

14.2.6.2 Preliminary results

Preliminary reconstructions were made using Intel Realsense's built-in default 3D processing (Figure 92).

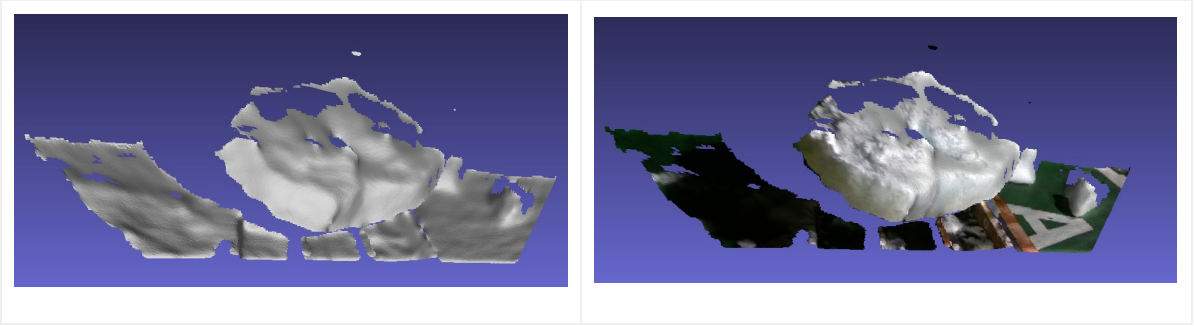

Figure 92 Scan outputs from the Intel Realsense of a pancake floe. (left) 3D surface model reconstructed using the Intel Realsense default processing algorithm. (right) 3D surface reconstruction with RGB data superimposed.

The 3D model envisioned is to be constructed by stitching the scans of the various viewpoints collected. The fusion of the collected LiDAR and the Realsense scans will allow for a detailed 3D model to be constructed. An investigation into the processing and stitching methodologies is needed to construct the desired model. Additional calibration experiments in the laboratory will be conducted to verify the accuracy of the generated model against ground truth and explore the various processing pipelines.

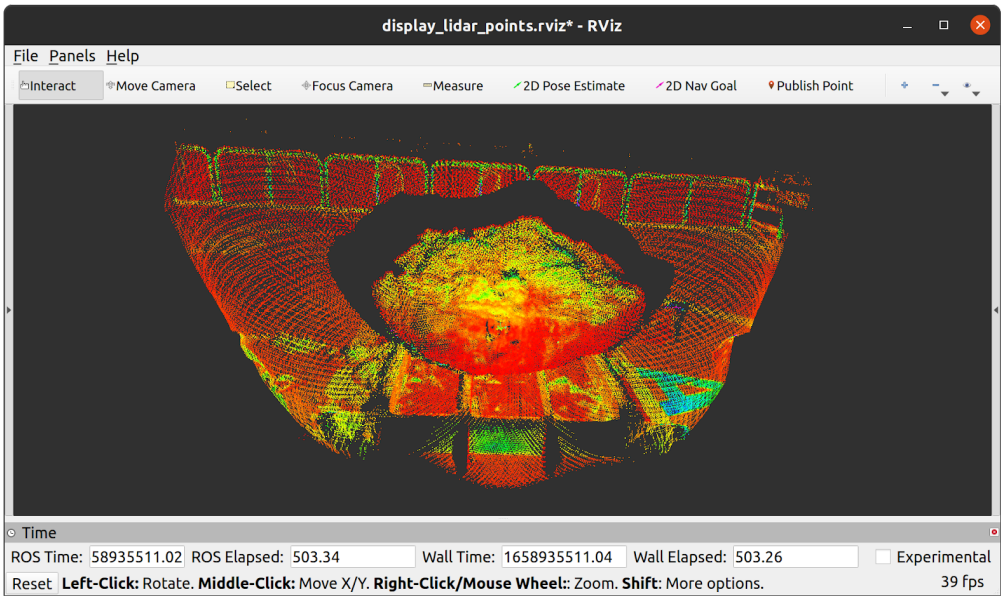

Figure 93 The LiDAR output scan of a single pancake floe collected during pancake retrieval operations.

14.2.6.3 Recommendations

The rig design requires improvement to allow for a more mobile system. This could be achieved by using a battery as the power supply instead of having to manage the extension cord link to the Livox. A single robust data capturing system can be designed to accommodate both LiDAR and Realsense acquisitions in a single rosbag. Additionally, the touch screen used to facilitate the Realsense scanning was faulty and difficult to use so a mouse and keyboard were used to start and stop the recordings.

14.2.7 Stereo GoPro recording of buoy deployment and retrievals

Stereo video was captured of the UCT SHARC buoy deployments and retrievals from a fixed location on deck 5 using two GoPro Hero 10 cameras. These data will be used in a preliminary investigation to extract and estimate the size and shape of pancake ice floes using image analysis. These physical estimates will be used to improve understanding of the inertial response of both the buoy and the ice floes to waves.

14.2.7.1 Method and equipment

A stereo imaging rig was designed using two GoPro Hero 10s attached to a bar using 3D printed connectors (Figure 94). The GoPro Hero 10s were selected due to their high resolution and suitability for outdoor recordings. The system was brought outdoors on Deck 5 as shown below.

The cameras were set to linear mode in a high-resolution video mode (30FPS, 4K resolution (3840x2160)). The recordings were started by clicking the trigger on the GoPro at the same time. An app called Camera Tools was used to trigger the cameras simultaneously, but it proved to be impractical since there exists a delay to connect to the cameras. Since the physical relationship between the cameras is known, depth can be estimated from the disparity shown in the two images.

Although movement of the cameras was kept to a minimum and the connectors are quite sturdy, it was still possible for a small amount of roll and pitch motion to occur between the GoPro and the 3D printed connector. For this reason, a calibration sequence was done in the heli-hangar after every acquisition to account for any movements in the camera orientation. The calibration board was an

A4 checkerboard pattern with 8x6 squares measuring 25 mm each. The board was printed using a gloss finish and then mounted to an A4 piece of hardboard for stability. These collected calibration data allow for the camera parameters for each scan to be mapped and hence a more accurate representation of the depth to be determined.

Figure 94 Stereo GoPro rig for imaging the UCT SHARC buoy deployment and retrievals.

Within each acquisition, several known physical markers were present in the scans: the side of the ship, the metre stick used for ice observations, the size of the carrier basket and the buoy and buoy stand dimensions. This allows for size estimates to occur without a stereo set up. Most of the buoy deployments and retrievals (Sec. 14.3) were captured using this stereo system, but there were occasions where this was not possible. In these cases, supplementary photos from mobile phones and cameras were taken of the buoy. Although these have less control than the stereo setup, there are sufficient markers in the image to estimate size. The processing of the data will yield whether size extractions are significantly improved with the use of the stereo cameras or if using a single image to estimate is sufficient. The GoPro footage was taken by **AS** except for deployment 4 and deployment 5 where the footage was taken by trained team members (**JR**, **RV**, **AA**, **GP**). **AS** was off duty for deployment 4 (SB05) and was on the basket for deployment 5 (SB04).

The system required at least two people to operate it, since the tripod had to be always held due to the strong winds. It was noted that the rig would gyrate slightly in strong wind conditions. Additional footage of the deployments was captured using a GoPro Hero 5 Session attached to a chest mount. A member of the deployment team would wear the harness to capture basket operations.

Station name	Date	Activity start time (UTC)	Location	Notes
ICE21 (I1)	2022/07/19	13:20	-58.67003, -1.24678	**SB01 deployment**: Only SHARC2 camera footage was found. SHARC1 did not record properly.
ICE22 (I2)	2022/07/19	18:00	-58.54985, -0.87618	**SB02 deployment**: Camera footage obtained from both GoPros.
ICE23 (I3)	2022/07/20	01:45	-58.58562, -0.46917	**SB03 deployment**: Camera footage obtained from both GoPros.
ICE12 (I5)	2022/07/20	07:40	-58.79702, -0.65042	**SB05 deployment**: Camera footage obtained from both GoPros.
ICE11 (I4)	2022/07/20	15:40	-58.58562, -0.46917	**SB04 deployment**: Camera footage obtained from both GoPros.
ICE00 (I0)	2022/07/20	19:10	-59.04377, -0.50618	**SB06 deployment**: Due to limited visibility and other ship activities which were occurring no GoPro footage was taken, instead, still images were captured with a mobile phone (**RV**).
SB06 (I0-PS)	2022/07/23	09:20	-59.39667, 0.10833	**SB06 retrieval**: Camera footage obtained from both GoPros.
SB04	2022/07/24	07:50	-59.16497, 0.86517	**SB04 retrieval**: The buoy stand sank, so retrieval needed to occur quickly – there was not sufficient time for set up of the rig. Photos taken from the bridge provided by Nicole Taylor.
SB01	2022/07/24	12:25	-59.1141, 0.66428	**SB01 retrieval**: Camera footage obtained from both GoPros.
SB05	2022/07/24	14:00	-58.97552, 1.00575	**SB05 retrieval**: The imaging rig had fallen over in the helihanger due to significant sea swells. This broke the 3D printed attachments and there was not sufficient time to fix/replace the rig. Data was collected by holding a single GoPro.

The GoPro Hero 10s were able to operate sub-zero temperatures. Only on a few occasions did a temperature warning appear on the GoPro screen. When this low temperature mode is activated, recordings are still able to proceed but the live view on the display turns off. It is also noted that the batteries should be as fully charged as possible for each session. In the cold weather, the cameras occasionally shut down with a low battery message when the battery is less than 50%.

14.2.7.2 Preliminary results

The ice conditions of the deployments and retrievals obtained from the imaging can be compared in Figure 95 to Figure 99.

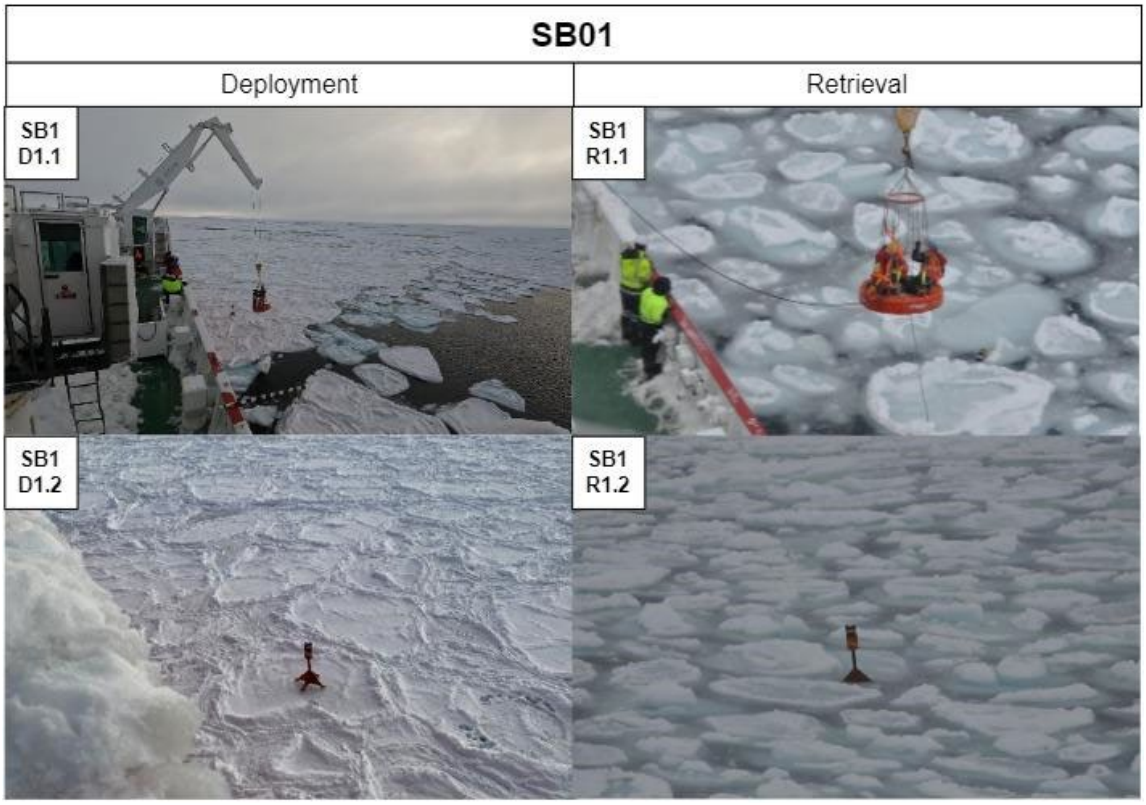

Figure 95 Images of the deployment and retrieval conditions of the UCT SHARC ice-tethered buoy SB01 during the SCALE 2022 Winter Cruise. These images highlight the greatly changing ice conditions between deployment and retrieval.

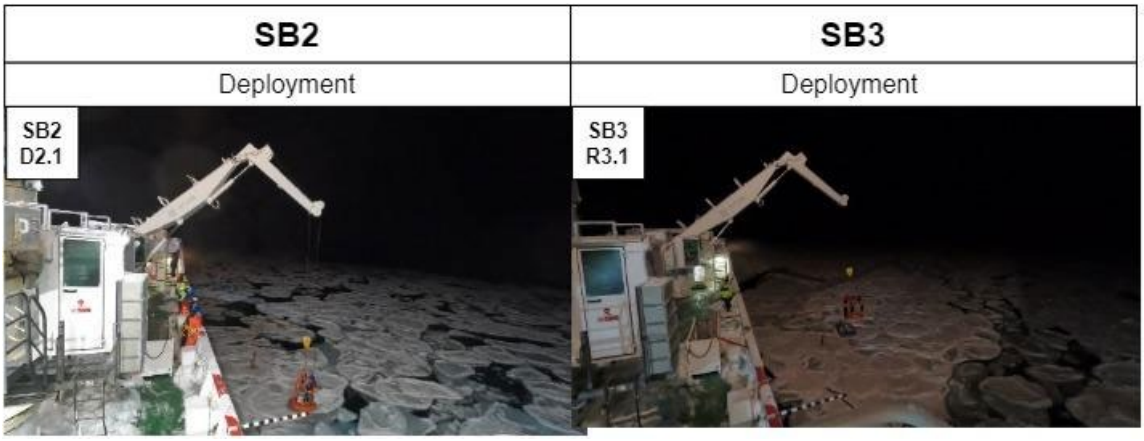

Figure 96 SB02 deployment. The buoy stopped transmitting.

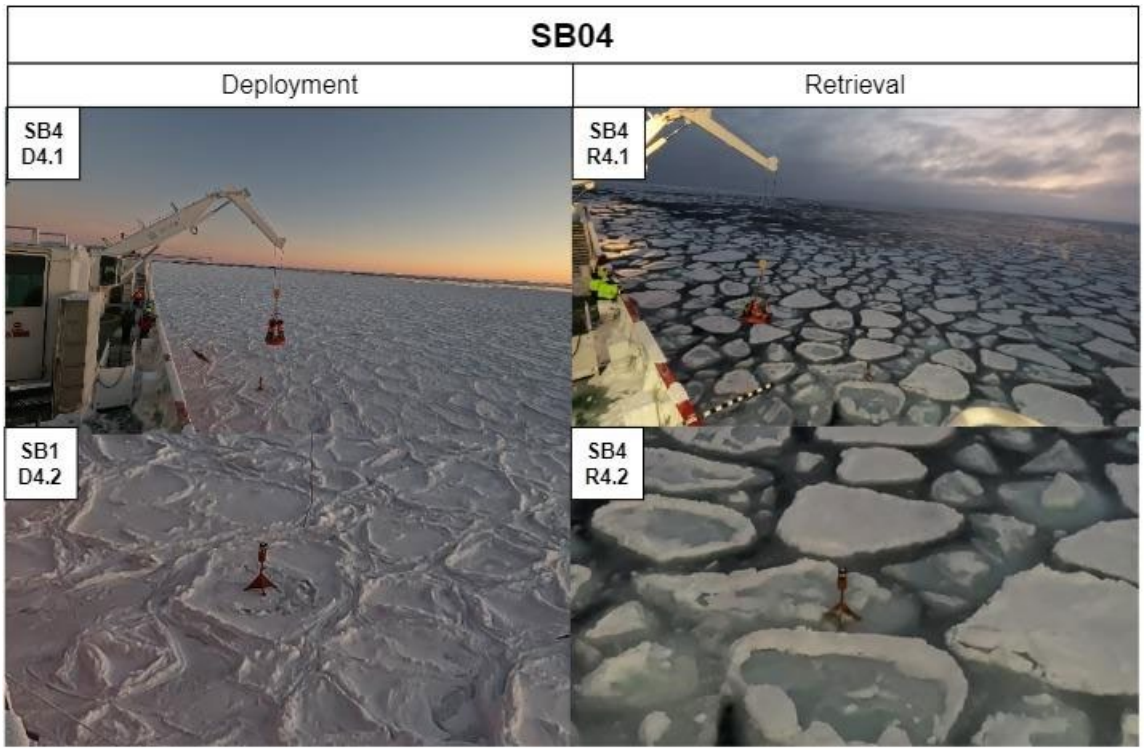

Figure 97 SB04 deployment and retrieval.

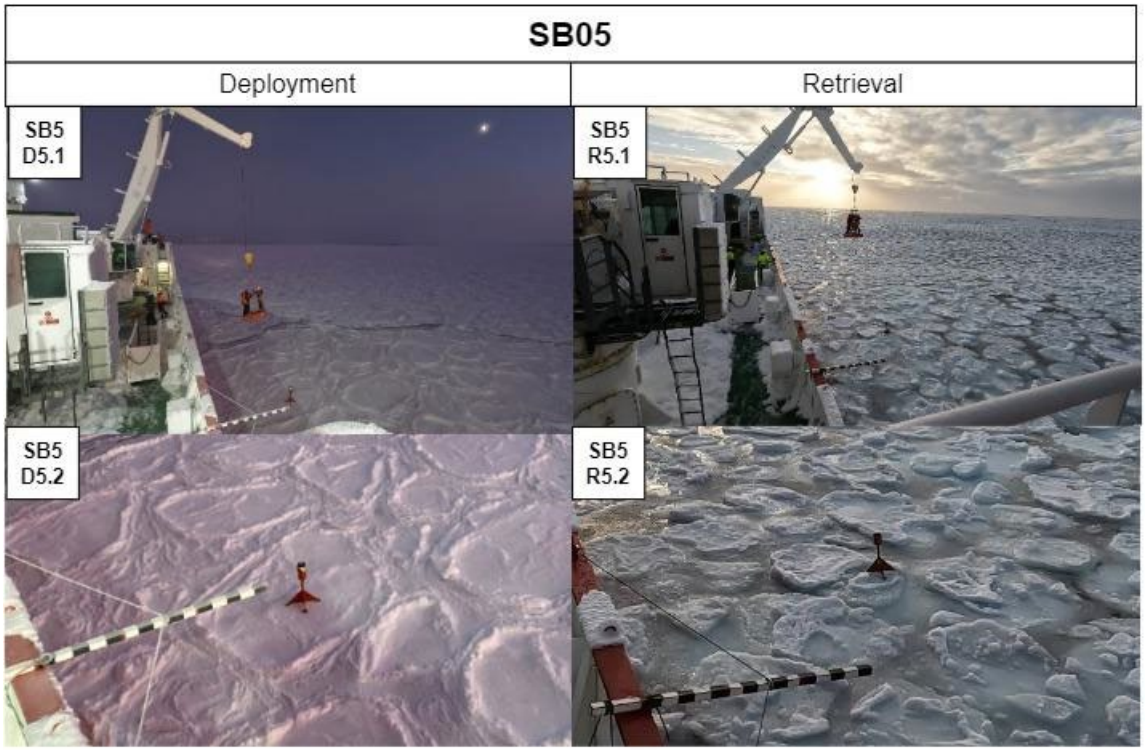

Figure 98 SB05 deployment and retrieval.

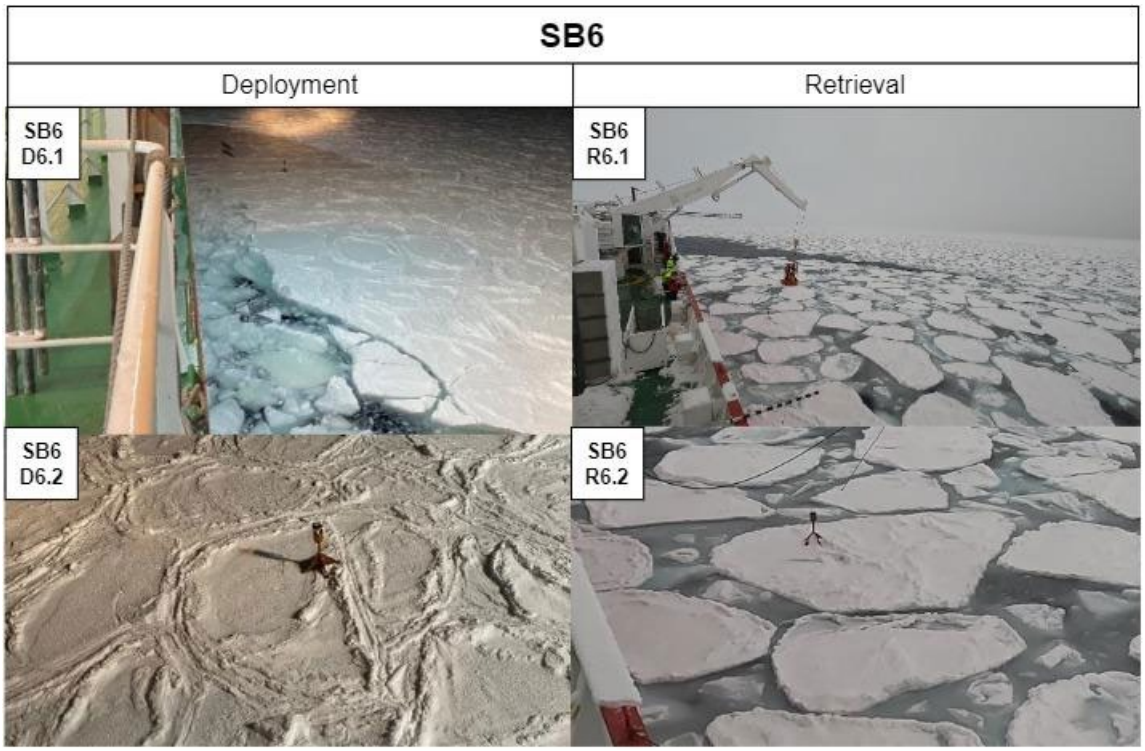

Figure 99 SB06 deployment and retrieval.

14.2.7.3 Recommendations

For future recordings, it is recommended that the GoPro mounting rig be improved to not rely on 3D printed parts and to be attached directly to the ship railing instead of using a tripod. A robust redesign of the data collection rig is recommended to collect a standardised collection of all deployment and retrieval activities. For synchronisation, the GoPro remote should be investigated compared to the app. Another method to improve synchronisation is to have a specific visual marker at the start of the recording (e.g. a flashlight turning on and off). This flashlight marker method was applied in some recordings but is also impractical unless there is a dedicated person with that responsibility. Overall, the system performed well and succeeded in collecting preliminary data for the image analysis of the specific ice floes that the buoys were deployed on.

14.3 BUOY DEPLOYMENTS AND RETRIEVALS

14.3.1 Scientific background

Autonomous devices have vastly changed our knowledge of the ocean in the past decade and have been contributing to the UN proclamation of the Decade of Ocean Science for Sustainable Development (2021-2030) to support joint efforts to observe the ocean and reverse its decline due to global change. The paucity of Southern Hemisphere observational data have, however, limited our understanding of climate variability in the region and how it contributes to overall Earth climate. There is currently a lack of technology to monitor Antarctic sea ice at scales that are relevant for Southern Hemisphere climate. Ice observations are mostly done through remote sensing proxies, which are validated through few in situ data collected by summer Antarctic expeditions and sporadic research campaigns. Autonomous devices are often deployed during these expeditions, but the highly variable features and seasonality of Antarctic sea ice limits their utilisation for extended periods of time. The expensive Arctic buoys deployed in thicker pack ice cannot be used as their cost

limits the scale of deployment needed to resolve spatial variability in the region. There is a major gap in the observational infrastructure, which can be filled by a network of affordable autonomous buoys.

14.3.2 Activity report

Six newly developed UCT SHARC ice-tethered instruments and three FMI open water wave buoys were deployed over a spatially distributed region (~25 km apart) in the Antarctic MIZ during a 5-day period during the SCALE 2022 winter cruise. Buoy placement was optimised to measure wave-in-ice and ice drift effects of a polar cyclone moving through the MIZ region during the deployment period. Buoys were placed in open drift to consolidated ice conditions to measure changes in significant wave height and wave period. Each wave buoy collected high frequency inertial time-series data of wave (FMI) and sea ice motion (UCT SHARC) as well as positional data to measure drift. Data were processed onboard and summary statistics were transmitted periodically via the Iridium satellite network.

The main activities undertaken by the buoy group during SCALE 2022 winter cruise were: (i) deployment and retrieval of the FMI open water and ice tethered buoys (**JVB**); and (ii) deployment and retrieval of the UCT SHARC buoy platforms (**RV**, **MV**, **MN, LS, JP, JVB, AS, JW**).

14.3.3 FMI wave buoy deployment and retrievals

14.3.3.1 Method and equipment

The floating open water buoys, which were deployed as drifters, were of type LainePoiss (Alari et al. 2022). Two of the Buoys (named here **LP2** and **LP4**) were of the first generation of platforms and were made out of fibreglass (Figure 100). These were deployed inside the MIZ. The third buoy (named here **LP8**) was of second generation and was made out of plastic (Figure 100).

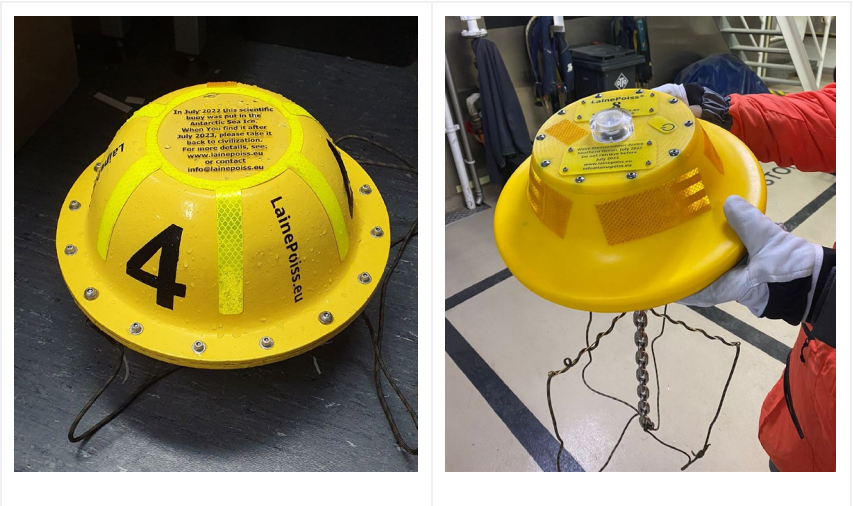

Figure 100 Three LainePoiss buoys were deployed as drifters during the SCALE WIN2022 cruise. (left) First generation of buoy made from fibreglass (LP2, LP4). (right) Second generation of buoy made from plastic (LP8). Photos by JVB.

All LainePoiss buoys log raw acceleration and gyroscope data at 50 Hz, which is saved to an SD-card. The data processed on board are downsampled to about 5 Hz. The wave spectrum is calculated from a 22-minute time series. The spectrum sent through the Iridium network contains 29 frequencies between 0.035095 Hz and 0.312805 Hz (frequency resolution ca 0.01 Hz).

Along with the spectrum the buoy sent some integrated parameters, the GPS position and the measured maximum single wave height. The LainePoiss buoys also use a magnetometer to record directional information, and the wave directions and the spreading are sent over the Iridium network. If the SD-card is retrieved, the full 2D wave spectrum can be obtained.

The wave buoy tethered to the ice (**BB01**) was of type OpenMetBuoy-v2021 (Rabault et al. 2022). The standard design was fitted inside an outer box for the purpose of being attached to the ice floe by sharpened screws (Figure 101). The buoy logs raw data at 800 Hz, but after the Kalman filtering the data is 10 Hz. The wave spectrum was calculated from a 20-minute time series and sent over the Iridium network. The spectrum that is sent has 55 frequencies between 0.0439453125 Hz and 0.3076171875 Hz (roughly 0.005 Hz resolution).

Figure 101 The FMI ice-tethered buoy (BB01) in its enclosure. The platform is based on the OpenMetBuoy-v2021 (Rabault et al. 2020) design. Photo by JVB.

Before deployment each buoy was configured and tested on board the ship in the Electronics Laboratory to ensure correct operation. As the LainePoiss buoys were going to be retrieved, they had rope attached around them to ease retrieval by the crew from the ships cranes (Figure 100). Buoys were turned on approximately half a day before deployment and were placed in a box on the deck 5 helideck with a clear view of the sky. This was done to ensure that the GPS and Iridium systems were configured and communicating correctly. All buoys were deployed by **JVB**.

Station name	Date	Activity start time (UTC)	Location	Notes
OD-1	2022/07/19	07:56	-58.22958, -1.35298	**LP8 deployment**: LP8 was deployed off the back of the poop deck in open-drift conditions.
ICE21 (I1)	2022/07/19	16:20	-58.66793, -1.12797	**LP4 deployment**: LP4 was deployed off the side of the poop deck in the MIZ.

ICE22 (I2)	2022/07/19	18:08	-58.54958, -0.86925	**BB01 deployment**: The FMI “box buoy” based on the OpenMetBuoy-v2021, was deployed on the same ice floe as the UCT SHARC buoy SB02.
ICE23 (I3)	2022/07/20	02:00	-58.58198, -0.46445	**LP2 deployment**: LP2 was deployed off the side of the poop deck in the MIZ. This device was not retrieved.
LP4	2022/07/24	11:40	-59.0608, 0.59938	**LP4 retrieval**: Retrieval started about 11:00 UTC. Extensive ice coverage made retrieval from the crane difficult. Photos available.
SB05	2022/07/24	14:00	-58.97552, 1.00575	**LP4 redeployment**: LP4 was redeployed off the side of the poop deck
LP8	2022/07/24	18:06	-58.58062, 0.47917	**LP8 retrieval**: Retrieval started about 17:30 UTC. Extensive ice coverage made retrieval from the crane difficult.
SAZr (PS)	2022/07/27	09:02	-46.9999, -0.00038	**LP8 redeployment**: LP8 was redeployed off the side of the poop deck after the station.

14.3.3.2 Preliminary results

Data from the FMI buoys were processed, and a selection of preliminary results are presented in the figures below.

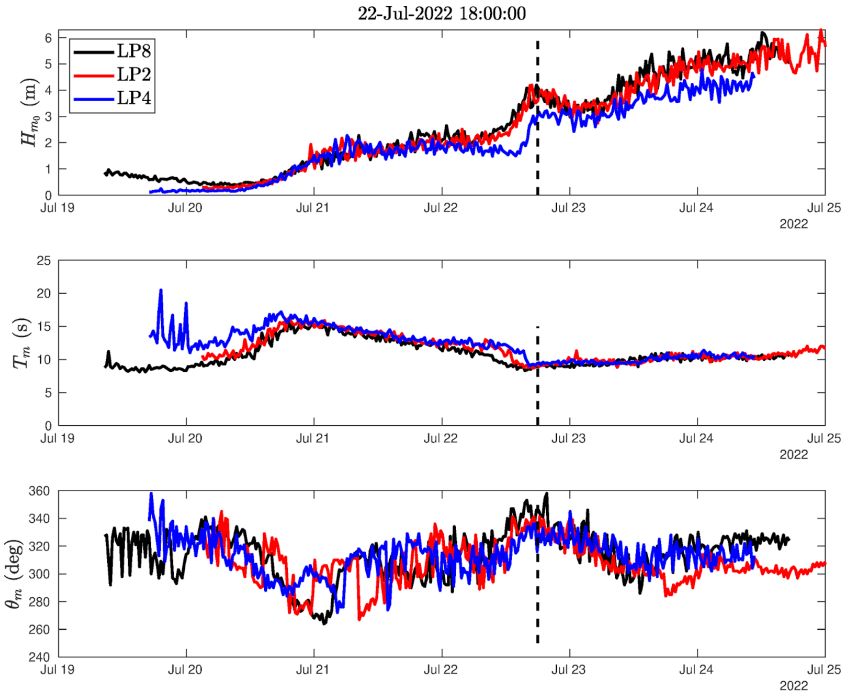

Figure 102 The significant wave height (top), mean wave period (middle), and mean wave direction (bottom) measured by the three floating wave buoys (LP2, LP4, LP8) during the experiment. The dashed vertical line marks the time for which spectra are shown in Fig. 2

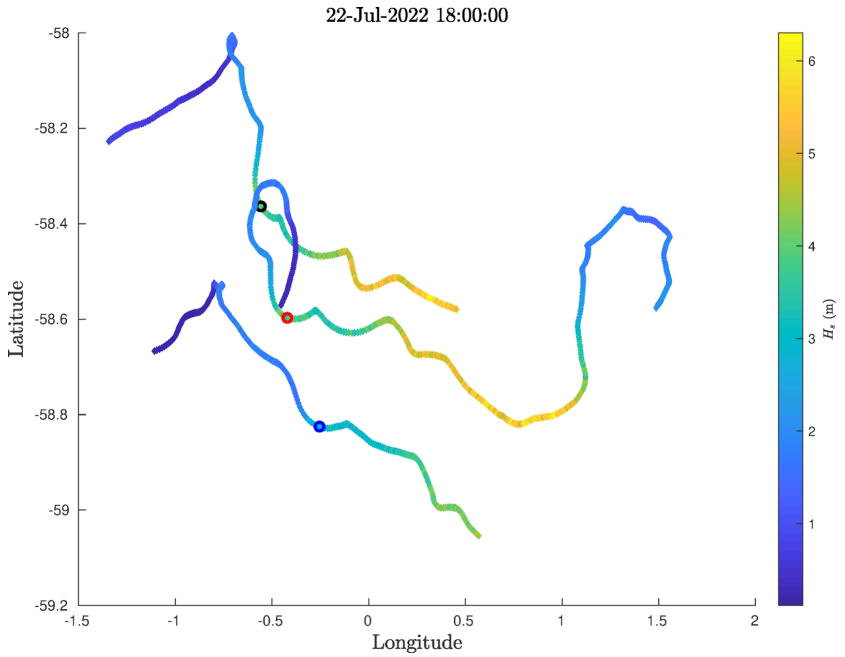

Figure 103 The drift and significant wave height of the three buoys. The circles (black: LP8, red: LP2, blue: LP4) marks the time for which spectra are shown in the next figure.

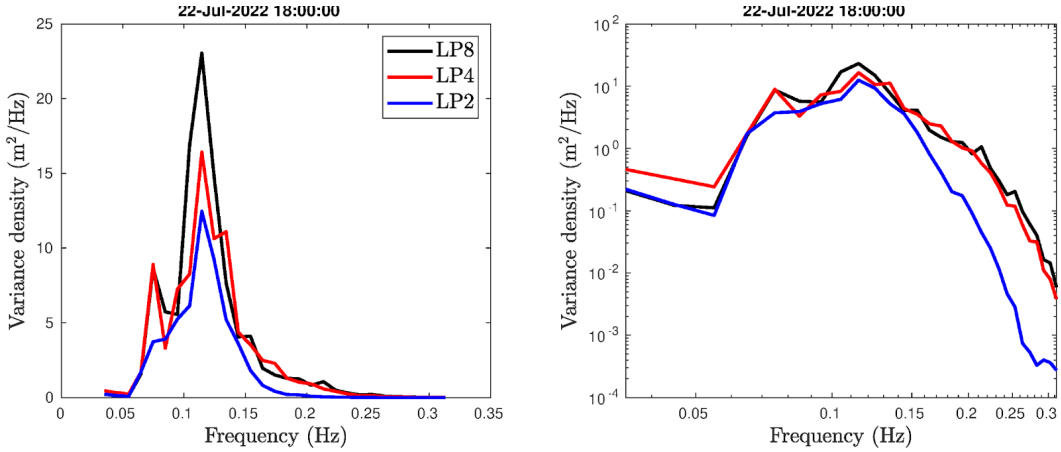

Figure 104 The wave spectra from the three different buoys showing the attenuation of the waves in ice. The wave spectra are an average of three 22-minute wave spectra closest to the time shown in the title.

14.3.4 UCT SHARC buoy deployment and retrievals

An ice-tethered instrument (UCT Southern Hemisphere Antarctic Research Collaborative Buoy) was prototyped and tested for the 2019 SCALE winter cruise, as part of the UCT NRF SANAP project on realistic modelling of the Marginal Ice Zone in the changing Southern Ocean (MISO). It was developed to collect in situ environmental and wave data in the Marginal Ice Zone. Three basic prototype units, equipped with ice drift (GNSS) and air temperature sensors were deployed during this mission to investigate survivability in Antarctic sea ice winter conditions. From these initial investigations, a number of key design improvements were identified and have been improved on in the SHARC V3.0 which was designed and produced for this cruise. These include: (a) improved hardware and onboard processing capability, (b) larger battery capacity and advanced power supply design, (c) an upgraded GNSS system for ice drift measurements (d) high frequency inertial measurement units (IMU) for waves-in-ice monitoring with an onboard wave processing algorithm (significant wave height and period, wave direction, power spectrum), which was calibrated in the the CSIR-BE wave tank facility. All platforms operate in two modes, (a) as a high frequency inertial data logger (100 Hz per inertial axes for 15 minutes), and (b) as an ice drift measurement buoy, where summarised GNSS and wave statistics data are transmitted every 40 minutes via the Iridium satellite network. An overview of the hardware design is presented in Figure 105.

Seven buoys were produced for deployment during the Targeted Observational Experiment and six were deployed at stations (**ICE21 - SB01**, **ICE22 - SB02**, **ICE23 - SB03**, **ICE12 - SB05**, **ICE11 - SB04** and **ICE00 - SB06**). An overview of the hardware in **Figure 23**. Four of the buoys were retrieved (**SB01**, **SB04**, **SB05** and **SB06**), with two of the platforms having been lost (most likely due to sinking events).

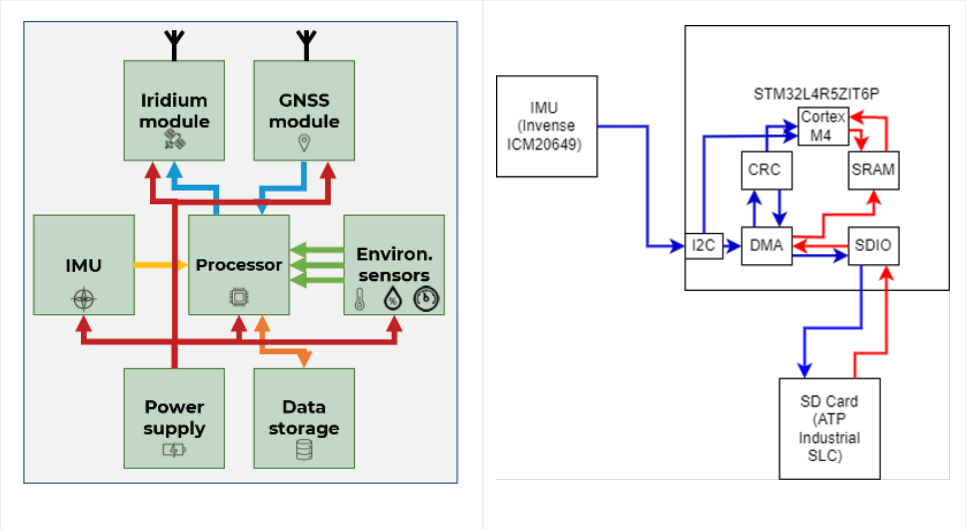

Figure 105 System hardware block diagrams of the UCT SHARC buoy architecture. (left) UCT SHARC V2.0 which contained inertial and environmental sensors with limited onboard wave processing and (right) the update UCT SHARC V3.0 which included high frequency inertial time-series data logging capability with data being saved on an SD-card for further analysis and processing

14.3.4.1 Method and equipment

Six SHARC Buoy V3.0s were deployed to capture the propagation of storm activity (specifically waves propagating through ice, known as waves-in-ice), into the MIZ.

Station name	Date	Activity start time (UTC)	Location	Notes
ICE21 (I1)	2022/07/19	13:20	-58.67003, -1.24678	**SB01 deployment (MN, JP, RV)**
ICE22 (I2)	2022/07/19	18:00	-58.54985, -0.87618	**SB02 deployment (JVB, MN, LS)**
ICE23 (I3)	2022/07/20	01:45	-58.58562, -0.46917	**SB03 deployment (MN, LS, RV)**
ICE12 (I5)	2022/07/20	07:40	-58.79702, -0.65042	**SB05 deployment (MV, RV, JW)**
ICE11 (I4)	2022/07/20	15:40	-58.58562, -0.46917	**SB04 deployment (JVB, AS, JW)**
ICE00 (I0)	2022/07/20	19:10	-59.04377, -0.50618	**SB06 deployment (MN, LS, RV)**
SB06 (I0-PS)	2022/07/23	09:20	-59.39667, 0.10833	**SB06 retrieval (MN, JP, RV)**
SB04	2022/07/24	07:50	-59.16497, 0.86517	**SB04 retrieval (JVB, MN, LS)**
SB01	2022/07/24	12:25	-59.1141, 0.66428	**SB01 retrieval (SM, MN, LS)**
SB05	2022/07/24	14:00	-58.97552, 1.00575	**SB05 retrieval (MN, LS, RV)**

The procedure for deployment of each buoy was as follows (Figure 106):

1. Before deployment, each buoy was assembled and tested on board the ship in the Electronics Laboratory to ensure correct operation. A new battery pack was fitted and a formatted SD-card was installed.
2. The buoy was placed in a stand on the deck 5 helideck for several hours to check the communication and GPS systems. This step was important for checking the functioning of the buoys prior to on-ice deployment.
3. All deployments were conducted from the personnel basket suspended from one of the starboard bow cranes. Three personnel were in the basket, with the buoy stand laid down in a horizontal position with the feet spikes facing outwards. The buoy itself was kept safely in the centre of the basket until deployment.
4. The buoy system was placed on ice by hand by first placing the stand as close to the centre of the selected pancake as possible, towards the bow of the ship. The ship is most likely to retreat related to the ice floe, reducing risk of collision of the personnel basket and buoy stand.
5. The buoy enclosure was then lowered into the holder on the stand.
6. Finally, the personnel basket was lifted from the ice as soon as the buoy was deployed.

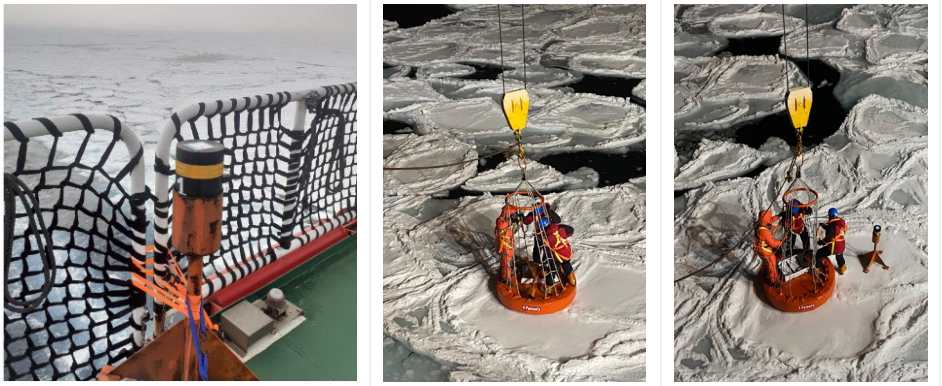

Figure 106 The deployment procedure for the UCT SHARC buoy during the SCALE WIN2022 cruise.

The procedure for retrieval of each buoy was as follows:

1. All retrievals were conducted from the personnel basket suspended from one of the starboard bow cranes. Three personnel were in the basket, to stabilise it, with one person responsible for lifting the buoy enclosure out of the stand.
2. Each enclosure was fitted with a handle on the side, which allowed for easy retrieval from the buoy stand.
3. Once the buoy was back on ship, the power was disconnected and the SD-card was retrieved. All data were then backed-up to a local hard drive.

14.3.4.2 Preliminary results

The SHARC buoys transmitted drift data via the Iridium satellite network as a key parameter of their in situ measurements of the MIZ. This measurement allows for calculations relating to how the ice sheet moves by comparing the paths of the buoys relative to each other, allowing the extraction of parameters such as ice sheet deformation over a time.

The high frequency IMU data collected by the buoys was processed to collect wave parameters that represent the general behaviour of waves in a region over a set period of time. It is worth noting that the high frequency IMU data retrieved from the buoys is the first such dataset to be collected in the region.

The general processing involves correcting the acceleration to the vertical, low pass filtering the high frequency noise, decimating the time series to a lower frequency, then performing a double integration in the frequency domain to get the wave amplitude (position time series) from the acceleration time series. From the amplitude time series, a power spectral density spectrum can be estimated using Welch's method. Finally, by integrating over the PSD, wave parameters such as significant wave height or period can be extracted. The general pipeline is depicted in figure 5 below.

Finally, as the raw data has been collected, several new analyses can be performed. For example, different approaches to filtering the raw data and extracting the wave parameters can be compared, high frequency phenomena such as ice floe impacts can also be investigated (see figure 6 below). Non-linear analyses of the time series data can also be performed.

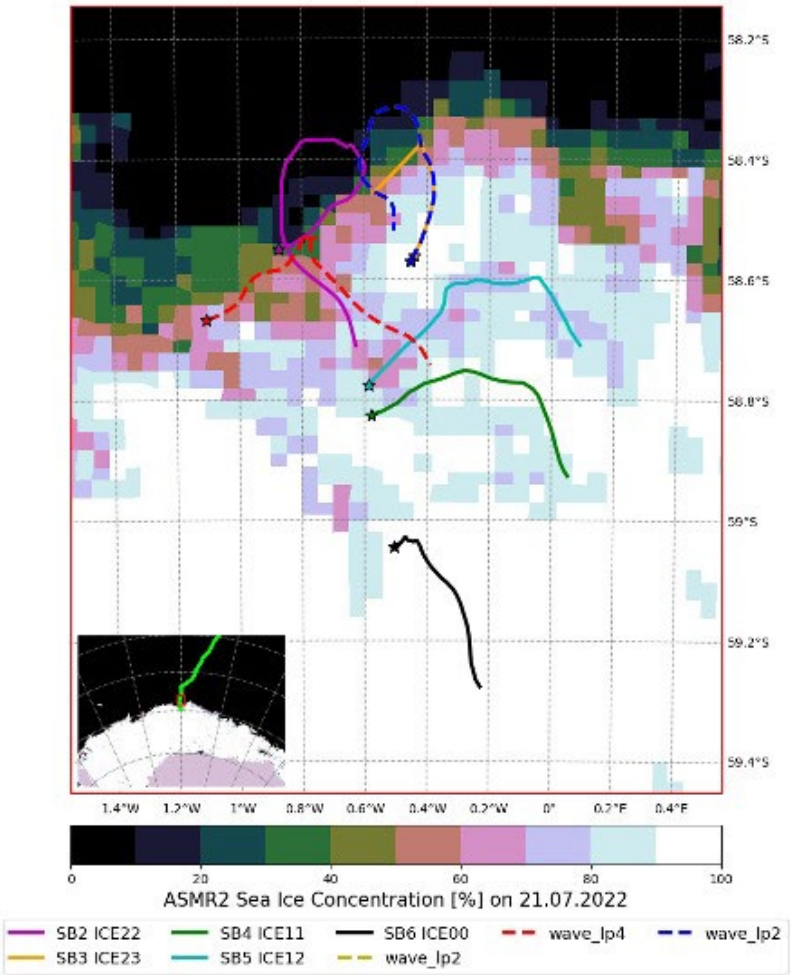

Figure 107 Buoy drift tracks for the duration of the experiment. Image credit R. Audh. SB01 path excluded

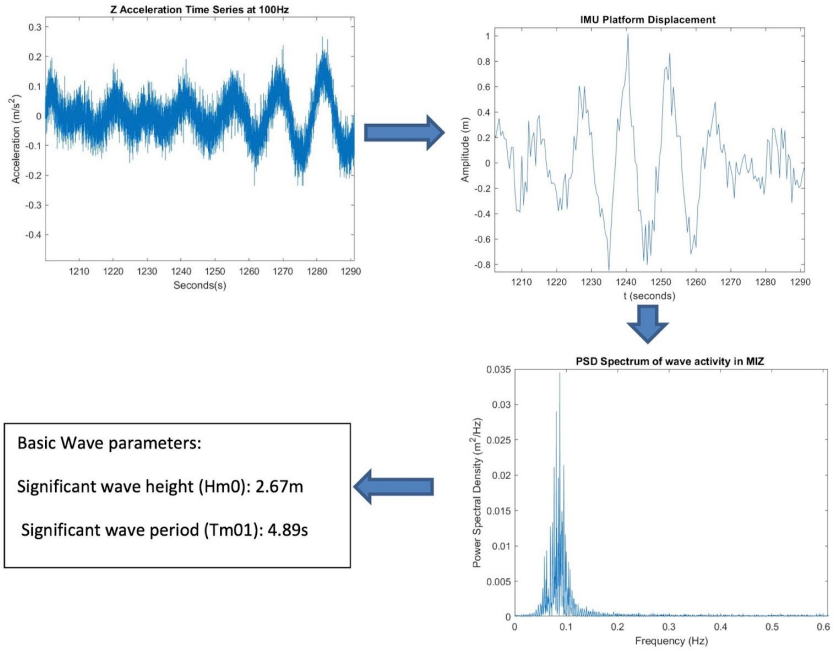

Figure 108 Overview of the wave parameter extraction pipeline

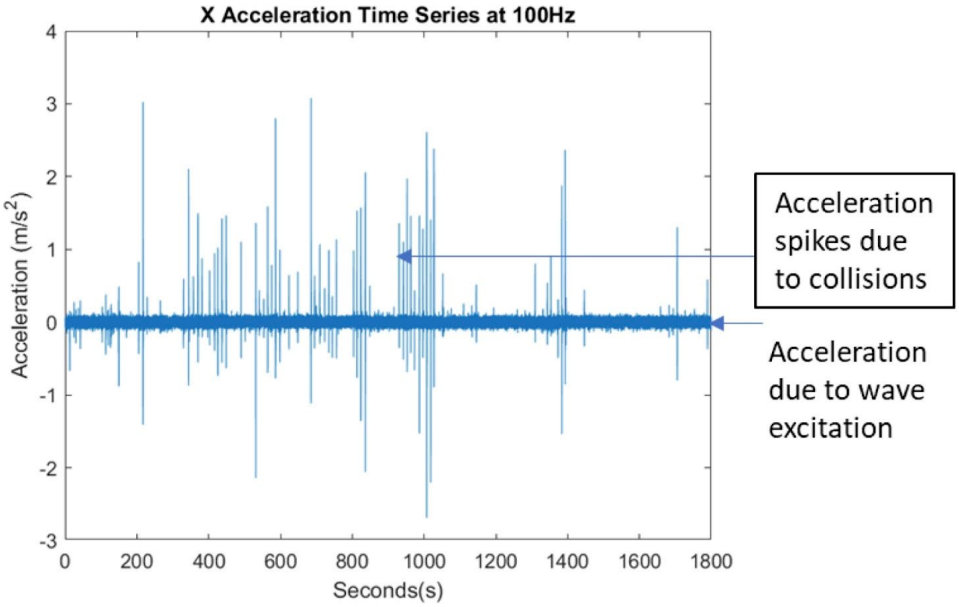

Figure 109 High acceleration events in the time-series which could be due to ice-ice collision events.

References

Arrigo, K.R., Worthen, D.L., Lizotte, M.P., Dixon, P. and Dieckmann, G., 1997. Primary production in Antarctic sea ice. Science, 276(5311), pp.394-397.

Eayrs, C., Holland, D., Francis, D., Wagner, T., Kumar, R. and Li, X., 2019. Understanding the Seasonal Cycle of Antarctic Sea Ice Extent in the Context of Longer-Term Variability. Reviews of Geophysics, 57(3), pp.1037-1064.

Eayrs, C., Li, X., Raphael, M.N. and Holland, D.M., 2021. Rapid decline in Antarctic sea ice in recent years hints at future change. Nature Geoscience, 14(7), pp.460-464.

Gryschka, M., Drüe, C., Etling, D. and Raasch, S., 2008. On the influence of sea-ice inhomogeneities onto roll convection in cold-air outbreaks. Geophysical Research Letters, 35(23).

Hall, D.K., Key, J.R., Casey, K.A., Riggs, G.A. and Cavalieri, D.J., 2004. Sea ice surface temperature product from MODIS. IEEE transactions on geoscience and remote sensing, 42(5), pp.1076-1087.

Hall, D.K., Nghiem, S.V., Rigor, I.G. and Miller, J.A., 2015. Uncertainties of temperature measurements on snow-covered land and sea ice from in situ and MODIS data during BROMEX. Journal of Applied Meteorology and Climatology, 54(5), pp.966-978.

Krishfield, R.A. and Perovich, D.K., 2005. Spatial and temporal variability of oceanic heat flux to the Arctic ice pack. Journal of Geophysical Research: Oceans, 110(C7).

Lytle, V.I., Massom, R., Bindoff, N., Worby, A. and Allison, I., 2000. Wintertime heat flux to the underside of east Antarctic pack ice. Journal of Geophysical Research: Oceans, 105(C12), pp.28759-28769.

Meehl, G.A., Arblaster, J.M., Bitz, C.M., Chung, C.T. and Teng, H., 2016. Antarctic sea-ice expansion between 2000 and 2014 driven by tropical Pacific decadal climate variability. Nature Geoscience, 9(8), pp.590-595.

Parkinson, C.L., 2014. Global sea ice coverage from satellite data: Annual cycle and 35-yr trends. Journal of Climate, 27(24), pp.9377-9382.

Rabault, J., Sutherland, G., Gundersen, O., Jensen, A., Marchenko, A., Breivik, Ø., 2020. An open source, versatile, affordable waves in ice instrument for scientific measurements in the Polar Regions. Cold Regions Science and Technology 170, 102955.

Rasmussen, T.A., Høyer, J.L., Ghent, D., Bulgin, C.E., Dybkjær, G., Ribergaard, M.H., Nielsen-Englyst, P. and Madsen, K.S., 2018. Impact of Assimilation of Sea-Ice Surface Temperatures on a Coupled Ocean and Sea-Ice Model. Journal of Geophysical Research: Oceans, 123(4), pp.2440-2460.

Sun, S. and Eisenman, I., 2021. Observed Antarctic sea ice expansion reproduced in a climate model after correcting biases in sea ice drift velocity. Nature communications, 12(1), p.1060.

15 MERCURY AND BIOACTIVE TRACE METALS IN THE SOUTHERN OCEAN

Team name and PI	MERCURY. Susanne Fietz (SU), Lynwill Martin (SAWS), Alakendra Roychoudhury (SU), Lars-Eric Heimbürger-Boavida
Authors	Fietz S, Labuschagne C, Jansen van Vuuren L, Buchanan K, Quinlan L, Walsh J, Gindorf S, Amptmeijr D, Roychoudhury, Martin, and Heimbürger-Boavida

15.1 BACKGROUND

Metals in the marine ecosystem can have two different main impacts: fertilizing or toxic. Here we focus on both aspects, in particular on bioactive trace metals as essential nutrients and on mercury as a key contaminant.

For bioactive trace metals, we focus particularly on the marginal ice zone during SCALE22, following up on ice and transect data collected during the SCALE19 winter and spring cruises. Sea ice winter formation is an important mechanism which accumulates and releases metals back into the system. However, the relative importance of this mechanism is still to be comprehensively determined (Lannuzel et al., 2011). The released metals play, potentially, a crucial role in the development of spring and summer phytoplankton blooms in the Southern Ocean (Grotti et al., 2005; Lannuzel et al., 2011, 2014). Hence seasonal sea-ice dynamics may play a significant role in the CO2 uptake mechanisms of the Southern Ocean.

For mercury, we focus on the transect, the ice and the atmosphere, as none of these environments has been sampled previously for mercury. Mercury, especially methylmercury is a neurotoxic contaminant in the ocean that affects ecosystem and human health. Over the past two decades, it became clear that processes in the seawater are largely responsible for the conversion from inorganic mercury to the bioaccumulative neurotoxin methylmercury. Members of the French team contributed to the thus far only Southern Ocean observations that show that this remote region is a source of methylmercury, likely transported as gaseous mercury in the atmosphere, entering the ocean via the sea-ice, converted into methylmercury by bacteria, taken up by phytoplankton and bioaccumulating along the marine food chain to harmful levels in top predator, including humans.

15.2 KEY RESEARCH QUESTIONS

Objective 1: “Mercury in Southern Ocean open waters and sea ice zone”:

1. What are the drivers controlling mercury (Hg) concentration, speciation and distribution in the Southern Ocean and how do these compare to other open ocean data?
2. How does the atmospheric Hg concentration change along the transect from Cape Town to Antarctica?
3. What is the GEM atmospheric mixing ratio along the transect from Cape Town to Antarctic Sea ice zone? Can this be successfully measured via an autonomous underway system?
4. What role does the formation of sea-ice play in the mercury (Hg) cycle?
5. Is there a microbial potential for Hg methylation and demethylation in the water column in the Southern Ocean along the transect?

6. Do the concentration and composition of dissolved organic matter (DOM) play a role for Hg speciation in the water column along the transect?
7. What is the quantitative and vertical behaviour of organic contaminants in the water column and can we use persistent organic pollutant (POP) data to quantify the anthropogenic influence in the Southern Ocean and relate the degree of human pollution to Hg concentrations and Hg speciation?

Objective 2: "Trace Metals in Sea Ice"

1. What is the distribution of trace netals within the Marginal Ice Zone during winter?
2. How does the vertical distribution of trace netals within the water column vary annually?
3. How does seasonal ice melt effect the concentration of dFe and other trace netals in the Southern Ocean?
4. How can the vertical and horizontal distribution of trace metals be further constrained by analysing the physico-chemical factors involved?

15.3 SAMPLING STRATEGIES

Two main types of samples were taken: **water** and **ice**. Both sampling strategies are described separately below. In addition, atmospheric mercury was measured continuously along the voyage. The continuous **atmospheric** mercury monitoring is described after the two sampling strategies (i.e. after water and ice).

15.4 WATER

15.4.1 Water samples: Stations

Seawater was collected from 4 Process Stations (PUZ, OD2, ICE00, SAZr, STZ) and 3 additional Ice Stations (ICE1/I21, ICE2/I22, ICE4/I11) (Table 1). "Ice Stations" refer to stations where GO-FLO bottles CTD casts were deployed while in the marginal sea ice zone.

Table 22: Station overview for water samples

Station ID	Station Type	Max sampled depth (m)	Date	Latitude	Longitude
PUZ1	Process	2300	2022/07/17	53°59.938' S	00°00.011 E
ICE1/I21	Ice	500	2022/07/19	58°40.131' S	01°09.934' W
ICE2/I22	Ice	500	2022/07/19	58°31.490' S	00°48.572' W
ICE4/I11	Ice	499	2022/07/20	58°51.069' S	00°40.824' W
OD2	Process	4500	2022/07/21	58°24.076' S	00°38.960' W
ICE00	Process/Ice	499	2022/07/23	59°24.023' S	00°07.872' E
SAZr/GT5	Process	3511	2022/07/26	46°59.983' S	00°00.121' E
STZ/GT10	Process	300	2022/07/29	38°4.1328' S	10° 57.222' E

15.4.2 Water samples: Sampling and sub-sampling

Water column samples were collected from 24 Teflon-coated, acid-cleaned GO-FLO bottles on a Seabird aluminium frame carousel CTD rosette attached to a Kevlar®(non-metallic) line, simultaneously measuring parameters such as salinity, temperature, and fluorescence. Empty GO-FLO bottles were stored in a certified class 100 (ISO) clean container with a zip lock bag covering the nozzle and shower caps covering the top and bottom of the bottles to protect them from particles.

At stations the GO-FLO bottles were carried to the carousel, loaded onto the frame, and prepared for deployment (Figure 1). Shower caps and zip lock bags were only removed directly before deployment. The bottles were triggered for closure during the upcast on the fly (Figure 1). Upon arrival back in the hanger, the filled bottles were immediately protected with fresh zip lock bags for the outlets and shower caps for the top and bottom. The flasks were transferred back into the clean container. After a 15-minute ventilation and re-equilibration period, sub-sampling was started.

Figure 110. GoFlo deployment. Top: Transport of Go-Flo bottles to the rosette and preparing Go-Flo triggers before deployment; Bottom: Deployment in open water and marginal ice zone. Photo credit: S. Fietz

Sub-sampling was conducted in the clean container for both unfiltered and filtered samples (Figure 2). All sub-sampling bottles, vials, and tubes were rinsed with sample water three times before filling. Some samples were taken unfiltered and others filtered. Similarly, some samples were stored directly after sub-sampling for processing and analysis on land and others were processed on board before storage. Hence, individual samples are described in more detail below.

Unfiltered samples: Unfiltered samples were taken for analysis of oxygen and deuterium isotopes, total mercury (THg), methylmercury (MeHg), monomethylmercury (MMHg), persistent organic contaminants, nutrients, genomics, and phytoplankton isolates. Samples were collected through a Teflon tube connected to the GoFLO bottle, under gravity.

Filtered samples: Filtered samples taken for *Team Mercury* and *Team Trace Metals* included dissolved trace metals (dTM), dissolved organic carbon (DOC) and fluorescent dissolved organic matter (FDOM). In addition, samples were taken for *Team Iron* that included dissolved iron (dFe),

soluble iron (sFe), iron ligands (FeL), humic substances (HS). To collect the filtered samples, each GO FLO bottle was connected to an ultra-pure Nitrogen gas line to push the sea water directly from the GO FLOs through a 0.45 +0.2µm filter (Sartorius Stedim Biotech Sartobran 300).

Figure 111. Sub-sampling the Go-Flos in the clean-container. Photo credit: S. Fietz

15.4.3 Water samples: Sample handling and processing on board

Oxygen and deuterium isotopes: Unfiltered samples were collected in 30 mL Teflon bottles without headspace and stored at room temperature.

Phytoplankton isolates: Unfiltered seawater was sampled directly into sterile 60 mL Falcon tubes and stored at 4˚C.

Macronutrients: Unfiltered samples were collected by filling 60 mL Falcon tubes with ca 40 mL of unfiltered sea water and frozen upright directly after collection.

Mercury: All Hg species samples were collected unfiltered and without headspace. THg was collected in 60 mL glass vials with septum tight screw caps that were wrapped with parafilm directly after collection. MeHg and MMHg samples were collected in 150 mL cubic PET bottles. MMHg samples were taken from clean container to dedicated ship laboratory, where they were reduced to a volume of 125 mL and purged with Argon gas (99.9995 % - 5.0 quality) for 12 minutes and 30 seconds to strip all dimethylmercury from the sample (Figure 3). MMHg and MeHg samples were acidified to 0.5 % v:v using Suprapure HCl. All mercury speciation samples were stored at 4˚C in the dark.

Persistent organic contaminants: Unfiltered samples were collected from selected depths at process stations. Six depths were sampled at stations PUZ, OD2 and SAZr and three samples were taken for STZ. Depths were selected to include surface, mixed layer depth, oxygen minimum, and deepest sampled depth. Samples were collected directly from the Go-Flos into 1L glass bottles. Glass bottles were then removed from the “GoFlo” clean container for processing the FIA clean container. For transport, all bottles were individually double-bagged in zip-lock bags. 10 µL of surrogate solution and one gel were added to each 800mL sample. Each bottle was then closed with muffled aluminium and lid. Samples were left for 48h in the zip lock bags at 4˚C in the dark to equilibrate. After 48h, the

gels with accumulated contaminants were recovered, placed in muffled aluminium foil and stored at -20 °C. 5 gel blanks were taken along the sampling.

Figure 112. David and Casper preparing methylmercury purging. Photo credit: S. Fietz

Bioactive trace metals: Filtered samples for dissolved trace metals were acidified to a pH of 1.7 with Merck Ultrapur® HCl (30%) and stored in 125ml LDPE bottles.

Organic matter: Filtered samples for FDOM and DOC were collected in 60 mL Falcon tubes filled to ca 40mL and frozen immediately.

Genomics: Approximately 4L of unfiltered seawater (two 2L Nalgene LDPE bottles) were sub-sampled from 6- 12 depths. Depths were selected to include at least from surface, mixed layer depth, oxygen minimum, and deepest sampled depth. All 4L unfiltered seawater samples were taken from the clean container to the dedicated ship laboratory and filtered through 0.2 µm membrane filters using a peristaltic pump (Figure 4). Three pump heads allowed pumping three samples simultaneously. Each sample was pumped through MasterFlex tubing, attached on the influent end to a pipette. Pipettes and tubing were cleaned with single ethanol rinse and 500ml Milli-Q water prior to each sample. Upon completing filtration of a 4L sub-sample, each filter was placed into bead-beater vial that were stored at -80 ˚C. For each sub-sample, the exact filtered volume was measured and recorded using measuring cylinders.

Figure 113. Jared and Liam preparing filtration system for Hg-specific genomics. Photo credit: S. Fietz

15.4.4 Water samples: Limitations

Due to malfunction of the electrical unit of 100 clean container, the ventilation of the clean container was not functional from station OD2 onwards (OD2, SAZr, STZ). All sampling activities were continued in the same manner described above (excluding *Team Iron*'s sampling for iron species). Acidification was carried out in the FIA container under a laminar flow fume hood for all remaining stations after OD2. To compensate for the lack of clean air ventilation, the container was thoroughly cleaned after every use.

15.4.5 Water samples: Stewardship

Following ship-board procedures, dTM and isotope samples are stored until analysis at Stellenbosch University. Mercury speciation and genomics samples are shipped to Institut Méditerranéen d'Océanologie, France, for analysis. FDOM and DOC samples were transported frozen to Stockholm University for analysis. POP gels were taken frozen to Europe, and will be analyzed at Institute of Research for Development, Marseille, France.

15.5 ICE

15.5.1 Ice samples: Stations

Ice cores and snow samples were collected in the Marginal Ice Zone (MIZ) at two sites, from four different pancakes (Table 3). A total of 14 ice cores and 4 frazil ice sampled were collected for mercury speciation and dTM analysis (7 and 2 each). From pancake 'A' we collected 4 cores for dTM and mercury (2 each), from pancake 'B' we collected 6 cores for dTM and mercury (3 each) and from pancake 'C' we collected 2.5 cores for dTM and 2 for mercury, from pancake 'D' we collected 1 core each. Snow samples were collected from 3 of the 4 sampled pancakes. Two additional cores were received from overboard sampling in collaboration with Chief Scientist and iMicrobiome specifically for Fe analysis.

Table 23: Station overview including coordinates for ice core sampling

Station	Pancake	Latitude	Longitude	Time on deck	Date
OD2	A	58° 22.714' S	00° 31.466' W	13:59	21/07/2022
OD2	B	58° 22.714' S	00° 31.466' W	14:17	21/07/2022

OD3	C	59° 24.960’ S	00° 1.862’ E	21:50	23/07/2022
OD3	D			10:46	24/07/2022

15.5.2 Ice samples: Ice coring and subsampling

Pancake ice recovery and ice core drilling in described in detail in Team SEAICE report. Briefly, ice pancakes on board were placed on a wooden pallets to provide stability and limit contamination from the deck. For mercury and trace metal sub-sampling, pancakes were partially covered with an acetone cleaned polyethylene sheet upon arrival on deck to prevent contamination.

Ice cores were drilled from the pancakes on board using an electrical drill and a barrel. Prior to collecting any core for trace metal or mercury analysis, the barrel was conditioned by coring at least two ice cores. Ice cores were transferred from the barrel directly into acid cleaned plastic liners wearing vinyl gloves and arm sleeves. Ice cores were then stored at -20˚C horizontally to prevent brine movements within the core. Mercury ice cores were sectioned into upper 15 cm, bottom 15 cm and 30 cm middle part using a ceramic knife within 24 hours from coring. dTM cores were sectioned into even segments. The outside of each section was generously scraped off with a ceramic knife in the clean container lab (FIA container). Mercury ice core sections were then transferred into zip lock bags and melted at room temperature. The melted cores were then transferred into 60 mL glass vials (THg) and 125 mL PET bottles (MeHg and MMHg) and processed as the seawater samples for each species (described above). The dTM sections were stored in acid cleaned zip lock bags and returned to -20˚C freezer for processing and analysis on land.

Figure 114. Pancake ice recovery and drilling. Top: recovery and snow sampling; Bottom: drilling and ice core display (Sonja, Caspar, Kayla, Lide). Photo credit: S. Fietz

15.5.3 Ice samples: Snow

Snow samples were collected from the top of the pancakes on board using an acid cleaned plastic shovel and transferred into acid cleaned zip lock bags. Samples for dTM were stored at -20°C freezer prior to processing at Stellenbosch. Samples for mercury were melted and further processed as the melted core sections and seawater as described above.

15.5.3.1 Ice samples: Frazil ice

Frazil ice was collected independently from the pancake ice, but at the same stations (i.e. as close as possible considering ship manoeuvres in the ice). Frazil ice for mercury and trace metals manually did not use *Team SEAICE*'s frazil ice collector as this method was not trace metal clean. Instead frazil ice for mercury and trace metals was collected from the aft deck using a polyethylene 1L jug on a long pole. Small holes in the bottom allowed seawater to drain when scooping the frazil ice. Samples for trace metals were transferred into acid cleaned zip lock bags and stored in a -20C˚ freezer until further processing on land. Frazil ice samples for mercury speciation were melted on board and transferred into sample vials as described for ice core sections above.

15.6 ATMOSPHERE

15.6.1 Atmospheric gaseous elemental mercury: Sampling and analysis

Underway sampling for atmospheric Gaseous elemental Mercury (GEM) was performed using a similar system to that being used at the Cape Point Global Atmosphere Watch Station (CPT GAW). A TEKRAN model 2537X was coupled to an existing on-board air intake line (~60m of 1.2-inch Dekoron) which served as the underway air intake line for the pCO_2 system (Figure 6). A flow rate of 1.5Lpm was required to flush the line sufficiently. The pCO_2 pump and TEKRAN instrument pump seemed to be adequate for this purpose (Refer to recommendation 1). The TEKRAN was coupled to a zero-air generator and a source of high purity Argon (99.999%) carrier gas. The instrument flow rate was kept low (in the order of 80 – 150mL/min). The instrument was set up to sample at 300s intervals whilst calibrations and zero checks were performed 4 – 6 hourly. Underway ship data (GPS location, atmospheric parameters etc.) was collected via SDS system (ship data system).

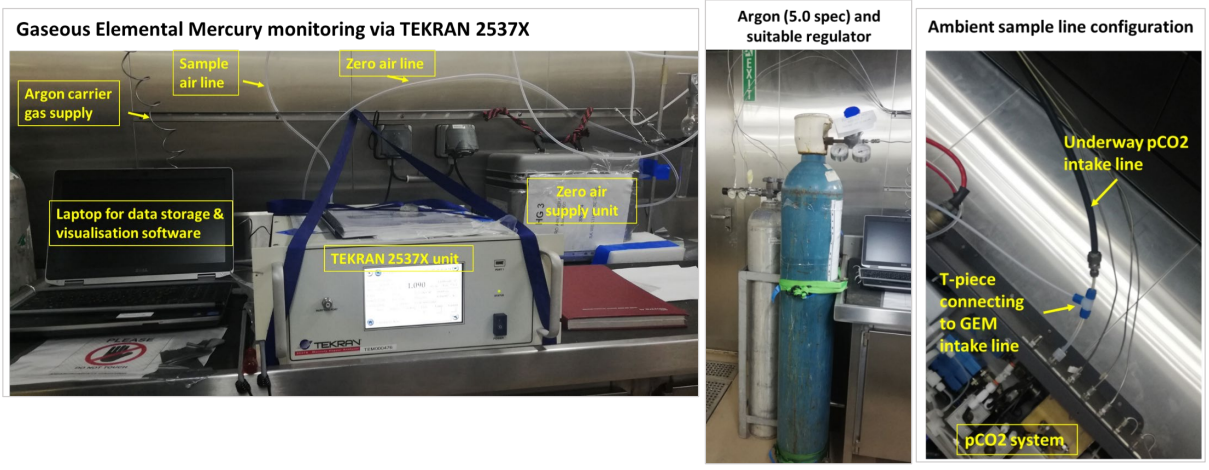

Figure 115: Left: Instrument setup configuration for GEM measurement in ambient air. Centre: Carrier gas supply cylinder, securely strapped; Right: Ambient sample line configuration with PCO2 system. Photo credit: C. Labuschagne

15.6.2 Atmospheric gaseous elemental mercury: Data

Raw data was collected from the laptop software (supplying an initial overview of the measurements and therefore acting as a good as an overall system health check) or downloadable as daily .txt files directly from the TEKRAN 2537X's USB drive (Figure 7). Off-line data processing can then be applied to QA/QC the data.

Overview of data file and column headers

C	D	E	F	G	H	I	J	K	L	M	N	O	P	X	Y	Z	AA	AB
Date Time	Activity	Cartridge	Zero Subtraction	Desorption	Event	AB Cycle	Sample Volume	Baseline Voltage	Baseline Std. Dev.	Peak Max. Voltage	Peak Magnitude	Concentration ng/m3	Event 0	Cartridge A	Cartridge B	Hourly ave A	Hourly ave B	
7/11/2022 12:00:00 AM	Continuous	B	0	OK	0	300	7.5	0.16	59.67	0.164	41534	1.236	1.236		1.236			
7/11/2022 12:05:00 AM	Continuous	A	0	OK	0	300	7.5	0.16	50.67	0.164	44241	1.283	1.283	1.283				
7/11/2022 12:10:00 AM	Continuous	B	0	OK	0	300	7.5	0.159	57.89	0.164	42520	1.265	1.265		1.265			
7/11/2022 12:15:00 AM	Continuous	A	0	OK	0	300	7.5	0.16	57.69	0.164	45000	1.305	1.305	1.305				
7/11/2022 12:20:00 AM	Continuous	B	0	OK	0	300	7.5	0.159	45.31	0.164	45845	1.365	1.365		1.365			
7/11/2022 12:25:00 AM	Continuous	A	0	OK	0	300	7.5	0.159	43.27	0.164	47987	1.392	1.392	1.392				
7/11/2022 12:30:00 AM	Continuous	B	0	OK	0	300	7.5	0.16	44.54	0.165	49025	1.459	1.459		1.459			
7/11/2022 12:35:00 AM	Continuous	A	0	OK	0	300	7.5	0.16	48.99	0.164	46031	1.335	1.335	1.335				
7/11/2022 12:40:00 AM	Continuous	B	0	OK	0	300	7.5	0.16	35.03	0.164	45055	1.341	1.341		1.341			
7/11/2022 12:45:00 AM	Continuous	A	0	OK	0	300	7.5	0.16	50.43	0.164	41847	1.214	1.214	1.214				
7/11/2022 12:50:00 AM	Continuous	B	0	OK	0	300	7.5	0.16	51.73	0.163	36039	1.072	1.072		1.072			
7/11/2022 12:55:00 AM	Continuous	A	0	OK	0	300	7.5	0.16	54.28	0.164	39677	1.151	1.151	1.151		1.280	1.258428571	
7/11/2022 1:00:00 AM	Continuous	B	0	OK	0	300	7.5	0.16	61.58	0.164	35969	1.071	1.071		1.071			
7/11/2022 1:05:00 AM	Continuous	A	0	OK	0	300	7.5	0.159	53.57	0.163	35851	1.04	1.04	1.04				
7/11/2022 1:10:00 AM	Continuous	B	0	OK	0	300	7.5	0.16	52	0.163	31678	0.943	0.943		0.943			
7/11/2022 1:15:00 AM	Continuous	A	0	OK	0	300	7.5	0.159	33.33	0.163	33548	0.973	0.973	0.973				
7/11/2022 1:20:00 AM	Continuous	B	0	OK	0	300	7.5	0.16	51.8	0.163	32139	0.957	0.957		0.957			

Figure 116: Overview of raw data file and column headers (col C – P). credit: C. Labuschagne

15.6.3 Atmospheric gaseous elemental mercury: Initial results

The figure below, shows some initial Gaseous Elemental Mercury (hourly averaged) atmospheric mixing ratios, along a transect from Cape Town to 59° South, and back again to 46° South (at the time of compiling this report) (Figure 10). The initial higher values (~1.5 ng/m3) are a result of some continental influences in the form of recirculating air masses (to be confirmed with air mass back trajectory calculations). This was followed by some very interesting features (draw down episodes) in the data as the measurements moved southwards. The mixing ratios of GEM is representative of the southern ocean and will form the foundation of comparisons with similar air masses, concurrently measured at the Cape Point GAW station and air mass back trajectory calculations.

The QA/QC parameters of importance is shown in Figure 10 and Figure 11. The individual tube A and tube B zero and span gives a good indication of "system health" and highlight possible analytical issues that requires intervention. It is recommended that these parameters are monitored on a continuous basis and that any remedial / interventions are performed timeously in order to ensure a good quality data set.

Overall, the GEM data collected during SCALE222, forms part of a very limited real-time (in situ) measurement collection for what otherwise constitutes a very sparsely sampled region of the globe. The data will be published in a peer reviewed journal as well as presented at one or more conference proceedings.

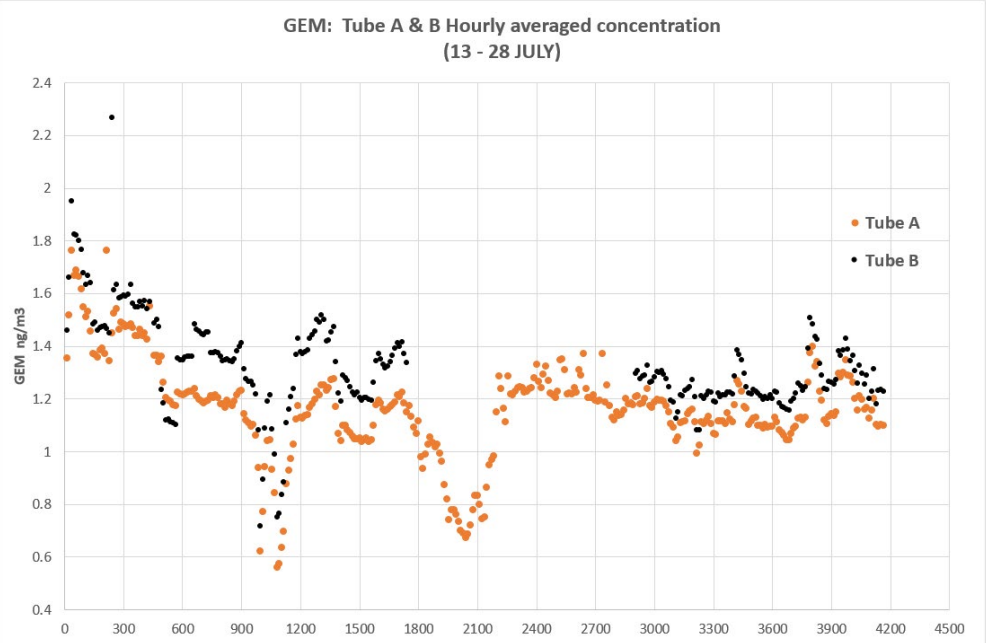

Figure 117: Overview of preliminary GEM hourly averaged atmospheric mixing ratios – on a transect from start (indicated by 0 on x-axis) to Antarctic Ocean region and back (as on time of compiling this report). credit: C. Labuschagne

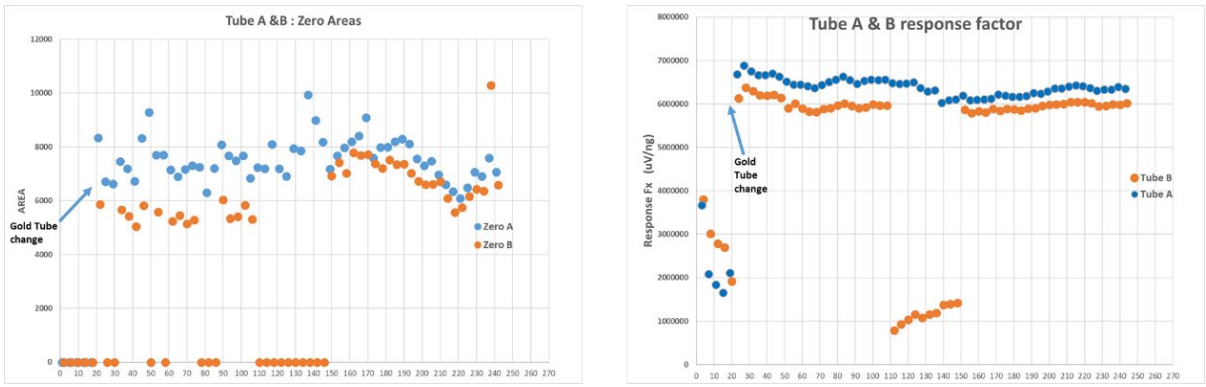

Figure 118: LEFT: Plot of individual 4-hourly zero (baseline) determinations; RIGHT: Plot of 4-hourly span calibration responses after applying a calibration gas. credit: C. Labuschagne

15.6.4 Atmospheric gaseous elemental mercury: Recommendations

It is suggested that a separate, dedicated line and flow pump (to ensure adequate line flushing) be installed in order to separate the GEM intake from the pCO2 intake line.

It seems possible to have this autonomously functioning system installed permanently on the SA Agulhas II for future voyages during its Southern Ocean activities. Any technician/scientist can be trained sufficiently prior to a voyage to be able to oversee such a system on future cruises.

16 SAPRI TRAINEES

Team name and PIs	SAPRI. Marcello Vichi (MARIS UCT), Juliet Hermes (SAPRI/SAEON) and Ria Olivier (ALSA/SU)
Authors	Whittingham J., Morake L., Ogugua U., Mahamba Y., Mthombeni A., Maluleke S., Wanda T., and Martin K.

The SCALE Winter Cruise 2022 provided the opportunity for the SAPRI trainees, who come from a range of academic backgrounds and institutions to learn and participate in a range of polar science activities. The team of SAPRI trainees consisted of:

Jennifer Whittingham (Social Science/Humanities/University of Cape Town) **JW**

Lefa Morake (Physical Geography/University of the Free State) **LM**

Udoka Ogugua (Agricultural Science/Unisa) **UO**

Yonela Mahamba (Marine Biology/Zoology/SANPARKS) **YM**

Annah Mthombeni (Fisheries Biology/Rhodes University) **AM**

Sandra Maluleke (Environmental Sciences/Unisa) **SM**

Thamsanqa Wanda (Marine Geology/Nelson Mandela University, SAIAB) **TW**

Kurt Martin (Humanities/Photographer) **KM**

16.1 SEMINAR SERIES

The team attended a series of evening seminars. This was an opportunity for the trainees to gain a broad understanding of the research occurring on the cruise and ask the researchers any questions. The seminars that were given included;

Prof Marcello Vichi, University of Cape Town: a) Introduction to Polar Oceanography, b) Antarctic Sea Ice variability and Climate Change

Davide Ampteijer & Sonja Gindorf, GMOS**:** The Biogeochemical Cycle of Mercury

Dr. Susanne Feitz, Stellenbosch University, South Africa: Phytoplankton and trace metals in the Southern Ocean

Marrick Muchow, Aalto University, Finland: Bridging Scales from Engineering to climate physics the representation of pressure ridges in sea-ice models

Makhudu Masotla, Department of Environment, Forestry, and Fisheries, South Africa: Top predators from the Southern Ocean

Dr. LetiziaTedesco, SYKE, University of Helsinki, Finland: Beyond ice worms – sea ice is a unique and extraordinary biome

16.2 Science Participation

Before the first deployment of the **CTD**, the trainees were given a talk by Prof Marcello Vichi in the operations room on the Poop Deck. This talk explained some of the physical and chemical properties of the water column and gave the trainees an understanding of the physical oceanographic characteristics of the Southern Ocean. LM had the opportunity to control and guide the CTD down through the water column in the operations room.

The team spent a morning with the **Top Predators** team where they learnt how to identify different seabird species by their wing and flight patterns, and beak shape. They also learnt how to document an observation, which includes noting the time, latitude/longitude, and how many were seen. They learnt how southern right whales are identified individually by the callosities on their face that act as a unique fingerprint. This observational data is collected in order to contribute to a wider data set that enables a better general understanding of distribution and frequency of top predators in the Southern Ocean.

The trainees learnt about the **McLane Pump** in one of the wet labs. Members of the N-Cycle Team explained how it was used to quantify the extent of carbon export below the mixed layer of the ocean. In addition to this, the trainees were exposed to the Marine Snow Catcher, another device that quantifies dissolved organic carbon that sinks below the mixed layer. This was followed by some hands-on experience filtering water collected by the Snow Catcher (JW, LM).

The trainees were integral to the **GoFlo** operations that occurred frequently throughout the cruise. This involved learning how to safely and without contamination prepare the CTD for deployment and how to avoid contamination and injury when carrying a CTD. Following this, some of the trainees (AM, SM, YM, UO) participated in water sampling for trace metals (mercury and nutrients) from the GoFlo bottles in the clean container. They were engaged in sample processing (purging and acidification) in the lab and in the freezing of the samples. TW participated in filtering the water collected from the GoFlo bottles for future genomic sequencing.

The trainees were invited by the SKYE team where the use and function of the **flow cytometer** was explained. The trainees witnessed a water sample taken from the underway water system go into the flow cytometer. This piece of equipment is used to detect, photograph, and identify the composition of phytoplankton communities in sea water.

JW, LM, KM had the opportunity to participate in some work with the **South African Weather Service**. They were involved in the deployment of drifters, XBTs (Expendable Bathythermograph), and several wave spotters. These sensors are used to collected various types of oceanographic data that will be used to inform global oceanographic and weather models.

Towards the end of the cruise, the trainees participated in **ice coring** on the Helideck. This involved how to dress for safety, how to assemble the ice corer, take a successful core sample, and measure the temperature accurately using a high accuracy thermometer, and finally how to make sense of the temperature readings. This practical was accompanied by an explanation of the physics of sea ice.

The team received a talk in the wet lab from the **MICROBIOME** team. They explained how they collect water from different depths using the Niskin bottles and look at microbial communities to try and understand how the microbiota react to different levels of metals (Manganese and Iron). This was accompanied by a practical with one of the team members. This involved sterilisation of equipment in order to filter 25L of water collected from the Niskins. A peristatic pump was used alongside a 0.2 micron and 0.3 micron filters. The filters were preserved in a -80 degree freezer to be used for metagenomic sequencing.

JW also conducted a series of interviews with the Team Leaders on the cruise and some members of the deck, navigation, and engine crew. This informed part of her PhD research.

KM was the photographer and documenter of the SCALE cruise. He moved freely around the ship and within the various scientific teams, meeting all participants. He photographed as many events as possible and organised team photos. He also edited and dispatched team updates, ensuring that the trainees were fully up to date with cruise activities.

The SAPRI Trainees would like to acknowledge; SAPRI, Antarctic Legacy Programme, National Research Foundation, APECS SA and all of the scientific teams that took the time to share their time and knowledge.

16.3 Images

Figure 119, OU assisting with the CTD

Figure 120 SM, YM, TW, JW, AM receiving a talk and demonstration on flow cytometry by Lumi Haraguchi

Figure 121 group photo of SAPRI Trainees with Prof Marcello Vichi

Figure 122 SAPRI Trainees with the Top Predators Team on the Monkey Island of the SA Agulhas II

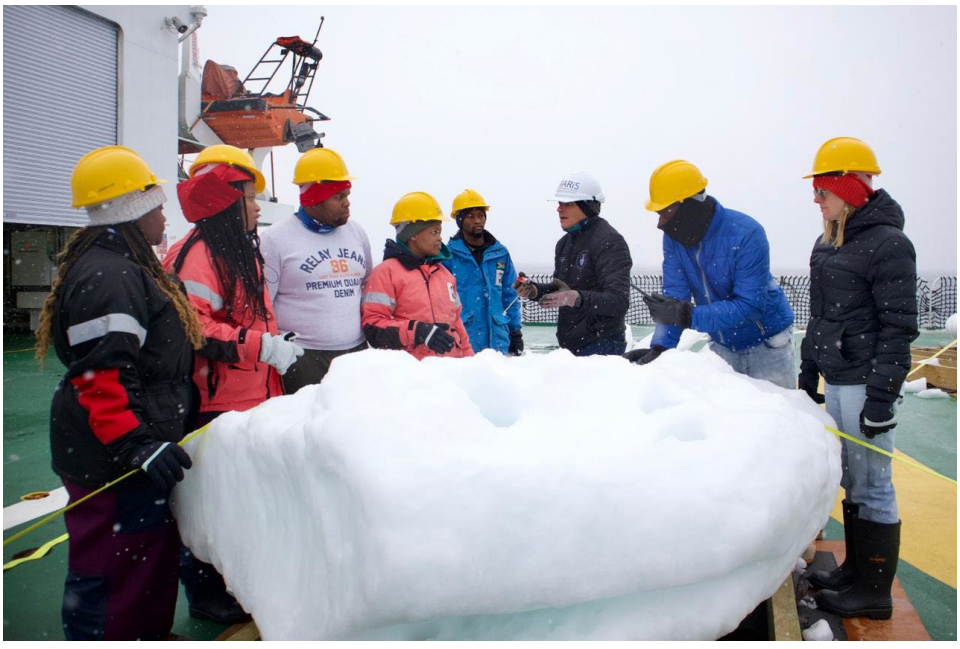

Figure 123 SM, AM, TW, YM, OU, JW learning how to take a sea-ice core from Prof Marcello Vichi

Figure 124 LM, OU, YM, SM, AM learning about the Marine Snow Catcher from Annicia Naicker

Figure 125 TW, LM, OU, AM, JW, YM receiving a talk from the Microbiome Team

Figure 127 AM, SM, YM assisting Sadiyah Rawat with the McLane Pump

Figure 126 LM assisting the Microbiome team with water filtering